Paranimfen: Tobias Nespital
Daphne Lelieveld

Printer: GVO printers & designers B.V.| Ponsen & Looijen

Cover: Ana Almeida & Nazaré Almeida

The work described in this thesis was performed in the department of Cell Biology of the University Medical Center Utrecht and supported by the Marie Curie Network, "UbiRegulators" (Grant MRTN-CT-2006-034555), and the European Network of Excellence, "Rubicon" (Grant LSHG-CT-2005-018683).

Understanding the Growth Hormone Receptor-βTrCP interactions:

Molecular Tools for controlling Growth Hormone Sensitivity

Inzicht in de binding tussen de groeihormoonreceptor en βTrCP: moleculair gereedschap om de gevoeligheid voor groeihormoon te regelen

(met een samenvatting in het Nederlands)

PROEFSCHRIFT

ter verkrijging van de graad van doctor aan de Universiteit Utrecht op gezag van de rector magnificus, prof.dr. G.J. van der Zwaan, ingevolge het besluit van het college voor promoties in het openbaar te verdedigen op vrijdag 30 september 2011 des middags te 12.45 uur.

door

Ana Carolina da Silva Almeida

geboren op 28 September 1984 te Caracas, Venezuela

Promotor: Prof.dr. G.J.A.M. Strous

Co-promotor: Dr. A.G.S.H van Rossum

The printing of this thesis was partly accomplished with financial support from Drug Discovery Factory B.V., and the J.E. Jurriaanse Stichting.

"I should keep my five senses perfectly trained, and my whole body, too, so that it would enjoy and understand. I should learn to run, to wrestle, to swim, to ride horses, to row, to drive a car, to fire a rifle. I should fill my soul with flesh. I should fill my flesh with soul. In fact, I should reconcile at last within me the two eternal antagonists."

Nikos Kazantzakis,
in Zorba the Greek

Contents

Abbreviations

AIDS	acquired immune deficiency syndrome
βTrCP	beta-transducin repeat protein
CHF	chronic heart failure
CK	casein kinase
COPD	chronic obstructive pulmonary disease
DUB	deubiquitinating enzyme
EPOR	erythropoietin receptor
ER	endoplasmic reticulum
ESCRTs	endosomal sorting complexes required for transport
GH	growth hormone
GHBP	GH binding protein GH receptor
GHR	GH receptor
GHRH	GH-releasing hormone
GSK3β	glycogen synthase kinase 3 beta
HECT	Homologous to E6-AP C-terminus
IFNAR	Interferon-α receptor
IGFs	insulin-like growth factors
IKK	inducible IκB kinase complex
IL	interleukin
IRS	Insulin receptor substrate 1
IκB	Inhibitor of I kappa B
JAK	Janus kinase
LBM	lean body mass
MAFbx	muscle atrophy F-box
MAPK	mitogen-activated protein kinase
MuRF1	muscle Ring Finger1
MVB	multivesicular bodies
NFκB	Nuclear factor kappa B
PI3-K	phosphoinositide 3-kinase
PKC	protein kinase C
PRLR	Prolactin receptor
PTP	protein tyrosine phosphatases
RA	rheumatoid arthritis
RING	really interesting new gene
SCF	SKP1-CUL1-F box protein
SFK	Src family kinases
SKP1	S-phase kinase-associated protein 1
SOCS	suppressor of cytokine signaling
SS	somatostatin
STAT	signal transducer and activator of transcription
TACE	tumour necrosis factor-receptor associated factor
TGF-β	transforming growth factor-beta
TGN	trans-Golgi-network
TNF-α	tumour necrosis factor alpha
Ub	ubiquitin
UBC	ubiquitin conjugating enzymes
UBD	ubiquitin binding domain
UbE	Ubiquitin dependent endocytosis motif
UIM	ubiquitin interacting motif
UPR	unfolded protein response

Introduction

Ana C. da Silva Almeida

Department of Cell Biology and Institute of Biomembranes,
University Medical Center Utrecht, Heidelberglaan 100, 3584
CX Utrecht, The Netherlands

Drug Discovery Factory BV, Albrechtlaan 14A, 1404 AK
Bussum, The Netherlands

Table of contents – Chapter 1

1. Growth Hormone physiology

1.1 GH Family and Structure

Growth Hormone (GH), also known as somatotropin or somatotrope hormone, is a peptide hormone produced in the anterior pituitary gland which promotes cell division, regeneration and growth (*1*). Philogenetically, GH is an ancestral hormone that has been found in the pituitary of primitive vertebrates, such as the jawless sea lamprey fish (*2*). Several GH isoforms have been identified, but in humans the majority of the circulating GH is a 22kDA form (*3*). GH belongs to the same family as prolactin, prolactin-like protein, placental lactogen, proliferin, proliferin-related protein and somatolactin (*4*). Crystallization of GH revealed its left twisted helical bundle structure composed by 4 antiparallel helixes (*5*). Two disulfide bounds were identified as necessary for its biological activity (*6*) (Fig.1). GH-related hormones, although differing in the primary amino acid, adopt a similar 3D structures (*7*). Bovine GH was isolated for the first time in 1944 from bovine pituitaries (*8*), but it was ineffective for the treatment of GH-deficient patients (*9*). Subsequently, human GH was purified for the first time in 1956 (*10*) and treatments using this preparation have been successful (*11*). These studies revealed the species specificity of GH.

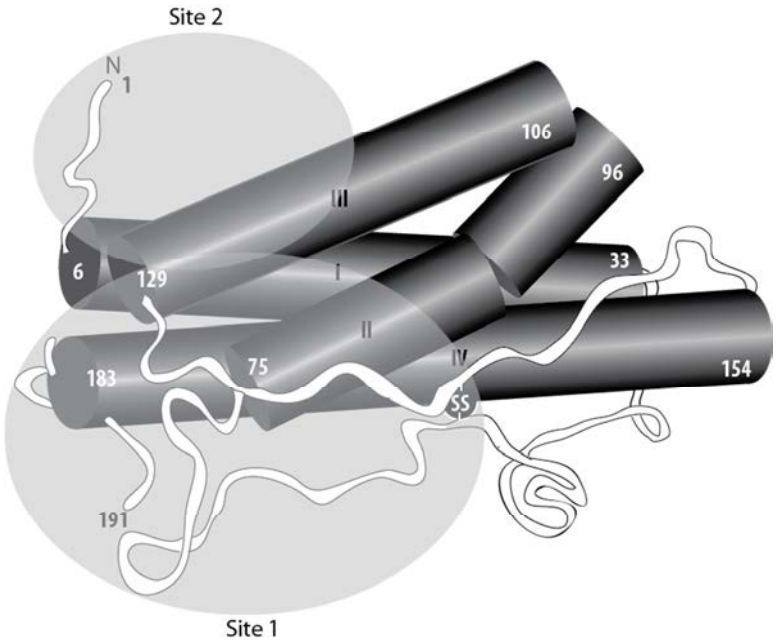

Fig.1: Schematic representation of GH crystal structure. The four antiparallel helical bundles are represented as cylindrical rods, labeled from I to IV, as obtained in the crystal structure of porcine GH. The amino- and carboxy termini of the protein are indicated with an N and a C. The amino-acid positions in the beginning and end of each independent helix are shown. Disulfide bonds connecting Cys53 to Cys165 and Cys182 to Cys189 are indicated. Site 1 and Site2 are roughly highlighted, referring to the two binding sites in GH to GHR. This figure is adapted from references (*5, 12*).

1.2 GH secretion and availability

The pituitary gland is the major source of the GH in circulation (*13*), but some extra-pituitary tissues (e.g. neural, immune, reproductive, alimentary, respiratory systems among others) have also been found to produce GH (*14*). GH is released from the somatotrophic cells in the anterior pituitary in a pulsatile manner. In man, GH is secreted episodically with a major surge at the onset of the slow-wave sleep, and less pronounced secretory episodes a few hours after meals (*15-17*). The pulsatility of GH secretion has a major impact on the pattern of GH-induced hepatic gene expression (*18*). The less pronounced pulsatile GH secretion pattern in females has been suggested to be responsible for sexual dimorphism in several physiologic processes, including hepatic metabolism (*19-21*). Pulses are regulated primarily by the interplay of hypothalamic hormones: a stimulatory GH-releasing hormone

(GHRH) and an inhibitory hormone, somatostatin (SS). These factors act via their receptors expressed at the cell surface of the somatotrophic cells. In addition, other peptides, called secretagogues (GHS), were identified to regulate GH secretion, such as GH releasing peptides (GHRP) originating from the brain (*22*), and Ghrelin, produced by stomach tissue (*23*). GHS act by activating their receptors (GHS-R), G-protein couped receptors expressed mainly in the anterior pituitary gland and hypothalamus (*24, 25*). Additionally, insulin-like growth factors (IGFs), of which the transcription is stimulated by GH, are able to inhibit GH release in a negative feedback loop (*26*). The details of the GH/IGF-1 system are discussed later in this chapter. Expression and release of GH are mainly regulated by the transcription factor Pit-1, which has additional functions in the differentiation and maintenance of somatotrophic cells (*27, 28*). GH secretion is also affected by other factors such as physical stress, body composition, metabolic status and others (Fig.2). For instance, during fasting and certain conditions of physical stress GH secretion is increased, and excess of glucose or lipid intermediates inhibits GH release in healthy man (*16, 29, 30*). After maximal GH secretion at puberty (*31*), adulthood is associated with its gradual decline (*32*). The degree to which this aspect is associated with aging-related changes in body composition and organ function remains controversial.

Besides the tight regulation of GH secretion, the availability of GH is also influenced by its clearance by the kidneys and by internalization through its receptor. A large part of the GH in the blood stream is bound to GH binding protein (GHBP), which corresponds to the extracellular domain of the GH receptor (GHR). GHBP increases the amounts of GH in circulation by protecting GH from its degradation and clearance. Therefore, GHBP may potentiate or inhibit GH physiologic activity.

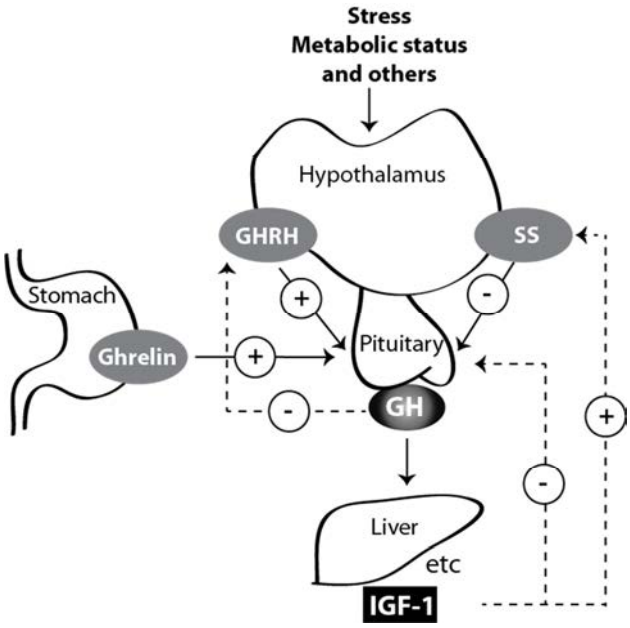

Fig.2: Factors that stimulate and suppress GH secretion under physiological conditions. Several factors influence GH secretion including stress, nutrition, and exercise among others. However, two factors are the main regulators: GH releasing Hormone (GHRH) and somatostatin (SS), which stimulate and inhibit GH secretion, respectively. Ghrelin produced in the stomach also stimulates GH release. GH stimulates the synthesis of insulin-like growth factor 1 (IGF1) by the liver, and other peripheral tissues. Both GH and IGF1 are involved in negative feedback loops. High GH levels inhibit its own secretion by stimulating the release of GHRH. High blood levels of IGF1 lead to decreased secretion of GH by direct suppression in the pituitary and by stimulating the release of SS.

1.3 Physiological roles of GH

1.3.1 Promotion of Growth

The promotion of postnatal growth is a major physiological function of GH. Initially, it was thought that GH indirectly stimulates growth via triggering the production of IGFs, or somatomedins, exclusively in the liver. This was called the "somatomedin hypothesis". This theory was challenged when direct actions of GH on several peripheral tissues were reported (*33*). In fact, liver-specific IGF-

1 gene-deleted mice show normal postnatal growth and development despite the low levels of IGF-1 in circulation. This indicates that direct effects of GH in target tissues (adipose tissue, bone and skeletal muscle) are involved in growth promotion, and probably in stimulation of local IGF-1 production (*34*). The critical importance of GH as the main endocrine mediator of growth is proven either by the dwarf phenotype occurring when the levels of GH are insufficient during early development, or by gigantism, due to hyper-secretion of GH before puberty (*13*). Apart from GH secretion, also defects in GHR and post-receptor signaling may result in phenotypes similar to GH hypo-secretion. Laron and coworkers described for the first time the clinical phenotype of severe growth defect, and for that reason it is named "Laron Syndrome"(*35*). Deletions and mutations in GHR have been described as causative for this phenotype (*36*). These facts described above confirm the important role of the GH system in growth promotion. On the other hand, pituitary adenomas that cause hypersecretion of GH in adulthood result in a clinical condition called acromegaly (*37*). In these patients excess of GH, besides affecting the size of hands, feet, fingers, has important metabolic consequences, suggesting additional functions for GH.

1.3.2 Metabolic regulation

GH holds important roles in metabolic regulation (Fig.3). As soon as human pituitary extracts became available it was shown that injection of large amounts of GH both in healthy subjects and GH-deficient patients stimulated lipolysis and led to hyperglycemia (*38-40*). Indeed, as expected, hyper-insulinemia, impaired glucose tolerance, and overt diabetes mellitus are common features of acromegaly (*41*). GH works as a metabolic switch between carbohydrate and lipid utilization: in conditions of energy surplus GH acts in concert with IGF-1 to promote nitrogen retention, while during starvation GH switches fuel consumption from carbohydrates and protein to lipids. This guarantees the preservation of protein stores and consequently maintains lean body mass (LBM). The direct acute metabolic effects of GH in the basal state are the stimulation of lipolysis and the consequent increase of free fatty acids (FFA) in the blood. Repetitive GH pulses in presence of adequate energy supply and concomitant increased insulin levels induces IGF-1 production (*42, 43*). Consequently, in the long range, protein stores and LBM increases, while body fat mass decreases.

Studies evaluating the acute effects of GH on protein metabolism in the basal state have produced inconsistent conclusions. While some studies indicated that acute GH stimulation leads to increased muscle protein synthesis, others did not detect any effects of GH withdrawal in protein metabolism (*44*). Less controversial are the studies evaluating the effects of GH on protein metabolism in pathological states (acromegaly and GH deficiency) and in stress (exercise and fasting). In fact, stress conditions are the natural domains of GH, in which the body benefits GH effects on substrate metabolism (*44*). During fasting GH is the only anabolic hormone to increase (*45*). GH administration has been shown to be beneficial for protein preservation in conditions of dietary restriction (*46*). Moreover, fasting in GH-deficient subjects resulted in 50% increase in urea-nitrogen excretion and 25% increase in muscle protein breakdown (*47, 48*). Also obesity has been associated with decreased levels of circulating GH, and consequent protein loss (*49*). Treatment of these patients with GH has been successful in preserving the protein stores and LBM (*50*). Although the metabolic functions of GH are well recognized, the underlying mechanisms of these actions are not yet well described.

Under certain conditions (e.g. if cells are deprived of GH for some hours), GH has acute and transient insulin-like effects (*51*). These effects include increased glucose utilization, increased glucose uptake, anti-lipolysis among others. It has been suggested that these effects are mediated by the insulin receptor substrate-1 (IRS-1) and phosphoinositide 3-kinase (PI3-K), which get activated by GH stimulation (*52*).

There is an extensive interest in taking advantage of the anabolic effects of GH for improving athletic performance (*53*). During moderate exercise GH appears to stimulate lipolysis without any effect on protein and glucose metabolism. Prolonged GH administration results in prevalent lipolysis and decreased protein oxidation (*44*). Although administration of supra-physiological doses of GH to athletes exerts potentially beneficial effects on body composition, it remains unclear whether these effects translate to improved performance (*54*). Nevertheless, GH abuse has been widespread among the athletes for more than 20 years, with potentially detrimental consequences (*55*).

1.3.3 Other functions

At the cellular level, GH stimulates differentiation and mitogenesis and prevents apoptosis (*56-58*). There are also reports that GH signaling results in tubulin polymerization (*59*), cell migration and chemotaxis(*60*). These cellular effects are implicated in a variety of biological actions of GH in immune cells. Both GH and its receptor are expressed in various immune cells as T lymphocytes, B lymphocytes, monocytes and neutrophils. GH enhances thymopoiesis and T cell development, modulates cytokine production, enhances B cell development and antibody production, activates neutrophils and monocytes, enhances neutrophil adhesion and monocyte migration, and it has an anti-apoptotic action (*61*). Additionally, GH is involved in the formation and functional activation of mature blood cells (*62*).

GH also plays important roles in fertility and reproduction (*63-67*). Additionally, GH has been described as modulator of stress response and behavior by acting directly on the brain (*68*). Also functions in stimulation of the heart development and regulation of cardiac function have been reported (*69*)

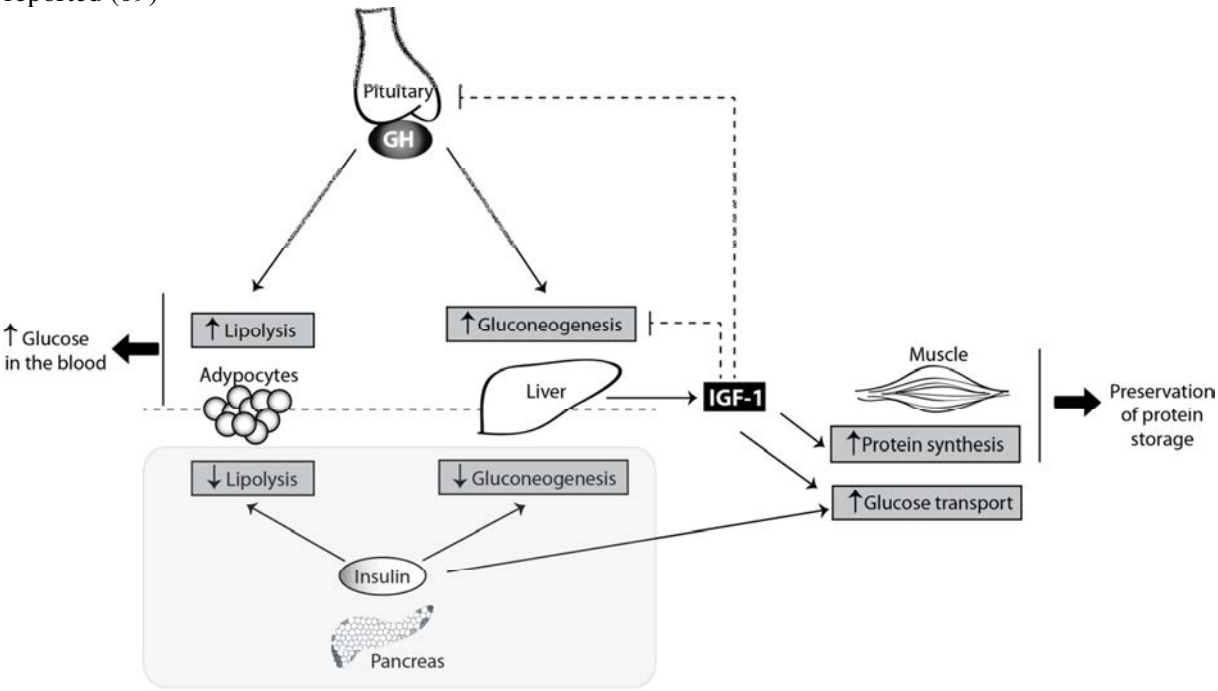

Fig.3: GH metabolic actions. GH has pleiotropic effects on carbohydrate, lipid and protein metabolism. GH antagonizes the effects of insulin, hormone secreted by the pancreas, by two direct ways: inhibiting gluconeogenesis in the liver, and increasing lipolysis in adipocytes. GH also stimulates the production of insulin-like growth factor 1 (IGF1) by the liver. IGF-1 suppresses gluconeogenesis in the liver via the insulin receptor. In the muscle, IGF-1 stimulates directly glucose uptake, and stimulates protein synthesis. IGF1 inhibits GH secretion by the pituitary gland, and therefore indirectly blocks the insulin antagonizing effects of GH, contributing for the glucose homeostasis. The main consequences of GH metabolic actions are the increase of glucose levels in the blood and preservation of protein storages.

1.4 GH antagonism

As referred previously, the pathological actions of excess GH are evident in the acromegaly patients, who have increased mortality and morbidity(*70*). Symptoms of these patients can be alleviated by surgery, radiotherapy, and by treatment with somatostatin (inhibitor of GH secretion), or the very effective GHR antagonist pegvisomant (*1*). While trying to produce a GH analogue with increased activity, GH antagonists were produced instead. Mutations in the amino acids at the positions 117, 119 and 122 were performed in order to correct the third imperfect α-helix of bovine GH. This resulted in a perfect amphiphathic α-helical molecule that bound GH receptor with the same affinity as the wild type but worked as GH receptor antagonist (*71*). Further systematic site-specific mutations revealed that by replacing glycine 120 in the third α-helix by an arginine (G120R), the hGH is converted into an efficient GH antagonist (*72*); pegvisomant contains the G120K mutation that

functions similarly. Additional amino acid changes combined with pegylation have increased the half-life in the circulation and reduced the immunogenicity of the recombinant molecule (*12*). Initially, the mechanism whereby a molecule that binds to its receptor with the same efficiency induces opposite effects was unclear. Recent advances have shed light on the underlying mechanism, which will be discussed later on in this thesis.

Pegvisomant could be also potentially used for treatment of patients with diabetes and microvascular complications, who have increased serum GH concentrations. Since there is a connection between excessive GH signaling and cancer (discussed further), blockade of the GH pathway with pegvisomant might be attractive for cancer therapy (*73*).

1.5 GH and ageing

Knockout mice for GHR ("Laron Dwarf") and mice with mutations causing GH deficiency or resistance ("Ames dwarf", and "Snell dwarf", and "Little") live longer than their genetically normal siblings (*74-76*). This extended longevity is remarkable and reproducible, ranging from 25 % to over 60%. These long-lived mice present many signs and indicators of a healthy delayed ageing process. These results would lead to the conclusion that GH normally released by the pituitary limits life expectancy, probably due to acceleration of the ageing process. This conclusion is supported by reports showing that reduced levels of IGF-1, or mutations interfering with IGF-1 signaling also result in increased mice longevity (*77, 78*). As expected, transgenic mice with elevated levels of GH and IGF-1 live shortly and reflect characteristics of an accelerated ageing process (*79*). Studies analyzing the influence of GH signaling and lifespan in several species have been performed. Although in most of the cases the negative correlation between GH and longevity seems to exist, in humans it is still unclear due to inconsistent reports. For instance, while Besson and co-workers reported that individuals with congenital GH deficiency live shorter (*80*), others reported that GH-deficient/resistant subjects live long with decreased incidence of cancer, atherosclerosis and vascular pathology, in spite of being obese (*81*) (*82*). These conflicting results may be connected to another key factor influencing the ageing process: the insulin sensitivity. In mouse models, GH-deficiency is associated with insulin sensitivity (low levels of circulating insulin), while GH-deficient people are insulin resistant (high levels of circulating insulin). In the mouse models, GH-deficiency allied with insulin sensitivity contributes to low blood glucose level. This biochemical feature has been negatively correlated with oxidative stress (*83*). Since oxidative stress is recognized as one of the major causes of ageing (*84*), GH may influence the ageing process by acting on oxidative stress pathways. Accordingly, Ames dwarf mice produce less metabolic oxidants, and have increased levels of anti-oxidants (*85*). On the other hand, in GH-deficient humans, insulin resistance increases the oxidative damage (*83*), induces accumulation of visceral fat mass (*86*), and increases the risk of several age-related diseases(*87*). Thus, differences in the ageing process between mice and humans suffering from GH-deficiency may be explained by their different insulin sensitivity.

In humans, during ageing the GH/IGF-1 axis is down regulated(*44*). On one hand, this probably contributes to the effects of ageing on body composition, skin characteristics and functional changes that decrease the quality of life. On the other hand, decrease in the amounts of GH with age may offer protection from cancer and other age-related diseases. Therefore, the GH replacement is controversial and as an anti-ageing therapy and involves both benefits and risks (*88*).

1.6 GH and cancer

Epidemiological studies reveal that high IGF-1 levels correlate with increased risk for development of prostate, breast and possibly colorectal cancer (*89*). There is also evidence, although controversial, that patients with acromegaly are at increased risk of colorectal carcinoma (*90*).

Some elegant experiments with rodents reveal an important role of GH in tumor development. Crossing GHR KO mice with mice predisposed to develop carcinomas significantly slowed down tumor progression (*91*). Additionally, GH deficient rats crossed with rats predisposed to prostatic cancer showed significantly reduced tumor incidence and burden (*92*). Interestingly, GH-deficient female rats are resistant to chemical induction of mammary carcinogenesis, whereas GH replacement

restores the risk of tumor development (*93*). Therefore, as concluded from rodent studies, there seems to be a clear connection between GH signaling and development of cancer.

In humans, elevated GHR expression has been found in colorectal, breast tumors and meningiomas (*94*). Moreover, there are many reports suggesting roles for the autocrine GH in oncogenic transformation and metastasis (*95, 96*). It has been shown that increased GH expression in human breast tissue is associated with increased epithelial cell proliferation and that metastatic mammary carcinoma cells have the highest levels of GH expression (*96-98*). Thus, autocrine GH signaling has an oncogenic potential.

2. Growth Hormone Receptor

2.1 Cytokine receptor superfamily

GHR is a single membrane spanning protein of 620 amino acids, isolated for the first time from rabbit liver (*99*). This was followed by cloning of the receptor from several species, which revealed a strong sequence homology (*100*). The human *GHR* is composed by 9 exons (*101*) encoding a cleavable amino acid signal peptide of 18 (exon 2), an extracellular domain of 246 (exon 3 to 7), a transmembrane domain of 24 (exon 8), and an intracellular domain of 350 residues (exon 9 and 10).

GHR belongs to the class 1 superfamily of cytokine receptors, which includes, erythropoietin (EPO), prolactin (PRL), granulocyte colony stimulating factor (G-CSF), interleukins (IL) 2-7, 9, 11-13, and 15, leukaemia inhibitory factor (LIF), ciliary neurotrophic factor (CNTF), oncostatin M (OSM) and leptin receptors (*100*). The GHR was the first member of the family to be characterized (*102*). Other receptors, such as the IL-10 receptor, or interferon (IFN)-α and –γ receptors are more distantly related and belong to the class 2 cytokine receptors superfamily (*100*).

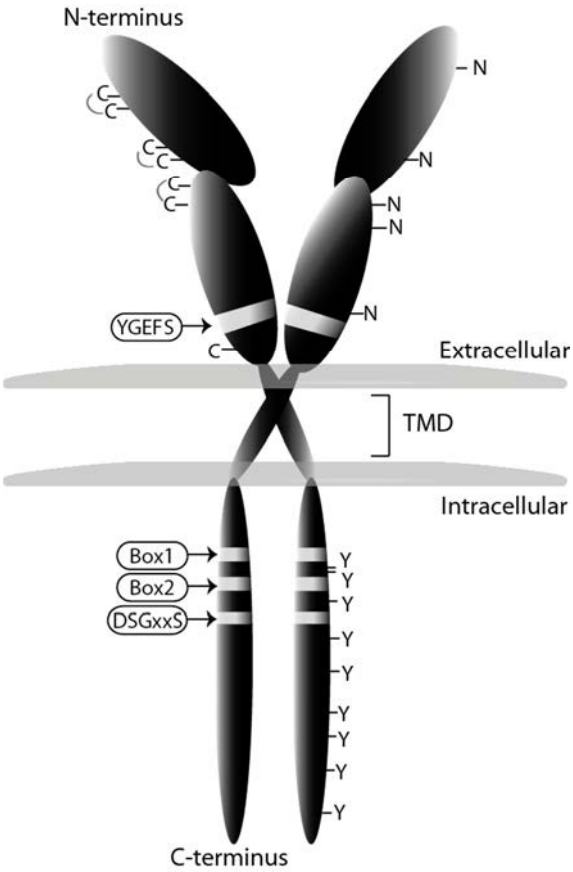

Fig. 4: Schematic representation of the GHR. GHR consists of an extracellular domain of 246 amino acids, a transmembrane domain (TMD) of 24 residues, and a cytoplasmic region of 320 amino acids. The extracellular domain contains 5 potential glycosylation sites (N), and seven cysteine residues, from which 6 form disulfide bonds. The YGEFS domain is located at the C-terminal part of the extracellular domain. The intracellular domain contains 9 tyrosine residues that can get phosphorylated upon receptor activation by GH. The Box-1 is responsible for JAK2 binding, and Box-2 for GHR internalization and degradation.

The class 1 cytokine receptors share many features. In the extracellular domain they contain conserved cysteine residues and a WSxWS (W, tryptophan, S, serine, x, any aminoacid) motif (*103*).

In the case of GHR, this motif is different, although homologous, YGEFS (Y, tyrosine; G, glycine; E, glutamic acid; F, phenylalanine; S, serine). This motif has been shown to be essential for GH binding (*104*). Despite the limited amino acid homology, the structures of GHR, EPOR and PRLR are similar, consisting on two fibronectin (FBN) type 3 domains (β-sandwich composed of seven β strands). In GHR the N-terminal domain is composed of amino acids 1-123 and the C-terminal composed of amino acids 128-328, separated by a four-amino acid hinge region (*105*). The GHR extracellular domain contains 3disulfide bridges, formed by 6 of its 7 cysteine residues (Fig. 4) (*106*). In the intracellular domain of this family there are two conserved membrane-proximal conserved sequences, referred to as box 1 and box 2, with functions in JAK2 binding and GHR endocytosis, respectively. These aspects will be discussed later in this chapter. Additionally, a conserved DSGxxS degradation motif is also present downstream of box-2, its function being revealed in this thesis.

2.2 GHR life cycle

While being translated on ribosomes, GHR is inserted in the endoplasmic reticulum (ER) membrane due the presence of the signal peptide. In the ER, the disulfide bounds are formed and GHR dimerizes (*107*). GHR is glycosylated with high mannose oligosaccharides important for the process of quality control in the ER. This GHR form is named precursor, and can be detected on western blotting as a double band running at 110 kDa. When correctly folded, GHR continues its route in to the Golgi apparatus. In the Golgi, the high mannose oligosaccharides of GHR are processed into complex oligosaccharides. This GHR form runs at 130 kDa in gels in the presence of sodium

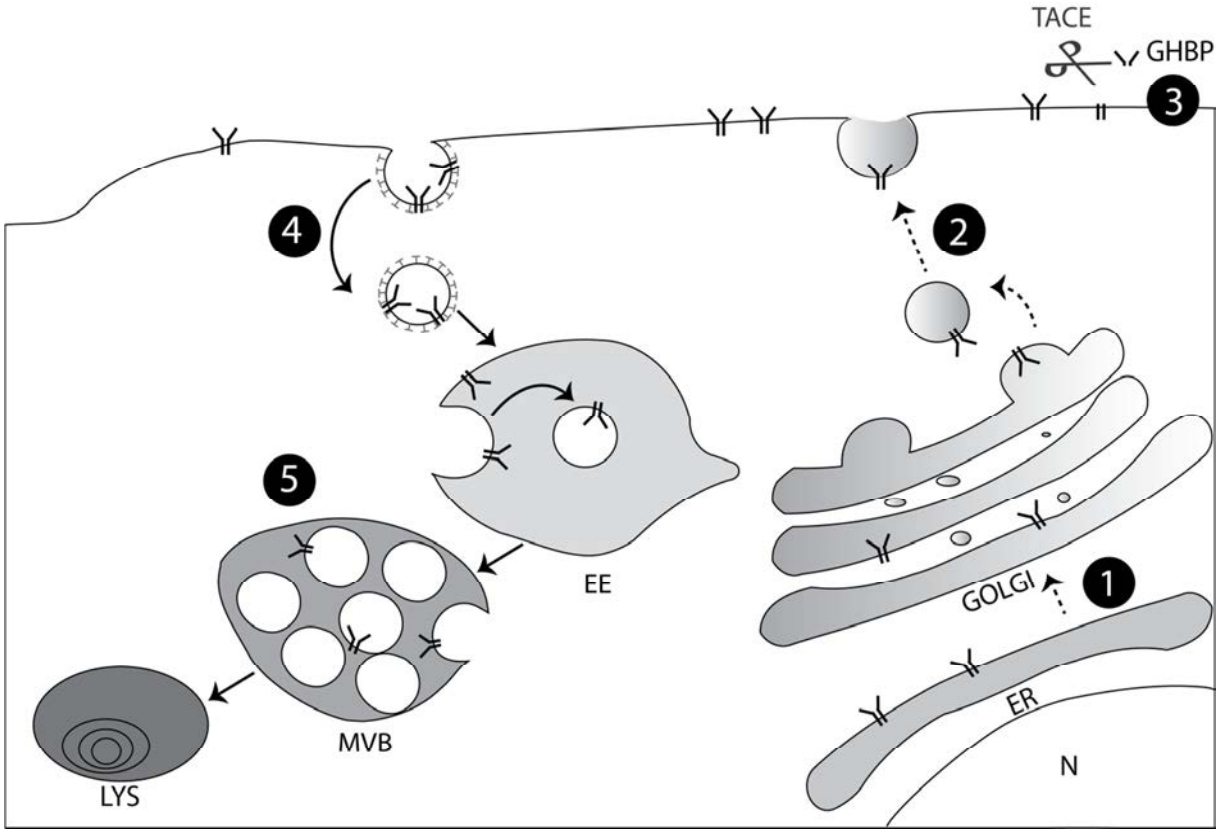

Fig.5: Life cycle of the GHR. The biosynthetic route is indicated with dashed arrows and the endocytic pathway with continuous arrows**.** GHR is synthesized in the endoplasmic-reticulum (ER) where it undergoes dimerization. The GHR dimer is sorted in the Golgi complex (1) and after transported to the plasma membrane (2). In the plasma membrane, GH can bind to GHRs and initiate signaling. Alternatively, GHRs are shedded into the blood by the action of TACE, with the generation of GHBP (3), or endocytosed via clathrin-coated pits into the cells (4). The endocytosed GHRs are then transported through the MVBs to the lysosome (LYS) for degradation (5).

dodecylsulphate (SDS). After this step, the GHRs traffic to the cell surface. GHR is constitutively endocytosed independently of GH presence (*108, 109*). When GH binds to GHRs at the cell surface, signaling cascades are triggered, followed by rapid endocytosis of the GHR (*110*), GHR is sorted into the multivesicular bodies (MVB), and eventually degraded in the lysosome (*111*).

Additionally, when the receptors are at the cell surface they can be cleaved by the metalloprotease tumor necrosis factor-α-converting enzyme (TACE), a process called shedding (*112, 113*). The cleaved extracellular domain circulates in the blood and is referred to as growth hormone binding protein (GHBP); the intracellular part is endocytosed and degraded. GHBP levels in the blood have been used as an indication of the amounts of GHR in the cells (*114*). When GH is bound to full length GHR, shedding is inhibited (*108, 115*). In the bloodstream, GHBP binding to the GH increases its half-life by decreasing its clearance (*116*). On the other hand, GHBP may antagonize GH actions by competing for its binding with GHR at the cell surface (*116*). Another function of the shedding process is downregulation of the responsiveness of the cells to GH. The availability for GH at the cells surface is determined by GHR endocytosis rate (75%), the rate of shedding (10%), and other (unknown) mechanisms (15%)(*117*).

3. GHR activation and signaling

3.1 Receptor activation mechanism

The class 1 cytokine receptors do not have intrinsic kinase activity (*118*). This role is mediated by JAK2 kinases that associate with the box-1 sequence in GHR (*119*), eight amino acid residues long, rich in proline (ILPPVPVP in GHR).

The first step in GH action is its binding to the GHR. The crystal structure of the extracellular domain of GHR bound to GH revealed that one GH molecule binds with two asymmetric binding sites two molecules of GHR (*105*) (Fig. 6). For a long time it was thought that GH binding to one GHR monomer at the plasma membrane recruits the second monomer of GHR to its second binding site.

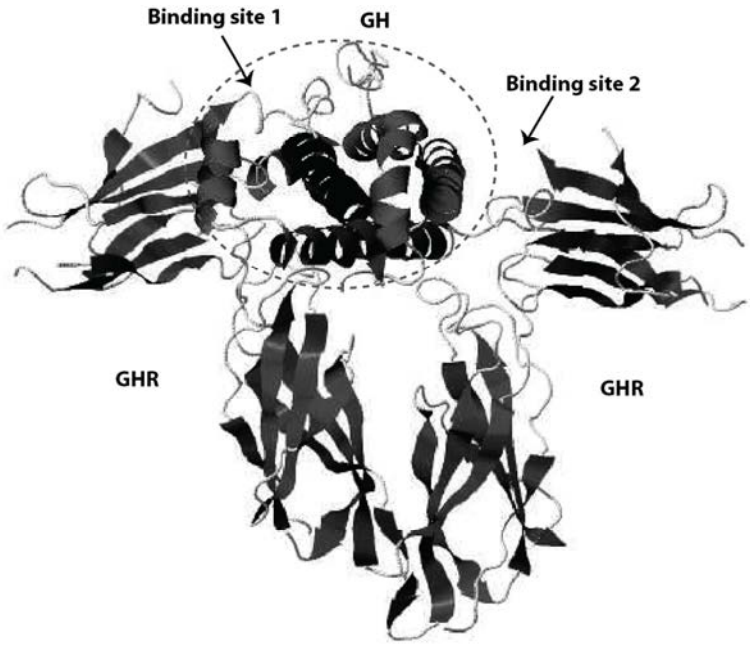

Fig.6: Crystal of GH-GHR dimer complex. A representation of the crystal structure of the extracellular domain of two GHR molecules binding to one GH molecule, determined by de Vos et al. 1992 is depicted (*105*); protein data base code: 3HHR. The extracellular domain of GHR is divided in two subdomains, each consisting on seven β-Strands arranged as one antiparallel β-sheet. The two subdomains are connected by a hinge region. The two binding sites of GH are indicated.

JAK2 activation was proposed to occur due to GHR dimerization itself. However, subsequent studies disproved this model. Studies by Gent and collaborators showed that GHR dimerizes in the ER, independently of GH, and travels to the cell surface as a pre-formed dimer (*107*). Subsequently, work by the group of Waters suggested that a change in conformation, induced by GH, rather than GHR dimerization, is responsible for GHR activation. In this study, the comparison of the crystal structure of the extracellular domain of GHR alone and the previous structure of GH-bound GHR revealed differences in conformation (*120*). Based on this knowledge, the current model for GHR activation proposes that GH binding to the GHR dimer causes a change in conformation in the extracellular binding domain which triggers the rotation of one monomer in relation to the other. This rotation brings the JAK2 molecules in close contact, which allows the catalytic activation of their kinase domains.

3.2 JAK2 activation

JAK2 is composed by four major domains: an N-terminal FERM (4.1 protein, ezrin, radixin, and moesin) domain, followed by a SH2 (Src homology 2) domain, pseudokinase and kinase domains. The binding to the box-1 of GHR occurs through the FERM domain (*121*). Normally JAK2 is held in an inactive conformation, where the kinase and pseudokinase domain interact with each other (*122*). The activation of JAK2 requires that two catalytic domains are brought in close proximity. This was concluded after realizing that often in human leukemia there is oligomerization of JAK2 molecules which renders them constitutively active; this aggregation is due to the occurrence of a genetic fusion between the JAK2 catalytic domain and the oncogenic transcription factor TEL (*123*). Analysis of other mutation also contributed to the understanding of JAK2 physiology. The mutation V617A, which turns JAK2 into a constitutively active state, is found in patients with myeloproliferative disorders (*124*). This mutation probably disrupts the inhibitory interaction between the pseudokinase and kinase domain (*125*). Following mutational analysis, the SH2-pseudokinase domain linker turned out to be important for JAK2 activation (*126*). JAK2 activation results in the phosphorylation of multiple tyrosines. Several of these tyrosines have been identified as important in the regulation of JAK2 function. For example, phosphorylation at tyrosine 1007 is thought to expose the substrate and/or ATP binding sites (*127*), and phosphorylation of tyrosine 119 is thought to promote JAK2 dissociation from its receptor (*128*). Phosphorylation of tyrosine 813 appears to enhance JAK2 activity (*129*), whereas phosphorylation of tyrosine 221 decreases it (*130*). The importance of many of the JAK2 tyrosines is related to their roles in recruiting ancillary molecules needed for signaling propagation or signal termination.

3.3 Signaling pathways of GH

The main pathways activated by GH are: the signal transducer and activator of transcription (STAT) pathway, the mitogen-activated protein kinase (MAPK) pathway, and the phosphoinositide-3 kinase (PI3K) pathway (Fig. 7). The extent by which each pathway is activated depends on the cell types, related to differences in relative expression levels of the components of each pathway.

For a long time JAK2 has been regarded as the only kinase activated directly via the GHR. However, recent data, indicating that not all the GH signaling events rely on JAK2, brought controversy to the field. In particular, the activation of Src Family kinases (SFK) can occur independently of JAK2. First evidence came from a study by Zhu et al, who showed this by using pharmacological inhibitors and kinase inactive proteins (*131*). Additional evidence came from Rowlison and co-workers, who reported that interfering with the GH-induced GHR conformational change affects JAK2 and Lyn activation differently (*132*). Activation of STAT5 by GH seems to require only JAK2, while activation of the small GTPases RalA, RalB, Rap1 and Rap2 by GH requires both c-Src and JAK2 (*131*). SFK activation by GH was shown to activate MAPKs, also referred to as extracellular signal-regulated kinase 1 and 2 (ERK1 and ERK2), through the phospholipase Cγ-Ras pathway (*132*). Barclay and co-workers showed that targeted mutation in the box-1 of GHR in mice although abrogating JAK2 activation did not decrease the hepatic activation of MAPK via Src (*133*).

3.1.1 The STAT pathway

STATs are latent transcription factors that upon activation by certain hormones or cytokines undergo tyrosine phosphorylation in the cytoplasm, dimerize via phosphotyrosine-SH2 interactions, and translocate into the nucleus where they activate transcription of specific genes (*134*). In mammals seven members of STAT have been identified with molecular weights ranging from 95 to 111 kDa (*135*). GH stimulation creates STATs binding sites in the GHR-JAK2 complex. The activation of STAT5a and STAT5b is critical for many of the GH biological functions, including metabolic changes, body growth and sex-dependent liver gene regulation (*136, 137*). STATs 1 and 3 have also been shown to become activated in response to GH (*136*), but their importance is still unclear. STAT5b binds to the promoter elements of the IGF-1 gene, regulating its transcription in a GH-dependent manner (*138*). A mutation in STAT5b, affecting its GH-induced tyrosine phosphorylation, caused severe growth retardation and immunodeficiency in one patient (*139*). This reiterates the importance of this STAT5 for IGF-1 expression. STAT5a and STAT5b, but not STAT3, require an intact and tyrosine phosphorylated GHR cytoplasmic tail for full activation (*140*). The key GHR tyrosines necessary for this event were identified (*141, 142*).

3.1.2 The MAPK pathway

The Ras/MAPK, or ERK/MAPK has also been shown to be activated by GH. GHR phosphorylation creates docking sites for Src homology 2 domain-containing transforming protein C (Shc) (*143*). Shc gets then phosphorylated by JAK2, and binds growth factor receptor-bound protein 2 (Grb2) which binds Son of Sevenless (SOS), a guanine nucleotide exchange protein. Subsequently, Ras, Raf, mitogen-activated protein kinase/extracellular-regulated protein kinase (MEK), and ultimately MAPKs are sequentially activated (*144*). Phosphorylated MAPKs translocates to the nucleus where it transactivates transcription factors, and changes gene expression to promote growth differentiation or mitosis. Data suggest that GH-dependent activation of the Ras/MEK/MAPK pathway contribute to GH-stimulated c-fos expression through serum response element (SRE). It remains controversial whether and how MAPK activation affects GH-induced proliferation and anti-apoptosis (*145*). As explained above, the activation of MAPKs may occur in a Src-dependent, JAK2 independent way. As STATs are also serine phosphorylated for full activity (*146*), it was suggested that this is mediated by MAPK pathway (*147*).

Some evidence suggests that GH signaling via MAPK pathway may engage in cross-talk with signaling pathways induced by other stimuli. Yamauchi and co-workers propose an interesting mechanism by which GH activates MAPK through stimulating the phosphorylation of a Gbr2 binding site in the epidermal growth factor (EGF) receptor (*148*). Additionally, studies by Kim at co-workers show that GH stimulation alters the phosphorylation status of ErbB-2, a tyrosine kinase growth factor receptor member of the EGF receptor family, in a MAPK dependent manner (*149*).

GH has also been described to activate other members of MAPK pathway, namely p38 MAP kinase and c-Jun amino-terminal kinase (JNK) (*150, 151*).

3.1.3 The PI3K pathway

GH has also been shown to stimulate the PI-3K pathway, probably through tyrosyl phosphorylation of the large adaptor proteins, the insulin receptor substrates (IRS). GH stimulates the phosphorylation of IRS-1, -2 and -3 by JAK2, which leads to their association with multiple signaling molecules including the p85 subunit of PI-3 kinase (*143, 152*). This pathway is shared by the insulin signaling, which may justify the insulin-like effects of acute GH stimulation under certain conditions, as discussed above. Particularly, activation of PI3-K mediates the GH-induced increase in glucose transport, via induction of translocation of the glucose transporter 4 (GLUT4) to the cell surface (*153*), and has been suggested to mediate the ability of GH to stimulate lipid synthesis (*51, 154*). Additionally, PI-3 kinase activation results in AKT activation, which has been implicated in GH-promotion of cell survival. Activation of AKT depends on JAK2 binding to box-1 in the GHR (*155*). Another kinase, p70S6K, involved in the control of cell proliferation and differentiation was shown to be activated by GH through PI-3 kinase and protein kinase C (PKC) (*156*). The NFκB pathway has also been shown to be activated by PI3-K and downstream AKT after GH stimulation (*58*).

3.4 GH desensitization

Termination of the GHR signaling is an important mechanism for controlling GH actions. As mentioned above, prolonged GH signaling may be associated with cancer. Therefore, the GH signaling is precisely regulated at multiple levels.

The suppressor of cytokine signaling (SOCS) family of proteins assumes a very important role in the GH-signal termination by mechanisms described below. This family is composed of eight members, and the expression of four of them is stimulated by GH, namely SOCS-1, -2, -3 and CIS (cytokine inducible SH2-constaining protein) (*157*). Structurally, SOCS proteins contain a central SH2 domain and a motif called SOCS box at their C-termini (*157*). The SOCS box mediates the formation of multi-subunit ubiquitin ligases, containing elongin BC, cullin 2 or 5 and the RING finger proteins Rbx1 or Rbx2 (*158*). SOCS-1 and SOCS-3 contain an additional kinase inhibitory region at their N-termini (KIR). Different SOCS apply different mechanisms for GH signaling downregulation. SOCS-1 is thought to bind Y1007 on JAK2 activation loop, and by doing so, to inhibit JAK2 activity through KIR (*159*). SOCS-3, besides binding to the same residue in JAK2 (*160*), also binds to phosphorylated tyrosines in GHR. Also SOCS-2 and CIS have been shown to bind to phosphorylated GHR, which was suggested to interfere with STAT5-GHR binding (*161*). SOCS-1, and possibly SOCS-2 and SOCS-3 use their ubiquitination activity to mediate JAK2 degradation and, therefore, signal termination (*157, 162*). A role of CIS as a stimulator of GHR internalization and proteasomal degradation has been proposed (*163*). Interestingly, there is evidence that some stimuli that reduce GH sensitivity, such as estrogen or sepsis, do so by increasing expression of certain SOCS proteins (*164, 165*). The physiological importance of SOCS in GH signaling regulation is unclear since $SOCS1^{-/-}$, $CIS^{-/-}$ and liver specific $SOCS\text{-}3^{-/-}$ are not bigger than normal (*166-168*). However, it cannot be excluded that these proteins have redundant functions.

Protein tyrosine phosphatases (PTPs) are also employed by the cells for negative regulation of GH signaling, namely SH2 domain-containing protein-tyrosine phosphatase (SHP-1), SHP-2, protein-tyrosine phosphatase (PTP)-H1, PTP1, TC-PTP and PT1b (*157*). Mice, deficient on SHP-1, have prolonged JAK-2 phosphorylation and STAT5 activity, which represents strong evidence for an important role of this kinase in the deactivation of GH signalling (*169*). There are conflicting reports concerning the physiologic importance of SHP-2 in GHR: while Frank et al. concluded that SHP-2 is a positive regulator (*170*), Stofega et al proposed SHP-2 as an inhibitor of GH signaling (*171*). GH stimulation has been shown to trigger the phosphorylation of JAK2-associated SIRP-α, signal regulatory protein alpha. This was suggested to promote SHP-2 recruitment and consequent attenuation of GH signaling (*172*). A study by Pasquali has identified PTP-H1, PTP1, PTP1b, and TC-PTP as specific interactors of phosphorylated GHR (*173*). PTP1b knockout mice display increased JAK2 and STAT5 phosphorylation, while PTP-H1 knockout mice display enhanced growth (*57, 174*). CD45 was shown to be a JAK2 phosphatase, being able to suppress its activity and regulate cytokine receptor signaling (*175*).

Other regulators are PIAS, "protein inhibitors of the activated STATs", which display SUMO ligase activity. PIAS can bind STAT proteins, and prevent their association to the DNA. Although the majority of the PIAS interactor proteins are prone to modification by SUMO, the exact mechanism by which PIAS influences STAT5 function is still unclear (*176*). Some studies have also implicated the adaptor protein Grb10 as regulator of GH signaling. Grb10 interacts with GHR upon GH stimulation, and downregulates GH signaling pathways downstream of JAK2 and independently of STAT5 (*177*). Work of Carter-Su and colleagues found that SH2B-β association with JAK2 enhances its activity (*178*). Thus, decrease in SH2B-β levels could contribute for GH-signaling termination.

Other cellular factors modulate GH sensitivity. The most important are insulin, thyroid and sex hormones, as well as inflammatory cytokines (*179, 180*).

The cells employ other mechanisms, besides direct interference with the signaling molecules, to terminate GH action. Manipulation of GHR levels at the cell surface is a very important mechanism not only to modulate the GH responsiveness of cells, but also to terminate GH signaling. As described in a previous section of this chapter, the extracellular domain of GHR can be cleaved in a process called shedding. One of the consequences of this process is the reduction of the number of signaling competent receptors at the cell surface, and consequent regulation of the cell sensitivity to GH (*145*). Since GH binding to GHR inhibits its shedding, this mechanism cannot be regarded as signal

terminator (*115, 181*). On the other hand, GHR is endocytosed both in the presence and absence of ligand. Therefore, besides regulating the responsiveness of the cells to GH, endocytosis of GHR provides a very efficient way for GH signaling attenuation. The next section in this chapter will be dedicated to the advances made in understanding GHR endocytosis.

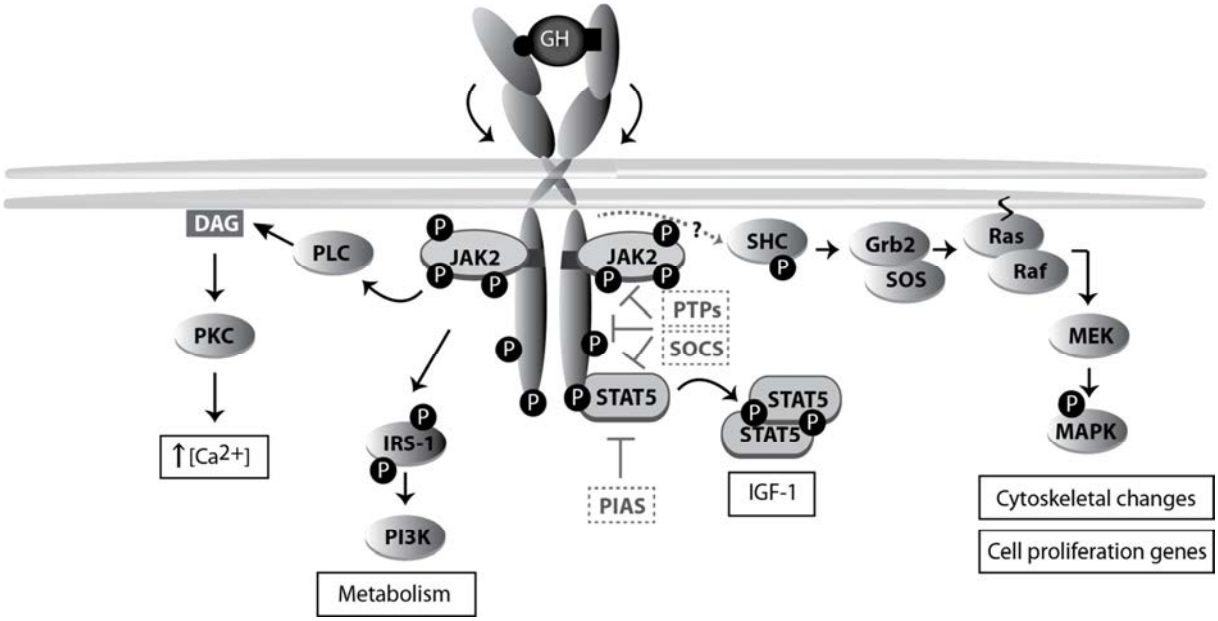

Fig.7: GHR activation and signaling. The binding of the two asymmetric binding sites of one GH molecule to the GHR dimer causes its rotation and subsequent activation of downstream signaling pathways, and ultimately specific gene transcription. The activation of different signaling pathways accounts for the multitude of GH functions. In the scheme also molecules involved in signal termination (PTPs, SOCS and PIAS) are indicated.

4. The ubiquitin system in receptor trafficking

Ubiquitin is a small molecule of 76 amino acids which C-terminus is attached to proteins upon sequential action of three enzymes: an ubiquitin activating enzyme (E1), an ubiquitin conjugating enzyme (E2), and an ubiquitin protein ligase (E3). Ubiquitin may be added as a single monomer or multiple monomers, or as a polyubiquitin chain. The addition of ubiquitin to target proteins covers a great variety of functions (see details in box 1) (Fig.8).

Endocytosis is the main way used by the cells to achieve the homeostatic regulation of plasma membrane protein abundance. Once a protein is endocytosed it is either recycled back to the cell surface or captured in the intraluminal vesicles of the MVBs, and eventually guided to lysosomes for degradation (*182*).

Ubiquitination has emerged as a central mechanism governing the subcellular trafficking of proteins. It is critically important for the regulation of the number of receptors and transporters at the plasma membrane. The first evidence for a role of ubiquitin in the membrane trafficking came from the work of Kolling and collaborators with the ABC-transporter Step6 (*183*). In mammalian cells, the first receptor reported to depend on the ubiquitination system for its endocytosis and degradation was GHR (*184*). From then on, many more receptors were shown to depend on the ubiquitin system to be endocytosed, often in response to ligand binding.

Ubiquitination works as an engagement tool of the proteins with the endosomal sorting complexes required for transport (ESCRTs) (*185*). In fact, ubiquitination has been reported at several points along the endocytic pathway. Although monoubiquitination has been regarded as a sufficient signal for sorting, K63 linked polyubiquitin chain are now considered as the primary sorting factor. Studies with the GAP-1 permease indicated that monoubiquitination is sufficient for initial internalization, but

further sorting in the endosomes requires K63-linked polyubiquitin (*186*). Also studies of the mammalian TrkA and MHC class 1 proteins showed the importance of this type of chains in their MVB sorting (*187, 188*). Within the endocytic system, ubiquitin acts as an interaction module that is recognized by a variety of ubiquitin binding domains (UBDs), including UIM, CUE, NZF, and certain VHS and SH3 domains present in several proteins (*189*).

After endocytosis, the next step in the sorting route is the selection by the ESCRT-0 complex, which acts at a branch point in endosomal traffic to bind a certain cargo and commit it to the lysosomal pathway; in the absence of any interaction, the cargo will be recycled instead of guided for degradation. ESCRT-0 is composed of HRS and STAM, both of which bearing UIM (ubiquitin interacting motif) and VHS (Vps27, HRS and STAM) domains, important for ubiquitin binding and cargo recognition (*190*). Additionally, ESCRT-0 is able to bind clathrin, and the downstream ESCRT-1 (*191*).

Other important components to consider in the endocytic regulation are the deubiquitinating enzymes (DUBs), which are specific proteinases able to remove ubiquitin moieties from proteins. Besides the catalytic domain, DUBs also contain domains that allow them to associate with scaffolding proteins and adaptors. The ESCRT machinery associates with at least two DUBs: AMSH and USP8 (UBPY). In yeast, Doa4 has been identified as an additional DUB, important for receptor recycling. Deubiquitination of endocytosed receptors before or after delivery into the MVBs may profoundly affect receptor trafficking, and ultimately substrate turnover rate (*192*).

It remains unclear how the ubiquitinated cargo is handed from one sorting step to the other. Models have been put forward based on a gradient of sorting proteins containing ubiquitin binding domains of increasing binding affinities. More complexity can be added to this model if we consider ubiquitin ligases and DUBs along the sorting pathway, which could perform additional chain editing (*182*). I will describe three examples of well-studied cargo to illustrate the importance of the ubiquitination system in trafficking.

4.1 Some examples

Carboxypeptidase S (Cps1), a vacuolar hydrolase in the budding yeast Saccharomyces cerevisiae, is a classical example of biosynthetic cargo which sorting is mediated by ubiquitin. Cps1 was the first cargo shown to depend on ubiquitin for entry in the MVBs (*193*). Cps1 is a type 2 integral membrane protein synthesized as a precursor form, pCps1. Cps1 cleavage in the vacuole (lysosome equivalent in yeast), is necessary for its proteolytic activation (*194*). pCps1 is ubiquitinated by Rsp5 already after exiting the Golgi, followed by sorting to the vacuole (*195*). Initially, it was thought the sorting of Cps1 was mediated by monoubiquitination but recent evidences pointed to a potential role of K63-linked chains (*186*). The DUB, Doa4, has been suggested to act on Cps1 (*196*).

The epithelial Na^+ channels, ENaC, are hetero-tetrameric channels with high selectivity for Na^+ over K^+. They are expressed in epithelial tissues such as sweat and salivary glands, nephrons and airway epithelia, where they display a polarized distribution to the apical membranes. After synthesis, ENaC channels are transported from the Golgi to the apical plasma membrane via the trans-Golgi-network (TGN)(*197*). Once in the plasma membrane, the endocytosis of the receptors contributes to their inactivation. After ubiquitination by the E3 ligase Nedd4-2, ENaC is endocytosed in a clathrin-dependent manner involving the ubiquitin-binding endocytosis adaptor epsin (*198*). It is unclear whether ENaC is modified with polyubiquitin chains, or with multiple ubiquitin monomers. The ubiquitinated ENaC is selected by the Hrs subunit of the ESCRT-0 into the ESCRT pathway and eventually lysosomally degradation (*199*). While being ubiquitinated, ENaC is committed to lysosomal degradation, but the DUBs, UCH-L3 and USP-2, are able to reverse this, promoting ENaC recycling, back to the apical plasma membrane (*200, 201*). Mutations in the ENaC, inhibiting Nedd4-2 binding, have been reported in patients suffering from Liddle syndrome, an autosomal dominant salt-sensitive hypertension syndrome. The phenotype of the syndrome is due to prolonged residence time of ENaC at the plasma membrane (*197*).

The epidermal growth factor (EGF) receptors (EFGR) have been intensively studied since their overexpression or gain function mutations are frequently associated with cancer. The EFGRs are expressed in several cell types and upon activation they mediate responses as proliferation, growth, survival and migration (*202*). From the eight described ligands, EGFα and transforming growth factor α (TGFα) are the best characterized. When they bind to the monomeric EGFR at the cell surface, they release the receptor from an autoinhibited state, and subsequently trigger their dimerization (*203*). This brings the two cytoplasmic tyrosine kinase domains together, which phosphorylate each other, and create docking sites for signaling mediators: PI3-K, the SH2- and SH3-dmain-containing adaptor Grb2, STAT3, and phospholipase Cγ (*204*). Additionally, the E3 ligase, c-Cbl, is rapidly recruited, which mediates the ubiquitination of EGFR involved in its endocytosis and trafficking to early endosomes (*205*). c-Cbl belongs to a subfamily of RING-domain-containing E3 ubiquitin ligases. Binding of c-Cbl to EGFR may occur directly on the phosphorylated tyrosine 1086, but also indirectly through the adaptor Grb2 (*206*). The E2 ubiquitin conjugating enzymes, Ube2D1-4, are involved. Six major ubiquitination sites have been identified, which are located within the kinase domain. Most of the ubiquitin chains, found in the EGFR, are in the form of Lys63-linked chains, but also multi-monoubiquitination occurs.

The endocytosis of EGFR can occur via several alternative ways, the most predominant of which is via clathrin-coated pits; there is evidence that the the internalization pathway depends on the extent of the ubiquitination. At low doses of EGF, the receptor is not ubiquitinated and is endocytosed through clathrin-dependent endocytosis, whereas at high doses of EGF the ubiquitination of the receptor results in its clathrin–independent endocytosis of EGFR (*207*). Four different mechanisms contribute to EGFR endocytosis through the clathrin-coated pits: ubiquitination of the tyrosine kinase domain, interaction with the clathrin adaptor AP-2, acetylation of three C-terminal lysine residues outside the tyrosine kinase domain, and interaction with the adaptor Grb2. Interestingly, when all major ubiquitination sites are mutated, EGFR still internalizes with similar efficiency as wild type, in a Cbl-dependent manner. This argues for an additional role of c-Cbl in EGFR endocytosis other than mediating EGFR ubiquitination. epsin and EPS15, ubiquitin-binding endocytosis adaptors are involved in EGFR internalization, confirming the importance of ubiquitination in EGFR endocytosis.

There is evidence that different ligands may trigger different EGFR trafficking pathways, probably related to different binding affinities to the receptor. EGF's strong binding to EGFR results in its sustained activation, ubiquitination and eventual degradation in the lysosomes; TGFα's weaker binding results in its fast dissociation, decreased ubiquitination and recycling instead of lysosomal sorting. These results support a scenario where EGFR is subjected to cycles of ubiquitination and deubiquitation, where the ubiquitination status dictates whether EGFR is degraded or recycled. In fact, the DUBs AMSH and USP8/UBPY have been implicated in the deubiquitination of the EFGR at an early stage, counteracting the entry of the receptor into the ESCRT pathway. While AMSH has specificity for Lys63-linked polyubiquitin chains, USP8 does not seem to have a preference.

4.2 Role of ubiquitin system in GHR endocytosis

The endocytosis and degradation of GHR depends on the ubiquitin conjugation system, as shown for the first time in a Chinese hamster lung cell line (ts20) with a temperature-sensitive mutation in the E1 enzyme. Whereas at the permissive temperature the endocytosis of GHR occurred normally, when the cells were put at non-permissive temperature the GHRs accumulate at the cell surface (*184*). Further evaluation revealed that GHR ubiquitination and clathrin dependent-GHR endocytosis are coupled events (*110, 208*). An important achievement in the mechanistic understanding of GHR endocytosis was the discovery of the "Ubiquitin-dependent endocytosis motif", which consists in the amino acid sequence DSWVEFIELD (*209*). If this motif is mutated the ubiquitination and endocytosis of GHR are strongly inhibited. Besides this motif, there is a di-leucine motif at the position 347-348. This motif mediates fast ubiquitin-independent, clathrin-dependent GHR endocytosis only if the receptor is truncated at position 349, probably due to its complete exposure in this case. The functionality of the di-leucine motif in the context of full length receptor is not apparent (*210*). Surprisingly, a GHR truncation (at amino acid 399), where all its lysines were mutated to arginines, although not being ubiquitinated, was normally endocytosed in an ubiquitin-system dependent

manner. This indicates that the ubiquitination of GHR itself is neither needed for its endocytosis nor for its degradation (*209*). Studies trying to discover which factor needs to be ubiquitinated before GHR is endocytosed have not been successful so far.

We recently found one reason that justifies the importance of the UbE motif in GHR endocytosis: it is a binding site for the $SCF^{\beta TrCP}$ E3 ligase (*211*). The role of the UbE motif and βTrCP has been also extended to sorting at the MVB and degradation at the lysosomes (*212*).

Recently another component was identified as an important regulator of GHR endocytosis: JAK2. Besides its role in signaling, merely binding of JAK2 to GHR is inhibitory for its endocytosis. The model is that GHR can only be endocytosed if JAK2 has detached from it, which was proposed to occur after GH stimulation. It is possible that JAK2 binding/dissociation cycles have direct effects in the ubiquitination events mediated by $SCF^{\beta TrCP}$, and thereby affect rate of GHR endocytosis (*213*).

Box-1: The Ubiquitin Proteasome System

Protein ubiquitination is the final result of an enzymatic cascade, in which each step involves a different enzyme class. In the first step, the E1 activating enzyme forms a high-energy thioester bound with the carboxy-terminus of ubiquitin which results in ubiquitin activation. Ubiquitin is then passed to the E2 conjugating enzyme through a transthiolation reaction. The ubiquitin-loaded E2 interacts then with the E3 ubiquitin ligase that will specifically recognize the substrate to which the ubiquitin will be attached. This final step occurs between the C-terminal glycine carboxyl group of ubiquitin and a free ε-amino group of a lysine in the target. In some cases, only a single ubiquitin is attached, resulting in monubiquitination; if a single ubiquitin is attached multiple times it results in multi-monoubiquitination. More often, poly-ubiquitination occurs, where multiple ubiquitin moieties are sequentially attached to one or more lysines of the previous ubiquitin molecule. Depending on the ubiquitin lysines chosen, different type of chains are formed, which have different physiologic roles. When the substrates are modified with chains formed via Lys-11 or Lys-48, they will be most likely degraded by the 26S proteasome, a 2.5 MDa proteolytic complex that hydrolyses the substrate and releases the intact ubiquitin moieties for reuse. Alternatively attachment of mono-ubiquitin or Lys63-linked polyubiquitin chain marks the substrates for internalization and sorting. Additionally, it was recently discovered that linear ubiquitin chain are important in NFκB activation. These chains are formed by LUBAC ("linear ubiquitin chain-assembly complex"), by conjugating ubiquitin moieties head-to-tail (*214, 215*). K63–linked chains are also involved in DNA repair and in a plethora of cellular signaling events.

Ubiquitination is reversed by deubiquitination, catalyzed by deubiquitinating enzymes (DUBs), proteases that cleave just the isopeptide bond and leave the substrate intact. The E3s bring specificity to the system: they recognize the substrates to be ubiquitinated and position them for optimal transfer of the ubiquitin moiety from the associated E2. Therefore, while there is only one E1 (UBA) (and UBA6 was also described to activate ubiquitin), there are approximately 35 active E2 enzymes identified to date, and a much larger collection of E3s exists. For example, comprehensive genome analysis of *Arabidopsis Thaliana* identified more than 1500 different E3s. Ubiquitin E3 ligases are classified into four main classes: HECT domain E3s, U-box E3s, monomeric RING finger E3s and multisubunit E3 complexes that contain a RING finger protein. The different classes differ in their E2 and substrate binding domains. The RING finger and the U-box domains have an adaptor function in correctly positioning the ubiquitin-loaded E2 to transfer the ubiquitin to the substrate. The HECT E3s form a thioester intermediate with ubiquitin before transferring it to the substrate (*216, 217*).

The ubiquitin is one of the most widely used protein modifications, which is very versatile due to its diverse surface architecture and possibility of forming chains. This signal is decoded by binding to ubiquitin-binding domains (UBDs). Two UBDs in the same protein are used to bridge two ubiquitinated substrates. Additionally, specialized UBDs are able to discriminate between different types of ubiquitin chains (*189*).

Several ubiquitin-like proteins (UBLs) have been identified, consisting of proteins that although having different primary amino acid sequence, share the characteristic three-dimensional ubiquitin fold. To date, 17 human UBLs have been identified, including NEDD8 ("neuronal precursor cell-expressed developmentally downregulated protein 8"), SUMO ("small ubiquitin-related modifier"), ISG-15 and FAT10. The different UBLs have their own E1-E2-E3 cascades, which cause distinct effects on their targets, and are involved in different biological pathways. NEDD8 conjugation to cullin enhances the enzymatic activity of the cullin-RING 3 ubiquitin ligases. Three SUMOs exist in humans, SUMO-1, -2, and -3; the attachment of SUMO alters the interaction between proteins, by mediating interactions with SUMO-binding motifs. ISG15 ("interferon-stimulated gene 15) and FAT10 are important in viral responses, consistent with their induction by type I interferons (*218*).

This process allows the dynamic modification of proteins, working like switches between different functional states of the substrate, therefore contributing to fine tuning of numerous cellular pathways.

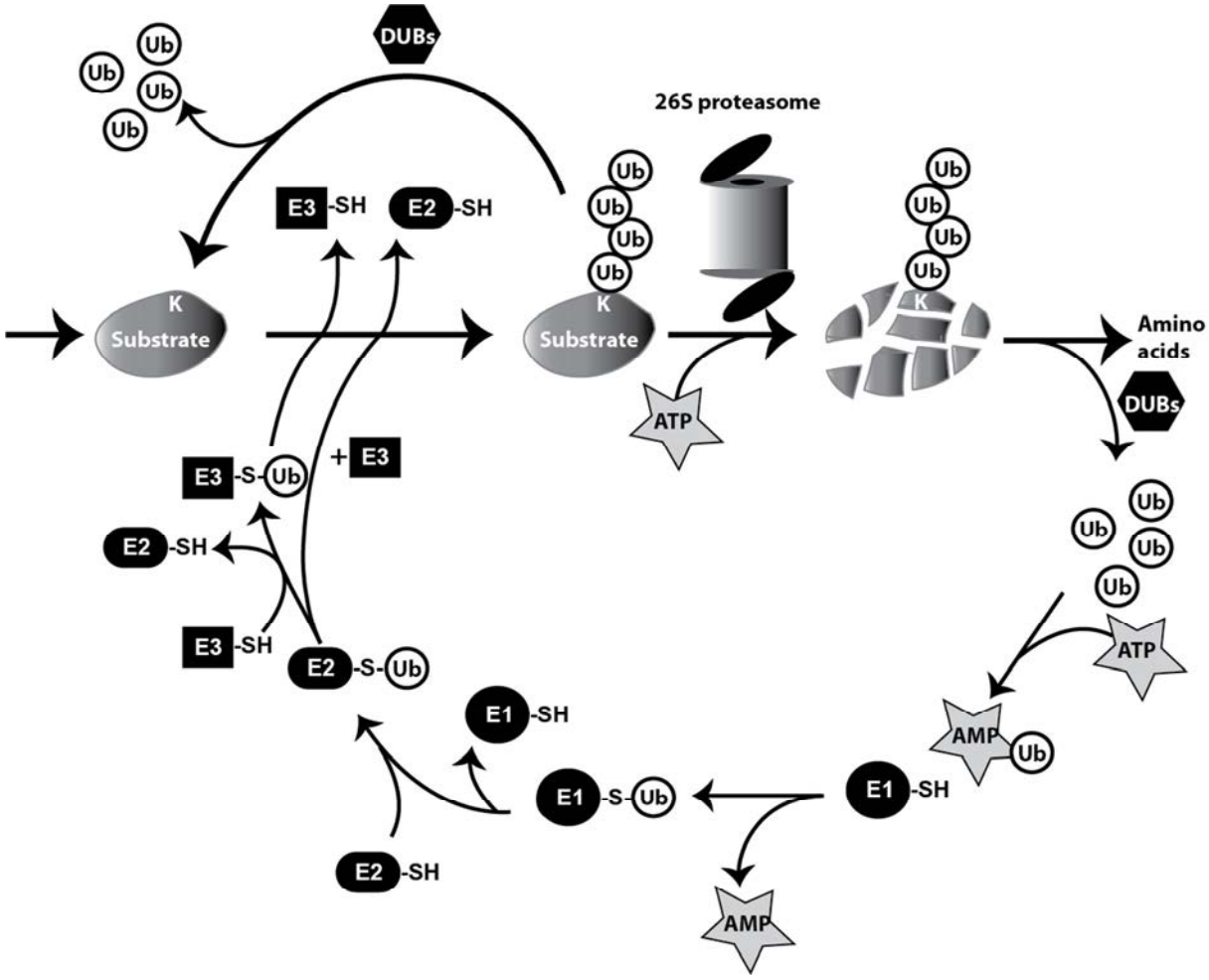

Fig.8: Schematic representation **of the ubiquitin-proteasome system (UPS).** The pathway starts with the activation of ubiquitin (Ub) by the E1, in an adenosine triphosphate (ATP)-dependent manner. Subsequently, the Ub is transferred to an E2, and finally attached to the substrate with the help of an E3. The final product is an Ub-protein conjugate where the C-terminal glycine carboxyl group of the ubiquitin is attached to a free amino group (typically lysine ε-amino) in the target or another Ub if poly-Ub chains are added. The ubiquitin-protein conjugate may be disassembled by the deubiquitinating enzymes (DUBs), or the target protein may be broken down by the 26S proteasome. Both processes result in the release of Ub molecules. (Adapted from (*216*))

5. SCF E3 ligases

SCF (SKP1-CUL1-F box protein) subfamily of E3 ligases was originally discovered and studied in budding yeast *S. cerevisae (219)*. They are the best characterized mammalian cullin RING ubiquitin ligases.

5.1 Structural organization

The determination of the crystal structure of SCF complex by Zheng and co-workers added some insights in the roles of each of its components and the mechanistic aspects of their interlinked actions (Fig. 9) (*220*). The cullin subunit, CUL1 is an elongated protein consisting of a long stalk and a globular domain. The N-terminus, contained in the long stalk, interacts with the adaptor protein SKP1 ("S-phase kinase-associated protein 1") and the C-terminal globular domain with a RING-finger protein RBX1 (or ROC1), RBX2 (or ROC2), or Ro52, by forming an intermolecular β-sheet. SKP1 brings into the complex an F-box protein that functions as the variable component on the enzyme, and

it is responsible for substrate recognition. The RING-finger protein RBX1 is involved in E2 conjugating enzyme binding, such as UBC3, UBC4 or UBC5. The SCF ligases are often referred to as super-enzymes, due to the fact that their mode of action implies concerted binding and action of several independent proteins. SCF ubiquitin ligases transfer ubiquitin via an activated UBC component to the substrate, bound by a specific-substrate binding protein, which positions the substrate in the optimal orientation for the reaction (*221*). CUL-1 is considered the scaffold or organizing center of this super-enzyme.

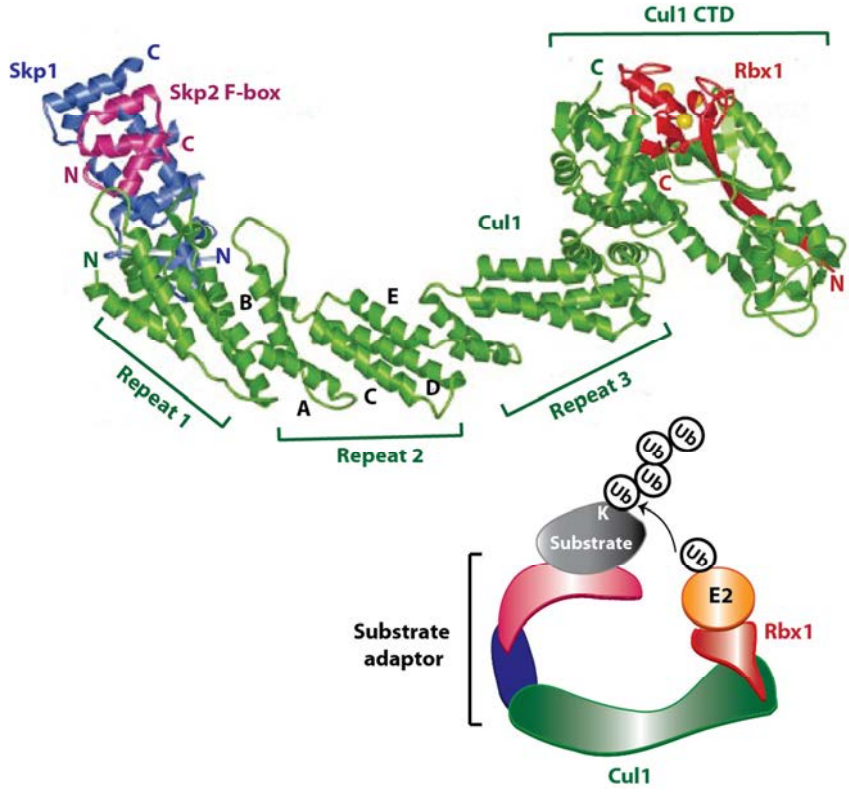

Fig.9: Representation of the crystal structure of SCF E3 ligases. *On the top:* overall structure of the Cul1-Rbx1-Skp1-F box (Skp2), where Cul1, Rbx1, Skp1 and F-box Skp2 are colored in green, red, blue and pink. The 5 helices from the 2nd cullin-repeat motif are marked from A to E (*220*). *On the bottom:* schematic diagram of the ubiquitin transfer from the E2 (bound to Rbx1) to the substrate, bound to the F-box protein and correctly positioned for the reaction (Adapted from (*216*)).

5.2 Dynamic regulation of assembly and activity

The complexity of the structural organization of the SCF complexes implies the need of regulation at multiple levels: abundance, assembly and activity. Considering that many adaptors are simultaneously delivering substrates, a failure or delay in one step will cause a multitude of deleterious effects in the cells. Changes in nuclear:cytoplasm partitioning of some SCF components, and regulation of expression levels of F-box proteins have been proposed as regulatory mechanisms (*216*). Additionally, there are reports that the F-box proteins get ubiquitinated in the assembled SCF complex in the absence of substrate. Since it is believed that the F-box proteins compete with each other for cullin scaffolds, their turnover has direct consequences for the relative proportion of each different SCF complexes (*222, 223*).

SCF complexes can dimerize through the F-box proteins, which contain a dimerization (D) domain immediately N-terminal of the F-box domain (*224*). It has also been demonstrated that CUL1 is able to dimerize (*225*). SCF dimerization has been proposed to allow optimal ubiquitin chain initiation and elongation or better tethering of the substrate for ubiquitination. Additionally, the proposed bivalent geometry of the dimeric SCF structure provides different distances between the substrate binding sites

and the two E2 docking sites. This may explain how SCF complexes are able to target different sized substrates and accommodate changes in the length of the elongating polyubiquitin chain (*226*).

Probably the best known mode of SCF E3 ligases regulation occurs through the cycles driven by NEDD8 together with the signalosome (CSN) and through CUL1-associated NEDD8-dissociated (CAND1). The first cycle is the conjugation of NEDD8 to CUL-1, in a process called neddylation. This is a 3-step enzymatic cascade similar to the ubiquitination reaction. It involves a heterodimeric E1 (APP-BP-1/Uba3) that activates Nedd8, the E2 UBC12 that conjugates Nedd8 to the CUL-1, and DCN1 (defective in cullin neddylation) and RBX1 as E3 (*227*). NEDD8 conjugation has been described to increase SCF complex catalytic activity (*228*). The mechanism is not elucidated but it has been proposed that NEDD8 and RBX1 form a common interface for recruiting the E2 (*229*). Neddylation is reversed by the activity of CSN, in particular through the isopeptidase activity of the metalloprotease CSN5/Jab1 subunit (*230*). CSN is evolutionary conserved and distantly related to the regulatory particle of the 26S proteasome (*231*). The second cycle involves the binding of CAND1, a 120-kDa protein, to CUL1. The three dimensional structure of CAND-1 in complex with CUL-1/RBX1 has been determined and revealed that CAND-1 has a U-shaped structure wrapped around the elongated CUL-1 surface (*232*). The inhibitory role of CAND-1 binding on SCF activity is partially due to a β hairpin at its C-terminus, which interferes with F-box protein binding. Additionally, the C-terminus of CAND-1 lies on top of the NEDD8 conjugation site, effectively blocking this modification as well. The currently most accepted model implies that the binding of CAND1 is transient and reversible, and once one F-box protein along with its substrate binds, NEDD8 is attached to CUL1 which prevents further interference by CAND1. After NEDD8 attachment, CSN binds to the SCF where it will have an important role in removing ubiquitin inadvertently attached to the SCF subunits in the course of the ubiquitination of the substrate. This deubiquitinating activity is performed by one or more DUBs, bound to the CSN. Once the ubiquitination of the substrate is complete, NEDD8 is removed by the CSN, the SCF is dissociated and CAND-1 is allowed to restart its binding/release cycles (*233*).

5.3 F-box proteins

In humans, 69 F-box proteins have been identified to date (*234*).The evolutionary conservation for each individual F-box protein is rare. The F-box proteins have the N-terminal F-box domain in common, named after its first discovery in cyclin F (or Fbxo1), and is composed of ~40 amino acids (*235*). This domain is used to bind SKP1 and to the rest of the E3 ligase complex. Although necessary, the F-box protein-SKP1 interaction is insufficient for a stable association with CUL1; additional stabilizing interactions between the F-box and CUL1 have been described. Importantly, not all the F-box proteins exist in the context of a SCF complex (*234*).

In their C-terminus, the F-box proteins harbor protein-protein interaction motifs involved in substrate binding. Typically, the F-box proteins use for this purpose WD40 repeats (FBW, F-box proteins with WD motifs), or leucine-rich repeats (FBL, F-box proteins with leucine-rich repeats). Additionally, there are F-box proteins with other motifs or without recognizable motifs (FBX). Most of the substrates are only recognized and bound by the F-box protein when they are post-translationally modified, usually by phosphorylation, which creates a degradation sequence (degron). The need of this modification before the F-box proteins can act, confirms their role as important physiological regulators able to respond to cellular stimuli. A single F-box protein is able to recognize multiple substrates, contributing for the wide biological action of the SCF ubiquitin ligases. Notably, the substrates of most of these F-box proteins remain unknown. Only nine SCF ubiquitin ligases are well established: SCF^{TrCP1}, SCF^{TrCP2}, SCF^{Skp2}, SCF^{FBLX3}, SCF^{FBLX20}, SCF^{FBXO4}, SCF^{FBXW7}, SCF^{FBXO7}, SCF^{FBXW8} (*221*).

In the next section of this chapter I will focus on the F-box protein βTrCP, very versatile in the regulation of a big variety of cellular processes.

5.4 $SCF^{\beta TrCP}$

Beta-transducin repeat containing protein (βTrCP), also termed Fbw1, interacts with its substrates via seven WD40 repeats domain, only when the two serine residues are phosphorylated in the destruction motif, $DSG(X)_{2+n}S$ (where X represents an hydrophobic amino acid) (*236, 237*).

βTrCPs are highly conserved from Xenopus to humans, particularly within the F-box and WD40 repeats region.

Mammals express two different paralogues of βTrCP-1 and -2, with no clear differences in their biochemical properties. The differences between βTrCP-1 and -2 are mainly present in their N-terminal parts, proximal to the F-box motif. Functionally, they seem to be redundant, as concluded from data from RNAi analysis and knockout mice for βTrCP-1 (*238, 239*). Additionally, alternative splicing mRNA mechanisms give rise to multiple isoforms (*240*). All of these isoforms contain the F-box and the seven WD40 repeats domain (*241, 242*).

After the action of a specific kinase on the serines of the $DSG(X)_{2+n}S$ motif, $SCF^{\beta TrCP}$ is recruited and mediates the ubiquitination on lysines, preferably located in the positions 9-13 upstream of this motif. The first identified substrate of βTrCP1 was the HIV protein Vpu (*243*). Since then , the list of βTrCP substrates has been increasing, and its involvement in ubiquitination and degradation of β-catenin and IκB is documented particularly well (*244-249*). Inclusively, the crystal structure of βTrCP in complex with a β-catenin fragment is available, which revealed that the phosphorylated degron is inserted in the surface of the funnel-like β-propellor barrel structure adopted by the seven WD40 repeats (Fig.10). The substrate is then placed in an optimal orientation toward the bound E2 to allow ubiquitination to occur (*250*). Importantly, there are some $SCF^{\beta TrCP}$ subtrates that are recognized via deviations of the classical motif, $DSG(X)_{2+n}S$ and it is unclear whether they employ similar ways of interaction with βTrCP. An important factor is to ensure that subtrate binding allows its correct positioning for ubiquitination. Many kinases have been described for specific phosphorylation of the serines in the $DSG(X)_{2+n}S$, being therefore key regulators of the turnover of it substrates, as glycogen synthase kinase 3β (GSK3β) and inducible IκB kinase complexβ (IKKβ), for β-Catenin and IκB, respectively (*251-255*)

5.4.1 Role in β-Catenin and IκB degradation

$SCF^{\beta TrCP}$-mediated β-catenin ubiquitination and subsequent degradation is important to keep the cytoplasmic levels of β-catenin low in basal conditions. This implies that β-catenin is constitutively phosphorylated in its degron serines. This occurs through tethering to the destruction complex composed of GSK3β, casein kinase 1 (CK1) tumor suppressor adenomatous poliposis coli (APC) protein and axin. Upon stimulation with WNT, a conserved family of secreted signalling molecules, the destruction complex disassembles through a mechanism that is not yet clear, β-catenin detaches and translocates to the nucleus, where it activates the transcription of target genes involved in cell differentiation and proliferation.The other classical $SCF^{\beta TrCP}$ substrate is the inhibitor of NFκB signalling, IκB. NFκB is a transcription factor mainly known for its role in inflammation responses. Normally, NFκB is sequestered in the cytoplasm bound to IκB. Once IκB is degraded by $SCF^{\beta TrCP}$ NFκB is allowed to migrate to the nucleus where it activates transcription of a large number of target genes, such as anti-apoptotic genes, and genes involved in cell growth. The degradation of IκB depends on its phosphorylation by IKK. Both accumulation of β-catenin and excessive activation of NFκB have been connected to cancer, making the $SCF^{\beta TrCP}$ a key player in tumor development.

5.4.2 $SCF^{\beta TrCP}$ and cytokine receptors

Another important activity of $SCF^{\beta TrCP}$ is in the endocytosis and degradation of cytokine receptors. The first cytokine receptor found to be degraded by $SCF^{\beta TrCP}$ was the alpha subunit of type 1 Interferon receptor (IFNAR) (*256*). Subsequently, $SCF^{\beta TrCP}$ was also reported in PRLR (*257*) and EpoR (*258*) degradation. IFNAR, PRLR and EpoR, all contain DSGxxS motifs that get phosphorylated upon ligand stimulation. Therefore, $SCF^{\beta TrCP}$ contributes to signaling termination of these receptors (*256-258*). Interestingly, IFNAR is also phosphorylated and ubiquitinated by unfolded protein response (UPR) inducers, including viral infections (*259*). We found that $SCF^{\beta TrCP}$ is also essential for GHR endocytosis, but in a different way compared to the regulation of the previously

described cytokine receptors. $SCF^{\beta TrCP}$ is functional both in the absence, and in the presence of GH, through its recruitment to the UbE motif. GHR also contains a DSGxxS which does not seem to be needed for GH-induced GHR downregulation (*211*).

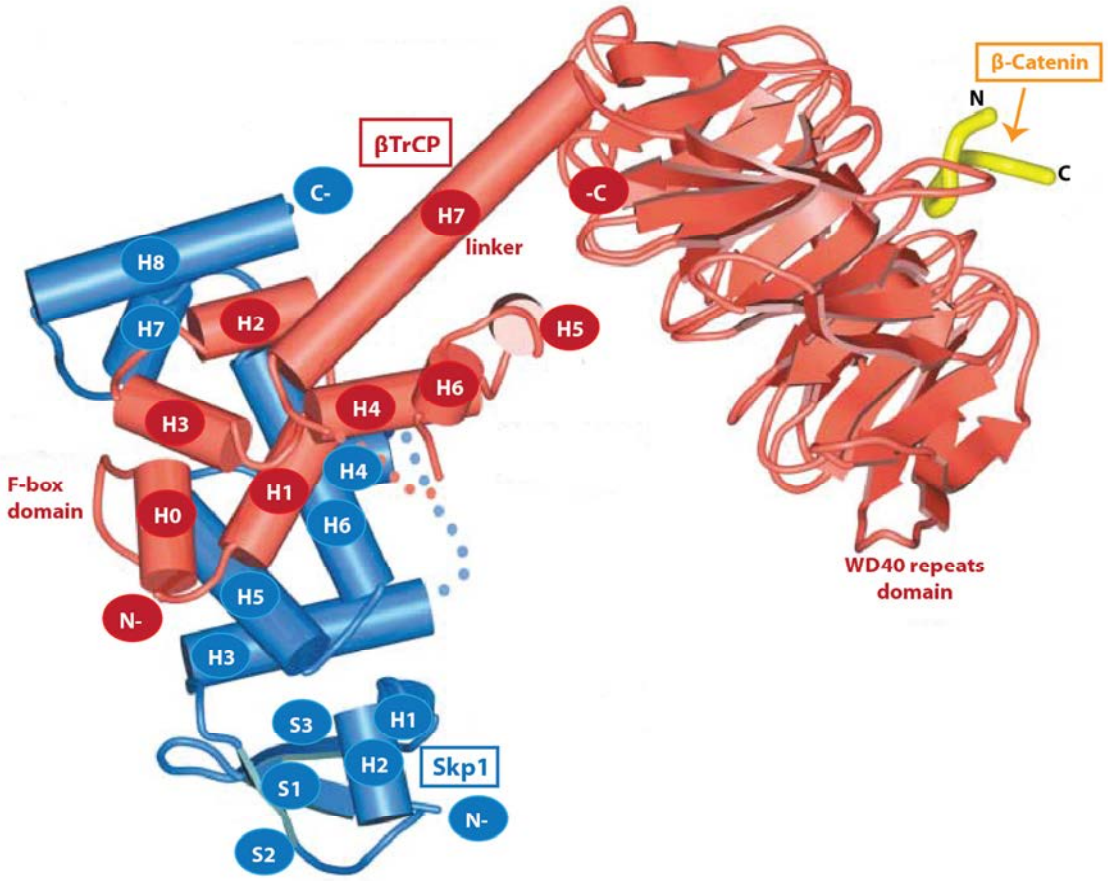

Fig.10: Structure of the complex βTrCP1-Skp1-phosphorylated β-catenin peptide. Overall view of the complex β-TrCP1 is colored red, Skp1 blue, and β-catenin yellow. The different domains of β-TrCP1 are indicated as well as the secondary structure elements for Skp1, F box and linker domains of β-TrCP1. Dotted lines represent disordered regions. Adapted from (*250*).

Box 2- Ubiquitin-Proteasome System as a drug target

The ubiquitin proteasome system (UPS) is responsible of the majority of degradative processes in the cell. Additionally, it has non-degradative functions. The action of the UPS occurs in multiple pathways in important physiological processes. For this reason, it is expected that many diseases, including numerous cancer types, cardiovascular disease, viral diseases and neurogenerative disorders originate from misregulations of the components of the UPS. These proteins should therefore be regarded as potential drug targets.

The first example of a UPS-related therapeutic target was the proteasome inhibitor bortezomib (Velcade; Millenium Pharmaceuticals) approved for cancer treatment, by the US Food and Drug Administration in 2003 (*260*). The proteasome represents the endpoint for the involvement of the UPS, which makes it a relatively unspecific drug target. Constant developments open new opportunities of using more components of the UPS as drug targets, like specific enzymes for certain pathways.

The E3 ligases are particularly good drug targets since they are the components that confer specificity. Several recent reports describe small molecule inhibitors targeting SCF E3 ubiquitin ligases. An inhibitor of SCF^{Met30} was identified, which acts by interfering with the binding of the F-box protein to the CUL1-RING complex (*261*). Another inhibitor was identified for the SCF^{Cdc4}, which interferes with substrate binding due to a distortion of the binding pocket through an allosteric mechanism (*262*). Thalomide is a compound that although used since 50 years as a sedative, only recently was identified as targeting cereblon (CRBN), which forms a cullin based E3 ligase, together with cullin 4 and damage-binding protein 1 (DDB1). Although the use of thalidomide is strictly controlled because of its teratogenic effects, it has been applied for treatment of myeloma and leprosy (*217*).

Development of inhibitors of E1 activating enzymes has also been described. One example is PYR41, a pyrazone derivative able to covalently modify the cysteine in the active site of the ubiquitin-activating enzyme (UAE). The effects of this compound in cells are inhibition of cytokine induced NFκB activation, and stabilization of p53 with consequent induction of p53 dependent transcription (*263*). A related compound, PYZD4409, with similar properties, had antileukaemic activity in a mouse cancer model (*264*). The activation of NEDD8 has also been targeted with MLN4924, an adenosine sulphamate analogue that binds to the nucleotide-binding pocket of NEDD8 activating enzyme (NAE) in its NEDD8 thioester form. This inhibitor forms a covalent adduct with NEDD8 by a mechanism called "substrate-assisted inhibition" (*265, 266*). The conjugation of NEDD8 to cullin is necessary for the full activation of the SCF E3. Therefore, we expect that blockage of the NAE activity will accumulate cullin-RING ligase substrates. Indeed, NAE inhibition has been reported to increase the levels of IκB, and, consequently, inhibit NFκB pathway activation in NFκB-dependent human cancer models (*267, 268*). This would support the use of this strategy as a potential treatment for disease associated with constitutively active NFκB signaling.
E2 conjugating enzymes from different ubiquitin-like protein (UBL) pathways have been connected to cancer and other diseases, such as UBE2O2, the SUMO E2 Ubc9, UBE2T and UbcH10 (*269-274*). A potential way of targeting E2 action is by interfering with its interaction with E1: a synthetic peptide corresponding to an extension of UBC12 (Ubc12N26) is able to compete for UBC12 binding to NAE (*275*). Alternatively, the E2-E3, or E2-thioester-substrate interactions may be regarded as targets.
Deubiquitinating enzymes (DUBs) are also attractive targets for drug discovery since they are involved in a great variety of processes in the cells (*276*). An example of success with this strategy is the inhibitor of the papain-like protease from the SARS coronavirus. This inhibitor was shown to block virus replication, specifically, without interfering with the host DUB activities (*277, 278*).
Thus, understanding of mechanistic details of ubiquitination pathways constitute specific opportunities for numerous therapies.

6. Cachexia

6.1 Definition

Cachexia (from the Greek kakos (bad) and hexia (condition)) is a multifactorial syndrome that frequently occurs in patients affected by chronic pathologies, such as cancer, AIDS, chronic heart failure (CHF), chronic obstructive pulmonary disease (COPD) or rheumatoid arthritis (RA). Hippocrates wrote about cachexia, in particular in association with CHF, around 2500 years ago, referring to it as: "The flesh is consumed by water, the feet and legs swell, the shoulders, clavicles, chest and thighs melt away. This illness is fatal" (*279*).

Cachexia is associated with high morbidity and mortality, which makes it clinically very relevant. A couple of years ago a consensus definition of cachexia was proposed: "cachexia is a complex metabolic syndrome associated with underlying illness and characterized by loss of muscle with or without loss of fat mass."(*280*)

6.2 Conditions associated with cachexia

A healthy body composition is ensured by a coordinated set of signaling pathways that modulates muscle mass in adults. When children enter in puberty their muscle mass is developed and strengthened through the action of GH, IGF-1, and sex steroids. Muscle mass peaks in the 20s or 30s and then declines. Loss of 40% of the body mass is fatal, while smaller losses have been demonstrated to have consequences, for example, in immune function or cancer mortality (*281, 282*). Different cachexia types may involve a combination of different factors.

Cancer cachexia is a wasting syndrome occurring during the course of most cancers. Although the definition of cancer cachexia is not well established, it is estimated that 55% of all the cancer patients acquires cachexia. Cancer cachexia has a large impact on prognosis of the cancer patients, being one of the ultimate cause of dead (*283*). The bad prognosis of CHF worsens even more, once cachexia is first diagnosed (*284*). Muscle wasting is a serious complication of the COPD patients, possibly related to their exercise intolerance. Especially when associated with systemic inflammation, cachexia becomes a very serious condition in these patients, with very important implications for their survival (*285*). Very often, AIDS patients also develop cachexia, which was considered as one important factor

in AIDS-defining diagnosis. The involuntary weigh loss in AIDS patients reflects metabolism alterations due to high anti-inflammatory responses and disturbances in hormone function (*286*). In RA patients the sustained increase in catabolic cytokines such as TNF-α, IL-1β, and IL-6, increases energy expenditure and muscle protein breakdown (*287*).

6.3 Molecular events underlying cachexia

6.3.1 E3 ubiquitin ligases MuRF1 and MAFbx/atrogin-1

The expression of the genes "Muscle atrophy F-box" (*MAFbx*), also called *Atrogin-1*, and "Muscle Ring Finger1" (*MuRF1)* is significantly upregulated under atrophy conditions (*288, 289*).

Knockout mice for MuRF1 ($MuRF1^{-/-}$) or for MAFbx ($MAFbx^{-/-}$) appear phenotypically normal, but under muscle atrophy conditions they lose significantly less muscle mass in comparison to control littermates (*288*). *MuRF1* encodes a RING-finger domain E3 ligase. The role of MurF1 in the progression of muscle atrophy depends on its E3 ligase activity, as concluded from the analysis of a mouse where only the RING domain of MuRF-1 was deleted (*290*). Firstly, MURF-1 was found to interact with myosin heavy chain (MyHC), and mediate its proteasomal degradation (*291*). Subsequently, additional proteins were described to be degraded in the muscle by MuRF1, including myosin light chain and myosin-binding protein C (*290*). MAFbx/Atrogin is an F-box protein in a SCF E3 ubiquitin ligase. Several substrates have been reported for MAFbx in skeletal muscle, such as MyoD (*292*) and eIF3f (*293*). Genetic activation of eIF3f is sufficient to induce hypertrophy, while its blockade induces atrophy in myotubes. The ubiquitination of eIF3f by MAFbx and its proteasomal degradation seems to account for MAFbx function during muscle atrophy (*293, 294*).Treatment of differentiated myotube cultures with the cachectic glucocorticoid dexamethasone enhances protein breakdown and increases expression of *MAFbx* and *MuRF1*. This can be reversed by treatment with IGF-1, acting through the PI3K/Akt pathway. In addition to triggering skeletal muscle hypertrophy, Akt signaling can inhibit the induction of atrophy signaling in a mechanism involving the FOXO family of transcription factors (*295-297*).

Other proteins besides IGF-1 have been demonstrated to perturb skeletal muscle size. Myostatin, a member of transforming growth factor-β (TGF-β) family, has been shown to be a negative regulator of muscle mass (*297-299*) and to inhibit activation of Akt in myoblasts and myotubules. Addition of IGF-1 blocks the effects of myostatin (*300, 301*).

6.3.2 Inflammatory cytokines and cachexia

Pro-inflammatory cytokines such as TNF-α and IL-6 have been proposed as the main mediators of cachexia. Elevated TNF-α level in the serum of pancreatic adenomacarcinoma patients was suggested to be related to development of cachexia (*302*). The mechanism by which TNF-α stimulates muscle wasting is largely unknown. The indirect effects may be related to the influence of TNF-α on circulating levels of hormones that regulate muscle grow, or to the stimulation of production of other catabolic cytokines. More directly, TNF-α has been suggested to inhibit myoblast differentiation, and to have a direct catabolic effect on differentiated muscle (*303*). NF-κB activation is the major center of the cellular responses to TNF-α, including TNF-α induced catabolism (*303*). However, episodic TNF-α administration has failed to induce cachexia in experimental animals; although repetitive administrations appeared to induce cachexia, tolerance to the administration is re-established and body weight returns to normal (*304*). Circulating IL-6 levels are a reliable predictor of weight loss in human cancer cachexia (*305*). Iwase *et al*. reported that IL-6 was the only cytokine measured that was elevated in all 28 cachectic patients included in their study, while circulating TNF-α was elevated in only 1 of 28 cachectic patients (*306*). Il-6 was revealed as an important mediator of muscle mass loss in several mouse models used to study cancer cachexia (*307*). IFN-γ, produced by activated T and natural killer (NK) cells, is another potential factor involved in cachexia. A monoclonal antibody against IFN-γ was able to reverse the wasting syndrome in tumor-bearing mice, indicating that IFN-γ mediates some metabolic changes characteristic of cancer cachexia (*308*). Further studies by the same group showed that mice inoculated with CHO cells constitutively producing IFN- γ develop severe cachexia (*309*).

Other cytokines, such as IL-1, leukemia inhibitory factor (LIF) and TGF-β have been suggested to mediate cachexia. Mice engrafted with tumors secretin LIF develop severe cachexia. The effects of IL-1 are most likely indirect, since administration of IL-1 receptor antagonist (IL-1ra) to tumor-bearing rats did not improve their cachexia condition.

6.4 GHR resistance in cachexia

The inherited phenotype of GH insensitivity, or resistance, occurs in patients suffering from Laron syndrome, as result of mutations affecting GHR signaling. It was first described in a family with short stature (*310*). GH resistance is characterized by high levels of circulating GH, with low levels of IGF-1, and poor IGF-1 and anabolic response to GH. A similar biochemical profile is found in acquired GH resistance as it occurs in catabolic states (*311-313*). In fact, the administration of GH to septic patients did not improve nitrogen balance or increase IGF-1 levels as shown by the controls. In several instances AIDS patients showed a limited IGF-1 response upon GH treatment when compared to the normal individuals (*314, 315*). On the other hand, in less severe cancer cachexia states, GH exerted some anabolic effects (*316*).

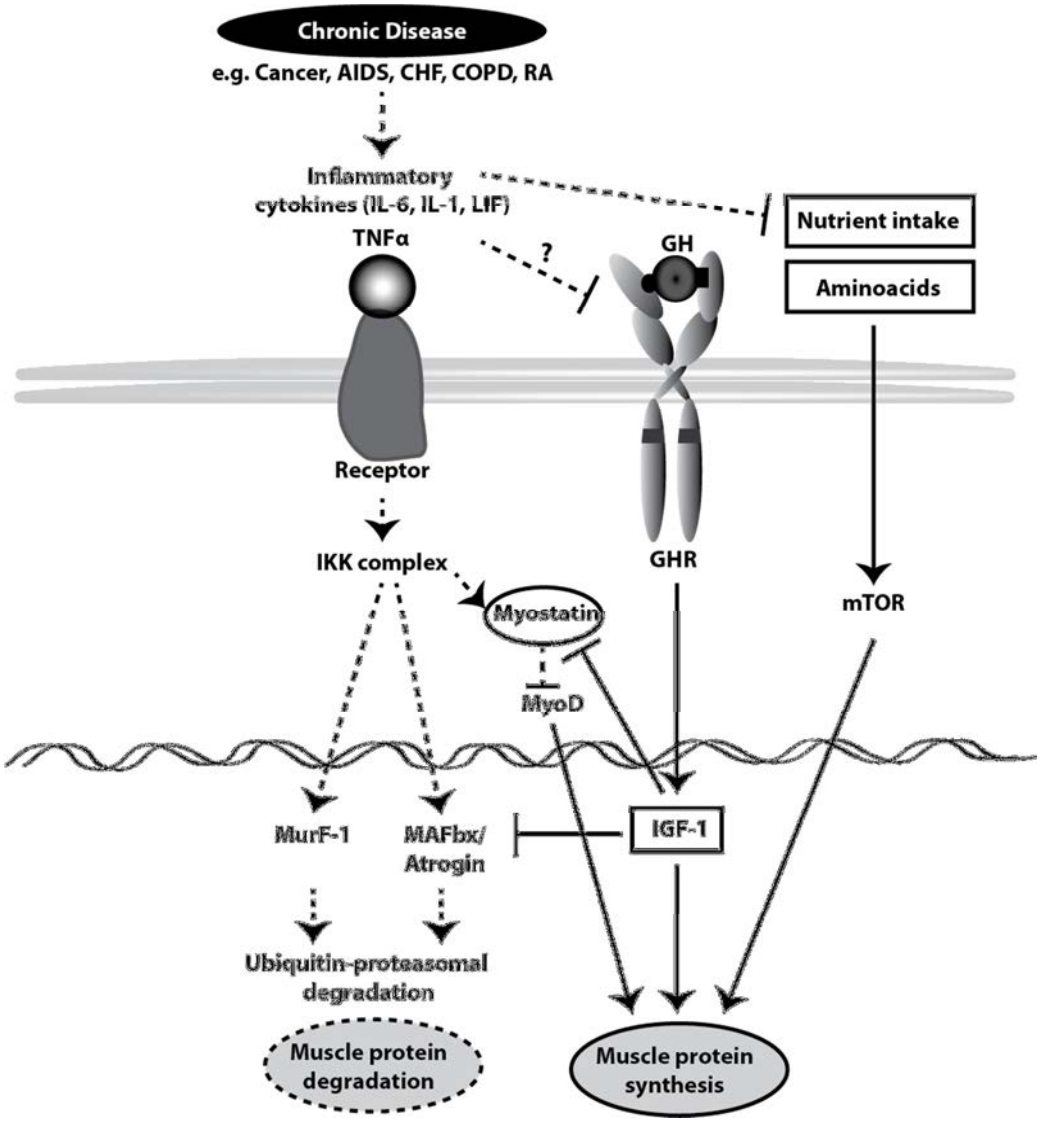

Fig.11: Molecular mechanisms of cachexia. In conditions of chronic disease, inflammatory cytokines (such as TNFα, IL-6, IL-1 and LIF) are major factors contributing to the development of cachexia. They can act by suppressing the appetite; stimulating the proteasomal degradation of muscle proteins (through the action of MurF-1 and MAFbx), or indirectly by

affecting GH signaling, and consequently IGF-1 production, by mechanisms not yet elucidated. *Continuous line*, anabolic pathways; *dashed line,* catabolic pathways. Adapted from Burckart et al, 2010.

The mechanisms responsible for the induction of GHR resistance in catabolic states are largely unknown and have been discussed for a long time (*317*). Initially, abnormal nutrition was considered a probable cause for acquired GH resistance. This view changed when it was demonstrated that patients with adequate nutritional support still failed to produce normal IGF-1 levels, indicating additional factors (*318*). Effects in IGF-1 synthesis, IGF-1 half-life or levels of IGF binding proteins (IGFBPs) have also been proposed as causative of acquired GH resistance (*313*) (*319*). Since GH is present in excess and the levels of IGF-1 are much reduced, the most likely scenario is failure in IGF-1 synthesis. This effect can be justified by decreased number of GHRs, or down-regulated GH signaling.

Several reports suggest that the elevated levels of inflammatory cytokines accompanying the GH resistance phenotype in cachexia might actually be the cause. This hypothesis is supported by several studies demonstrating the negative impact of cytokines in GH actions. Transgenic mice overexpressing IL-6 have reduced IGF-1 levels and are small (*320*). Accordingly, GH resistance phenotype could be induced in rats by injection of LPS, effect mediated indirectly by TNF-α and IL-6, and correlating with decrease GHR mRNA expression and up-regulation of SOCS-3 mRNA (*321*). Moreover, IL-1 and TNF-α inhibit IGF-1 expression in response to GH stimulation in rat hepatocytes (*322*) and TNF-α neutralization in mice with chronic colitis up-regulated GHR abundance and restored GH signaling (*323*). Based on this evidence, inflammation is considered the cause of GH resistance. However, there are also studies suggesting that anti-inflammatory agents like glucocorticoids inhibit GH actions. The synthetic glucocorticoid dexamethasone has been shown to inhibit the induction of IGF-1 expression triggered by GH, most likely due to diminished amounts of GHR (*324, 325*). Therefore, it remains unclear what is the pathophysiological mechanism of acquired GH resistance in cachexia syndrome.

6.5 Cachexia treatment

Several approaches have been proposed for therapy or prevention of cachexia in experimental models and cancer patients. A combination of adequate dietary protein, energy and exercise was proven to be efficacious in clinical trial settings, but its translation to a generalized treatment of cachexia patients did not result in clear benefits (*326*). Therefore, the critical need of new medical treatments together with the growing scientific insight in the ontogeny of the cachexia syndrome has urged the creation of new drugs.

The possibility of interfering with the pro-inflammatory cytokines at several levels has been particularly explored as a strategy for cachexia treatment. These include molecules able to inhibit cytokine production and release, such as Pentoxifylline, Thalidomide, and inhibitors of TNF-α converting enzyme, as well as molecules interfering with cytokine-receptor interaction, such as monoclonal anti-TNF-α antibodies, soluble TNF-α receptors, IL-1 receptor antagonists, anti-IL-6, and anti-IL-6 receptor antibodies). Additionally, the use of suramin has been explored for cachexia treatment due to its ability to interfere with cytokine bioactivity. However, the results obtained to date on the effects of these strategies for the treatment of cachexia are not promising, probably due to the multi-factorial nature of the cachexia syndrome. On the other side, the use of anti-cytokine agents may affect the essential physiological functions of cytokines in immune responses (*327*).

Anti-oxidants, branched-chain amino acids, agonists of the melanocortin receptor, ghrelin and anti-myostatin agents are some other explored anti-cachexia strategies among many (*328*).

Decrease of testosterone levels during aging, correlates with the loss of muscle mass(*329*). Therefore, the use of testosterone or analogs has been suggested as a potential treatment of cachexia. Favorable effects of testosterone in enhancing body weight, lean body mass, and muscle strength, with an acceptable safety profile have been demonstrated (*330-334*). The limitation with the application of these molecules is related to their non-selectivity in terms of anabolic versus androgenic effects.

Molecules interfering with the myostatin pathway have also been attempted. The use of anti-myostatin antibodies did not appear to improve muscle strength (*335*). Alternatively, compounds that inhibit signal transduction of myostatin by blocking activin receptors have been tried in early-phase clinical trials (*285*). Angiotensin II has been suggested to be involved in cachexia, both in patients and

in experimental animal models. ACE inhibitors, which inhibit angiotensin II formation, have been shown to reduce cachexia in cancer and CHF patients. Additionally the blockade of angiotensin II receptors has been shown to prevent skeletal muscle atrophy in rats (*285*).

GH has been explored for the treatment of cachexia. As described before in this chapter, GH stimulates production of IGF-1, which triggers protein synthesis, myoblast differentiation, muscle growth. At the same time it suppresses protein oxidation and proteolysis. Therefore, GH is very important for muscle homeostasis. The use of recombinant GH is currently approved by the U.S. FDA for treatment of muscle wasting in AIDS patients, parenteral nutrition-dependent short bowel syndrome, pediatric chronic kidney disease, and in adult and pediatric GH-deficiency states. In several studies in HIV patients, recombinant GH has significantly improved the cachectic phenotype (*336*). Additional beneficial effects of GH treatment have been reported in adult catabolic patients with chronic renal failure (CRF)(*337*). However, GH treatment failed to improve the cachectic status of CHF patients, probable due to acquired GH resistance (*338*). Treatment with GH has some side effects, including dose-related paresthesias and arthralgias, insulin resistance, sodium retention, and peripheral edema (*339-342*). Ghrelin is also considered an attractive candidate for cachexia treatment, because of its anabolic actions, via increasing GH secretion, its actions on increasing appetite and ghrelin-mediated anti-inflammatory activity (*285*). Several experimental studies in animal models and patients in few clinical trials have shown promising results of the use of ghrelin for cachexia treatment (*343-347*). The successful use of GH or ghrelin on cachexia treatment is limited to patients that do not suffer from GH resistance, which is a common condition of cachexia patients (*see section 6.4*).

A successful treatment of cachexia most likely requires a combination of several therapies covering the broad range of factors involved in the syndrome, including a strategy to prevent GHR degradation that may be the cause of GH insensitivity.

Outline of this thesis

GH signaling plays major roles in the organism and, therefore, the sensitivity of the cells to GH and the signaling duration are under a tight control. GHR endocytosis is one of the main mechanisms that determine the amount of GHRs at the cell surface, and allow the cells to regulate GH signaling. In this thesis we characterized the interaction between GHR and βTrCP, an essential factor that mediates ubiquitination events necessary for GHR endocytosis, and explored the potential of this interaction as a tool for manipulating the sensitivity of the cells to GH.

In **chapter 2**, we showed that βTrCP binds two motifs in GHR: the previously described UbE motif, and the downstream DSGRTS sequence, that corresponds to a consensus degron (DSGxxS) present in other βTrCP substrates. Interestingly, we found that while the UbE motif is necessary for both basal and GH-induced endocytosis, the DSGRTS sequence is only necessary for basal endocytosis. Therefore, besides the UbE motif, the DSGRTS has a crucial importance in the regulation of the cellular levels of GHR, and consequently the responsiveness of the cells to GH. βTrCP binds to the DSGRTS sequence with the same residues as it binds to its other substrates, such as βcatenin or IκB. On the other hand, the UbE motif (DSWVEFIELD) seems to interact differently. In **chapter 3**, we characterized in detail the interaction between βTrCP and the UbE motif. By *in vitro* binding assays using purified βTrCP and GHR tails we proved that this interaction is direct. Additionally, we showed that βTrCP ubiquitinates GHR *in vitro* in an UbE motif-dependent manner. The amino acid residues in βTrCP and UbE motif necessary for the interaction were determined and used together with NMR data, in the computation modeling of the interaction. This revealed that the interaction βTrCP-UbE motif is unconventional. In **chapter 4** we showed that the affinity of the βTrCP-UbE motif interaction can be regulated by phosphorylation of the Ser323 in the UbE motif. This suggests that Ser323 phosphorylation could be a mechanism of increasing the rate of GHR endocytosis, in response to certain stimuli. We showed that GH stimulation works as such a stimulus. Therefore, GH-induced phosphorylation at the Ser323 can be considered as a mechanism used by the cells for rapid signal-termination. In **chapter 5** we showed that tumor-bearing mice suffering from cachexia have reduced amount of GHRs in the liver. Decrease in amount of GHRs in cachexia patients may be the reason of their GH resistance phenotype. The unconventional interaction βTrCP –GHR is a potential target for discovery of drugs that, by interfering with it, inhibit GHR endocytosis, and as such, increase the number of GHRs at the cell surface and consequently improve GH sensitivity of the cells. Cachexia patients would therefore benefit from such a drug. Based on this, we developed a robust screening route, from a simple molecular high throughput screening, to several cell based assays and a mouse model, to find potential lead compounds for future therapeutic development against cachexia.

In **chapter 6**, we explored and discussed the potentialities of Bioluminescence energy transfer (BRET) technology for studying molecular mechanisms involved in the regulation of GHR endocytosis. This technology allowed us to study the interaction of JAK2 and βTrCP with GHR in real time. We confirmed that both interactions occur in basal conditions. When GHR is occupied by JAK2 its endocytosis is inhibited. GH stimulation induces the detachment of JAK2 from GHR, as concluded by decreased BRET signal, which allows GHR to endocytose.

The findings of this thesis represent a significant progress in the understanding of the molecular mechanisms regulating GHR endocytosis, with focus on the translation of this knowledge into drug discovery, for the benefit of patients with chronic diseases suffering from cachexia.

References

1. A. J. Brooks, M. J. Waters, *Nat Rev Endocrinol* **6**, 515 (Sep, 2010).
2. H. Kawauchi, S. A. Sower, *Gen Comp Endocrinol* **148**, 3 (Aug, 2006).
3. G. Baumann, *Endocrine Rev.* **12**, 424 (1991).
4. V. Goffin, K. T. Shiverick, P. A. Kelly, J. A. Martial, *Endocr Rev* **17**, 385 (Aug, 1996).
5. S. S. Abdel-Meguid *et al.*, *Proc Natl Acad Sci U S A* **84**, 6434 (Sep, 1987).
6. A. Besson *et al.*, *J Clin Endocrinol Metab* **90**, 2493 (May, 2005).
7. H. R. Mott, I. D. Campbell, *Curr Opin Struct Biol* **5**, 114 (1995).
8. C. H. Li, H. M. Evans, M. E. Simpson, *J Biol Chem* **159**, 353 (1945).
9. E. Knobil, R. O. Greep, *Recent Prog Horm Res* **15**, 1 (1959).
10. C. H. Li, H. Papkoff, *Science* **124**, 1293 (1956).
11. J. C. Beck, E. E. McGarry, I. Dyrenfurth, E. H. Venning, *Science* **125**, 884 (May 3, 1957).
12. J. J. Kopchick, *Horm Res* **60 Suppl 3**, 103 (2003).
13. S. Okada, J. J. Kopchick, *Trends Mol Med* **7**, 126 (2001).
14. S. Harvey, *Endocrine* **38**, 335 (Dec, 2010).
15. M. L. Hartman *et al.*, *Am J Physiol* **260**, E101 (Jan, 1991).
16. K. Y. Ho *et al.*, *J Clin Invest* **81**, 968 (Apr, 1988).
17. Y. Takahashi, D. M. Kipnis, W. H. Daughaday, *J Clin Invest* **47**, 2079 (Sep, 1968).
18. H. K. Choi, D. J. Waxman, *Growth Horm IGF Res* **10 Suppl B**, S1 (Apr, 2000).
19. J. O. Jansson, S. Eden, O. Isaksson, *Endocr Rev* **6**, 128 (Spring, 1985).
20. G. S. Tannenbaum, H. K. Choi, W. Gurd, D. J. Waxman, *Endocrinology* **142**, 4599 (Nov, 2001).
21. C. A. Gebert, S. H. Park, D. J. Waxman, *Mol Endocrinol* **13**, 213 (Feb, 1999).
22. C. Chen, *Clin Exp Pharmacol Physiol* **27**, 323 (May-Jun, 2000).
23. M. Kojima *et al.*, *Nature* **402**, 656 (1999).
24. R. G. Smith *et al.*, *Horm Res* **51 Suppl 3**, 1 (1999).
25. X. M. Guan *et al.*, *Brain Res Mol Brain Res* **48**, 23 (Aug, 1997).
26. M. L. Hartman *et al.*, *J Clin Invest* **91**, 2453 (Jun, 1993).
27. I. Pellegrini *et al.*, *Mol Endocrinol* **20**, 3212 (Dec, 2006).
28. B. Andersen, M. G. Rosenfeld, *J Biol Chem* **269**, 29335 (Nov 25, 1994).
29. J. Roth, S. M. Glick, R. S. Yalow, S. A. Berson, *Metabolism* **12**, 577 (Jul, 1963).
30. A. P. Hansen, *Diabetes* **22**, 619 (Aug, 1973).
31. J. D. Veldhuis, J. N. Roemmich, E. J. Richmond, C. Y. Bowers, *Endocr Rev* **27**, 101 (Apr, 2006).
32. E. Corpas, S. M. Harman, M. R. Blackman, *Endocr Rev* **14**, 20 (1993).
33. A. J. D'Ercole, G. T. Applewhite, L. E. Underwood, *Dev Biol* **75**, 315 (Mar 15, 1980).
34. D. Le Roith, C. Bondy, S. Yakar, J. L. Liu, A. Butler, *Endocr Rev* **22**, 53 (Feb, 2001).
35. Z. Laron, A. Pertzelan, S. Mannheimer, *Isr J Med Sci* **2**, 152 (Mar-Apr, 1966).
36. Z. Laron, *Rev Endocr Metab Disord* **3**, 347 (Dec, 2002).
37. R. Reddy, S. Hope, J. Wass, *BMJ* **341**, c4189 (2010).
38. S. E. Fineberg, T. J. Merimee, *Diabetes* **23**, 499 (Jun, 1974).
39. D. Rabinowitz, G. A. Klassen, K. L. Zierler, *J Clin Invest* **44**, 51 (Jan, 1965).
40. K. L. Zierler, D. Rabinowitz, *Medicine (Baltimore)* **42**, 385 (Nov, 1963).
41. P. H. Sonksen *et al.*, *J Clin Endocrinol Metab* **27**, 1418 (Oct, 1967).
42. M. I. Wurzburger, G. M. Prelevic, P. H. Sonksen, L. A. Balint-Peric, M. Wheeler, *J Clin Endocrinol Metab* **77**, 267 (Jul, 1993).
43. D. R. Clemmons, L. E. Underwood, *Annu Rev Nutr* **11**, 393 (1991).
44. N. Moller, J. O. Jorgensen, *Endocr Rev* **30**, 152 (Apr, 2009).
45. J. Gjedsted *et al.*, *Acta Physiol (Oxf)* **191**, 205 (Nov, 2007).
46. J. M. Manson, D. W. Wilmore, *Surgery* **100**, 188 (Aug, 1986).

47. H. Norrelund, N. Moller, K. S. Nair, J. S. Christiansen, J. O. Jorgensen, *J Clin Endocrinol Metab* **86**, 3120 (Jul, 2001).
48. H. Norrelund, K. S. Nair, J. O. Jorgensen, J. S. Christiansen, N. Moller, *Diabetes* **50**, 96 (2001 Jan, 2001).
49. J. D. Veldhuis *et al.*, *J Clin Endocrinol Metab* **72**, 51 (Jan, 1991).
50. P. Felig, E. B. Marliss, G. F. Cahill, Jr., *J Clin Invest* **50**, 411 (Feb, 1971).
51. M. Ridderstrale, *Curr Drug Targets Immune Endocr Metabol Disord* **5**, 79 (Mar, 2005).
52. C. Carter-Su *et al.*, *Endocr J* **43 Suppl**, S65 (Oct, 1996).
53. H. Liu *et al.*, *Ann Intern Med* **148**, 747 (May 20, 2008).
54. J. Gibney, M. L. Healy, P. H. Sonksen, *Endocr Rev* **28**, 603 (Oct, 2007).
55. V. Birzniece, A. E. Nelson, K. K. Ho, *Trends Endocrinol Metab*, (Mar 17, 2011).
56. P. Colosi, K. Wong, S. R. Leong, W. I. Wood, *J. Biol. Chem.* **268**, 12617 (1993).
57. I. Pilecka, A. Whatmore, R. Hooft van Huijsduijnen, B. Destenaves, P. Clayton, *Trends Endocrinol Metab* **18**, 12 (Jan-Feb, 2007).
58. S. Jeay, G. E. Sonenshein, M. C. Postel-Vinay, P. A. Kelly, E. Baixeras, *Mol Cell Endocrinol* **188**, 1 (Feb 25, 2002).
59. E. L. Goh, T. J. Pircher, P. E. Lobie, *Endocrinology* **139**, 4364 (Oct, 1998).
60. C. J. Wiedermann, N. Reinisch, H. Braunsteiner, *Blood* **82**, 954 (Aug 1, 1993).
61. N. Hattori, *Growth Horm IGF Res* **19**, 187 (Jun, 2009).
62. S. Merchav, *J Pediatr Endocrinol Metab* **11**, 677 (Nov-Dec, 1998).
63. S. Mukhina *et al.*, *Endocrinology* **147**, 1819 (Apr, 2006).
64. S. T. Ng *et al.*, *Nat Med* **3**, 1141 (Oct, 1997).
65. K. L. Hull, S. Harvey, *Endocrine* **13**, 243 (Dec, 2000).
66. K. L. Hull, S. Harvey, *J Endocrinol* **168**, 1 (Jan, 2001).
67. A. V. Sirotkin, *Vet J* **170**, 307 (Nov, 2005).
68. H. Yoshizato, T. Fujikawa, H. Soya, M. Tanaka, K. Nakashima, *Endocrinology* **139**, 2545 (May, 1998).
69. G. Lombardi *et al.*, *Horm Res* **48 Suppl 4**, 38 (1997).
70. J. Ayuk, M. C. Sheppard, *Rev Endocr Metab Disord* **9**, 33 (Mar, 2008).
71. W. Y. Chen, D. C. Wight, T. E. Wagner, J. J. Kopchick, *Proc Natl Acad Sci U S A* **87**, 5061 (Jul, 1990).
72. W. Y. Chen, N. Chen, J. Yun, T. E. Wagner, J. J. Kopchick, *J Biol Chem* **269**, 20806 (Aug 12, 1994).
73. C. E. Higham, P. J. Trainer, *Exp Physiol* **93**, 1157 (Nov, 2008).
74. K. T. Coschigano *et al.*, *Endocrinology* **144**, 3799 (Sep, 2003).
75. K. E. Borg, H. M. Brown-Borg, A. Bartke, *Proc Soc Exp Biol Med* **210**, 126 (Nov, 1995).
76. K. Flurkey, J. Papaconstantinou, R. A. Miller, D. E. Harrison, *Proc Natl Acad Sci U S A* **98**, 6736 (2001).
77. M. Holzenberger *et al.*, *Nature* **421**, 182 (Jan 9, 2003).
78. C. Selman *et al.*, *FASEB J* **22**, 807 (Mar, 2008).
79. A. Bartke, *Neuroendocrinology* **78**, 210 (Oct, 2003).
80. A. Besson *et al.*, *J Clin Endocrinol Metab* **88**, 3664 (Aug, 2003).
81. Z. Laron, *Mech Ageing Dev* **126**, 305 (Feb, 2005).
82. O. Shevah, Z. Laron, *Growth Horm IGF Res* **17**, 54 (Feb, 2007).
83. G. Paolisso, D. Giugliano, *Diabetologia* **39**, 357 (Mar, 1996).
84. A. D. Romano, G. Serviddio, A. de Matthaeis, F. Bellanti, G. Vendemiale, *J Nephrol* **23 Suppl 15**, S29 (Sep-Oct, 2010).
85. H. M. Brown-Borg, A. M. Bode, A. Bartke, *Endocrine* **11**, 41 (Aug, 1999).
86. W. T. Cefalu *et al.*, *Metabolism* **44**, 954 (Jul, 1995).
87. F. S. Facchini, N. Hua, F. Abbasi, G. M. Reaven, *J Clin Endocrinol Metab* **86**, 3574 (Aug, 2001).
88. A. Bartke, *Clin Interv Aging* **3**, 659 (2008).
89. A. G. Renehan *et al.*, *Lancet* **363**, 1346 (Apr 24, 2004).
90. A. G. Renehan *et al.*, *Horm Metab Res* **35**, 712 (Nov-Dec, 2003).

91. X. Zhang *et al.*, *Carcinogenesis* **28**, 143 (Jan, 2007).
92. Z. Wang *et al.*, *Endocrinology* **149**, 1366 (Mar, 2008).
93. Q. Shen *et al.*, *Endocrinology* **148**, 4536 (Oct, 2007).
94. H. M. Khandwala, I. E. McCutcheon, A. Flyvbjerg, K. E. Friend, *Endocr Rev* **21**, 215 (Jun, 2000).
95. T. Zhu *et al.*, *Cancer Res* **65**, 317 (Jan 1, 2005).
96. S. Mukhina *et al.*, *Proc Natl Acad Sci U S A* **101**, 15166 (Oct 19, 2004).
97. M. Raccurt *et al.*, *J Endocrinol* **175**, 307 (November 1, 2002, 2002).
98. M. J. Waters, B. L. Conway-Campbell, *Proc Natl Acad Sci U S A* **101**, 14992 (Oct 19, 2004).
99. B. I. Posner, P. A. Kelly, R. P. Shiu, H. G. Friesen, *Endocrinology* **95**, 521 (Aug, 1974).
100. P. A. Kelly, J. Djiane, M. C. Postel-Vinay, M. Edery, *Endocr Rev* **12**, 235 (1991).
101. P. J. Godowski *et al.*, *Proc Natl Acad Sci U S A* **86**, 8083 (Oct, 1989).
102. D. W. Leung *et al.*, *Nature* **330**, 537 (Dec 10-16, 1987).
103. C. J. Bagley, J. M. Woodcock, F. C. Stomski, A. F. Lopez, in *Blood*. (1997), vol. 89,, pp. 1471-1482.
104. J. W. Baumgartner, C. A. Wells, C. M. Chen, M. J. Waters, *J Biol Chem* **269**, 29094 (Nov 18, 1994).
105. A. M. de Vos, M. Ultsch, A. A. Kossiakoff, *Science* **255**, 306 (1992).
106. G. Fuh *et al.*, *J. Biol. Chem.* **265,**, 3111 (1990).
107. J. Gent, P. van Kerkhof, M. Roza, G. Bu, G. J. Strous, *Proc Nat Acad Sci USA* **99**, 9858 (July 23, 2002, 2002).
108. P. van Kerkhof, M. Smeets, G. J. Strous, *Endocrinology* **143**, 1243 (Apr 1, 2002).
109. G. J. Strous, P. van Kerkhof, R. Govers, P. Rotwein, A. L. Schwartz, *J. Biol. Chem.* **272**, 40 (1997).
110. P. van Kerkhof, M. Sachse, J. Klumperman, G. J. Strous, *J. Biol. Chem.* **276**, 3778 (2000).
111. P. van Kerkhof, G. J. Strous, *Biochem Soc Trans* **29**, 488 (2001).
112. A. Sotiropoulos *et al.*, *Endocrinology* **132**, 1863 (1993).
113. Y. Zhang, J. Jiang, R. A. Black, G. Baumann, S. J. Frank, *Endocrinology* **141**, 4342 (Dec, 2000).
114. T. Amit, M. B. Youdim, Z. Hochberg, *J Clin Endocrinol Metab* **85**, 927 (Mar, 2000).
115. Y. Zhang *et al.*, *J Biol Chem* **276**, 24565 (Jul 6, 2001).
116. G. Baumann, *J Pediatr Endocrinol Metab* **14**, 355 (Apr, 2001).
117. G. J. Strous, P. van Kerkhof, *Mol Cell Endocrinol* **197**, 143 (Nov 29, 2002).
118. I. Firmbach-Kraft, M. Byers, T. Shows, R. Dalla-Favera, J. J. Krolewski, *Oncogene* **5**, 1329 (Sep, 1990).
119. L. S. Argetsinger *et al.*, *Cell* **74**, 237 (1993).
120. R. J. Brown *et al.*, *Nat Struct Mol Biol*, (Aug 21, 2005).
121. S. J. Frank *et al.*, *J Biol Chem* **270**, 14776 (Jun 16, 1995).
122. P. Saharinen, M. Vihinen, O. Silvennoinen, *Mol Biol Cell* **14**, 1448 (Apr, 2003).
123. V. Lacronique *et al.*, *Science* **278**, 1309 (Nov 14, 1997).
124. R. Kralovics *et al.*, *N Engl J Med* **352**, 1779 (Apr 28, 2005).
125. T. S. Lee *et al.*, *Cancer* **115**, 1692 (Apr 15, 2009).
126. L. Zhao *et al.*, *J Biol Chem* **284**, 26988 (Sep 25, 2009).
127. J. Feng *et al.*, *Mol Cell Biol* **17**, 2497 (May, 1997).
128. M. Funakoshi-Tago, S. Pelletier, T. Matsuda, E. Parganas, J. N. Ihle, *Embo J* **25**, 4763 (Oct 18, 2006).
129. J. H. Kurzer *et al.*, *Mol Cell Biol* **24**, 4557 (May 15
Jul, 2004).
130. L. S. Argetsinger *et al.*, *Mol Cell Biol* **24**, 4955 (Jun, 2004).
131. T. Zhu, L. Ling, P. E. Lobie, *J Biol Chem* **277**, 45592 (November 22, 2002).
132. S. W. Rowlinson *et al.*, *Nat Cell Biol* **10**, 740 (Jun, 2008).
133. J. L. Barclay *et al.*, *Mol Endocrinol* **24**, 204 (Jan, 2010).
134. J. N. Ihle, *Curr Opin Cell Biol* **13**, 211 (Apr, 2001).
135. M. Chatterjee-Kishore, F. van den Akker, G. R. Stark, *Trends Cell Biol* **10**, 106 (2000).

136. J. Herrington, L. S. Smit, J. Schwartz, C. CarterSu, **19**, 2585 (2000).
137. D. J. Waxman, C. O'Connor, *Mol Endocrinol*, (Mar 16, 2006).
138. J. Woelfle, D. J. Chia, P. Rotwein, *J Biol Chem*, (Oct 7, 2003).
139. R. G. Rosenfeld *et al.*, *Pediatr Nephrol* **20**, 303 (Mar, 2005).
140. W. S. Yi *et al.*, *Mol.Endocrinol.* **10**, 1425 (1996).
141. L. H. Hansen *et al.*, *J Biol Chem* **271**, 12669 (May 24, 1996).
142. L. S. Smit *et al.*, *Mol. Endocrinol.* **10**, 519 (1996).
143. A. C. P. Thirone, C. R. O. Carvalho, M. J. A. Saad, *Endocrinology* **140**, 55 (1999).
144. J. A. Vanderkuur *et al.*, *Endocrinology* **138**, 4301 (Oct, 1997).
145. S. J. Frank, *Growth Horm IGF Res* **11**, 201 (Aug, 2001).
146. T. Decker, P. Kovarik, *Oncogene* **19**, 2628 (May 15, 2000).
147. T. J. Pircher, H. Petersen, J. A. Gustafsson, L. A. Haldosen, *Mol Endocrinol* **13**, 555 (Apr, 1999).
148. T. Yamauchi *et al.*, *Nature* **390**, 91 (1997).
149. S. O. Kim *et al.*, *J Biol Chem* **274**, 36015 (1999).
150. T. Zhu, P. E. Lobie, *J Biol Chem* **275**, 2103 (2000).
151. T. Zhu, E. L. K. Goh, D. Leroith, P. E. Lobie, *Journal of Biological Chemistry* **273**, 33864 (1998).
152. T. Yamauchi *et al.*, *J Biol Chem* **273**, 15719 (Jun 19, 1998).
153. I. Yokota *et al.*, in *Biochimica et Biophysica Acta - Molecular Cell Research*. (1998), vol. 1404, pp. 451-456.
154. M. Ridderstrale, H. Tornqvist, *Biochem Biophys Res Commun* **203**, 306 (Aug 30, 1994).
155. J. A. Costoya *et al.*, *Endocrinology* **140**, 5937 (Dec, 1999).
156. S. J. MacKenzie *et al.*, *Proc Nat Acad Sci USA* **95**, 3549 (1998).
157. A. Flores-Morales, C. J. Greenhalgh, G. Norstedt, E. Rico-Bautista, *Mol Endocrinol* **20**, 241 (February 1, 2006, 2006).
158. B. T. Kile *et al.*, *Trends Biochem Sci* **27**, 235 (May, 2002).
159. H. Yasukawa *et al.*, *Embo J.* **18**, 1309 (1999).
160. A. Sasaki *et al.*, *Genes Cells* **4**, 339 (Jun, 1999).
161. P. A. Ram, D. J. Waxman, *J. Biol. Chem.* **274**, 35553 (1999).
162. D. Ungureanu, P. Saharinen, I. Junttila, D. J. Hilton, O. Silvennoinen, *Mol Cell Biol* **22**, 3316 (May 15, 2002).
163. T. Landsman, D. J. Waxman, *J. Biol. Chem.* **280**, 37471 (November 11, 2005, 2005).
164. K. C. Leung *et al.*, *Proc Natl Acad Sci U S A*, (Jan 27, 2003).
165. G. Yumet, M. L. Shumate, D. P. Bryant, C. H. Lang, R. N. Cooney, *Crit Care Med* **34**, 1420 (May, 2006).
166. W. S. Alexander *et al.*, *Cell* **98**, 597 (1999).
167. B. A. Croker *et al.*, *Nat Immunol* **4**, 540 (Jun, 2003).
168. R. Starr *et al.*, *Proc Natl Acad Sci U S A* **95**, 14395 (Nov 24, 1998).
169. R. H. Hackett *et al.*, *J. Biol. Chem.* **272**, 11128 (1997).
170. S. O. Kim, J. Jiang, W. Yi, G. S. Feng, S. J. Frank, *J Biol Chem* **273**, 2344 (Jan 23, 1998).
171. M. R. Stofega, J. Herrington, N. Billestrup, C. Carter-Su, *Mol Endocrinol* **14**, 1338 (Sep, 2000).
172. M. R. Stofega, L. S. Argetsinger, H. Wang, A. Ullrich, C. Carter-Su, *J Biol Chem* **275**, 28222 (Sep 8, 2000).
173. C. Pasquali *et al.*, *Mol Endocrinol*, (Aug 7, 2003).
174. F. Gu *et al.*, *Mol Cell Biol* **23**, 3753 (Jun, 2003).
175. J. Irie-Sasaki *et al.*, *Nature* **409**, 349 (2001).
176. K. Rakesh, D. K. Agrawal, *Biochem Pharmacol* **70**, 649 (Sep 1, 2005).
177. S. Moutoussamy, F. Renaudie, F. Lago, P. A. Kelly, J. Finidori, *J Biol Chem* **273**, 15906 (1998).
178. L. Rui, C. Carter-Su, *Proc Natl Acad Sci U S A* **96**, 7172 (Jun 22, 1999).
179. V. Birzniece, A. Sata, K. K. Ho, *Rev Endocr Metab Disord* **10**, 145 (Jun, 2009).
180. S. von Laue, R. J. Ross, *Growth Horm IGF Res* **10 Suppl B**, S9 (Apr, 2000).
181. K. Loesch *et al.*, *Endocrinology* **147**, 2839 (June 1, 2006, 2006).

182. J. H. Hurley, H. Stenmark, *Annu Rev Biophys*, (Jul 21, 2010).
183. R. Kölling, C. P. Hollenberg, *EMBO J.* **13**, 3261 (1994).
184. G. J. Strous, P. van Kerkhof, R. Govers, A. Ciechanover, A. L. Schwartz, *EMBO J.* **15**, 3806 (1996).
185. M. J. Clague, S. Urbe, *Trends Cell Biol* **16**, 551 (Nov, 2006).
186. E. Lauwers, C. Jacob, B. Andre, *J Cell Biol* **185**, 493 (May 4, 2009).
187. L. M. Duncan *et al.*, *Embo J* **25**, 1635 (Apr 19, 2006).
188. T. Geetha, M. W. Wooten, *Traffic* **9**, 1146 (Jul, 2008).
189. I. Dikic, S. Wakatsuki, K. J. Walters, *Nat Rev Mol Cell Biol* **10**, 659 (Oct, 2009).
190. X. Ren, J. H. Hurley, *EMBO J* **29**, 1045 (Mar 17, 2010).
191. R. L. Williams, S. Urbe, *Nat Rev Mol Cell Biol* **8**, 355 (May, 2007).
192. M. H. Wright, I. Berlin, P. D. Nash, *Cell Biochem Biophys*, (Mar 30, 2011).
193. F. Reggiori, H. R. Pelham, *Embo J* **20**, 5176 (2001).
194. D. O. Spormann, J. Heim, D. H. Wolf, *J Biol Chem* **267**, 8021 (Apr 25, 1992).
195. D. J. Katzmann, S. Sarkar, T. Chu, A. Audhya, S. D. Emr, *Mol. Biol. Cell* **15**, 468 (February 1, 2004, 2004).
196. D. J. Katzmann, M. Babst, S. D. Emr, *Cell* **106**, 145 (2001).
197. M. B. Butterworth, *Biochim Biophys Acta* **1802**, 1166 (Dec, 2010).
198. O. Staub *et al.*, *EMBO J.* **16**, 6325 (1997).
199. R. Zhou, R. Kabra, D. R. Olson, R. C. Piper, P. M. Snyder, *J Biol Chem* **285**, 30523 (Oct 1, 2010).
200. M. B. Butterworth *et al.*, *J Biol Chem* **282**, 37885 (Dec 28, 2007).
201. P. Fakitsas *et al.*, *J Am Soc Nephrol* **18**, 1084 (Apr, 2007).
202. E. Witsch, M. Sela, Y. Yarden, *Physiology (Bethesda)* **25**, 85 (Apr, 2010).
203. K. M. Ferguson *et al.*, *Mol Cell* **11**, 507 (Feb, 2003).
204. Y. Yarden, *Eur J Cancer* **37**, 3 (2001).
205. G. Levkowitz *et al.*, *Genes Dev* **12**, 3663 (1998).
206. I. H. Madshus, E. Stang, *J Cell Sci* **122**, 3433 (Oct 1, 2009).
207. S. Sigismund *et al.*, *Proc Natl Acad Sci U S A* **102**, 2760 (Feb 22, 2005).
208. R. Govers, P. van Kerkhof, A. L. Schwartz, G. J. Strous, *EMBO J.* **16**, 4851 (1997).
209. R. Govers, T. ten Broeke, P. van Kerkhof, A. L. Schwartz, G. J. Strous, *EMBO J.* **18**, 28 (1999).
210. R. Govers, P. van Kerkhof, A. L. Schwartz, G. J. Strous, *J. Biol. Chem.* **273**, 16426 (1998).
211. P. van Kerkhof, J. Putters, G. J. Strous, *J. Biol. Chem.* **282**, 20475 (July 13, 2007, 2007).
212. P. van Kerkhof, M. Westgeest, G. Hassink, G. J. Strous, *Exp Cell Res* **317**, 1071 (Apr 15, 2011).
213. J. Putters *et al.*, *PLoS One* **6**, e14676 (2011).
214. K. Iwai, F. Tokunaga, *EMBO Rep* **10**, 706 (Jul, 2009).
215. F. Tokunaga *et al.*, *Nat Cell Biol* **11**, 123 (Feb, 2009).
216. Z. Hua, R. D. Vierstra, *Annu Rev Plant Biol*, (May 18, 2010).
217. L. Bedford, J. Lowe, L. R. Dick, R. J. Mayer, J. E. Brownell, *Nat Rev Drug Discov* **10**, 29 (Jan, 2011).
218. B. A. Schulman, J. W. Harper, *Nat Rev Mol Cell Biol* **10**, 319 (May, 2009).
219. E. E. Patton, A. R. Willems, M. Tyers, *Trends in Genetics* **14**, 236 (1998).
220. N. Zheng *et al.*, *Nature* **416**, 703 (Apr 18, 2002).
221. D. Frescas, M. Pagano, *Nat Rev Cancer* **8**, 438 (Jun, 2008).
222. J. M. Galan, M. Peter, *Proc Natl Acad Sci U S A* **96**, 9124 (Aug 3, 1999).
223. P. Zhou, P. M. Howley, *Mol Cell* **2**, 571 (Nov, 1998).
224. H. Suzuki *et al.*, *Journal of Biological Chemistry* **275**, 2877 (2000).
225. E. H. Chew, T. Poobalasingam, C. J. Hawkey, T. Hagen, *Cell Signal* **19**, 1071 (May, 2007).
226. X. Tang *et al.*, *Cell* **129**, 1165 (Jun 15, 2007).
227. D. Liakopoulos, G. Doenges, K. Matuschewski, S. Jentsch, *EMBO J.* **17**, 2208 (1998).
228. M. A. Read *et al.*, *Mol Cell Biol* **20**, 2326 (Apr, 2000).
229. E. Sakata *et al.*, *Nat Struct Mol Biol* **14**, 167 (Feb, 2007).

230. S. Lyapina *et al.*, *Science* **292**, 1382 (May 18, 2001).
231. C. Schwechheimer, *Biochim Biophys Acta* **1695**, 45 (Nov 29, 2004).
232. S. J. Goldenberg *et al.*, *Cell* **119**, 517 (Nov 12, 2004).
233. D. R. Bosu, E. T. Kipreos, *Cell Div* **3**, 7 (2008).
234. J. R. Skaar, J. K. Pagan, M. Pagano, *Cell* **137**, 1160 (Jun 12, 2009).
235. C. Bai *et al.*, *Cell* **86**, 263 (1996).
236. J. D. Laney, M. Hochstrasser, *Cell* **97**, 427 (1999).
237. T. Maniatis, *Genes & Development* **13**, 505 (1999).
238. D. Guardavaccaro *et al.*, *Developmental Cell* **4**, 799 (2003).
239. K. Nakayama *et al.*, *PNAS* **100**, 8752 (July 22, 2003, 2003).
240. J. Putters, J. A. Slotman, J. P. Gerlach, G. J. Strous, *Cell Signal* **23**, 641 (Apr, 2011).
241. A. Yaron *et al.*, *Nature* **396**, 590 (Dec 10, 1998).
242. J. Koike *et al.*, *Biochem Biophys Res Commun* **269**, 103 (Mar 5, 2000).
243. F. Margottin *et al.*, *Mol Cell* **1**, 565 (1998).
244. A. Yaron *et al.*, *Nature* **396**, 590 (1998).
245. S. Y. Fuchs, A. Chen, Y. Xiong, Z. Q. Pan, Z. Ronai, *Oncogene* **18**, 2039 (1999).
246. S. Hatakeyama *et al.*, *Proceedings of the National Academy of Sciences of the United States of America* **96**, 3859 (1999).
247. M. Kitagawa *et al.*, *Embo Journal* **18**, 2401 (1999).
248. E. Spencer, J. Jiang, Z. J. J. Chen, *Genes & Development* **13**, 284 (1999).
249. H. Suzuki *et al.*, *Biochemical and Biophysical Research Communications* **256**, 127 (1999).
250. G. Wu *et al.*, *Mol Cell* **11**, 1445 (Jun, 2003).
251. P. Tan *et al.*, *Molecular cell* **3**, 527 (Apr, 1999).
252. J. T. Winston *et al.*, *Genes Dev* **13**, 270 (Feb 1, 1999).
253. E. Latres, D. S. Chiaur, M. Pagano, *Oncogene* **18**, 849 (Jan 28, 1999).
254. M. Hart *et al.*, *Curr Biol* **9**, 207 (Feb 25, 1999).
255. Z. J. Chen, L. Parent, T. Maniatis, *Cell* **84**, 853 (Mar 22, 1996).
256. K. G. Kumar *et al.*, *Embo J* **22**, 5480 (Oct 15, 2003).
257. Y. Li, K. G. Kumar, W. Tang, V. S. Spiegelman, S. Y. Fuchs, *Molecular and cellular biology* **24**, 4038 (May, 2004).
258. L. Meyer *et al.*, *Blood* **109**, 5215 (Jun 15, 2007).
259. J. Liu *et al.*, *Cell host & microbe* **5**, 72 (Jan 22, 2009).
260. E. S. Lightcap *et al.*, *Clin Chem* **46**, 673 (May, 2000).
261. M. Aghajan *et al.*, *Nat Biotechnol* **28**, 738 (Jul, 2010).
262. S. Orlicky *et al.*, *Nat Biotechnol* **28**, 733 (Jul, 2010).
263. Y. Yang *et al.*, *Cancer Res* **67**, 9472 (Oct 1, 2007).
264. G. W. Xu *et al.*, *Blood* **115**, 2251 (Mar 18, 2010).
265. T. A. Soucy *et al.*, *Nature* **458**, 732 (Apr 9, 2009).
266. T. A. Soucy, P. G. Smith, M. Rolfe, *Clin Cancer Res* **15**, 3912 (Jun 15, 2009).
267. M. A. Milhollen *et al.*, *Blood* **116**, 1515 (Sep 2, 2010).
268. R. T. Swords *et al.*, *Blood* **115**, 3796 (May 6, 2010).
269. H. Maeda *et al.*, *Mol Cancer Res* **7**, 1553 (Sep, 2009).
270. X. Duan, J. O. Trent, H. Ye, *Anticancer Agents Med Chem* **9**, 51 (Jan, 2009).
271. S. Zhu, M. Sachdeva, F. Wu, Z. Lu, Y. Y. Mo, *Oncogene* **29**, 1763 (Mar 25, 2010).
272. J. Hao *et al.*, *Tumour Biol* **29**, 195 (2008).
273. J. H. van Ree, K. B. Jeganathan, L. Malureanu, J. M. van Deursen, *J Cell Biol* **188**, 83 (Jan 11, 2010).
274. S. Chen *et al.*, *J Cancer Res Clin Oncol* **136**, 419 (Mar, 2010).
275. D. T. Huang *et al.*, *Nat Struct Mol Biol* **11**, 927 (Oct, 2004).
276. L. Daviet, F. Colland, *Biochimie* **90**, 270 (Feb, 2008).
277. A. K. Ghosh *et al.*, *J Med Chem* **52**, 5228 (Aug 27, 2009).
278. K. Ratia *et al.*, *Proc Natl Acad Sci U S A* **105**, 16119 (Oct 21, 2008).

279. A. M. Katz, P. B. Katz, *Br Heart J* **24**, 257 (May, 1962).
280. W. J. Evans *et al.*, *Clin Nutr* **27**, 793 (Dec, 2008).
281. R. Roubenoff, J. J. Kehayias, *Nutr Rev* **49**, 163 (Jun, 1991).
282. W. D. Dewys *et al.*, *Am J Med* **69**, 491 (Oct, 1980).
283. A. Laviano, M. M. Meguid, A. Inui, M. Muscaritoli, F. Rossi-Fanelli, *Nat Clin Pract Oncol* **2**, 158 (Mar, 2005).
284. S. D. Anker *et al.*, *Lancet* **349**, 1050 (Apr 12, 1997).
285. D. Glass, R. Roubenoff, *Ann N Y Acad Sci* **1211**, 25 (Nov, 2010).
286. C. A. Wanke *et al.*, *Clin Infect Dis* **31**, 803 (Sep, 2000).
287. R. Roubenoff *et al.*, *J Clin Invest* **93**, 2379 (Jun, 1994).
288. S. C. Bodine *et al.*, *Science*, (Oct 25, 2001).
289. M. D. Gomes, S. H. Lecker, R. T. Jagoe, A. Navon, A. L. Goldberg, *Proc Natl Acad Sci U S A* **98**, 14440 (Dec 4, 2001).
290. S. Cohen *et al.*, *J Cell Biol* **185**, 1083 (Jun 15, 2009).
291. B. A. Clarke *et al.*, *Cell Metab* **6**, 376 (Nov, 2007).
292. L. A. Tintignac *et al.*, *J Biol Chem* **280**, 2847 (Jan 28, 2005).
293. J. Lagirand-Cantaloube *et al.*, *EMBO J* **27**, 1266 (Apr 23, 2008).
294. A. Csibi, M. P. Leibovitch, K. Cornille, L. A. Tintignac, S. A. Leibovitch, *J Biol Chem* **284**, 4413 (Feb 13, 2009).
295. M. Sandri *et al.*, *Cell* **117**, 399 (Apr 30, 2004).
296. T. N. Stitt *et al.*, *Mol Cell* **14**, 395 (May 7, 2004).
297. S. W. Lee *et al.*, *J Am Soc Nephrol* **15**, 1537 (Jun, 2004).
298. A. C. McPherron, A. M. Lawler, S. J. Lee, *Nature* **387**, 83 (May 1, 1997).
299. A. C. McPherron, S. J. Lee, *Proc Natl Acad Sci U S A* **94**, 12457 (Nov 11, 1997).
300. A. U. Trendelenburg *et al.*, *Am J Physiol Cell Physiol* **296**, C1258 (Jun, 2009).
301. R. Sartori *et al.*, *Am J Physiol Cell Physiol* **296**, C1248 (Jun, 2009).
302. R. Talar-Wojnarowska *et al.*, *Neoplasma* **56**, 56 (2009).
303. M. B. Reid, Y. P. Li, *Respir Res* **2**, 269 (2001).
304. J. M. Argiles, S. Busquets, M. Toledo, F. J. Lopez-Soriano, *Curr Opin Support Palliat Care* **3**, 263 (Dec, 2009).
305. H. R. Scott, D. C. McMillan, A. Crilly, C. S. McArdle, R. Milroy, *Br J Cancer* **73**, 1560 (Jun, 1996).
306. S. Iwase, T. Murakami, Y. Saito, K. Nakagawa, *Eur Cytokine Netw* **15**, 312 (Oct-Dec, 2004).
307. G. Strassmann, M. Fong, J. S. Kenney, C. O. Jacob, *J Clin Invest* **89**, 1681 (May, 1992).
308. P. Matthys, H. Heremans, G. Opdenakker, A. Billiau, *Eur J Cancer* **27**, 182 (1991).
309. P. Matthys *et al.*, *Int J Cancer* **49**, 77 (Aug 19, 1991).
310. Z. Laron, *Birth Defects Orig Artic Ser* **10**, 231 (1974).
311. G. Mazzoccoli *et al.*, *Anticancer Res* **19**, 1397 (Mar-Apr, 1999).
312. R. Ross *et al.*, *Clin Endocrinol (Oxf)* **35**, 47 (Jul, 1991).
313. J. Bentham, J. Rodriguez-Arnao, R. J. Ross, *Horm Res* **40**, 87 (1993).
314. M. S. Dahn, M. P. Lange, L. A. Jacobs, *Arch Surg* **123**, 1409 (Nov, 1988).
315. M. Gottardis *et al.*, *J Trauma* **31**, 81 (Jan, 1991).
316. J. A. Tayek, J. A. Brasel, *J Clin Endocrinol Metab* **80**, 2082 (Jul, 1995).
317. R. C. Jenkins, R. J. Ross, *Baillieres Clin Endocrinol Metab* **10**, 411 (Jul, 1996).
318. W. J. Chwals, B. R. Bistrian, *Crit Care Med* **19**, 1317 (Oct, 1991).
319. B. M. Moats-Staats, J. L. Brady, Jr., L. E. Underwood, A. J. D'Ercole, *Endocrinology* **125**, 2368 (Nov, 1989).
320. F. De Benedetti *et al.*, *J Clin Invest* **99**, 643 (Feb 15, 1997).
321. P. Wang, N. Li, J. S. Li, W. Q. Li, *World J Gastroenterol* **8**, 531 (Jun, 2002).
322. J. P. Thissen, J. Verniers, *Endocrinology* **138**, 1078 (Mar, 1997).
323. L. M. Difedele *et al.*, *Gastroenterology* **128**, 1278 (May, 2005).

324. V. Beauloye, J. M. Ketelslegers, B. Moreau, J. P. Thissen, *Growth Horm IGF Res* **9**, 205 (Jun, 1999).
325. J. M. Luo, L. J. Murphy, *Endocrinology* **125**, 165 (Jul, 1989).
326. R. Roubenoff, V. A. Hughes, *J Gerontol A Biol Sci Med Sci* **55**, M716 (Dec, 2000).
327. F. Penna *et al.*, *Expert Opin Biol Ther* **10**, 1241 (Aug, 2010).
328. E. Tazi, H. Errihani, *Indian J Palliat Care* **16**, 129 (Sep, 2010).
329. J. E. Morley *et al.*, *Metabolism* **46**, 410 (Apr, 1997).
330. S. Grinspoon *et al.*, *Clin Infect Dis* **28**, 634 (Mar, 1999).
331. S. Bhasin *et al.*, *JAMA* **283**, 763 (Feb 9, 2000).
332. S. Grinspoon *et al.*, *J Clin Endocrinol Metab* **82**, 1332 (May, 1997).
333. R. Casaburi *et al.*, *Am J Respir Crit Care Med* **170**, 870 (Oct 15, 2004).
334. P. E. Knapp *et al.*, *Am J Physiol Endocrinol Metab* **294**, E1135 (Jun, 2008).
335. K. R. Wagner *et al.*, *Ann Neurol* **63**, 561 (May, 2008).
336. M. Gelato, M. McNurlan, E. Freedland, *Clin Ther* **29**, 2269 (Nov, 2007).
337. O. Mehls, S. Haas, *Growth Horm IGF Res* **10 Suppl B**, S31 (Apr, 2000).
338. M. Cicoira, P. R. Kalra, S. D. Anker, *J Card Fail* **9**, 219 (Jun, 2003).
339. T. R. Ziegler, L. S. Young, J. M. Manson, D. W. Wilmore, *Ann Surg* **208**, 6 (Jul, 1988).
340. T. A. Byrne *et al.*, *Ann Surg* **218**, 400 (Oct, 1993).
341. L. B. Pupim, P. J. Flakoll, C. Yu, T. A. Ikizler, *Am J Clin Nutr* **82**, 1235 (Dec, 2005).
342. T. A. Byrne *et al.*, *Ann Surg* **242**, 655 (Nov, 2005).
343. M. M. Kamiji, A. Inui, *Curr Opin Clin Nutr Metab Care* **11**, 443 (Jul, 2008).
344. M. D. DeBoer, *Nutrition* **24**, 806 (Sep, 2008).
345. F. Strasser *et al.*, *Br J Cancer* **98**, 300 (Jan 29, 2008).
346. N. Nagaya *et al.*, *Circulation* **110**, 3674 (Dec 14, 2004).
347. N. Nagaya *et al.*, *Chest* **128**, 1187 (Sep, 2005).

βTrCP controls growth hormone receptor degradation via two different motifs

2

Ana C. da Silva Almeida[1,2], Ger J Strous[1], Agnes G S H van Rossum[1,2]

[1] Department of Cell Biology and Institute of Biomembranes, University Medical Center Utrecht, Heidelberglaan 100, 3584 CX Utrecht, The Netherlands

[2] Drug Discovery Factory BV, Albrechtlaan 14A, 1404 AK Bussum, The Netherlands

(Manuscript submitted)

Abstract

The physiological roles of growth hormone (GH) are broad and include metabolism regulation and promotion of somatic growth. Therefore, the responsiveness of cells to GH must be tightly regulated. This is mainly achieved by a complex and well-controlled mechanism of GH receptor (GHR) endocytosis. GHR endocytosis occurs independently of GH and requires the ubiquitin ligase SCF(βTrCP) that is recruited to the ubiquitin-dependent endocytosis (UbE) motif in the cytoplasmic tail of the GHR. In this study we report that, in addition to the UbE motif, a downstream degron, DSGRTS, binds to βTrCP. The WD40 residues on βTrCP involved in the interaction with this sequence are identical to the ones necessary for binding the "classical" motif, DSGxxS, in IκB, and βcatenin. Previously, we showed that this motif is not involved in GH-induced endocytosis. We show here that the DSGRTS sequence significantly contributes to GHR endocytosis/degradation in basal conditions, while the UbE motif is involved both in basal and GH-induced conditions. These findings explain the high rate of GHR degradation under basal conditions, which is important for regulating the responsiveness of cells to GH.

Introduction

Growth Hormone (GH) is a 22-kDa peptide produced in the anterior pituitary gland, under the control of GH releasing hormone (GHRH) and somatostatin. GH is widely used, clinically, to promote growth and metabolism (1). GH exerts its extensive physiological actions by binding the GH receptor (GHR). GHR is a protein of 620 amino acids, and although expressed in all tissues, GHR is mainly found in the liver, adipose tissue and muscle. The receptor is synthesized in the endoplasmic reticulum, processed in the Golgi complex, and transported to the plasma membrane as a dimer (5). GHR is a member of the class 1 superfamily of cytokine receptors, together with prolactin receptor (PRLR), interferon α receptor (IFNAR), erythropoietin receptor (EpoR), interleukins receptors, among others. Similarly to other cytokine receptors, GHR does not have intrinsic kinase activity. Asymmetric GH binding to the extracellular domain of GHR dimer induces a conformational change (2) that results in the cross-activation of two JAK2 molecules associated to box 1 of the GHR cytoplasmic tail. Although JAK-STAT pathway is the major effector of GHR signaling, by inducing IGF-1 expression (3), strong evidence indicates that Src family kinases are directly activated upon GH binding (4).

Effective GH signaling not only depends on the amounts of GH in circulation but also on the availability of GHRs at the cells surface. In order to control responsiveness of cells to GH, the amounts of GHRs are dynamically regulated, reflecting a balance of receptor endocytosis/degradation, and transport of newly synthesized receptors to the plasma membrane (6). GHR turnover is rapid and occurs constitutively; in the presence of GH the receptor degradation is accelerated, probably due to the release of JAK2 from the GHR (7-9).

Endocytosis of GHR depends on a functional ubiquitin conjugation system (10). This dependency is related to the presence of the ubiquitin-dependent endocytosis (UbE) motif in the cytoplasmic tail of the receptor. Recently, we identified β-transducing repeat-containing protein (βTrCP) as an essential factor for GHR endocytosis and degradation, through its recruitment to this motif (11). βTrCP is the F-box substrate recognition subunit of a multi-subunit cullin-based E3 ligase, SCF(βTrCP) (12). βTrCP recognizes the degron, $DSGx_{n2-4}S$, where x represents a hydrophobic residue, only if the two serines are phosphorylated. Classical examples of βTrCP substrates are βcatenin and IκB which have GSK3β and IKK, as regulatory kinases, respectively (12-16).

Interestingly, in addition to the UbE motif, GHR contains a conserved sequence corresponding to the classical βTrCP degron, the DSGRTS sequence. Endocytosis of homologous cytokine receptors, such as IFNAR (17), PRLR (18), and EpoR (19), depends on βTrCP binding to the classical degron when the two serines are phosphorylated after ligand binding. βTrCP acts, therefore, as a negative regulator of signaling of these receptors (17-19). Our previous studies indicated that the DSGRTS sequence was not involved in GH-induced endocytosis (9, 11). However, an important difference between GHR and other homologous receptors is its very high rate of basal degradation (at steady state in the absence of GH).

Since the phosphorylated DSGRTS sequence displays an intrinsic affinity for βTrCP, we hypothesized that it might play a role in the endocytosis of GHR under different conditions. Of note is that βTrCP binding through the UbE motif is important for both basal, and GH-induced endocytosis (20).

In this study, we show that two motifs bind βTrCP and contribute to the endocytosis/degradation of GHR, under basal conditions. Stimulation with GH results in a predominant role of UbE motif. Therefore, in addition to the UbE motif, the DSGRTS sequence significantly contributes to the GHR homeostasis of cells. This study reveals an interplay between two βTrCP binding motifs in the GHR tail, with important implications for understanding the mechanisms controlling the responsiveness of the cells to GH.

Materials and methods

Reagents

GHR antibodies (anti-T and anti-B) recognizing aminoacid residues 271–318 and aminoacids 327-493 of GHR, respectively, were raised in rabbit (51) (10). Monoclonal antibody against ubiquitin (clone FK2) was purchased from Biomol (Raamsdonksveer, The Netherlands), anti-actin (Clone C4) was obtained from MP Biomedicals Inc (Amsterdam, The Netherlands), and Monoclonal anti-Flag (M2) from Sigma (Saint Louis, MO, USA). Goat anti-mouse IgG Alexa 680 was from Molecular Probes (Eugene, OR, USA, and Goat anti-rabbit IgG IR Dye800 from Rockland Immunochemicals Inc (Gilbertsville, PA, USA). Streptavidin beads were purchased from Pierce (Rockford, IL, USA). Protein A-beads were purchased from Repligen (Waltham, MA, USA). Human GH was a kind gift from Eli Lilly Research Labs (Indianapolis, IN, USA). Biotinylated-GH (biotin-GH) was made according to the manufacturer's protocol, Pierce. Cycloheximide was purchased from Sigma.

DNA constructs

Full-length rabbit GHR cDNA in pcDNA3 has been previously described (10). The mutations were inserted with Quick Change mutagenesis kit from Stratagene (Santa Clara, CA, USA). GHR F327A pcDNA3 construct was generated as described before (20). GHR DAGxxA (S366A, S370A) was generated with the oligonucleotides,
5'_GGATGACGACGCTGGACGAACCGCCTGTTACGAACC_3' and
3'_CCTACTGCTGCGACCTGCTTGGCGGACAATGCTTGG, on GHR WT template. The same oligonucleotides were used on GHR F327A template, to generate the double mutant F327A+DAGxxA.GHR DEGxxE was generated with the oligonucleotides, 5'_ GCAAAGGATGACGACGAGGGACGAACCGAGTGTTACGAACC_3'and 5'_ CGTTTCCTACTGCTGCTCCCTGCTTGGCTCACAATGCTTGG_3', on GHR WT template.

The Flag-tagged wild type mouse βTrCP2 (Flag-βTrCP2) construct was a generous gift from Prof. Carter-Su (University of Michigan, Ann Arbor, USA). Structural studies on βTrCP1 interaction with its substrates revealed that Y271, R431, R474 and Y488 in the WD40 repeats are important for binding to its substrate βcatenin and IκB (25). The WD40 domains of βTrCP1 and 2 are very similar. For the experiments described in this paper we used βTrCP2, since previous results gave indications that this is the most relevant isoform for GHR endocytosis(11). The βTrCP1 residues indicated above are conserved in βTrCP2 (Y244, R404, R447, Y461, respectively). These residues were mutated to alanine with Quick Change mutagenesis kit from Stratagene, using Flag-βTrCP2 as a template, with the following oligonucleotides: Y244 A
(5'_CTGAAAATAGTAAAGGTGTCGCCTGTTTACAGTACG_3' and
3'_GACTTTTATCATTTCCACAGCGGACAAATGTCATGC_5'); R404A (5'_ CAATGGGCACAAGGCGGGCATTGCCTGTCTCC_3' and
3'_GTTACCCGTGTTCCGCCCGTAACGGACAGAGG_5'); R447A (5'_ CATGAAGAATTGGTCGCATGCATCCGGTTTGATAACAAGAGG_3' and 3'_ GTACTTCTTAACCAGCGTACGTAGGCCAAACTATTGTTCTCC_5'); Y461A (5'_GGATTGTCAGTGGGGCCGCTGATGGGAAAATTAAAGTTTGG_3' and
3'_CCTAACAGTCACCCCGGCGACTACCCTTTTAATTTCAAACC_5').

Cell culture, transfections and stable cell lines

Culture media, fetal calf serum and antibiotics for tissue culture were purchased from Gibco (Invitrogen, Groningen, The Netherlands). Human embryonic kidney 293 (HEK293) cells, stably expressing the Tetracycline Repressor (HEK293-TR), were a gift from Dr. Madelon Maurice (University Medical Centre Utrecht, Utrecht, The Netherlands).

HEK293-TR cells were grown in Dulbecco's modified Eagle's medium (DMEM) supplemented with 10% fetal calf serum, 100 units/ml penicillin, 0.1 mg/ml streptomycin and 12 μg/ml Blasticidin S (MP Biomedicals). HEK293-TR cells, stably expressing GHR WT and mutants were maintained in DMEM high glucose (4.5 g/l), supplemented with 10% FCS, 100 units/ml penicillin, 0.1 mg/ml streptomycin, 12 μg/ml Blasticidin S, and 600 μg/ml Geneticin (G418) (Invitrogen). Cells were grown at 37°C with 5.0% CO_2. Twice a week the cells were washed with phosphate-buffered saline (PBS),

detached from the flask with trypsin-EDTA (Invitrogen) diluted in fresh growth medium, and split into new culture flasks. DNA transfections were performed using FuGene 6 (Roche, Applied Sciences, Almere, The Netherlands). Seventy percent confluent cultures in 6-wells plates were transfected with 1 µg of DNA, according to the manufacturer's protocol. For fluorescence microscopy experiments, cells were grown on top of coverslips placed in 12 wells plates and transfected with 0.5 µg of DNA. Twenty four hours after transfection, cells were used for pull down experiments, western blotting, and fluorescence microscopy experiments. HEK293-TR stable cell lines expressing GHR WT, F327A, DAGxxA, and F327A+DAGxxA mutants were created by transfecting HEK293-TR cells with the correspondent constructs, using Fugene 6, according to the manufacturer's instructions. Selection of clones expressing GHR-Rluc was done using Geneticin (G418) (Invitrogen). In conditions of GH stimulation, human GH was added at a concentration of 180 ng/ml. When indicated, cells were treated with 20 µg/ml cycloheximide.

^{125}I binding and internalization

^{125}I-Human GH was prepared using chloramine T (10). For degradation experiments, cells grown in 12-well plates were washed with 1 ml of serum-free DMEM, supplemented with 20mM Hepes pH 7.4, and 0.1% bovine serum albumin, and incubated 60 min at 37ºC. ^{125}I-GH (180 ng/ml in DMEM/Hepes/0.1% bovine serum albumin) was added, and the cells were incubated for 15 min at 37ºC. After 15 min, the unbound ^{125}I-GH was aspirated, and 0.75 ml of DMEM/Hepes/0.1% bovine serum albumin was added to each well, while keeping the plate at 37ºC. After 1 hour of incubation at 37ºC, the medium was collected, and 0.75 ml of ice cold 20% TCA solution was added. The samples were incubated on ice for 30 min to allow the precipitation of the non-degraded GH. TCA-soluble radioactivity was determined in the supernatant after centrifugation and was used as a measurement for degraded ligand. Meanwhile, the cells were washed once with 2 ml ice-cold PBS-c (PBS with 0.135 g/L $CaCl_2$ and 0.1g/L $MgCl_2$). Cell surface ^{125}I-GH was removed by treating the cells twice with 0.75 ml acid wash (0.15 M NaCl, 50 mM glycine, 0.1% bovine serum albumin, pH 2.5) for 5 min on ice. Acid wash was collected in counting tubes, and radioactivity was measured using a LKB counter. Cells were solubilized overnight in 1 N NaOH. Internalized ^{125}I-GH was determined by measuring the radioactivity in the collected NaOH fraction.

For internalization experiments, cells, grown in 12-well plates, were washed with 1 ml of minimal essential medium supplemented with 20 mM Hepes pH7.4, and 0.1% bovine serum albumin, and put on ice. ^{125}I-GH (180 ng/ml in DMEM/Hepes/0.1% bovine serum albumin) was added to the cells. After 2h binding on ice, cells were placed at 37ºC for 15 min, to allow receptor endocytosis. Cells were then washed once with 2 ml of PBS-c (PBS with 0.135g/liter $CaCl_2$ and 0.1 g/liter $MgCl_2$). Cell surface ^{125}I-GH and internalized ^{125}I-GH was determined following the procedure described above. GH internalization at time point 0 and 15 min is expressed as percentage of the total radioactivity (cell surface and internalized). Unspecific counts were determined by incubating the cells with ^{125}I-GH together with excess unlabeled GH (90 µg/ml).

Confocal microscopy

Cy3-GH was prepared using a fluorolink-Cy3 label kit according to the manufacturer's protocol (Amersham Biosciences, Roosendaal, The Netherlands). Transfected cells, grown on coverslips, were incubated for 30 min with Cy3-GH (180ng/ml), washed with PBS and fixed for 30 min in 4% paraformaldeyde in PBS. After fixation, cells were embedded in Mowiol, and confocal pictures were taken using LeicaTCS 4D system.

Biotin-GH pull downs and immunoprecipitations

24 h after transfection, HEK293-TR cells were placed on ice and the medium was replaced with cold DMEM (20 mM Hepes, pH7.4), after which biotin-GH (180 ng/ml) was added. After 2 h of incubation, which result in saturating GHR binding to biotin-GH, cells were washed three times with PBS, and lysed with cold lysis buffer (1% Triton X-100, 1 mM EDTA, 1 mM PMSF, 10 µg/ml aprotinin, 10 µg/ml Leupeptine, 1 mM Na_3VO_4 and 100 mM NaF in PBS) for 20 minutes. After 5 min centrifugation at maximum speed at 4°C, the supernatant was incubated for 1 h with 25 µl streptavidin beads at 4°C. Beads were boiled and subjected to SDS-PAGE, and western blotting. Alternatively, the pull down was also performed by adding biotin-GH (180 ng/ml) directly to the cell culture medium, in

the incubator, at 37°C, for 10 min. The cells were washed three times with the PBS, lysed and the pull down was performed as described above. For ubiquitination experiments, HEK293-TR cells stably expressing GHR variants were lysed in 1% Triton X-100 with inhibitors (1 mM EDTA, 1 mM PMSF, 10 μg/ml aprotinin, 10 μg/ml leupeptin, 10 mM NEM, 1 mM Na_3VO_4 and 100 mM NaF). The cell lysates were centrifuged at maximum speed, for 5 min, at 4°C, and the supernatants were used for GHR isolation with anti-GHR antibody (anti-T) and protein A beads, in 1% Triton X-100, 0.5% SDS, 0.25% sodium deoxycholate, 0.5% BSA and inhibitors. Immunoprecipitates were subjected to reducing SDS-PAGE and western blotting.

Immuno Blotting

Following SDS-PAGE, proteins were transferred to an Immobilion-FL PVDF membrane (Millipore, Amsterdam, The Netherlands). The membranes were blocked with Odyssey blocking buffer (Li-Cor Biosciences, Lincoln, NE, USA) diluted two times with PBS for 1 hour at room temperature. The blots were incubated with the indicated primary antibodies for 1.5 hour, and after washing in PBS 0.1% Tween-20, membranes were incubated for 1 hour with secondary antibody. Detection and analysis of the immunoblots was performed with an Odyssey infrared imaging system (Li-Cor Biosciences, Lincoln, Nebraska).

Statistical analysis

For data analysis SPSS 15.0 was used. All data are presented as means with the standard errors of the means (SEM). The results were analyzed by analysis of variance (ANOVA) at $p \leq 0.05$.

Results

1. The conserved DSGRTS sequence contributes to βTrCP binding.

Our previous studies identified βTrCP as an essential factor for GHR endocytosis (11) as well as for sorting at the multivesicular bodies (MVBs) (21). The role of βTrCP in GHR endocytosis and degradation was dependent on its interaction with the UbE motif (11, 20). However, βTrCP classically recognizes the degron, DSGxxS, when both serines are phosphorylated in substrates such as βcatenin, IκB, PrLR, IFNAR (22). GHR contains such a conserved degron, DSGRTS, 30 amino acid residues downstream of the UbE motif (Fig. 1A). To investigate whether the DSGRTS sequence binds to βTrCP, we generated mutants where either the UbE motif or the DSGRTS sequence were mutated (F327A, DAGxxA, DEGxxE), or both (F327A + DAGxxA). The Phe327 in the UbE has been shown to be critical for GH-induced endocytosis (20, 23, 24), due to a reduced binding to βTrCP (11). Replacement of the serine residues of the DSGRTS sequence with alanine residues (DAGxxA) should render this motif non-functional. On the other hand, replacement of the serine residues to the phosphomimetic glutamate residues (DEGxxE) should result in a constitutively active motif. To investigate the binding affinity of the GHR mutants to βTrCP, pull down experiments were performed. GHR complexes were isolated from HEK293-TR cells expressing Flag-tagged βTrCP (Flag-βTrCP) together with the various GHR constructs as indicated in Fig. 1B, using biotin-GH bound on ice. It is important to note that these conditions do not trigger GH signaling, and reflect basal (steady state) conditions. If we correct the mature receptors for the amounts of precursor (reflecting the synthesis) and we assume that the mutations do not affect the maturation rate, the different mutations in GHR affected the stability of the receptor differently as is apparent from the ratios mature-precursor in the total cell lysates (Fig. 1B, 4th panel; quantified in Fig. 1C, right panel). As previously described, the F327A mutation stabilized the GHR as seen by increased mature form of the GHR. Remarkably, the DAGxxA mutant was stabilized to the same extent as the UbE mutant (Fig. 1B, 4th panel, lane 3;

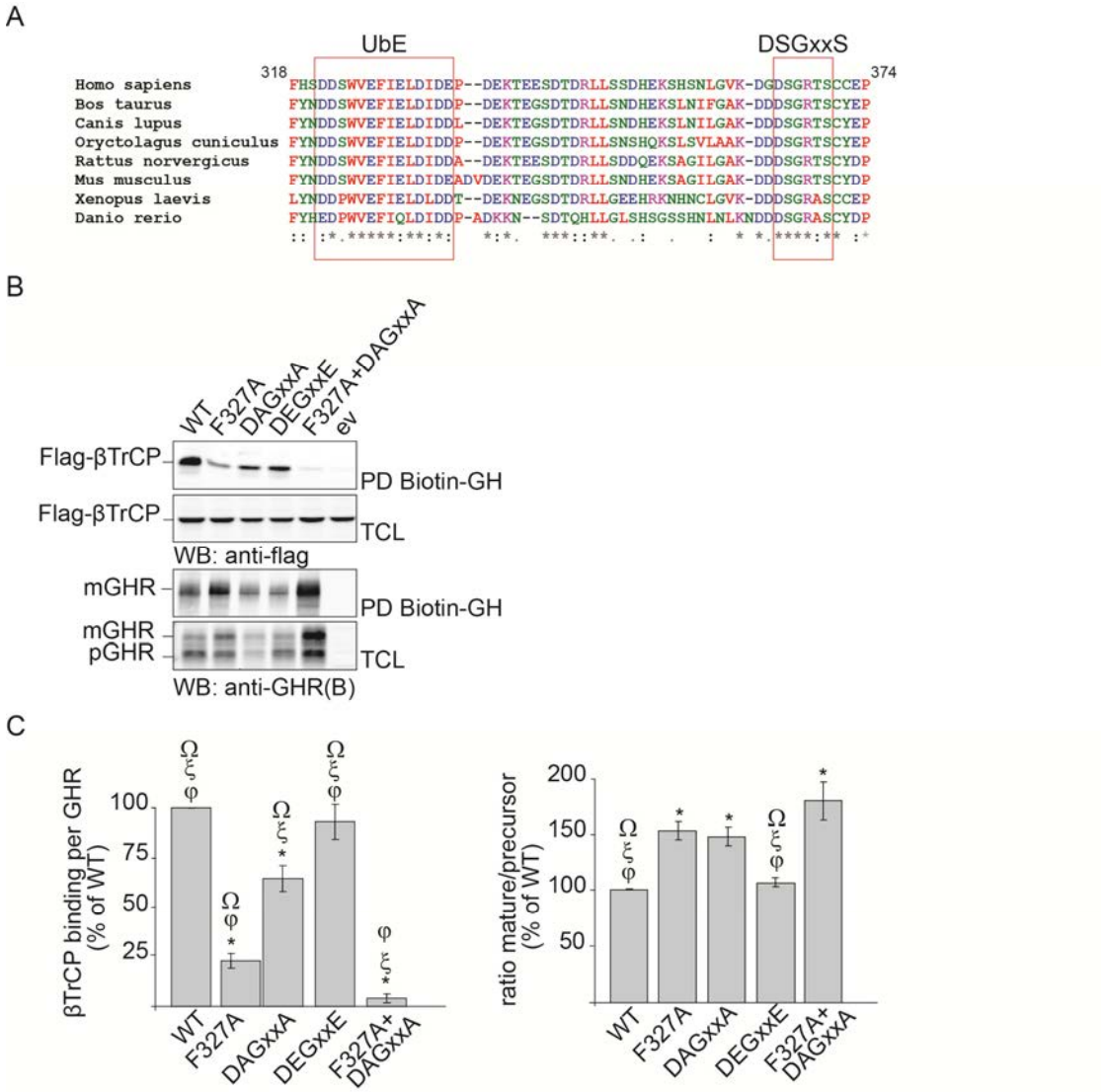

FIG. 1. The conserved DSGRTS sequence contributes to βTrCP binding.
(A) Alignment of the UbE and DSGRTS sequences of the GHR protein from *Homo sapiens* (human), *Bos taurus* (cow), *Canis lupus* (dog), *Oryctolagus cuniculus* (lapin), *Rattus norvegicus* (rat), *Mus musculus* (mouse), *Xenopus laevis* (frog), *Danio rerio* (fish). The alignment was performed with the CLUSTALW tool, EMBL-EBI server: "*", means that the residues in that column are identical in all sequences in the alignment; ":" and "." mean that conserved and semi-conserved substitutions, respectively, are observed; the colors represent different physicochemical properties shared by groups of aminoacids. **(B)** HEK293-TR cells were transiently transfected with GHR WT or mutants (F327A, DAGxxA, DEGxxE, F327A+DAGxxA) and co-transfected with Flag-βTrCP. GHR complexes were pulled from the cell surface using biotin-GH bound on ice for 2 hours. The samples resulting from the pull down were subjected to western blotting (WB), and detected with anti-GHR (B) and anti-Flag (for Flag-βTrCP detection) antibodies (left panel). Equal aliquots from the total cell lysates were analyzed by western blotting with the same antibodies (right panel). mGHR, mature GHR; pGHR, precursor GHR in the endoplasmic reticulum; PD, pull down; TCL, total cell lysate; ev, empty vector. Note that only mature GHR is detected in the PD samples (left panel) due to experimental set up. **(C)** Quantification of 1B. The effect of each GHR mutant was expressed as amount of βTrCP binding per GHR (left panel), and stabilization of GHR, expressed as ratio mGHR:pGHR in percentage of the WT (right panel). The data represent the mean of three independent experiments ± SEM ($p \leq 0.05$: ∗ vs. WT; ξ vs. F327A; ϕ vs. DAGxxA; Ω vs. F327A+DAGxxA).

quantified in Fig. 1C, right graph), suggesting that DSGRTS sequence is also involved in GHR endocytosis/degradation. These differences correlate with the extent of βTrCP binding, which is expressed as the amount of βTrCP bound to an identical amount of GHR mutant. As previously described, the F327A mutant resulted in 80% decreased βTrCP binding due to its non-functional UbE motif ((11) and Fig.1B, 1st panel, compare lanes 1 and 2; quantified in Fig. 1C, left graph). Hardly any βTrCP was able to bind the double mutant (DAGxxA+F327A) (Fig. 1B, 1st

panel, lane 5; quantified in Fig. 1C, left graph), suggesting that the difference between the double mutant and the F327A mutant is due to interaction of βTrCP with the DSGRTS sequence (Fig. 1B, lane5). Indeed, the DAGxxA mutant bound 35% less βTrCP, as compared to the WT (Fig.1B, 1st panel, compare lanes 1 and 3; quantified in Fig. 1C, left graph). On the other hand, mutation of the serine residues to glutamates restored the βTrCP binding to approximately 90% of the WT, which suggests that this mutation indeed
functions as phosphomimetic (Fig.1B, 1st panel, compare lanes 1 and 4; quantified in Fig. 1C, left graph). These results implicate that the serine residues in the DSGRTS sequence of GHR WT are fully phosphorylated under the experimental conditions used. Mass spectrometry analysis failed to identify peptides carrying the DSGRTS sequence neither in trypsin, nor in elastase and V8 digests. We conclude that the GHR DSGRTS sequence is fully phosphorylated, can bind βTrCP independently of the UbE domain under basal, GH-independent conditions.

2. DSGRTS and UbE motifs interact in a different way with the WD40 domain of βTrCP

βTrCP recognizes its substrates through its WD40 domain. Structural studies on βTrCP-substrate interactions revealed residues in this domain that are important for interacting with the classical DSGxxS degron (25). In order to investigate the modes of interaction of the DSGRTS sequence and the UbE motif with βTrCP, we mutated these residues (Y244A, R404A, R447A, andY461A) and performed binding assays. HEK293-TR cells were co-transfected with Flag-βTrCP WT or WD40 mutants, together with GHR WT, UbE mutant (F327A), or DSGRTS mutant (DAGxxA). GHR complexes were isolated from the plasma membrane with biotin-GH bound on ice. Note that βTrCP binding to the GHR F327A mutant represents binding through the DSGRTS sequence, binding to the GHR DAGxxA mutant represents binding through the UbE motif, while binding to the GHR WT represents the effects on βTrCP binding through both motifs. Transfection of the different βTrCP WD40 point mutants had different effects on the amount of GHR, due to their different stabilization effects of the mature receptor. This resulted in different amounts of pulled GHRs (Fig. 2A). Overexpression of all the βTrCP WD40 mutants with GHR F327A mutant resulted in the stabilization of the mature GHR (Fig. 2A, 4th left panel). This can be explained by a dominant negative effect, where the mutated βTrCP, which is not able to bind DSGRTS sequence, competes with the endogenous βTrCP for the other subunits of the SCF complex. This results in GHR endocytosis inhibition, and consequent stabilization of GHR. Only overexpression of Y244A and R447A WD40 mutants resulted in the same stabilization effect when co-expressed with GHR DAGxxA (Fig. 2A, 6th left panel). This indicates that only Y244 and R447 are involved in βTrCP function through the UbE motif. These residues are indeed important for βTrCP binding to the UbE motif (Fig. 2A, 5th right panel; quantified in figure 2B). On the other hand, like the βTrCP interaction with DSGxxS motif in βcatenin (25), all four WD40 residues tested are important for βTrCP-GHR-DSGRTS interaction (Fig. 2A, 3rd right panel; quantified in Fig. 2B). The effects of the βTrCP mutants on GHR stabilization correlate exactly with their ability to bind βTrCP. Remarkably, the interaction of βTrCP with GHR UbE motif requires only the residue Y244 and R447, and neither the residues R404 nor Y461 are involved. We conclude that βTrCP binds DSGRTS in a classical way, while the binding to the UbE motif is clearly different.

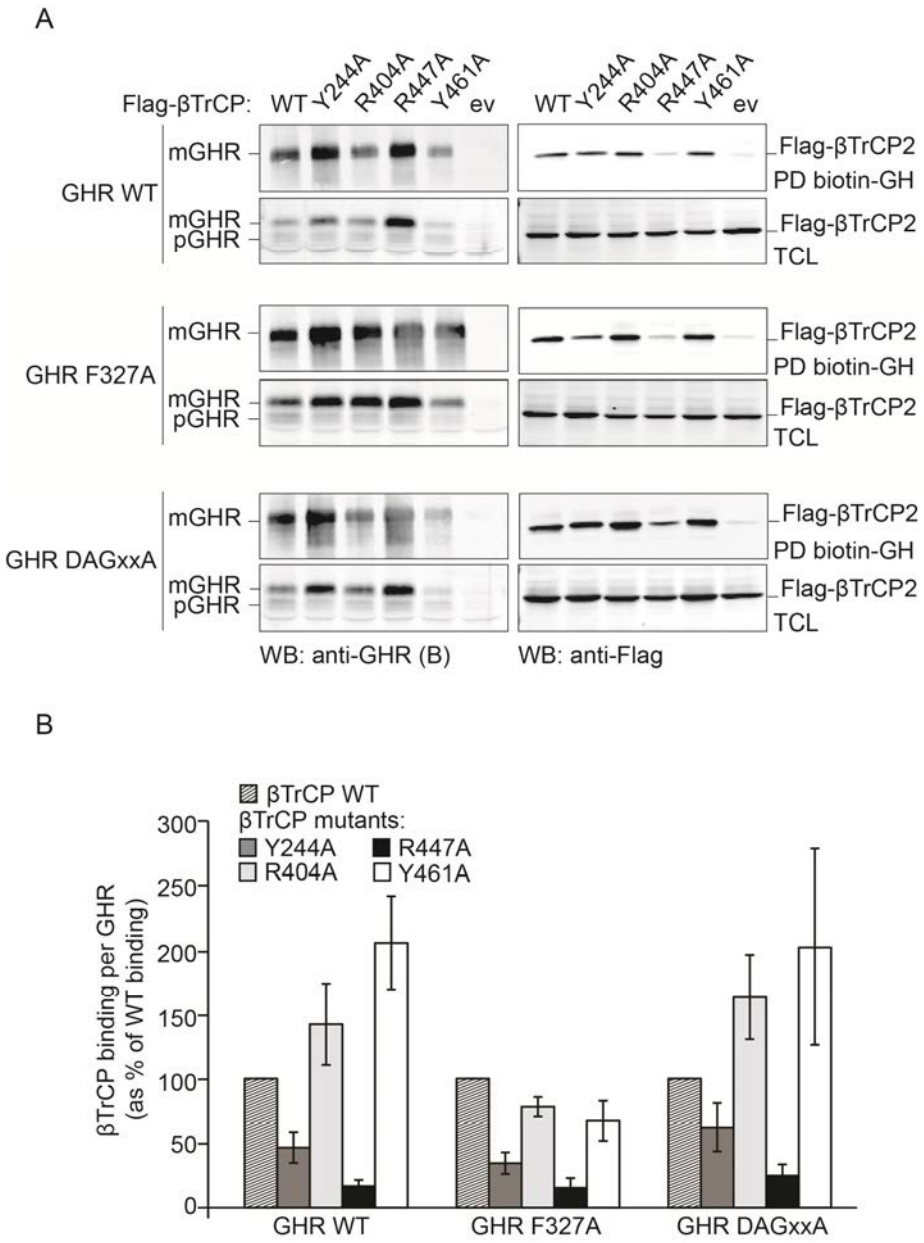

FIG. 2. DSGRTS and UbE motifs interact in a different way with the WD40 domain of βTrCP

(A) HEK293-TR cells were transiently transfected with GHR WT, F327A or DAGxxA mutants. The cells were co-expressing either Flag-βTrCP WT or βTrCP mutants with point mutations in the WD40 domain (Y244A, R404A, R447A, Y461A). GHR complexes were pulled from the cell surface by using biotin-GH bound on ice for 2 hours. The samples resulting from the pull down were subjected to western blotting (WB), and detected with anti-GHR (B) (left panel) and anti-Flag (for Flag-βTrCP detection, right panel) antibodies. Equal aliquots from the total cell lysates were analyzed by western blotting with the same antibodies. mGHR, mature GHR; pGHR, precursor GHR in endoplasmic reticulum; PD, pull down; TCL, total cell lysate; ev, empty vector. Note that only the mature GHR is detected in the PD samples. (**B)** Quantification of 2A. The effects of βTrCP WD40 point mutations on the binding to the UbE motif, DSGRTS sequence, or to both motifs were quantified (WT, diagonal line pattern bars; Y244A, dark grey bars; R404A, light grey bars; R447A, black bars; Y461A, white bars). The results shown in the graph were expressed as βTrCP mutant binding per GHR, as percentage of the binding of βTrCP WT. Data represent the mean of three independent experiments ± SEM.

3. The DSGRTS sequence contributes to GHR ubiquitination in basal conditions, but not upon GH stimulation

Classically, the functionality of the DSGxxS motif under different physiological conditions depends on its phosphorylation status. For instance, ligand-induced phosphorylation of the DSGxxS motifs in PRLR and EpoR cause βTrCP recruitment, which

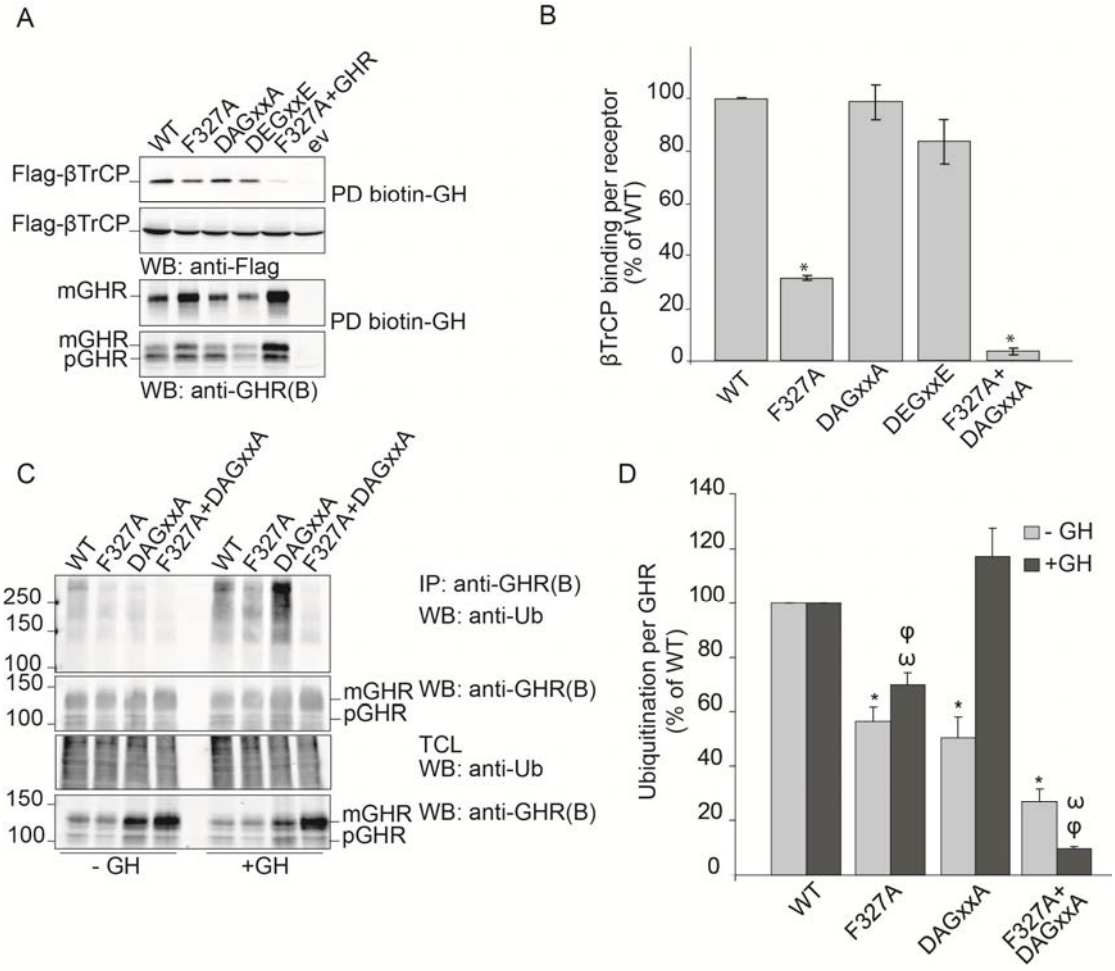

FIG. 3. The DSGRTS sequence contributes to GHR ubiquitination in basal conditions, but not upon GH stimulation
(A) HEK293-TR cells were transiently transfected with GHR WT and mutants (F327A, DAGxxA, DEGxxE, F327A+DAGxxA) and co-transfected with Flag-βTrCP. The cells were incubated with 180 ng/ml biotin-GH for 10 min at 37°C, then lysed, and GHR complexes were pulled from the cell surface using streptavidin beads. The samples were subjected to western blotting and detected with anti-GHR (B) and anti-Flag (for Flag-βTrCP detection) antibodies. Note that only mature GHR is detected in the PD samples. Aliquots of cell lysates were also analyzed by western blotting with the same antibodies. mGHR, mature GHR; pGHR, precursor GHR in the endoplasmic reticulum; PD, pull down; TCL, total cell lysates; ev, empty vector. **(B)** Quantification of 3A. The effect of each GHR mutant was expressed as amount of βTrCP binding per GHR in percentage of the WT. The data represent the mean of three independent experiments ± SEM ($p \leq 0.001$ ∗ vs. WT). **(C)** GHRs were isolated by immunoprecipitation, with anti-GHR (T) antibody, from HEK293-TR cells stably expressing GHR WT, F327A, DAGxxA or F327A+DAGxxA mutants stimulated or not for 15 min at 37°C with 180 ng/ml GH. The immunoprecipitations were performed under denaturating conditions to guarantee that ubiquitination signal is coming only from GHRs. The samples were subjected to western blotting (WB) and detected for ubiquitin (with FK2 antibody: anti-Ub) and GHR (with anti-GHR (B)) antibodies. Aliquots of cell lysates were analyzed by western blotting with the same antibodies. mGHR, mature GHR; pGHR, precursor GHR in the endoplasmic reticulum; IP, immunoprecipitations; TCL, total cell lysates. **(D)** Quantification of 3C. The ubiquitination status of GHR was expressed as ratio ubiquitination:GHR. The ubiquitination detected on GHR WT samples, in the conditions -/+ GH, was set at 100 %. The data represent the mean of three independent experiments ± SEM. ($p \leq 0.05$: ∗ vs. WT (-GH); ω vs. WT (+GH); ϕ vs. DAGxxA (+GH)).

mediates receptor endocytosis and, consequently, signal termination (18, 19). We wondered whether GH stimulation influences βTrCP binding and function through the DSGRTS sequence on GHR.

Firstly, we repeated the pull downs performed in Fig. 1B, but instead of binding biotin-GH on ice, the cells were incubated with biotin-GH at 37°, to trigger GH signaling. Under these conditions, the DAGxxA mutant did not show decreased Flag-βTrCP binding, compared to GHR WT (Fig 3A, compare lane 1 with 3; quantified in Fig. 3B), while the F327A mutant showed 70% less βTrCP binding (Fig 3A, compare lane 1 with 2; quantified in Fig. 3B). We conclude that the DSGRTS sequence of GHR does not bind to βTrCP when cells are stimulated with GH.

SCF(βTrCP) mediates K48 ubiquitination of the GHR (9). To investigate the role of the DSGRTS sequence in basal and GH-induced GHR ubiquitination, HEK293-TR cells, stably expressing GHR WT, F327A, DAGxxA or the double mutant (F327A+DAGxxA) were stimulated or not with GH, and the ubiquitination status of GHR was analyzed. Without GH, GHR WT was ubiquitinated at a basal level. GH stimulation enhanced the GHR WT ubiquitination (Fig. 3C, compare lanes 1 and 5). The F327A mutant was less ubiquitinated in both basal and GH-induced conditions compared to the corresponding GHR WT (Fig. 3C, compare lanes 1 to 2 and lanes 5 to 6; quantified in Fig. 3D). On the other hand, the DAGxxA mutant showed impaired ubiquitination in the absence of GH stimulation compared to WT (Fig. 3C, compare lane 1 to lane 3; quantified in Fig. 3D) to a similar extent as the F327A mutant, while its ubiquination status was not reduced compared to WT, if the cells were stimulated with GH (Fig. 3C, compare lane 5 to lane 7; quantified in Fig. 3D). In the double mutant (F327A+DAGxxA), hardly any ubiquitination of the receptor was detected, both in presence and absence of GH (Fig. 3C, lane 4 and 8; quantified in Fig. 3D). These results indicate that the role of the DSGRTS sequence in mediating GHR ubiquitination is restricted to basal conditions, while the UbE motif is involved in both basal and GH-induced conditions. Normal GH-dependent induction of GHR DAGxxA ubiquitination correlates well with the absence of βTrCP binding to the DSGRTS sequence after GH stimulation (Fig. 3A). From the results shown in Fig.1, we concluded that under basal conditions the DSGRTS sequence can bind βTrCP independently of the UbE motif. Together, the results support the hypothesis that the SCF(βTrCP) acts exclusively via the UbE motif in GH-induced conditions, while both motifs support ubiquitination in basal conditions.

4. GH-induced GHR endocytosis does not require a functional DSGRTS sequence

Ubiquitination of the GHR, although not necessary (20), precedes its endocytosis (26). Therefore, we assume that the ubiquitination status of GHR correlates with its endocytosis efficiency. Since the DSGRTS sequence is not involved in GH-induced GHR ubiquitination (Fig. 3C and Fig. 3D), we would expect that this sequence is not required for GH-induced GHR endocytosis. To investigate this, we evaluated the relative contribution of the UbE motif and DSGRTS sequence in GH-induced GHR endocytosis and degradation in HEK293-TR cells stably expressing GHR WT, the mutants F327A, DAGxxA, or the double mutant (F327A+DAGxxA). Fig. 4A shows that GH uptake was very efficient in GHR WT expressing cells, and, therefore, all the Cy3-GH appears as small punctae inside the cells without any detectable surface labeling. The GH uptake by the GHR UbE mutant (F327A) was inefficient and resulted in a strong labeling at the plasma membrane, and few punctae inside the cell (Fig. 4A and previously described in (23)). GHR DAGxxA mutant internalized GH normally, without cell surface labeling. The labeled dots inside seem to be larger and brighter than in the WT cells, probably due to higher levels of GHR DAGxxA, compared to GHR WT (see Fig. 3C, 4th panel). This may be explained by defective basal degradation of GHR DAGxxA mutant, suggested by the increased ratio mature/precursor of this mutated receptor compared to the WT (Fig. 1C and 3C). Cells expressing GHR double mutant, showed Cy3 labeling exclusively at the plasma membrane, indicating a complete block in GHR endocytosis.

Similar results were obtained when measuring the internalization and degradation of ^{125}I-GH by the different GHR forms (Fig. 4B). The F327A mutation caused an impaired GH endocytosis and consequently impaired degradation of the receptor. ^{125}I-GH was normally internalized and degraded by the DAGxxA mutant, while the double mutant showed a complete inhibition of GH endocytosis and degradation, with a stronger phenotype than the F327A mutant alone. In the GHR F327A mutant there might be an "artificial" gain of function of the DSGxxS motif, which normally, according to our model, is not active under GH stimulation. This would justify the different phenotype between the F327A mutant and the double mutant in GH-induced conditions. Although both assays show the importance of the UbE motif in GH-induced endocytosis of GHR, the DSGRTS sequence does not

seem to contribute to this process. However, in both experiments we measured the effects of GH stimulation after 30 min (Cy3-GH) or 60 min (^{125}I-GH). In order to verify whether at earlier time points after GH stimulation, the DSGRTS sequence has a role, the rates of ^{125}I-GH endocytosis in cells expressing GHR WT and GHR DAGxxA were compared after 15 min stimulation (Fig. 4C). The DAGxxA mutant internalized ^{125}I-GH slightly less efficiently (~10%) after 15 min. We conclude that the DSGRTS sequence does not contribute to GH-induced endocytosis and degradation of the GHR.

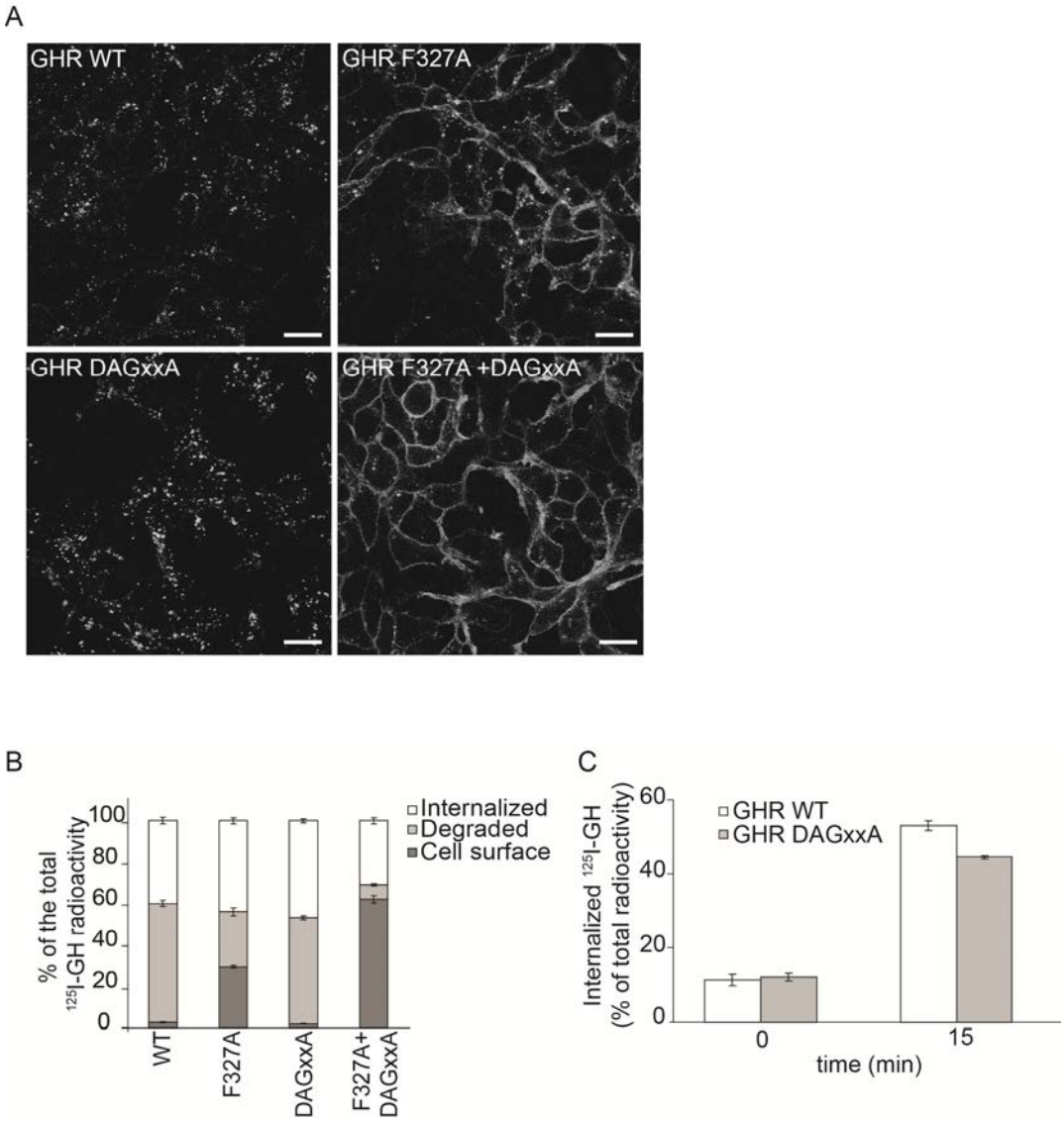

FIG. 4. GH-induced GHR endocytosis does not require a functional DSGRTS sequence.
(A) HEK293-TR cells stably expressing GHR WT, F327A, DAGxxA and F327A+DAGxxA, cultured on coverslips, were incubated with Cy3-GH 180 ng/ml for 30 min at 37°C, and fixed in formaldehyde. Representative confocal pictures are shown. Bar, 20 µm **(B)** ^{125}I-GH was bound to HEK293-TR cells stably expressing GHR WT, F327A, DAGxxA and F327A+DAGxxA, for 15 min at 37°C. The medium was exchanged to Hepes-buffered medium. After 1 hour at 37°C, the amounts of cell surface, internalized and degraded ^{125}I-GH were determined, as described in *Materials and Methods.* The results were expressed as percentage of radioactivity of each fraction in relation to the total radioactivity (cell surface, intracellular and degraded). The data represent the mean of four independent measurements ± SEM. **(C)** HEK293-TR cells stably expressing GHR WT and DAGxxA were incubated on ice for 2 hours with 180 ng/ml ^{125}I-GH (saturating amounts), and then placed at 37°C for 15 min, or not (time = 0 min), in order to allow internalization to occur. ^{125}I-GH internalized at time point 0 and 15 min is expressed as percentage of the total radioactivity (cell surface and intracellular). The data represent the mean of four independent experiments ± SEM.

5. Basal GHR degradation requires both UbE and DSGRTS motifs.

The results from Fig.1 suggested that the DSGRTS sequence is involved in the basal endocytosis/degradation of the GHR, judging from the accumulation of mature GHR in relation to precursor. This was supported by the involvement of the DSGRTS sequence in βTrCP binding and GHR ubiquitination in basal conditions (Figs. 1 and 3). However, when cells were stimulated with GH, neither a role of the DSGRTS sequence in βTrCP binding nor GHR ubiquitination/endocytosis could be detected (Figs. 3 and 4). To investigate directly the relative contribution of the two motifs to basal and GH-induced GHR endocytosis/degradation, HEK293-TR cells stably expressing GHR WT, F327A, DAGxxA, or double mutant (F327A+DAGxxA) were treated with cycloheximide, in the presence or absence of GH. In absence of GH stimulation, after 90 min of cycloheximide treatment, GHR WT decreased to approximately 50% of the initial amount due to basal endocytosis and lysosomal degradation (Fig. 5A; quantified in Fig. 5B, *closed circles*). However, the degradation of both GHR F327A and DAGxxA mutants was strongly affected: more than 50% of the receptors were still present after 180 min, which most likely reflects impaired receptor endocytosis (Fig. 5A; quantified in 5B, *closed squares* and *open circles*, respectively). When both motifs were mutated the amount of GHRs remained constant over time, indicating a block in the basal degradation of GHR (Fig. 5A; quantified in 5B, *open squares*). The degradation of GHR WT was twice as fast when cells treated with cycloheximide were stimulated with GH: already after approximately 45 min GHR WT amounts decreased 50% (Fig. 5C; quantified in Fig. 5D, *closed circles)*. In the same experiment, the degradation of GHR DAGxxA mutant occurred at the same rate as GHR WT, confirming our hypothesis that the DSGRTS sequence is not involved in GH-induced GHR degradation (Fig. 5C; quantified in Fig. 5D, *open circles,*). On the other hand, the degradation of GHR F327A mutant is impaired in the presence of GH: 50% of the receptors were still present after 90 min. This is in agreement with the requirement of the UbE motif for both basal and GH-induced GHR endocytosis/degradation. The degradation of the double mutant (F327A+DAGxxA) was blocked as can been seen by no significant change in the amounts of the mutant over time after cycloheximide treatment and GH stimulation (Fig. 5C; quantified in Fig. 5D, *open squares*). We conclude that βTrCP binding to both UbE and DSGRTS motifs is needed for degradation of the GHR in basal conditions (in the absence of GH), while under GH stimulation, binding to UbE motif only is sufficient for GHR endocytosis/degradation.

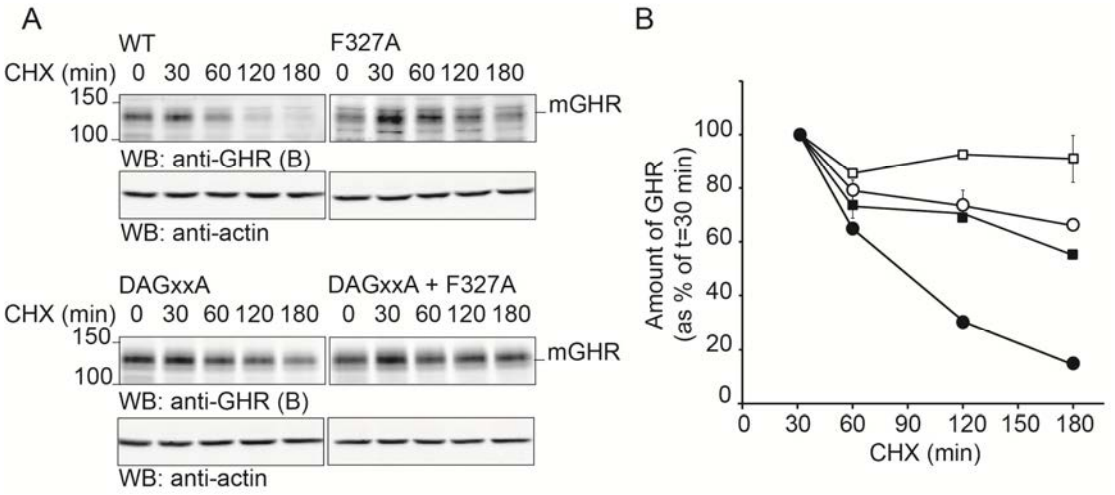

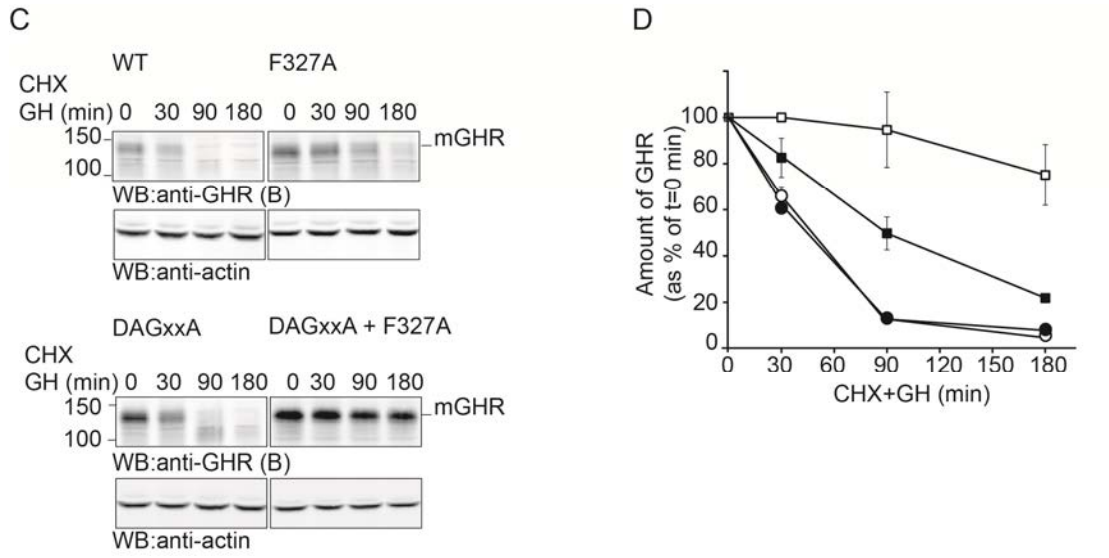

FIG. 5. Basal GHR degradation requires both UbE and DSGxxS motifs.
(A) Stable HEK293-TR cell lines expressing GHR WT, F327A, DAGxxA or F327A+DAGxxA mutants were subjected to cycloheximide (C= 20 μg/ml) treatment for the different indicated time points (0, 30, 60, 120, or 180 min). The cells were lysed and equal amount of lysates were analyzed by western blotting (WB), using anti-GHR (B) and anti-actin antibodies. CHX, cycloheximide; mGHR, mature GHR. **(B)** Quantification of 5A. The total amount of GHRs was determined, corrected for actin, and expressed in relation to the amount of receptor after 30 minutes of cycloheximide treatment, which was set at 100%. The data represent the mean from two independent experiments ± SEM. (*closed circles*, WT; *closed squares*, F327A; *open circles*, DAGxxA; *open squares*, F327A+DAGxxA). **(C)** The same cell lines used in 5A were subjected to cycloheximide (C= 20 μg/ml) treatment combined with 180 ng/ml GH, for the different indicated time points (0, 30, 90, or 180 min). The cells were lysed and equal amount of lysates were analyzed by western blotting (WB), using anti-GHR (B) and anti-actin antibodies. CHX, cycloheximide; mGHR, mature GHR. **(D)** Quantification of 5C. The total amount of GHRs was determined, corrected for actin, and expressed in relation to the amount of receptor present when no treatment was applied, which was set at 100%. The data represent the mean from two independent experiments ± SEM. (*closed circle*, WT; *closed square*, F327A; *open circle*, DAGxxA; *open square*, F327A+DAGxxA).

Discussion

The endocytosis and degradation of GHR depends on the role of $SCF^{\beta TrCP}$ E3 ligase, which mediates ubiquitination event(s) essential for GHR endocytosis. We have previously described that $SCF^{\beta TrCP}$ ligase complex is recruited to the UbE motif, present in the cytoplasmic tail of GHR, allowing the receptor to be endocytosed and degraded (11). In the present study, we found that the conserved DSGxxS motif, DSGRTS, present downstream of the UbE in the cytoplasmic tail of GHR is also able to bind βTrCP. The GHR DSGRTS sequence binds in a classical manner to WD40 domain of βTrCP, like βcatenin, but different from GHR UbE motif. We show for the first time a functional role for this motif in GHR. It is involved in the basal, or GH-independent, endocytosis/degradation of the receptor. In fact, in the absence of GH stimulation, the UbE and DSGRTS motifs contribute equally to the endocytosis rate of GHR, while no role of DSGRTS sequence was detected upon GH stimulation.

Since βTrCP binds equally well to the WT and the DEGxxE mutant receptor, likely the serine residues in the DSGRTS sequence are fully phosphorylated under basal conditions. This seems to be a specific feature of GHR. However, these experiments were done in overexpression systems, which may represent a stressful condition that triggers DSGRTS serine phosphorylation. Thus, we cannot exclude that under physiological levels of GHR the regulation is different.

There might be other pathways that indirectly modulate GHR levels in the cells by influencing the DSGRTS sequence phosphorylation status, and consequently the rate of basal degradation of GHR. For example, pro-inflammatory cytokines such as TNFα, IL-6 have a role in inducing a state of GH insensitivity (27, 28). Additionally, insulin has been described to modulate GHR levels and consequently GH signaling, depending on the activity of PI-3 kinase and MEK/ERK signaling (29, 30).

Besides affecting the expression levels of GHR, insulin might influence the phosphorylation status of the DSGRTS sequence as well. In some chronic situations the body would profit from higher GH sensitivity at steady state, e.g. growth plate chondrogenesis in children (31, 32). Inhibition of the DSGRTS kinase is one mechanism through which cells can increase the number of GHRs, and consequently GH sensitivity.

In literature, several kinases have been described for phosphorylating the DSGxxS motif serines in different substrates. In Vpu, involved in HIV infection, βTrCP binds to the DSGxxS motif, where both serines are constitutively phosphorylated by CK2 (33). We could not find evidence for a role of CK2 in the phosphorylation of the serines of the DSGRTS sequence in GHR by using CK2 inhibitor (data not shown). The DSGxxS motifs of the IFNAR and PRLR are phosphorylated by CK1 (34) and GSK3β (35), respectively. Probing both kinases with specific inhibitors neither specifically decreased the interaction of the GHR DSGRTS sequence with βTrCP nor decreased GHR endocytosis/degradation. Therefore, we conclude that these kinases are not involved in the phosphorylation of GHR DSGRTS sequence (data not shown). Future studies need to be performed to find the kinase responsible for the phosphorylation of DSGRTS of GHR. This will give more insight into GH-independent mechanisms of regulation of GHR endocytosis.From our results we concluded that phosphorylation of GHR DSGRTS sequence is GH-independent (Fig. 4). This differs from the regulation present in the homologous receptors PrLR, IFNAR1 and EpoR. The phosphorylation of the motif in PrLR is triggered by its ligand (35). For the IFNAR, treatment of cells with IFNα/β triggers Tyk2 activity and induces the phosphorylation of the serine535 in the DSGxxS motif, and its subsequent ubiquitination and degradation (34). These events can be stimulated also by unfolded protein response (UPR) inducers, including viral infection (36). In an analogous way, βTrCP is only described to bind EpoR after Epo stimulation, depending on JAK2 activation (19). In contrast, βTrCP binds to UbE and DSGRTS sequences in GHR under basal conditions, ensuring its continuous endocytosis and degradation (Fig. 5).

A basally regulated process of endocytosis guarantees that the levels of GHR at the plasma membrane are kept at the right level so that the cells are appropriately sensitive to GH. JAK2 binding to the GHR slows down the endocytosis of the receptor (9). Upon GH stimulation, JAK2 is released momentarily, allowing βTrCP to bind more effectively to the receptor. Consequently, GH binding accelerates GHR endocytosis. Thus, the cellular concentration of JAK2 is a third factor to consider on the regulation of the basal endocytosis/degradation of GHR. The DSGRTS sequence is involved only in basal GHR endocytosis, and not after GH stimulation. It is important to consider that in the hypothetical case of a defective UbE motif, the balanced interplay between the functions of the UbE and DSGRTS sequences is most likely disturbed. In this case, the DSGRTS sequence might partially cover for the function of the UbE, which justifies the different phenotype of the F327A mutant compared to the double mutant (F327A + DAGxxA) in conditions of GH stimulation (Fig. 3, 4 and 5). In addition, these results implicate that the DSGRTS sequence is kept phosphorylated under GH stimulation. In our model (Fig. 6) we speculate that GH stimulation triggers certain events that result in increased affinity of βTrCP to the UbE motif, masking or overcoming the necessity for a role of the DSGRTS sequence. The detachment of JAK2 from the GHR could be one of these events. Alternatively, GH stimulation might trigger post-translational modifications on the UbE motif resulting in increased βTrCP affinity for this motif (manuscript in preparation). This possibility is currently under investigation. In addition, it is possible that GHRs are allowed to internalize through the DSGRTS sequence, even when JAK2 is bound to the receptor. This makes DSGRTS a potential candidate motif for regulating GHR levels by other pathways independent of GH stimulation or JAK2 binding.

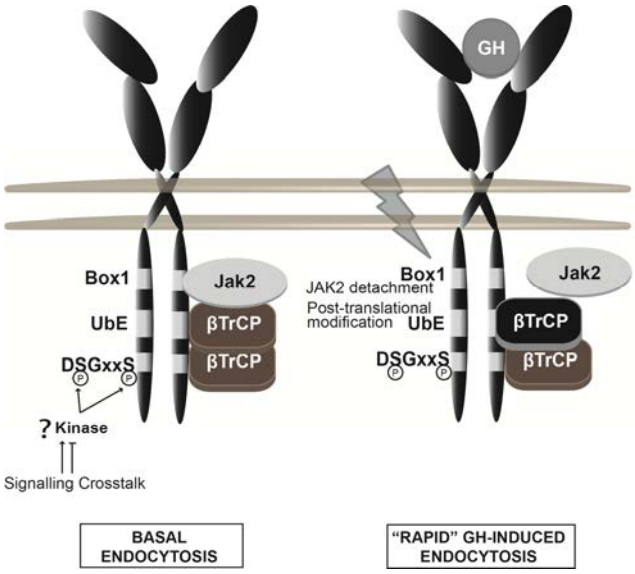

FIG. 6. Model
Under basal conditions βTrCP binds to the UbE motif and to the constitutively phosphorylated DSGRTS sequence. Both motifs contribute equally to the continuous GH-independent turnover of the GHR. This is essential to guarantee a proper regulation of the GH sensitivity of the cells. Yet, the kinase responsible for the DSGRTS phosphorylation is unknown. Other pathways may influence GHR cellular levels by modulating DSGRTS phosphorylation status. Under conditions of GH stimulation certain events (such as JAK2 release from the receptor, or post-translational modification on the UbE) may result in an increased βTrCP binding to the UbE motif, and consequent faster endocytosis.

Whether both UbE and DSGRTS motifs can be active and occupied by βTrCP at the same time is not clear. GHR exists as a dimer at the cell surface (5), and therefore each GHR unit contains two UbE motifs and two DSGRTS sequences. Additionally, $SCF^{\beta TrCP}$ complexes have been reported to undergo dimerization (37, 38) . Therefore, it is possible that multiple $SCF^{\beta TrCP}$ complexes bind on one GHR tail at the same time. The functional relevance of this potential phenomenon and regulating factors involved are still elusive. Other βTrCP substrates have been proposed to contain multiple motifs cooperatively recognized by βTrCP, such as Cubitus interruptus (39), Mdm2 (40), and Gli3 (41). Employing multiple binding sites, involving potentially multiple differently regulated phosphorylation events, allows the possibility of a more fine-tuned βTrCP action.

Recently, we also reported a role of βTrCP in the endosomal sorting of the GHR (21). The DSGRTS sequence might be involved in GHR sorting at the multi vesicular body (MVB) as well. The relative functional involvement of UbE versus DSGRTS motifs might differ between GHR endocytosis at the cell surface and GHR sorting at the MVBs. Further research is needed to clarify a role for GHR DSGRTS sequence in endosomal sorting.

Various mechanisms exist to modulate GH responsiveness of cells and terminate GH signaling (42). Studies by us and others indicate that the sensitivity of cells to GH is mainly dictated by the GHR levels on the surface of the cells (43-45). The present study shows an important role for the DSGRTS sequence in regulating cellular levels of GHR, which is a crucial factor for avoiding too much responsiveness of cells to GH. In fact, excessive GH signaling has been recently connected to cancer (*46, 47*). The study by Shen *et al.* showed convincingly that dwarf rats lacking GH do not develop tumors when treated with the carcinogen N-methyl-N-nitrosourea (48). Additionally, increased GHR expression has been detected in breast cancer compared with adjacent normal tissue (49, 50).

The present study reveals that the important high rate of GHR degradation is guaranteed by two motifs, UbE and DSGRTS, through a mechanism involving βTrCP-mediated ubiquitination. This is the first time that a functional role is assigned for the GHR DSGRTS sequence in basal GHR endocytosis, but not in GH-induced GHR endocytosis. The GHR DSGRTS sequence provides a new platform for regulating the GH sensitivity of cells. How UbE motif and DSGRTS sequence influence each other to fine tune the process of GHR endocytosis and degradation remains to be elucidated.

Acknowledgments

This research was supported by the European Network of Excellence, Rubicon "Role of ubiquitin and ubiquitin-like modifiers in cellular regulation" (Grant LSHG-CT-2005-018683), and the Marie Curie network, "UbiRegulators", (Grant MRTN-CT-2006-034555).

We thank Dr. Peter van Kerkhof for the critical reading of the manuscript and suggestions.

We thank all other members of the GHR group.

References

1. Brooks AJ, Waters MJ 2010 The growth hormone receptor: mechanism of activation and clinical implications. Nat Rev Endocrinol 6:515-525
2. Brown RJ, Adams JJ, Pelekanos RA, Wan Y, McKinstry WJ, Palethorpe K, Seeber RM, Monks TA, Eidne KA, Parker MW, Waters MJ 2005 Model for growth hormone receptor activation based on subunit rotation within a receptor dimer. Nat Struct Mol Biol 12:814-821
3. Lanning NJ, Carter-Su C 2006 Recent advances in growth hormone signaling. Rev Endocr Metab Disord 7:225-235
4. Rowlinson SW, Yoshizato H, Barclay JL, Brooks AJ, Behncken SN, Kerr LM, Millard K, Palethorpe K, Nielsen K, Clyde-Smith J, Hancock JF, Waters MJ 2008 An agonist-induced conformational change in the growth hormone receptor determines the choice of signalling pathway. Nat Cell Biol 10:740-747
5. Gent J, van Kerkhof P, Roza M, Bu G, Strous GJ 2002 Ligand-independent growth hormone receptor dimerization occurs in the endoplasmic reticulum and is required for ubiquitin system-dependent endocytosis. Proc Natl Acad Sci U S A 99:9858-9863
6. Strous GJ, van Kerkhof P 2002 The ubiquitin-proteasome pathway and the regulation of growth hormone receptor availability. Mol Cell Endocrinol 197:143-151
7. Gorin E, Goodman HM 1985 Turnover of growth hormone receptors in rat adipocytes. Endocrinology 116:1796-1805
8. Murphy LJ, Lazarus L 1984 The mouse fibroblast growth hormone receptor: ligand processing and receptor modulation and turnover. Endocrinology 115:1625-1632
9. Putters J, da Silva Almeida AC, van Kerkhof P, van Rossum AG, Gracanin A, Strous GJ 2011 Jak2 is a negative regulator of ubiquitin-dependent endocytosis of the growth hormone receptor. PLoS One 6:e14676
10. Strous GJ, van Kerkhof P, Govers R, Ciechanover A, Schwartz AL 1996 The ubiquitin conjugation system is required for ligand-induced endocytosis and degradation of the growth hormone receptor. Embo J 15:3806-3812
11. van Kerkhof P, Putters J, Strous GJ 2007 The ubiquitin ligase SCF(betaTrCP) regulates the degradation of the growth hormone receptor. J Biol Chem 282:20475-20483
12. Winston JT, Strack P, Beer-Romero P, Chu CY, Elledge SJ, Harper JW 1999 The SCFbeta-TRCP-ubiquitin ligase complex associates specifically with phosphorylated destruction motifs in IkappaBalpha and beta-catenin and stimulates IkappaBalpha ubiquitination in vitro. Genes Dev 13:270-283
13. Tan P, Fuchs SY, Chen A, Wu K, Gomez C, Ronai Z, Pan ZQ 1999 Recruitment of a ROC1-CUL1 ubiquitin ligase by Skp1 and HOS to catalyze the ubiquitination of I kappa B alpha. Mol Cell 3:527-533
14. Latres E, Chiaur DS, Pagano M 1999 The human F box protein beta-Trcp associates with the Cul1/Skp1 complex and regulates the stability of beta-catenin. Oncogene 18:849-854
15. Hart M, Concordet JP, Lassot I, Albert I, del los Santos R, Durand H, Perret C, Rubinfeld B, Margottin F, Benarous R, Polakis P 1999 The F-box protein beta-TrCP associates with phosphorylated beta-catenin and regulates its activity in the cell. Curr Biol 9:207-210
16. Chen ZJ, Parent L, Maniatis T 1996 Site-specific phosphorylation of IkappaBalpha by a novel ubiquitination-dependent protein kinase activity. Cell 84:853-862
17. Kumar KG, Tang W, Ravindranath AK, Clark WA, Croze E, Fuchs SY 2003 SCF(HOS) ubiquitin ligase mediates the ligand-induced down-regulation of the interferon-alpha receptor. Embo J 22:5480-5490
18. Li Y, Kumar KG, Tang W, Spiegelman VS, Fuchs SY 2004 Negative regulation of prolactin receptor stability and signaling mediated by SCF(beta-TrCP) E3 ubiquitin ligase. Mol Cell Biol 24:4038-4048
19. Meyer L, Deau B, Forejtnikova H, Dumenil D, Margottin-Goguet F, Lacombe C, Mayeux P, Verdier F 2007 beta-Trcp mediates ubiquitination and degradation of the erythropoietin receptor and controls cell proliferation. Blood 109:5215-5222

20. Govers R, ten Broeke T, van Kerkhof P, Schwartz AL, Strous GJ 1999 Identification of a novel ubiquitin conjugation motif, required for ligand-induced internalization of the growth hormone receptor. Embo J 18:28-36
21. van Kerkhof P, Westgeest M, Hassink G, Strous GJ 2011 SCF(TrCP) acts in endosomal sorting of the GH receptor. Exp Cell Res 317:1071-1082
22. Frescas D, Pagano M 2008 Deregulated proteolysis by the F-box proteins SKP2 and beta-TrCP: tipping the scales of cancer. Nat Rev Cancer 8:438-449
23. Govers R, van Kerkhof P, Schwartz AL, Strous GJ 1997 Linkage of the ubiquitin-conjugating system and the endocytic pathway in ligand-induced internalization of the growth hormone receptor. Embo J 16:4851-4858
24. Allevato G, Billestrup N, Goujon L, Galsgaard ED, Norstedt G, Postel-Vinay MC, Kelly PA, Nielsen JH 1995 Identification of phenylalanine 346 in the rat growth hormone receptor as being critical for ligand-mediated internalization and down-regulation. J Biol Chem 270:17210-17214
25. Wu G, Xu G, Schulman BA, Jeffrey PD, Harper JW, Pavletich NP 2003 Structure of a beta-TrCP1-Skp1-beta-catenin complex: destruction motif binding and lysine specificity of the SCF(beta-TrCP1) ubiquitin ligase. Mol Cell 11:1445-1456
26. Sachse M, van Kerkhof P, Strous GJ, Klumperman J 2001 The ubiquitin-dependent endocytosis motif is required for efficient incorporation of growth hormone receptor in clathrin-coated pits, but not clathrin-coated lattices. J Cell Sci 114:3943-3952
27. Wang P, Li N, Li JS, Li WQ 2002 The role of endotoxin, TNF-alpha, and IL-6 in inducing the state of growth hormone insensitivity. World J Gastroenterol 8:531-536
28. DiFedele LM, He J, Bonkowski EL, Han X, Held MA, Bohan A, Menon RK, Denson LA 2005 Tumor necrosis factor alpha blockade restores growth hormone signaling in murine colitis. Gastroenterology 128:1278-1291
29. Ji S, Guan R, Frank SJ, Messina JL 1999 Insulin inhibits growth hormone signaling via the growth hormone receptor/JAK2/STAT5B pathway. J Biol Chem 274:13434-13442
30. Bennett WL, Keeton AB, Ji S, Xu J, Messina JL 2007 Insulin regulation of growth hormone receptor gene expression: involvement of both the PI-3 kinase and MEK/ERK signaling pathways. Endocrine 32:219-226
31. De Luca F 2006 Impaired growth plate chondrogenesis in children with chronic illnesses. Pediatr Res 59:625-629
32. Gevers EF, Hannah MJ, Waters MJ, Robinson IC 2009 Regulation of rapid signal transducer and activator of transcription-5 phosphorylation in the resting cells of the growth plate and in the liver by growth hormone and feeding. Endocrinology 150:3627-3636
33. Schubert U, Henklein P, Boldyreff B, Wingender E, Strebel K, Porstmann T 1994 The human immunodeficiency virus type 1 encoded Vpu protein is phosphorylated by casein kinase-2 (CK-2) at positions Ser52 and Ser56 within a predicted alpha-helix-turn-alpha-helix-motif. J Mol Biol 236:16-25
34. Kumar KG, Krolewski JJ, Fuchs SY 2004 Phosphorylation and specific ubiquitin acceptor sites are required for ubiquitination and degradation of the IFNAR1 subunit of type I interferon receptor. J Biol Chem 279:46614-46620
35. Plotnikov A, Li Y, Tran TH, Tang W, Palazzo JP, Rui H, Fuchs SY 2008 Oncogene-mediated inhibition of glycogen synthase kinase 3 beta impairs degradation of prolactin receptor. Cancer Res 68:1354-1361
36. Liu J, HuangFu WC, Kumar KG, Qian J, Casey JP, Hamanaka RB, Grigoriadou C, Aldabe R, Diehl JA, Fuchs SY 2009 Virus-induced unfolded protein response attenuates antiviral defenses via phosphorylation-dependent degradation of the type I interferon receptor. Cell Host Microbe 5:72-83
37. Suzuki H, Chiba T, Suzuki T, Fujita T, Ikenoue T, Omata M, Furuichi K, Shikama H, Tanaka K 2000 Homodimer of two F-box proteins betaTrCP1 or betaTrCP2 binds to IkappaBalpha for signal-dependent ubiquitination. J Biol Chem 275:2877-2884
38. Chew EH, Poobalasingam T, Hawkey CJ, Hagen T 2007 Characterization of cullin-based E3 ubiquitin ligases in intact mammalian cells--evidence for cullin dimerization. Cell Signal 19:1071-1080
39. Jia J, Zhang L, Zhang Q, Tong C, Wang B, Hou F, Amanai K, Jiang J 2005 Phosphorylation by double-time/CKIepsilon and CKIalpha targets cubitus interruptus for Slimb/beta-TRCP-mediated proteolytic processing. Dev Cell 9:819-830

40. Inuzuka H, Tseng A, Gao D, Zhai B, Zhang Q, Shaik S, Wan L, Ang XL, Mock C, Yin H, Stommel JM, Gygi S, Lahav G, Asara J, Xiao ZX, Kaelin WG, Jr., Harper JW, Wei W 2010 Phosphorylation by casein kinase I promotes the turnover of the Mdm2 oncoprotein via the SCF(beta-TRCP) ubiquitin ligase. Cancer Cell 18:147-159
41. Tempe D, Casas M, Karaz S, Blanchet-Tournier MF, Concordet JP 2006 Multisite protein kinase A and glycogen synthase kinase 3beta phosphorylation leads to Gli3 ubiquitination by SCFbetaTrCP. Mol Cell Biol 26:4316-4326
42. Frank SJ 2001 Growth hormone signalling and its regulation: preventing too much of a good thing. Growth Horm IGF Res 11:201-212
43. Gebert CA, Park SH, Waxman DJ 1999 Termination of growth hormone pulse-induced STAT5b signaling. Mol Endocrinol 13:38-56
44. Ji S, Frank SJ, Messina JL 2002 Growth hormone-induced differential desensitization of STAT5, ERK, and Akt phosphorylation. J Biol Chem 277:28384-28393
45. van Kerkhof P, Vallon E, Strous GJ 2003 A method to increase the number of growth hormone receptors at the surface of cells. Mol Cell Endocrinol 201:57-62
46. Waters MJ, Barclay JL 2007 Does growth hormone drive breast and other cancers? Endocrinology 148:4533-4535
47. Kleinberg DL, Wood TL, Furth PA, Lee AV 2009 Growth hormone and insulin-like growth factor-I in the transition from normal mammary development to preneoplastic mammary lesions. Endocr Rev 30:51-74
48. Shen Q, Lantvit DD, Lin Q, Li Y, Christov K, Wang Z, Unterman TG, Mehta RG, Swanson SM 2007 Advanced rat mammary cancers are growth hormone dependent. Endocrinology 148:4536-4544
49. Mertani HC, Garcia-Caballero T, Lambert A, Gerard F, Palayer C, Boutin JM, Vonderhaar BK, Waters MJ, Lobie PE, Morel G 1998 Cellular expression of growth hormone and prolactin receptors in human breast disorders. Int J Cancer 79:202-211
50. Gebre-Medhin M, Kindblom LG, Wennbo H, Tornell J, Meis-Kindblom JM 2001 Growth hormone receptor is expressed in human breast cancer. Am J Pathol 158:1217-1222
51. van Kerkhof P, Govers R, Alves dos Santos CM, Strous GJ 2000 Endocytosis and degradation of the growth hormone receptor are proteasome-dependent. J Biol Chem 275:1575-1580

The interaction of βTrCP with the ubiquitin-dependent endocytosis motif of growth hormone receptor is unconventional

3

Ana C. da Silva Almeida[1,2], Henry G Hocking[3], Rolf Boelens[3], Ger J Strous[1], Agnes G S H van Rossum[1,2]

[1] Department of Cell Biology and Institute of Biomembranes, University Medical Center Utrecht, Heidelberglaan 100, 3584 CX Utrecht, The Netherlands

[2] Drug Discovery Factory BV, Albrechtlaan 14A, 1404 AK Bussum, The Netherlands

[3] Department of NMR Spectroscopy, Bijvoet Center for Biomolecular Research, Utrecht University, Padualaan 8, 3584 CH Utrecht, The Netherlands

(Manuscript in preparation)

Abstract

Growth Hormone (GH) binding to the GH receptor (GHR) triggers essential signaling pathways that promote growth and metabolic regulation. The sensitivity of the cells to GH is mainly controlled by the endocytosis of the receptor. βTrCP an essential factor regulating GHR endocytosis. In this study we show that βTrCP interacts directly via its WD40 repeats domain with the ubiquitin dependent endocytosis motif (UbE) in GHR. The E3 ligase SCF(βTrCP) mediates GHR ubiquitination *in vitro* in a UbE dependent manner. The role of βTrCP WD40 residues in GHR binding, *in vitro* ubiquitination and endocytosis was analysed and revealed the unconventionality of the UbE-βTrCP interaction. With structural data of this interaction, obtained by NMR, combined the functional mapping of the UbE and βTrCP WD40 aminoacid residues involved, a computational model of the interaction was constructed. This model shows a unique interaction of βTrCP with GHR-UbE, different from the one occurring with canonical motifs present in all other βTrCP substrates. This unique interaction is a promising specific target to discover drug that inhibit GHR endocytosis in order to increase GH sensitivity in cancer cachexia patients.

Introduction

Growth Hormone receptor (GHR), is a protein of 620 amino acids, member of the class 1 cytokine receptors superfamily, that exists as a dimer at the cell surface of all the cells in the body (*1*). Upon binding of the growth Hormone (GH) to the GHR, Janus kinase 2 (JAK2) molecules associated to the cytoplasmic tails of the receptors (*2*) are activated, and consequently signalling cascades are triggered. The JAK-STAT pathway is the major effector of GHR signaling by inducing IGF-1 expression, but also the mitogen-activated protein kinase (MAPK) and phosphoinositide-3 kinase (PI3K) pathways are activated by GH (*3*). Apart from promoting longitudinal body growth, GHR signaling regulates metabolism and cellular functions such as proliferation and differentiation (*1*). Therefore, a proper control of the tissue sensitivity to the GH is required, since excessive GH signalling has been connected to cancer (*4, 5*), and GH resistance has been reported in cachexia patients (*6, 7*). Cachexia is a complex metabolic disorder, occurring in cancer and AIDS patients, characterized by extensive loss of muscle mass and decreased quality of life (*8, 9*). Patients suffering from this condition would benefit from a treatment increasing the responsiveness of the cells to GH.

The availability of GHRs in cells is important for the GH responsiveness in the body, and is mainly determined by the rate of GHR endocytosis/degradation (*10*). GHR endocytosis requires an intact ubiquitination system (*11*) and depends on the Ubiquitin-dependent endocytosis (UbE) motif present in its cytoplasmic tail (*12*). Protein ubiquitination involves the sequential action of three classes of enzymes: E1 or ubiquitin activating enzyme, E2 or ubiquitin conjugating enzyme, and E3 or ubiquitin ligases. The E3 ligase introduces substrate specificity in the system. The F-box protein βTrCP, substrate recognition subunit of the E3 ligase $SCF^{\beta TrCP}$, is necessary for GHR endocytosis (*13*). A role for the complete $SCF^{\beta TrCP}$ in GHR endocytosis has been suggested (*13*). $SCF^{\beta TrCP}$ is a heterotetrameric complex belonging to the family of RING type ubiquitin ligases (*14*). The scaffold protein Cullin1 interacts on its N-terminus domain with Skp1, and on its C-terminus with Rbx1, a RING finger protein. Skp1 binds to βTrCP and Rbx1 recruits transiently the E2 that adds the ubiquitin molecules to the substrate. Mammalian SCF E3 ligases can collaborate with Cdc34 or E2s of the Ubc4/5 family *in vitro,* but it is unclear whether this is also true *in vivo* (*15*).

$SCF^{\beta TrCP}$ is involved in the ubiquitin dependent endocytosis of receptors homologous to GHR, e.g. interferon-alpha receptor (IFNAR)(*16*), erythropoietin receptor (EpoR)(*17*), and prolactin receptor (PrLR)(*18*). After ligand binding to these receptors, the serine residues of the DSGxxS motifs become phosphorylated and $SCF^{\beta TrCP}$ is recruited, mediating their ubiquitin-dependent endocytosis. Also GHR contains a DSGxxS motif. However, recently we demonstrated that the GHR-DSGxxS motif is not involved in GH-mediated, but in GH-independent basal GHR endocytosis and degradation (da Silva Almeida AC *et al*, manuscript submitted). GHR- UbE motif regulates GHR endocytosis and degradation, both in presence or absence of GH stimulation.

βTrCP interacts with its substrates through its WD40 repeats domain. The crystal structure of a complex of βTrCP in complex with β-catenin was solved and revealed the characteristics of this interaction in molecular detail (*19*). Additionally, Nuclear Magnetic Resonance (NMR) studies have characterized the interaction of βTrCP with several substrates via the classical phosphorylated degron $DSG(X)_{2+n}S$ (*20-25*). For the binding of the GHR- DSGxxS to βTrCP, the same residues in the WD40 domain are involved (*da Silva Almeida AC et al*, manuscript submitted). On the other hand, the GHR-UbE motif sequence (DDSWVEFIELD) differs substantially from the one of the conserved classical $DSG(X)_{2+n}S$ motif. Therefore, we predict that the interaction of the GHR-UbE motif with βTrCP is unconventional, and as such can act as a promising specific target to discover drugs able to inhibit GHR endocytosis specifically, and consequently increase GH sensitivity in cachexia patients.

In this study we report that βTrCP binds directly to the UbE motif *in vitro* in a different manner than to the classical $DSG(X)_{2+n}S$ motif. Furthermore, $SCF^{\beta TrCP}$ mediates GHR ubiquitination *in vitro*. Mutations in WD40 repeats domain residues decreased GHR-βTrCP interaction, GHR ubiquitination *in vitro*, and GHR endocytosis. Functional mapping of amino acid residues of the UbE motif and WD40 domain was combined with structural data obtained by NMR, and a computational model of the interaction was constructed. This model shows a unique interaction of βTrCP with GHR-UbE, different from the one with canonical motifs present in all other described βTrCP substrates.

Materials and Methods

Reagents

Anti-poli-His monoclonal antibody was purchased from Sigma (Saint Louis, MO, USA). Anti-GHR (B) was raised in rabbit, against aminoacids 327-493 of the cytosolic tail of the rabbit GHR as previously described (*11*). Anti-GST antibody was raised in rabbit against GST peptides (*11*). Monoclonal antibody against ubiquitin (clone FK2) was purchased from Biomol (Raamsdonksveer, The Netherlands), monoclonal anti-Flag (M2) from Sigma, polyclonal anti-Myc from Millipore (Billerica, MA, USA) and anti-T7 from Novagen (Madison, WI, USA). Goat anti-mouse IgG Alexa 680 was from Molecular Probes (Eugene, OR, USA) and Goat anti-rabbit IgG IRDye800 from Rockland Immunochemicals Inc (Gilbertsville, PA, USA). Streptavidin beads were purchased from Pierce (Rockford, IL, USA) and streptactin beads from GE healthcare (Hoevelaken, The Netherlands). Anti-Flag (M2) agarose beads and 3XFlag peptide were purchased from Sigma. Human GH was a kind gift from Eli Lilly Research Labs (Indianapolis, IN, USA). Glutathione (GSH)-beads were purchased from Amersham Biosciences (Freiburg, Germany).

Biotinylated-GH (biotin-GH) was prepared using Biotinylation kit purchased from Pierce (Rockford, IL, USA), according to the manufacturer's protocol. GH(his-TEV-STREP3-his)C was purified by U-Protein Express BV (Utrecht, The Netherlands). The primers were purchased from Sigma. Peptides were chemically synthesized by Pepscan (Lelystad, The Netherlands). The sequence was as following: UbE (GHR fragment aminoacid 314-335), 22 aminoacids, Acetyl-YKPEFHSDDSWVEFIELDIDEP-amide; UbE-mutant (F327A/D331A), 22 aminoacids, Acetyl-YKPEFHSDDSWVEAIELAIDEP-amide; and the β-catenin peptide (fragment 17-48), 32 aminoacids, with phosphorylated serines 33 and 37, DRKAAVSHWQQQSYLDSGIHSGATTTAPSLSG.

DNA constructs

Full-length rabbit GHR cDNA in pcDNA3 has been previously described (*11*). The mutations were inserted with Quick Change mutagenesis kit from Stratagene (Santa Clara, CA, USA). GHR F327A mutant in pcDNA3 was generated as previously described (*12*). GHR DAGxxA (S366A, S370A) was generated with the oligonucleotides, 5'_GGATGACGACGCTGGACGAACCGCCTGTTACGAACC_3' and 3'_CCTACTGCTGCGACCTGCTTGGCGGACAATGCTTGG, on full length GHR template. GHR 326EFIxxD (GHR-EFID mutant) was generated as previously described(*26*).

βTrCP2 cDNA N-terminally fused with a flag tag cloned in pcDNA3 (Flag-βTrCP) was a generous gift from Prof. Tomoki Chiba (University of Tsukuba, Tsukuba-shi, Japan).

The constructs Myc-Cullin, Flag-Skp1 and T7-Rbx in pcDNA3.1 were a gift from Prof. Kazuhiro Iwai (Osaka University, Osaka, Japan). Structural and biochemical studies on the interaction of βTrCP1 with classical substrates as βCatenin and IκB identified residues in the WD40 domain of βTrCP1 involved in their interaction (Tyr271, Arg431, Arg474, Tyr488)(*19*). To investigate the effects of these mutations on the interaction with GHR-UbE, site-directed mutagenesis was performed to replace the respective conserved residues with alanine in flag-tagged βTrCP2 (Flag-βTrCP), by using Quick Change mutagenesis kit from Stratagene. Flag-βTrCP2 was used as a template, and the following oligonucleotides were used: Y244 A (5'_CTGAAAATAGTAAAGGTGTCGCCTGTTTACAGTACG_3' and 3'_GACTTTTATCATTTCCACAGCGGACAAATGTCATGC_5'); R404A (5'_CAATGGGCACAAGGCGGGCATTGCCTGTCTCC_3' and 3'_GTTACCCGTGTTCCGCCCGTAACGGACAGAGG_5'); R447A (5'_CATGAAGAATTGGTCGCATGCATCCGGTTTGATAACAAGAGG_3' and 3'_GTACTTCTTAACCAGCGTACGTAGGCCAAACTATTGTTCTCC_5'); Y461A (5'_GGATTGTCAGTGGGGCCGCTGATGGGAAAATTAAAGTTTGG_3' and 3'_CCTAACAGTCACCCCGGCGACTACCCTTTTAATTTCAAACC_5').

Other single mutants of the WD40 domain were also generated: G242A (5'GAAAATAGTAAAGGTGTCTACTGTTTAACAG3' and 3'CTGTAAACAGTAGACACCTTTACTATTTTC5'), R258A (5'CAGTGGCCTACGAGATAATTCTATTAAG3' and

3'CTTAATAGAATTATCTCGTAGGCCACTG5'), S282A (5'CAGGACACACAGGCTCTGTCCTCTGTCTGC3' and 3' GCAGACAGAGGACAGAGCCTGTGTGTCCTG5'), S298A (5'GTAACTGGCTCTTCAGATTCTACGG3' and 3'CCGTAGAATCTGAAGAGCCAGTTAC5'), S421A (5'GTTAGTGGATCATCAGATAATACCATTAGG3' and 3' CCTAATGGTATTATCTGATGATCCACTAAC5'), L445A (5' GGACATGAAGAATTGGTCCGATGCATCC3' and 3' GGATGCATCGGACCAATTCTTCATGTCC5'), R494A (5'GAACATTCTGGACGTGTGTTTCGGCTCC3' and 3'GGAGCCGAAACACACGTCCAGAATGTTC5').

All Flag-tagged βTrCP WD40 triple alanine mutants were obtained following the strategy described before (*27*). Briefly, two PCR products were made for creating each triple alanine mutant, using Flag-βTrCP2 as template. The first PCR segment was obtained with the forward primer common for every mutant annealing in Flag tag, 5'GATCGGATCCATGGACTACAAAGACGATGACGACAAGATGGAGCCCGACTCG3', and a reverse primer, specific for each mutation that creates a Not1 site while replacing three codons with alanine encoding ones. The second PCR fragment was generated with a forward primer specific for each mutation, where a Not1 site is created while replacing three codons with alanine encoding ones, and a common reverse primer, annealing in the end of Flag-βTrCP2 sequence, 3' GATCGAATTCTTATCTAGAGATGTAAGTG-5'. After Not1 digestion, the two fragments originated from PCR1 and PCR2 were ligated, and cloned using BamH1 and EcoRI restriction sites in pcDNA3.

Cell culture and transfections

Culture media, foetal calf serum and antibiotics for tissue culture were purchased from Gibco (Invitrogen, Groningen, The Netherlands). Human embryonic kidney 293 (HEK293) cells, stably expressing the Tetracycline Repressor (HEK293-TR), were a gift from Dr. Madelon Maurice (University Medical Centre Utrecht, Utrecht, The Netherlands).

HEK293-TR cells were grown in Dulbecco's modified Eagle's medium (DMEM) supplemented with 10% fetal calf serum, 100 units/ml penicillin, 0.1 mg/ml streptomycin and 12 μg/ml Blasticidin S (MP Biomedicals, Amsterdam, The Netherlands). Cells were grown at 37°C with 5.0% CO_2. Twice a week the cells were washed with phosphate-buffered saline (PBS), detached from the flask with trypsin-EDTA (Invitrogen) diluted in fresh growth medium, and split into new culture flasks. DNA transfections were performed using FuGene 6 (Roche, Applied Sciences, Almere, The Netherlands). Seventy percent confluent cultures in 6-wells plates were transfected with 1 μg DNA, according to the manufacturer's protocol. 10 cm dishes were transfected with 6 μg DNA, for subsequent purification of the SCF(βTrCP) complex and GHR proteins to be used in the *in vitro* ubiquitination assays. For fluorescence microscopy experiments, the cells were grown on coverslips placed in 12 wells plates and transfected with 0.5 μg DNA. Twenty four hours after transfection, the cells were used for pull down experiments, immunoprecipitations, western blotting, and fluorescence microscopy experiments.

Protein expression and Purification

The C-terminal part of βTrCP2 (114-542), including SkpI binding domain, but excluding dimerization domain, was amplified by PCR with forward primer GATGCCATGGGAATGTTGCAGCGGGACTTTATT and reverse primer GATCAAGCTTTTATCTAGAGATGTAAGTGTATG (short form of βTrCP2: SF- βTrCP2). After NcoI and HindIII digestion, the fragment was cloned into pFastBac-HT-B Baculoviral vector with a His-tag (Invitrogen, Groningen, The Netherlands). SkpIΔΔ, lacking unstructured loops of amino acids 38-43 and 71-82 in the pAcSG2 vector, was a generous gift from Dr. Brenda Shulman (St. Jude Children's Research Hospital, Memphis, USA). A PCR fragment was generated by amplifying SkpIΔΔ with the forward primer GATGCCATGGGAATGCCTTCAATTAAGTTGCAG and reverse primer GATCCTCGAGTCACTTCTCTTCACACCACTGG. This PCR fragment was cloned into pFastBac-HT-B (with His tag) using Nco1 and Xho1 restriction sites. The generation of the full-length rabbit GHR cDNA in pcDNA3 was previously described (*11*). The generation of the baculovirus for His-tagged SF-βTrCP2 (His-SF-βTrCP) and His-tagged SkpIΔΔ (His-SkpIΔΔ) was performed according

to the manufacturers of the Bac-to-Bac® Baculovirus expression system (Invitrogen, Groningen, The Netherlands). The virus titer was further amplified in 50 ml of Sf9 cells cultured in suspension. The efficiency of the virus was tested by infecting SF9 insect cells with increasing amounts of baculovirus and screened for the day post infection that resulted in the highest amount of protein. For expression of high amounts of functional His-SF-βTrCP protein, co-expression with His-SkpIΔΔ was necessary to stabilize the βTrCP protein, as reported previously by Wu et al (*19*). To scale up the protein expression, large volumes of SF9 cell suspension cultures at density of $2x10^6$ cells/ml were infected with a 1:500 dilution of the virus stock of His-SF-βTrCP, and 1:2000 dilution of the virus of His-SkpIΔΔ. Two days after infection, infected cells were spun down, washed in Phosphate Buffer Saline (PBS), and pellets were stored at -20^o until further use. For protein purification, $2x10^8$ SF9 cells were lysed in 5 ml lysisbuffer (50 mM NaH_2PO_4 pH 8, 200 mM NaCl, 5 mM β-Mercaptoethanol, 5% glycerol, 20 mM imidazole, 1 mM PMSF, 10 µg/ml leupeptine, 10 µg/ml aprotinine). After sonication, cells were centrifugated for 60 min at 30,000 rpm at 4^0C in Ti50.2 rotor (Beckman coulter, Woerden, The Netherlands). Lysates were filtered over 0.22 µm filter, and then loaded on a Histrap HP column (GE Healthcare, Hoevelaken, The Netherlands) connected to the Äkta Explorer high-performance liquid chromatography (HPLC) (GE Healthcare). The His-SF-βTrCP/His-SkpIΔΔ complex was optimally eluted from the column by using an optimized step gradient of increasing imidazole concentrations until reaching 500 mM (50 mM NaH_2PO_4 pH 8, 200 mM NaCl, 5 mM β-Mercaptoethanol, 5% glycerol, 500 mM imidazole, 1 mM PMSF, 10 µg/ml leupeptine, 10 µg/ml aprotinine). This purification resulted in two distinct peaks. The first peak, eluting at lower imidazole concentration (approximately 100 mM) corresponded to background and excess of Skp1ΔΔ that is not in complex with His-SF-βTrCP. The second peak, eluted at a higher imidazole concentration (approximately 250 mM) was the His-SF-βTrCP/His-SkpIΔΔ complex in a stoichiometric ratio 1:1. The fractions from the second peak were concentrated to 500 µl using vivaspin 20 (Lab Technology Products, Goettingen, Germany), and loaded on a S200 gel filtration column with gel filtration buffer (50 mM NaH_2PO_4 pH 7.2, 200 mM NaCl). The purified complex was then concentrated with vivaspin 20 until reaching appropriate concentration.

GHR cytoplasmic tails of two different lengths, residues 270-318 or 217-334 (without or with UbE motif, respectively), were expressed as a GST phusions in *E. coli* (strain BL21), and purified with Glutathione (GSH)-beads (Amersham Biosciences) by a standard protocol previously described (*28*). After purification the proteins were freeze dried in aliquots and stored at -20^{0}C. The UbE alanine scan was performed in GST-GHR270-339 tails, with the Quick Change mutagenesis kit from Stratagene. The expression and purification was performed as described previously for GST-GHR 270-318 and GST-GHR 270-334.

$SCF^{\beta TrCP}$ complexes were expressed in HEK293-TR cells co-transfected with Flag-Skp1, Myc-Culin1, T7-Rbx1 and Flag-βTrCP2 (WT and WD40 point mutants). 24 hours after transfection, the cells were lysed in 15 mM Tris HCl pH7.4, 500 mM NaCl, 0.35% NP40, 5 mM EDTA, 5 mM EGTA, 1 mM PMSF, 10 µg/ml leupeptine, 10 µg/ml aprotinine. $SCF^{\beta TrCP}$ was isolated by adding Flag agarose beads to the lysates overnight, with subsequent elution with 3XFlag peptide (Sigma-Aldrich) in the concentration 100µg/ml in TBS (10 mM Tris HCl, 150 mM NaCl, pH7.4).

GHRs (WT or EFID mutant) were transiently overexpressed in HEK293-TR cells. 24 hours after transfection, the receptors were bound to 180 ng/ml GH(his-TEV-STREP3-his)C for 30 min at 37^{o}C, and pulled with Streptactin beads (GE Healthcare) after lysis in 100 mM Tris-HCl pH8, 150 mM NaCl, 1 mM EDTA and 0.5% TritonX100. GHRs were eluted with desthiobiotin (Sigma) 2.5 mM, 100 mM Tris-HCl pH8, 150 mM NaCl, 1 mM EDTA.

In vitro Binding assays

GST-GHR 270-318 (GST-GHR-UbE) or GST-GHR 270-334 (GST-GHR+UbE) were dissolved in PBS supplemented with 1% BSA and protease inhibitors (1 mM PMSF, 10 µg/ml aprotinin, 10 µg/ml leupeptine) and incubated with GSH beads for 2 hours at 4^0C (10 µg GST phusions were used for saturation of 25 µl of GSH beads). The beads were washed twice with the same buffer and twice with

binding buffer (50 mM Tris pH8, 100 mM NaCl, 0.1 % Triton X-100, 0.1%BSA, 1 mM PMSF, 10 μg/ml aprotinin, 10 μg/ml leupeptine)

His-SF-βTrCP2/His-Skp1ΔΔ complex was then incubated for 2 hours with the GSH beads coupled to GST-GHR phusions in the binding buffer at 4^0. The beads were washed twice with binding buffer and twice with 0.1 X PBS. In case of competition with peptides, the beads were incubated for 2 additional hours with increasing concentrations of the indicated GHR peptides (0.7, 7 and 70 μM) diluted in binding buffer. The beads were washed twice with binding buffer and twice with 0.1 X PBS. The beads were boiled in sample buffer, run on SDS-PAGE and immunoblotted with anti-GST and anti-His antibodies.

In vitro Ubiquitination assays

The purified Uba1 and UbcH5 were a kind gift of Prof. Titia Sixma (Nederlands Kanker Instituut (NKI), Amsterdam, The Netherlands).

GHR ubiquitination reactions were performed at 37°, for 1 hour, in a total volume of 60 ul. The reactions contained 50 mM TrisHCl pH7.4, 75 mM NaCl, 0.6 mM DTT, 5 mM $MgCl_2$, 2 mM ATP, 2 mM NaF, 1 ug ubiquitin, 0.15 pmol Uba1 (E1), 90 pmol UbcH5 (E2). As source of E3 ligase, $SCF^{\beta TrCP}$ complexes purified from HEK293 cells were used: 1/5th of the total $SCF^{\beta TrCP}$ purified from a confluent 10 cm dish was used per reaction.

Purified GST-GHR tails (50 pmol per reaction) or full length GHR receptors (1/7th from the total amount of GHR purified from a 10 cm dish per reaction) were used as substrates.

Biotin-GH pull downs, immunoprecipitations

24 h after co-transfection of the indicated GHR and βTrCP constructs, biotin-GH (180 ng/ml) was added to HEK293-TR for 10 min at 37°C. Subsequently, cells were washed three times with PBS, and lysed with cold lysis buffer (1% Triton X-100, 1 mM EDTA, 100 mM NaF, 1 mM Na_3VO_4, 1 mM PMSF, 10 μg/ml aprotinin, and 10 μg/ml Leupeptine, in PBS). After 5 min centrifugation at maximum speed at 4°C, the supernatant was incubated for 1 h with streptavidin beads at 4°C. Beads were boiled and subjected to SDS-PAGE, and western blotting.

For the anti-Flag co-immunoprecipitations HEK293-TR cells were lysed in 50 mM Tris pH7.4, 100 mM NaCl, 50 mM NaF, 1% Triton X-100, 1 mM EDTA, 1 mM Na_3VO_4, 1 mM PMSF, 10 μg/ml aprotinin, and 10 μg/ml Leupeptine. After 5 min centrifugation at maximum speed at 4°C, the supernatant was incubated for 1 h with anti-Flag agarose beads at 4°C. Beads were boiled and subjected to SDS-PAGE, and western blotting.

Immuno Blotting

Following SDS-PAGE, proteins were transferred to an Immobilion-FL PVDF membrane (Millipore, Amsterdam, The Netherlands). The membranes were blocked with Odyssey blocking buffer (Li-Cor Biosciences, Lincoln, NE, USA) diluted two times with PBS for 1 hour at room temperature. The blots were incubated with the indicated primary antibodies for 1.5 hour, and after washing in PBS 0.1% Tween-20, membranes were incubated for 1 hour with secondary antibody. The detection and analysis of the immunoblots was performed with an Odyssey infrared imaging system (Li-Cor Biosciences, Lincoln, Nebraska).

Confocal Microscopy

Cy3-GH was prepared using a fluorolink-Cy3 label kit according to the manufacter's protocol (Amersham Biosciences). Transfected cells, grown on coverslips, were incubated for 30 min with Cy3-GH (180ng/ml), washed with PBS and fixed for 30 min in 4% paraformaldeyde in PBS. After fixation, the cells were embedded in Mowiol. Representative confocal pictures were taken using LeicaTCS 4D system (Leica Microsystems,Wetzlar, Germany).

NMR Spectroscopy

All NMR experiments were carried out at 278 K on a Bruker AVANCE 600 MHz spectrometer equipped with 5-mm triple-resonance z-shielded cryogenic probe. Spectra were processed using

Bruker Topspin (Bruker BioSpin B.V, Netherlands) and analyzed using CcpNmr Analysis v2.1.5(*29*). Secondary structure of the UbE peptide was determined from a consensus of chemical shift indices of $^{1}H\alpha$, $^{13}C\alpha$ and $^{13}C\beta$ nuclei using the CSI software (*30*). Restraints were derived and structures calculated in torsion angle space using the software CYANA 2.1 (*31*).

NMR samples contained the UbE motif peptide, Acetyl-YKPEFHSDDSWVEFIELDIDEP-amide, with or without the purified β-TrCP2 (His-SF-βTrCP/His-SkpIΔΔ complex). Both UbE peptide and β-TrCP samples were prepared in 50 mM phosphate buffer pH 7.2, 200 mM NaCl, 5% D_2O. ^{1}H chemical shifts were directly referenced to the resonance of 2,2-dimethyl-2-silapentane-5-sulfonate sodium salt.

The following two-dimensional (2D) experiments were performed: 2D-TOCSY (*32*) (4096 × 600 complex points), 2D-TRNOESY(*33, 34*) (1024 × 1024 complex points), 2D heteronuclear ^{1}H-^{13}C HMQC(*35*) (centered on aliphatic signals) and ^{1}H-^{13}C CT-HSQC (*36*) (centered on aromatic signals).

The fast exchange regime between the bound and free states required for "Transfer Nuclear Overhauser effect spectroscopy"(TRNOESY) NMR experiments was investigated using "Saturation transfer difference" (STD) across a range of concentration ratios 1:600 – 1:10 (protein : peptide) (*37*). Saturation transfer was achieved with on-resonance selective low power irradiation (60 db attenuation) at -2 ppm, and off-resonance at -10 ppm for the reference spectrum. The optimal protein: peptide ratio was set at 1:350, corresponding to a protein and peptide concentrations of 4.5μM. and 1.6 mM, respectively. The 1D STD spectra were obtained by internal subtraction of saturated spectra from reference spectra. Residual positive signals are present when a ligand undergoes reversible binding. The intensity of the STD signal is proportional to the proximity of the ligand residues to the protein. ^{1}H-^{1}H NOE peaks of the UbE peptide were collected from TRNOESY spectra with 100 ms mixing time in both absence and presence of β-TrCP (at protein: peptide ratio of 1:350). Peak volumes were converted to distance restraints using the CYANA 2.1 internal calibration protocol. Of the two hundred structures minimized in CYANA 2.1, twenty, with the lowest target function values, were selected as the representative ensemble and used for the molecular docking stage to β-TrCP.

Modeling of β-TrCP2 structure and molecular docking of UbE peptide

Ten models of β-TrCP2 were derived from the homologous structure of β-TrCP1 (PDB code 1P22) using the Modeller (9v1) software (*38, 39*). All ten models were used in the subsequent docking stage to the TRNOESY derived structures of the UbE peptide. Molecular docking was generated using the HADDOCK server (*40*). The docking consists of three stages, namely, a rigid body minimization (it0), a semi-flexible simulated annealing in torsion angle space (it1) and finally a refinement in explicit solvent. Structures in each stage are ranked according to their HADDOCK score and based on this ranking are selected for the next stage. The HADDOCK score is a weighted sum of the buried surface area and the following four energy terms; Van der Waals, electrostatic, desolvation and restraint violation. One thousand structures are minimized in it0, from which 200 with the lowest HADDOCK score are selected for it1 and the water refinement stage. Based on the mutagenesis studies described in this study, the following Ambiguous Interaction Restraints (AIRs) were incorporated as active restraints in the docking protocol: E13 (E326 in full length GHR), F14 (F327 in full length GHR), D18 (D331 in full length GHR) from the UbE peptide, and Y244, R258, S282, R447 from β-TrCP2. After water-refinement, the cluster with the lowest HADDOCK score (-107.3 ± 17.5) and smallest RMSD from the lowest energy structure (1.1 ± 0.8 Å) was chosen as the representative ensemble of the complex. Consistent with the HADDOCK score this cluster displayed the largest buried surface area (1434.1 +/- 137.2 Å2) of all clusters. The lowest energy structure within this cluster was chosen for the comparison with previously published β-TrCP1 – ligand complexes (*20-25*).

Results

The UbE motif of GHR interacts directly with βTrCP

Previously, we found that the ubiquitin ligase SCF(βTrCP) regulates the endocytosis and degradation of the GHR (*13*). The UbE motif of GHR and the WD40 domain of βTrCP appeared to be crucial for this interaction. However it was not formally proven whether this interaction was direct. In

order to show the direct interaction, we purified GST-GHR tails from *E.coli*, and βTrCP from Sf9 cells. βTrCP was purified in complex with Skp1, since Skp1 is required to guarantee βTrCP solubility and stability (*19*). The optimized purification procedure resulted in a stoichiometric complex His-SF-βTrCP/His-Skp1ΔΔ (Fig. 1A). The purified βTrCP/Skp1 complex bound specifically to the GST–GHR tails containing the UbE

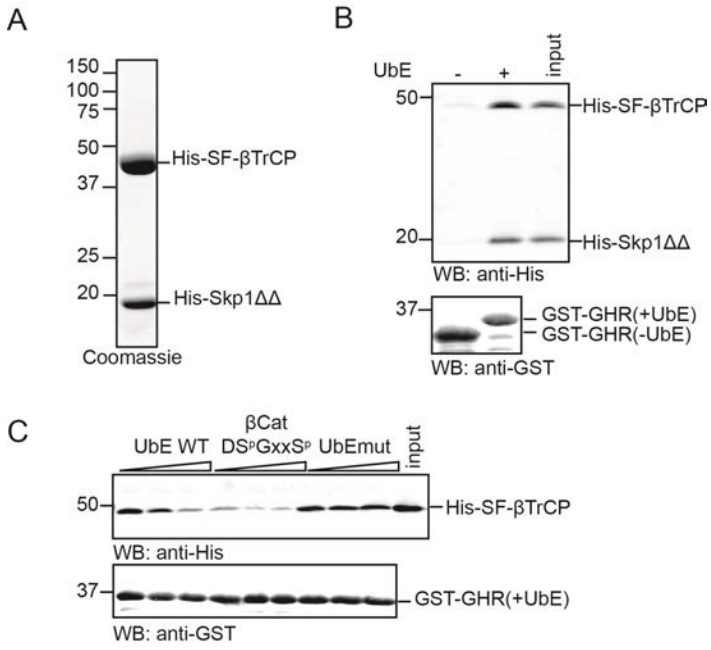

Fig. 1- The UbE motif of GHR interacts directly with βTrCP

(A) Coomassie staining of purified His tagged-short form of βTrCP (His-SF-βTrCP) from Sf9 cells in a stoichiometric complex with His-Skp1ΔΔ (detailed procedure, see Materials and Methods). **(B)** GST-GHR tails with (+) or without (-) the UbE motif were coupled to glutathione beads and allowed to bind His-SF-βTrCP/His-Skp1ΔΔ complex. The samples were analysed by western blotting with anti-His and anti-GST antibodies. In the 3rd lane the input of His-SF-βTrCP/His-Skp1ΔΔ complex used in the binding assay is shown. **(C)** GST-GHR tails containing the UbE motif were coupled to glutathione beads and saturated with His-SF-βTrCP/His-Skp1ΔΔ complex. Increasing concentrations of peptides (0.7, 7 and 70 μM) containing the WT UbE motif, phosphorylated DSGxxS motif of βCatenin (βCat $DS^{P}GxxS^{P}$), or a mutated UbE motif (F327 and D331 mutated to alanines), were used to compete for the binding of βTrCP. The samples were analysed by western blotting with anti-His and anti-GST antibodies.

motif (GST-GHR(+UbE)) and not if the UbE motif was absent (GST-GHR(-UbE)) (Fig. 1B). The specificity of the interaction was confirmed by a competition assay (Fig. 1C). The binding of the purified His-SF-TrCP/His-Skp1ΔΔ to the GST-GHR(+UbE) tails was competed off by addition of increasing concentrations of peptides containing the UbE motif sequence. As a result, the higher the concentration of UbE peptide added, the lower is the amount of His-SF-βTrCP/His-Skp1ΔΔ retained in the beads coupled to GST-GHR(+UbE) (Fig. 1C, lane 1-3). A peptide with a mutated UbE motif sequence was not able to interfere with the GHR-βTrCP protein interaction (Fig. 1C, lane 7-9), confirming the specificity of the interaction. A peptide containing the phosphorylated DSGxxS motif sequence was able to compete more efficiently for βTrCP binding than the UbE motif peptide (Fig. 1C, lane 4-6).

These results show that the UbE motif interacts directly and specifically with βTrCP, with a lower affinity than the phosphorylated DSGxxS motif.

$SCF^{\beta TrCP}$ ubiquitinates the GHR upon interaction with the UbE motif, *in vitro*.

Interaction of $SCF^{\beta TrCP}$ with the phosphorylated $DSG(X)_{2+n}S$ motif on its substrates results in their ubiquitination (*41*). To investigate whether SCF(βTrCP) is able to mediate the ubiquitination of the receptor, an *in vitro* ubiquitination assay was developed. The multi-subunit $SCF^{\beta TrCP}$ complex (E3) was immunoprecipitated from HEK293-TR cells (Fig. 2A), and together with purified Uba1 (E1) and UbcH5b (E2), was used in the *in vitro* ubiquination of GST-GHR tails (+/-UbE motif). GST-GHR(+UbE) was clearly ubiquitinated in the rection as can be seen by several discrete bands and a smear up in the gel, detected with both anti-GST (Fig. 1B, top panel, lane 2) and anti-ubiquitin antibodies (Fig. 2B, low panel, lane 2). When GST-GHR(-UbE) was used as substrate, or either E2 or E3 were absent in the reaction, no characteristic ubiquitination pattern could be detected (Fig. 2B, top panel, lane 5, 3 and 4, respectively). This shows that ubiquitination of the GST-GHR tails depends on the direct interaction on SCF(βTrCP) with the UbE motif, correlating with the binding results of Fig. 1. When detected with anti-ubiquitin antibody, a smear up in the gel is detected that occurs

independently of substrate addition (Fig. 1B, low panel, lane 1), most likely due to ubiquitination of other components of the reaction.

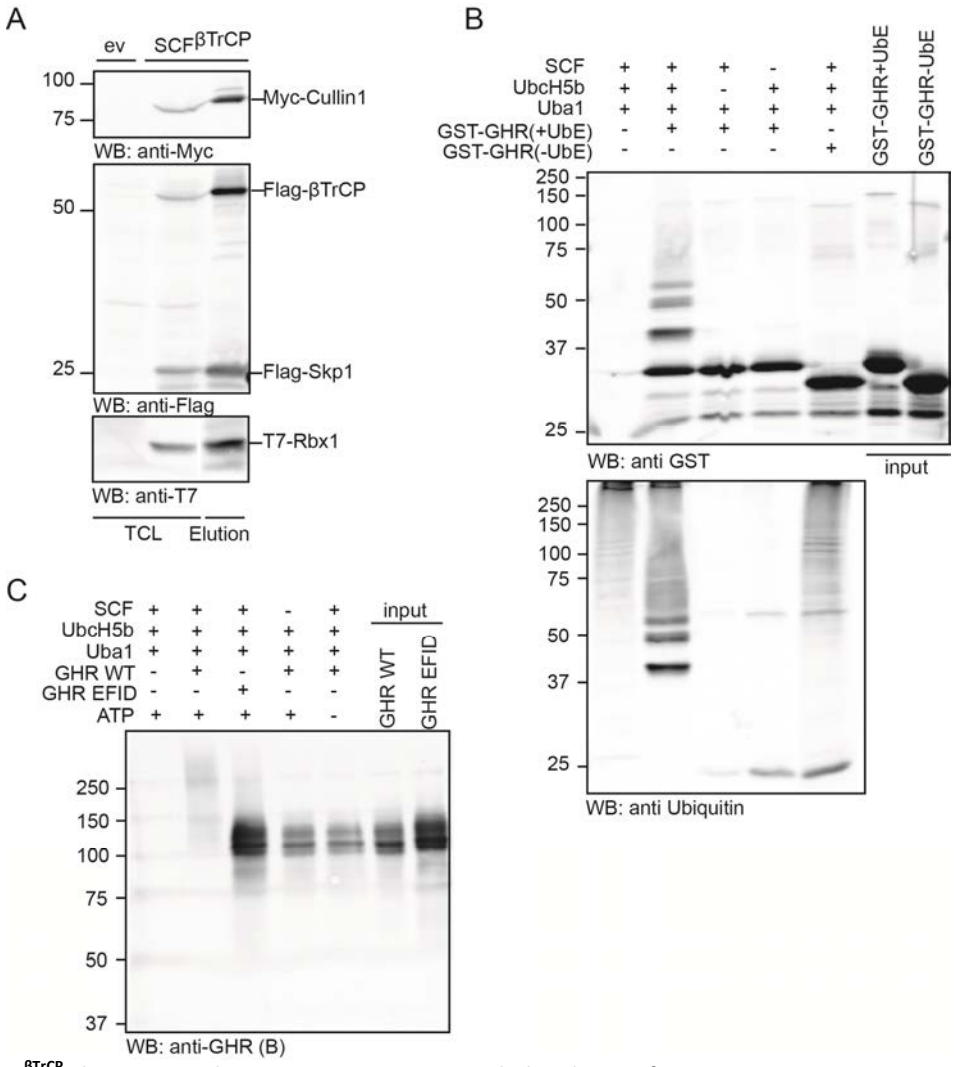

Fig. 2- SCF$^{\beta TrCP}$ ubiquitinates the GHR upon interaction with the UbE motif, *in vitro*.
(A) HEK293-TR cells were transiently co-transfected with Flag-Skp1, Myc-Culin1, T7-Rbx1 and Flag-βTrCP2, or with empty vector as control. The SCF(βTrCP) complex was isolated with anti-flag agarose beads and eluted with 3X Flag peptide. The elution (lane 3) was analysed by western blotting with anti-Myc, anti-Flag, and anti-T7 antibodies. An aliquot of the lysates used for SCF(βTrCP) isolation is shown in lane 2. ev, empty vector; TCL, total cell lysates. **(B)** GST-GHR tails with (+) or without (-) UbE motif were used as substrates in *in vitro* ubiquitination reactions. The reactions contained Uba1 as E1, UbcH5 as E2, and SCF(βTrCP) complex from elutions as shown in figure 2A, as E3. After 1 hour incubation at 37^{0}C, the reactions were subjected to western blotting and detected with anti-GST (upper panel) and anti-ubiquitin (anti-Ub) antibodies (lower panel). The substrates used in the reaction are shown in lane 6 and lane 7 (input). **(C)** GHR WT and GHR-EFID mutant were overexpressed in HEK293-TR cells, pulled from the cell surface with STREP-tagged GH, bound to streptactin beads and eluted with desthiobiotin. Elutions were used as substrates in *in vitro* ubiquitination reactions, as explained in figure 2B. The reactions were subjected to western blotting and detected with anti-GHR (B) antibody. The substrates used in the reaction are shown in lane 6 and lane 7 (input).

To demonstrate that ubiquitination of GHR also takes place under physiological conditions, we performed the assay with full length receptors pulled from HEK293-TR cells transiently transfected with wild type GHR (WT), or the UbE mutant (EFID) (*12*). GHR WT was ubiquitinated very efficiently, as seen by a complete shift of GHR signal up in the gel, provided that SCF (βTrCP) and ATP were present (Fig. 2C, compare lane 2 to lanes 4 and 5). The GHR-EFID mutant was hardly ubiquitinated (Fig. 2C, lane 3).

Taken together, we conclude that SCF (βTrCP) mediates GHR ubiquitination directly, in an UbE motif dependent manner.

GHR-βTrCP interaction has unconventional characteristics.

Previously, we showed that the GHR-βTrCP binding depends on the WD40 domain (*42*). In the previous sections of this paper we proved that βTrCP binds directly to the UbE motif, and as a consequence it mediates GHR ubiquitination. This classifies GHR as a genuine βTrCP substrate. As the UbE sequence significantly differs from the classical $DSG(X)_{2+n}S$ degron, we expect the characteristics of the GHR-βTrCP interaction to differ as well. Structural studies have identified βTrCP WD40 amino acid residues that contribute for the binding to the phosphorylated DSGxxS motif (*19*). We evaluated the role of some of these residues (Y244A, Y404A, R447A, and Y461A) on the interaction with GHR.

Firstly, we performed binding assays to evaluate the effect of these mutations. HEK293-TR cells were co-transfected with Flag-βTrCP WT and WD40 mutants, together with GHR WT. GHR F327A mutant (with mutation in the crucial residue of the UbE motif)(*12*), co-transfected with βTrCP, was used as a control to ascertain that the conditions of the assay are optimal. Biotin-GH was used to isolate GHR complexes from the plasma membrane of the cells. As expected, Flag-βTrCP WT was pulled with GHR (Fig. 3A, lane 1), while its interaction with the GHR F327A was decreased (Fig. 3A, lane 7; quantified in Fig. 3B).The expression of the different Flag-βTrCP mutants affected the stability of the GHR differently, as can be seen in total cell lysates by differences in the ratio mature/precursor (Fig. 3A, 4th panel). This can be explained as follows: Overexpressed Flag-βTrCP mutants compete with the endogenous βTrCP for the other components of the SCF complex; if the mutants have impaired binding to GHR, they work as dominant negative, and the endocytosis/degradation of GHR will be impaired, resulting in accumulation of mature GHR. Overexpression of the Y244A and R447A mutants resulted in the stabilization of mature GHR, which indicates that these mutations most likely affected the binding to GHR. Particularly, the mutation R447A resulted in a stabilization of GHR comparable with GHR F327A.When βTrCP amounts (Fig. 3A, 1st panel) are corrected for the amount of pulled receptor (Fig. 3A, 3rd panel), the binding of the R447A mutant to GHR was indeed strongly impaired (25% of the WT), at similar extent as βTrCP binding to the GHR F327A mutant (Fig. 3A, compare lane 4 to lane 6; quantified in Fig. 3B). With the same analysis, the mutant Y244A also bound GHR less efficiently (75% of the WT) (Fig. 3A; quantified in Fig. 3B). The mutants Y404A and Y461A bound GHR WT normally and, consequently, no stabilization of the mature GHR was seen (Fig. 3A, lanes 3 and 5, respectively; quantified in Fig. 3B). These results argue that R447 and Y244 are involved in βTrCP interaction with GHR-UbE motif, while the residues R404 and Y461 are not. The βTrCP Y244A mutant resulted in an intermediate level of ubiquitination (Fig.3B, lane 3), in agreement with its intermediate capacity to bind GHR. The smear and bands above 60 kD detected with the anti-GST antibody, are unrelated to the specific ubiquitination reaction of GHR, because they are also present in the input (Fig. 3B, upper panel, lane 9). Ubiquitination did not occur on GST-GHR(-UbE) (Fig. 3B, upper panel, lane 2). The effects of the βTrCP mutations on endocytosis of GHR in living cells were addressed by analysing the uptake of Cy3-GH in cells transiently overexpressing GHR together with Flag-βTrCP constructs (WT and mutants)(Fig. 3C). Co-expression of GHR F327A mutant with WT βTrCP was performed as a control, and resulted in inhibition of Cy3-GH uptake as seen by plasma membrane labelling of Cy3-GH (Fig. 3C). In the WT situation Cy3-GH is efficiently internalized, and therefore, all the Cy3-GH appears as small punctae inside the cells, without any detectable surface labelling. The same phenotype was seen when overexpressing βTrCP Y244A, R404 or Y461A mutants. In contrast, overexpressing βTrCP R447A mutant resulted in inhibition of Cy3-GH uptake, in a comparable extent to GHR F327A mutant.

Overall, we conclude that from the four tested WD40 residues needed for βcatenin and IκB binding (*19*), only R447 and to a lesser extent Y244 are involved in GHR binding, GHR ubiquitination and GHR endocytosis. Interestingly, R404 and Y461 seem not to be involved. These characteristics reveal that the interaction GHR-βTrCP is unconventional. Since GHR is the only protein described so far that uses the UbE motif for βTrCP binding, we can classify GHR-βTrCP interaction as unique.

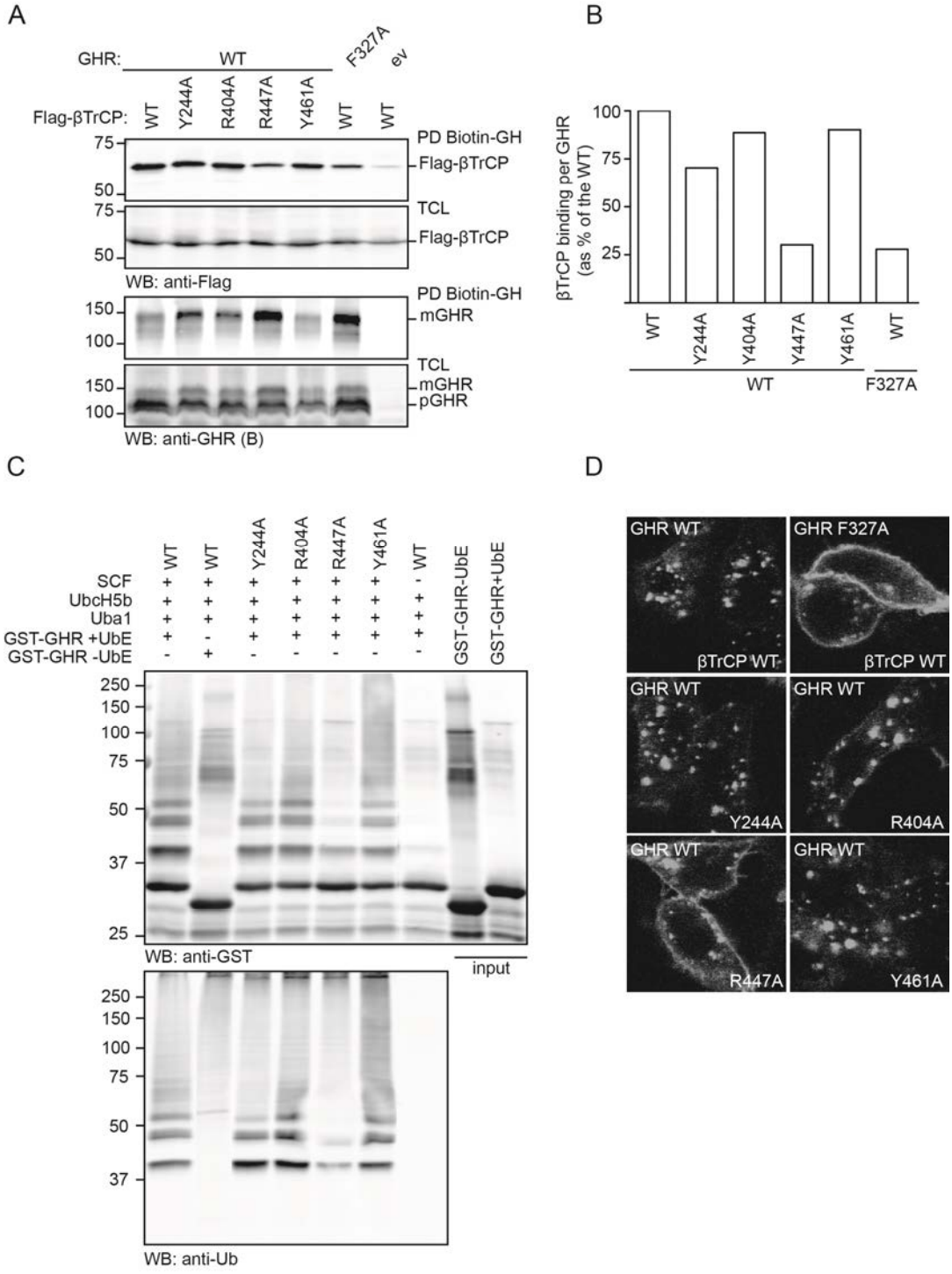

Fig. 3. GHR-βTrCP interaction has unconventional characteristics.

(A) HEK293-TR cells were transiently co-transfected with GHR WT together with Flag-βTrCP WT or Flag-βTrCP containing point mutations in its WD40 domain (Y244A, R404A, R447A and Y461A). In lane 5, GHR F327A mutant was co-transfected with Flag-βTrCP WT. GHR complexes were pulled from the cell surface with biotin-GH, bound for 10 min at 37^{o}C, and streptavidin beads. The samples resulting from the pull down were subjected to western blotting and detected with anti-GHR (B) and anti-Flag (for Flag-βTrCP detection) antibodies. ev, empty vector; PD, pull down; TCL, total cell lysates; mGHR, mature GHR; pGHR, precursor GHR in the endoplasmatic reticulum. **(B)** Quantification of Fig. 3A. The effect of each mutant was expressed as amount of βTrCP binding per GHR, as a percentage of the binding of the βTrCP WT to GHR WT. **(C)**HEK293-TR cells were transiently co-transfected with Flag-Skp1, Myc-Culin1, T7-Rbx1 and Flag-βTrCP2 WT or Flag-βTrCP containing point mutations in its WD40 domain (Y244A, R404A, R447A and Y461A). SCF(βTrCP) complexes were isolated by co-immunoprecipitation as shown in figure 2A. GST-GHR tails with (+) or without (-) the UbE motif were used as substrates in *in vitro* ubiquitination reactions. The reactions contained Uba1 as E1, UbcH5 as E2, and SCF with Flag-βTrCP WT or Flag-βTrCP mutants (Y244A, R404A, R447A and Y461A) as E3. After 1 hour incubation at 37^{0}C, the reactions were subjected to western blotting and detected with anti-GST (upper panel) and anti-ubiquitin (anti-Ub) antibodies (lower panel). The

substrates used in the reaction are shown in lane 8 and lane 9 (input). **(D)** HEK293-TR cells cultured on coverslips were transiently co-transfected with GHR WT together with Flag-βTrCP WT or Flag-βTrCP mutants (Y244A, R404A, R447A, or Y461A). GHR F327A mutant was co-transfected with Flag-βTrCP WT. The cells were incubated 30 min with Cy3-GH 180 ng/ml at 37^{o} C, and fixed in formaldehyde. Representative confocal pictures are shown.

Mapping more residues in the UbE and WD40 domain of betaTrCP2 involved in the interaction

To characterize the UbE-βTrCP interaction further we evaluated the relative contributions of each UbE aminoacid residue in an *in vitro* binding assay. A series of GST-GHR tails were generated in which each residue in the UbE sequence was mutated to alanine. These tails were coupled to glutathione beads and incubated with purified His-SF-βTrCP/His-Skp1ΔΔ complex. The amount of βTrCP/Skp1 bound per each GHR tail is shown and quantified in Fig. 4A. Especially the residues E326, F327, and D331 were involved in the GHR-βTrCP interaction.

Next, we extended our analysis to the complete WD40 repeats domain of βTrCP, in an attempt of mapping the residues of this domain involved in GHR- βTrCP interaction. Wu and collaborators (*19*) have shown that the residues contacting βCatenin are distributed along all the blades and are located mainly in three positions. The most commonly used residue is the second of the A strand. The residue immediately preceding the A strand (A-1) and immediately after the B strand (B+1) were also used. The same positions are used in other interaction involving the WD40 domain, e.g. transducin $G_t\beta\gamma$ and its interactor phosphoducin (*43*). To identify residues in the WD40 domain involved in UbE motif binding, we performed site directed mutagenesis of WD40 repeats of βTrCP. Triple alanine mutants and some single alanine mutants were generated from the A strands (including A-1) residues, and from the loops connecting the strands B and C, of all the 7 repeats (supplementary data). All these Flag-tagged mutants were transiently transfected in HEK293-TR cells together with GHR mutated in the DSGxxS motif (DAGxxA mutant). Recently we found that the DSGxxS motif in the GHR is able to bind βTrCP as well, in a conventional manner (da Silva Almeida AC *et al*, manuscript submitted). Therefore, the GHR DAGxxA mutant was used instead of GHR WT to eliminate any influence of βTrCP binding occurring through the DSGRTS sequence in the GHR. Flag-βTrCP WT or βTrCP mutants were immunoprecipitated and the amount of GHR interacting was analysed. The results obtained for the single βTrCP mutants are shown in Fig. 4B, while the results of the triple mutants are shown in the supplementary data. The differences in the amounts of GHR are a result of the different effects of the overexpressed βTrCP mutants on GHR endocytosis/degradation. In the quantification shown in Fig. 4B (lower panel) and in supplementary data this aspect was taken in consideration. In agreement with Fig. 3, we show again the importance of the residue R447 and to a lesser extent Y244 for the interaction with GHR; R258 and S282 were identified as additional important residues (Fig. 4B). Mutation of the residues S298, S421, L445 and Y461 resulted in increased binding to GHR. Perhaps mutation in these residues caused steric effects that increased the UbE-βTrCP interaction. For the analysis of the effects of the triple alanine mutations, two phenotypes were considered: (1) decreased GHR binding to βTrCP (Supplementary data, left graph) and (2) stabilization of GHR, as shown by increased ratio matureGHR/precursorGHR (Supplementary data, right graph). It is important to consider that by mutating three successive residues, folding problems might arise, with consequences on the general structure of βTrCP. The summary of the effects of each βTrCP mutant on GHR binding and stabilization are shown in the table of the supplementary data. Based on the two phenotypes mentioned above, residues mutated in L1, L4, L7, L9, L10, L12, L13, L17 and L22 triple mutants seem to be involved in the GHR-βTrCP interaction. The triple mutants L1 and L17 contain the residues Y244 and R447 respectively, which were proved to be important for the binding (Fig. 4B). The residue S282, important for βTrCP binding is immediately prior to the residues mutated in L4, which implies an important role of the strand A in blade 2 on UbE binding. The triple mutant L13, with compromised UbE binding, contains R404, which is not important for the interaction when mutated individually. Therefore, it could be that either G405 or I406 are important for the GHR-βTrCP interaction. Interestingly, while the mutant R258A has decreased binding to βTrCP, the triple mutant L3, where this residue was one of the mutated residues, did not show impaired binding. This would argue for a negative role of the other mutated residues (D259 and/or N260) in the interaction. In order to discard the possibility that the effects of the triple mutations on GHR binding arise from folding or steric problems a new set of mutagenesis of single βTrCP residues will be performed.

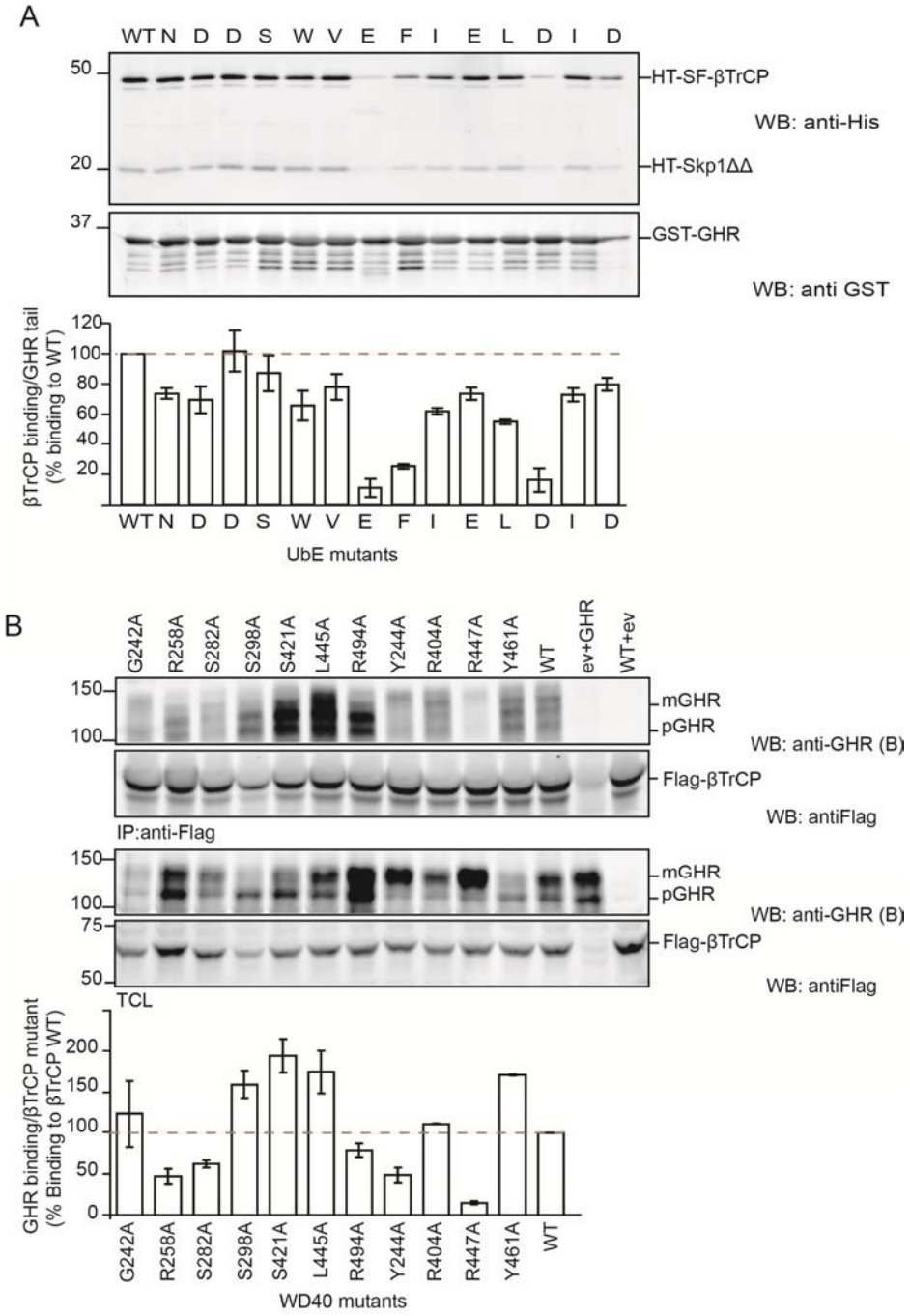

Fig. 4. Mapping more residues in the UbE and WD40 domain of betaTrCP2 involved in the interaction
(A) GST-GHR tails, WT, or where each of the indicated UbE residues were mutated to alanines, were coupled to glutathione beads, and incubated with purified His-SF-βTrCP/His-Skp1ΔΔ complex. The samples were analysed by western blotting with anti-His and anti-GST antibodies. The graph represents the quantification of βTrCP bound to GHR, corrected for the amount of GST-GHR tail, and expressed as percentage of βTrCP binding GST-GHR WT. **(B)** HEK293-TR cells were transiently co-transfected with GHR DAGxxA mutant together with Flag-βTrCP WT or Flag-βTrCP containing point mutations in the WD40 domain. The samples resulting from co-immunoprecipitation with anti-Flag agarose beads, were subjected to western blotting and detected with anti-GHR (B) and anti-Flag (for Flag-βTrCP detection) antibodies. The graph represents the quantification of the amount of GHR bound per immunoprecipitated Flag-βTrCP, corrected for the differences in GHR expression, and expressed as a percentage of GHR binding to Flag-βTrCP WT. ev, empty vector; IP, immunoprecipitation; TCL, total cell lysates; mGHR, mature GHR; pGHR, precursor GHR in the endoplasmatic reticulum.

Taken together, we conclude that βTrCP-UbE interaction requires the residues E326, F327 and D331 on GHR, and the residues R258, S282, Y244 and R447A on the WD40 domain of βTrCP.

Transfer-NMR studies data of the UbE-βTrCP interaction

NMR based methods have been extensively used in the last years for characterizing interactions of βTrCP with the $DSG(X)_{2+n}S$ motif in its substrates (*20-25*). We used this technique to get a detailed understanding how the unconventional UbE motif fits into the WD40 pocket. A peptide of the UbE motif 22 amino acids long was used with or without addition of purified βTrCP in STD and TRNOESY experiments.

Initially, the analysis of the Chemical Shift Index (CSI) obtained from the $^{13}C\alpha$, $^{13}C\beta$ and $^{1}H\alpha$ resonance assignments for the UbE peptide alone, supported a random-coil secondary structure (Fig. 5A). Accordingly, the majority of the NOE restraints, for both unbound (without βTrCP addition) and bound UbE peptide (with βTrCP addition), were intra-residual (Table 1). The random-coil secondary structure is also supported by the low percentage of dihedral angles occupying the most favored region in the Ramachandran plot (Table 1). This limited the ability to find a unique fold from the structure calculation.

Table 1: Structural Statistics for unbound and bound UbE peptide

	Unbound GHR peptide	Bound GHR peptide
Structural Ensemble	20	20
No. of distance restraints	286	183
Short-range (|i-j| ≤ 1)	244	171
Medium-range (1 < |i-j| < 5)	42	9
Long-range	0	3
Global RMSD (Å)		
Av. Backbone	3.27 ± 1.07	4.24 ± 1.39
Av. Heavy atom	3.89 ± 1.02	5.24 ± 1.26
Ramachandran plot		
Most favoured region	42.6 %	49.2 %
Additionally allowed region	57.4 %	49.5 %
Generously allowed region	0 %	0.8 %
Disallowed region	0 %	0.5 %

STD NMR spectroscopy experiments allow the identification of the amino acids of the peptide that are in close proximity with the protein. Irradiation of the protein at a resonance where no ligand signals are present leads to selective and very efficient saturation of the protein by spin diffusion. The entire protein is quickly saturated; the saturation is then transferred to the binding protons of the ligand by intermolecular saturation transfer. The protons in the closest proximity with the protein will show the highest degree of saturation. The STD signals result from the transfer of saturation from the bound to the free ligand, which requires fast exchange between these two states (*37*). The selective magnetization of βTrCP resulted in saturation transfer from βTrCP to the UbE peptide, at the ratio 1:350 (protein: peptide), suggesting that the condition of fast exchange is satisfied (Fig. 5B, middle panel). As a control we used the UbE peptide sample without any βTrCP added. Under these conditions, no signals of the UbE peptide were present, confirming that the observed signals depend on the selective saturation of βTrCP resonances and subsequent transfer of magnetization to the UbE peptide (Fig. 5B, bottom panel). Although all the STD peaks were attributable to the UbE peptide, no quantitative analysis of their intensities could be performed, due to the low signal to noise ratio. Therefore, based on the STD data no clear conclusions can be drawn about the proximity of the residues in UbE motif involved in βTrCP binding. However, from scrutinising the amide region in the STD spectra it is clear that the residue Phe14 of UbE (Phe327 in the full length GHR) is involved in binding.

Since the UbE-βTrCP interaction is a fast exchange system, as concluded by the STD experiments, we could incorporate the TRNOEs for a meaningful structure calculation of the bound peptide (Fig.

5B). A small number of medium and long range NOEs, observed in both the bound and unbound UbE peptide forms (Fig.5 5C), conferred a residual structure to the peptide, accessed by a bend formed between residues 11-16 (W324-E329 in GHR full length). This bend is more prominent in the bound form of the peptide (Fig.5 D).

We conclude that although the UbE motif has tendency to be unstructured it adopts a residual structure when bound to βTrCP.

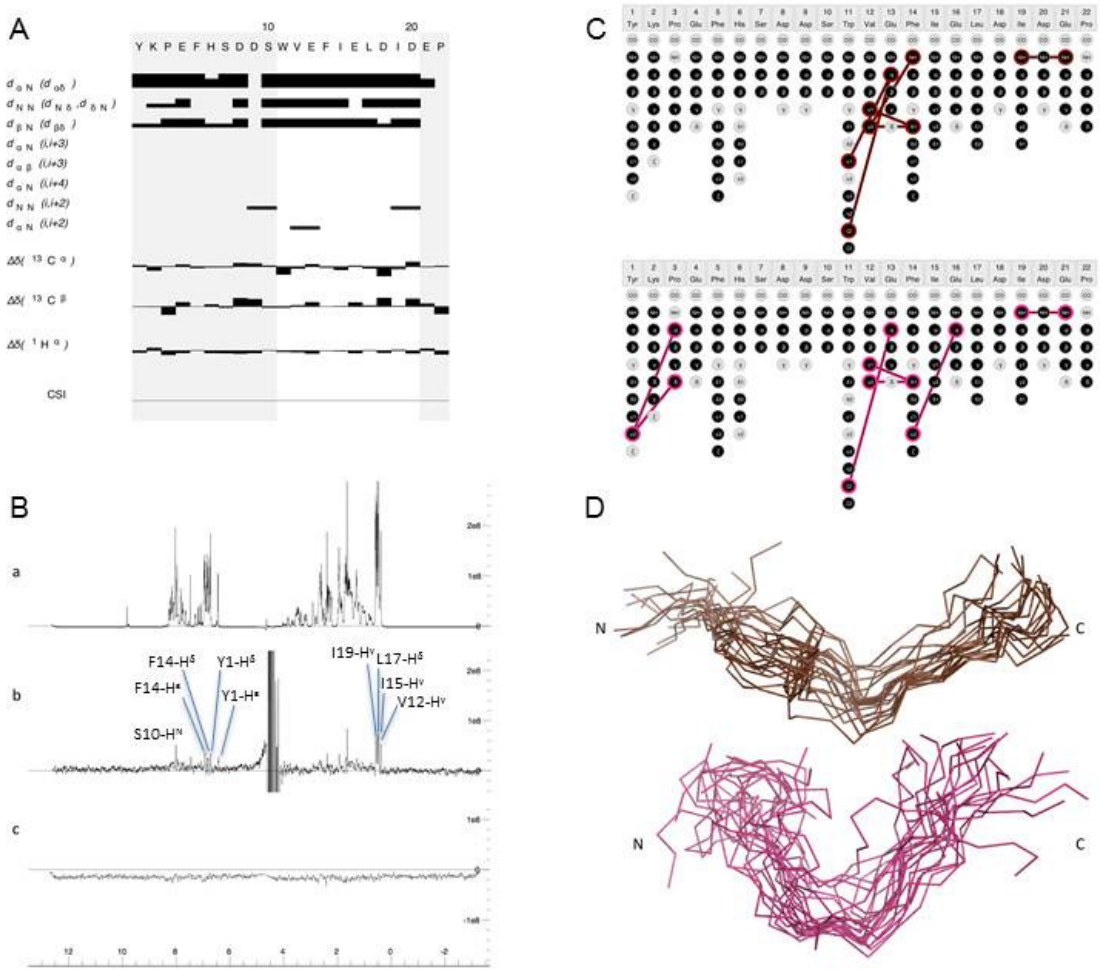

Fig.5 NMR data on UbE-βTrCP interaction. (A) Sequential and medium range NOE patterns and chemical shift index (CSI) for the unbound form of GHR peptide show no significant deviations from random coil values (**B)** a) 1D watergate spectrum for unbound GHR peptide b) 1D STD experiment at 1:350 (protein:peptide) condition under which protein binding is observed as indicated by the net transfer of magnetization from protein to peptide c) Control 1D STD on unbound peptide **(C)** NOE connectivities between protons separated by more than two residues for unbound (top) and bound (bottom) forms of GHR peptide. Absence of long range NOEs indicate extended coil structures in both cases. **(D)** Ensemble of NOE-derived structures calculated from NOESY of unbound (top) and from TRNOESY of bound (bottom) form of GHR peptide. TRNOESY was performed at 1:350 (protein:peptide) as observed under STD conditions.

Computational modelling of the UbE-βTrCP interaction

Based on the mutagenesis data (Fig.4) and NMR experiments (Fig. 5) we sought to obtain a model of the structure of the UbE- βTrCP interaction. We first modelled the structure of βTrCP2 based on the crystal structure of βTrCP1 bound to a β-catenin peptide (*19*). The structures of the bound form of the UbE peptide, obtained by TRNOESY, were then used for docking using the HADDOCK server. The structure of the βTrCP2-UbE complex with the lowest HADDOCK score is shown in Fig. 6. In this model, a succession of turns form a bend in the N-terminal region of the peptide between residues

Tyr1 and Phe14 while the C-terminal region (residues 15-22) remains extended. Two distinct β-turns occur in the middle of the sequence: a type II β-turn from residues 8 to 10 and a type VIII β-turn from residues 12 to 14. The UbE-βTrCP interaction involves mainly hydrogen bonds, hydrophobic and electrostatic (ionic) interactions, as predicted with the webserver-based Protein Interaction Calculator software (*44*). Also some cation-pi interactions contribute to the binding. A summary of the formed interactions is shown in Table 2 and Fig.7. The importance of some UbE motif residues (Glu326 (Glu13 in the peptide), Phe327 (Phe14), and Asp331 (Asp18)) and βTrCP2 residues (Tyr244, Arg258, Ser282, and Arg447) on UbE-βTrCP2 interaction is in agreement with the results from the binding assays (Fig. 4). This was expected, since these residues were used as restraints during the docking procedure. Interestingly, Phe327 forms cation-pi interaction with Arg447 while being placed in a βTrCP hydrophobic pocket. This type of interactions can reach the same order of energy as hydrogen bonds or electrostatic interactions, and therefore play an important role in stabilizing binding. This may justify why the residue Arg447, despite not forming hydrogen or electrostatic bonds with the UbE motif, is essential for the UbE-βTrCP interaction, as concluded from the binding assays (Fig.4B). Based on this model, additional βTrCP2 residues were predicted to bind the UbE motif, such as Leu324, Glu444, Lys338, Lys241 and Arg383. Interestingly, some of these residues were contained in the triple alanine βTrCP mutants that had a strong effect in GHR binding, and degradation: Leu324(mutant L7), Lys338 (mutant L9), Arg383 (mutant L12). The involvement of these individual residues in the interaction will be tested, and will allow us to verify the validity of the model.

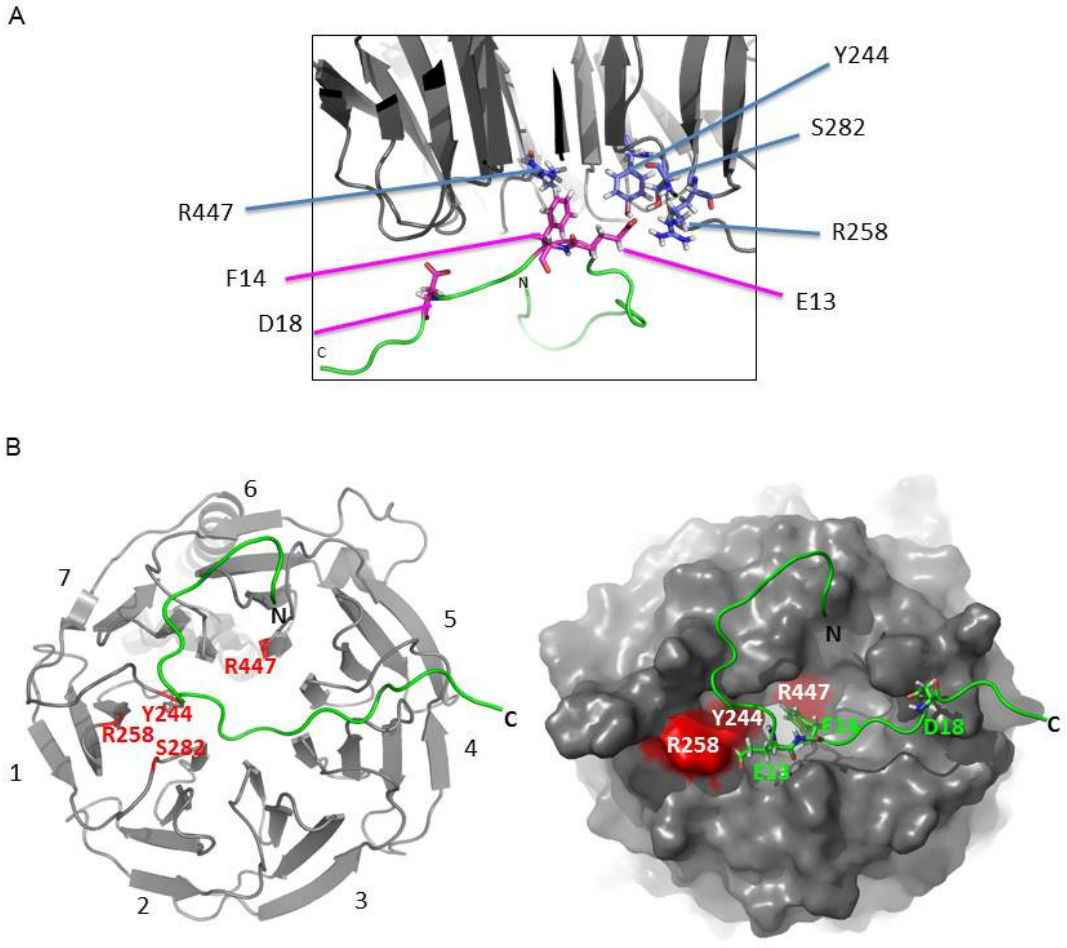

Fig. 6. UbE peptide-TrCP2 complex. (A) Site of interaction between WD40 domain of βTrCP2 and GHR peptide in the best scoring Haddock complex. βTrCP2 WD40 domain is shown in grey and the UbE motif peptide in green. Mutational analysis-based ambiguous interaction restraints (AIRS) used in the docking run are highlighted: UbE residues are in pink, and βTrCP2 residues in blue. **(B)** Bottom view (surface) of the complex. The seven blades of the WD40 domain are numbered from 1 to 7. βTrCP2 residues are shown in red, and UbE motif residues are green.

Table 2: Summary of the intermolecular interactions in lowest HADDOCK scoring UbE- βTrCP2 complex

	Y	K	P	E	F	H	S	D	D	S	W	V	E	F	I	E	L	D	I	D	E	P
Ube peptide	1	2	3	4	5	6	7	8	9	10	11	12	13	14	15	16	17	18	19	20	21	22
GHR full length	314	315	316	317	318	319	320	321	322	323	324	325	326	327	328	329	330	331	332	333	334	335

	UbE-peptide	**β-TrCP2**	
Hydrophobic interactions (< 5Å)	Tyr 1	Tyr 461	
	Phe 14	Tyr 244	
	Phe 14	Leu 324	
	Ile 15	Ala 365	
	Leu 17	Ala 364	
Main chain-Side chain hydrogen bonds			**Donor-Acceptor dist. (Å)**
	Tyr 1 N	Glu 444 $O\varepsilon_1$	2.80
	Tyr 1 N	Glu 444 $O\varepsilon_2$	2.75
	Glu 13 O	Lys 338 $N\zeta$	3.33
	Leu 17 O	Arg 383 $N\eta_2$	2.95
	Trp 11 O	Arg 494 $N\eta_2$	3.16
Side chain-Side chain hydrogen bonds	Asp 9 $O\delta_2$	Lys 241 ζ	2.81
	Glu 13 $O\varepsilon_1$	Tyr 244 $O\eta$	2.71
	Glu 13 $O\varepsilon_1$	Arg 258 $N\eta_2$	2.83
	Glu 13 $O\varepsilon_2$	Arg 258 $N\eta_2$	3.46
	Glu 13 $O\varepsilon_1$	Ser 282 $O\gamma$	2.72
	Glu 13 $O\varepsilon_2$	Ser 298 $O\gamma$	2.66
	Asp 18 $O\delta_1$	Arg 383 $N\varepsilon$	2.88
	Asp 18 $O\delta_1$	Arg 383 $N\eta_2$	3.04
	Glu 16 $O\varepsilon_2$	Arg 404 $N\eta_1$	3.18
	Glu 16 $O\varepsilon_2$	Arg 404 $N\eta_2$	2.62
	Asp 18 $O\delta_1$	Arg 404 $N\varepsilon$	3.37
	Asp 18 $O\delta_2$	Arg 404 $N\varepsilon$	3.42
	Asp 18 $O\delta_2$	Arg 404 $N\eta_2$	2.66
Ionic interactions	Lys 2	Glu 444	
	Asp 9	Lys 241	
	Glu 13	Arg 258	
	Glu 16	Arg 404	
	Asp 18	Arg 383	
	Asp 18	Arg 404	
Aromatic-aromatic interactions (<7Å)			**Inter-centroid distance (Å)**
	Tyr 1	Tyr 461	6.47
Cation-pi interactions (<6 Å)			**Cation-Pi distance (Å)**
	Trp 11	Lys 241	5.76
	Trp 11	Arg 258	4.82
	Phe 14	Arg 447	5.05

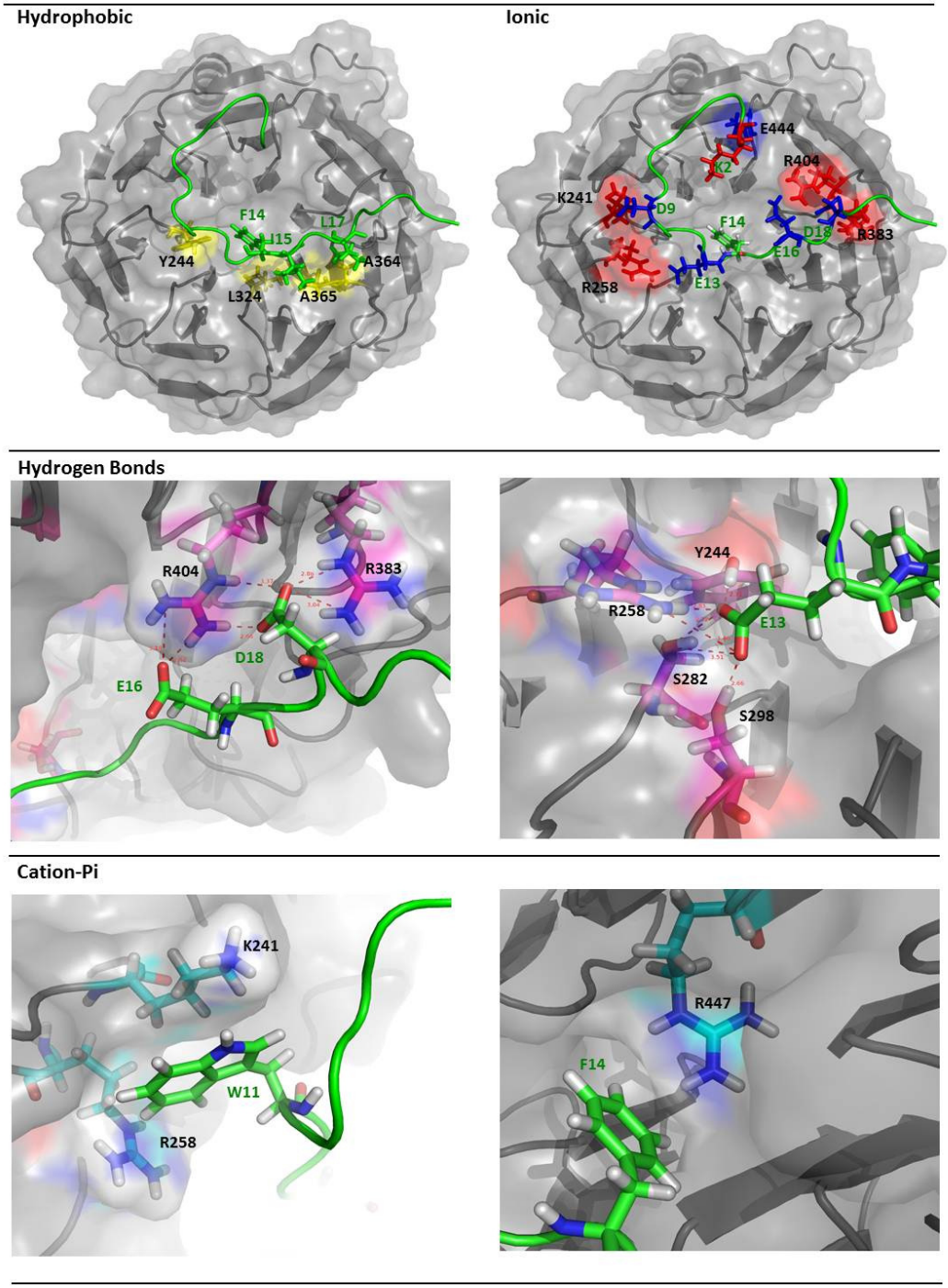

Fig. 7. Intermolecular interactions in the lowest HADDOCK scoring UbE-βTrCP2 complex. Interactions (Hydrophobic, ionic, cation-Pi, and Hydrogen bonds) maintaining the UbE-βTrCP2 complex are represented. βTrCP2 is shown in grey (residue numbers in black) and the UbE motif peptide in green (residue numbers in green).

As mentioned previously, since the sequence of the UbE motif differs substantially from the sequence of the $DSG(X)_{2+n}S$ motif we expected the UbE-βTrCP2 interaction to be unique. To investigate this, we compared the interactions of βTrCP2 with the UbE motif, with the interactions of βTrCP1 with the classical $DSG(X)_{2+n}S$ motif present in other substrates. Data present in literature resulting from docking studies starting with the NMR bound structure of β-catenin, Vpu, IκB and ATF4 were used for comparison (Table 4)(*25*). All the ligand-βTrCP interactions are stabilized

through a network of contacts, electrostatic interactions and hydrogen bounds (table 4, squares filled in grey) involving all the WD40 repeats of βTrCP. Additionally, some hydrophobic interactions are formed that may increase the affinity of the binding region (table 4, squares filled in black).

Table 4: Summary of the interactions in NMR bound Structures of β-catenin, Vpu, IκB, and ATF4 (docked to βTrCP1) and of UbE-GHR (docked to βTrCP2)

		β-catenin							Vpu									IκBa								ATF4						
βTrcP1		^{32}DpSGIHpSG^{38}							^{50}EDpSGNEpSEGE^{59}									^{29}RHDpSGLDpSMKD^{39}								^{217}NDpSGICMpSPE^{226}						
		D	S	G	I	H	S	G	E	D	S	G	N	E	S	E	G	E	R	H	D	S	G	S	K	D	N	D	S	I	S	P	E
W1	K268																																
	Y271																					■											
	R285		■													■	■	■				■						■	■				
W2	S309																												■				
	S325		■													■		■				■							■				
W3	L351			■																										■			
	K365													■	■						■												
W4	A391																																
	A392								■																								
	N394			■	■																									■			
	G408							■																									
	R410					■																				■					■	■	
W5	R431					■				■	■															■				■			
	G432					■				■																■						■	
	A434			■															■											■			
	S448					■				■																						■	
W6	E471																																
	R474			■								■	■						■	■										■			
	Y488											■												■									
W7	R521	■																				■	■							■			

		UbE - GHR							
βTrCP2		^{314}YKPEFHSDDSWVEFIELDIDEP^{335}							
		Y	D	W	E	F	I	L	D
W1	K241		■						■
	Y244				■	■			
	R258				■				
W2	S282				■				
	S298				■				
W3	L324					■			
	K338				■				
W4	A364							■	
	A365						■		
	N367								
	G381								
	R383							■	■
W5	R404								
	G405								
	A407								
	S421								
W6	E444	■							
	R447								
	Y461	■							
W7	R494			■					

Note: This table is adapted from ref. (25) where the information on βTrCP-UbE interactions was added. The βTrCP1 residues (*top* table) correspond directly to the indicated homologous βTrCP2 residues (bottom table) The filled squares represent predicted interactions between βTrCP and its substrates (grey squares represent hydrogen bonds, and black squares represent hydrophobic interactions).

Importantly, the peptides bind βTrCP in such a way that one hydrophobic residue is centered into a hydrophobic binding pocket in βTrCP. In the cases of β-catenin and ATF4 the hydrophobic residues are Gly34 and Ile221, respectively (see table 4, black squares). In the case of UbE, this role is played by Phe327. Additionally, important electrostatic interactions and hydrogen bonds are mostly established by the phosphorylated serines or negatively charged aminoacids, as aspartates and glutamates, in all the analyzed examples. We conclude UbE binds to βTrCP by similar principles used

by the other βTrCP substrates, involving an extensive network of hydrogen bonds and electrostatic interactions with βTrCP, stabilized by its placement into a βTrCP hydrophobic pocket.

Discussion

The interaction of the UbE motif of GHR with βTrCP is essential for the endocytosis and degradation of GHR (*13*). The present study adds crucial information for the structural understanding of this interaction. Firstly, we proved formally that βTrCP binds to the UbE motif directly. Furthermore, $SCF^{\beta TrCP}$ mediates GHR ubiquitination *in vitro* in an UbE motif-dependent manner. Initial binding and ubiquitination assays (Fig.3) suggested that βTrCP binds to the UbE motif differently than to $DSG(X)_{2+n}S$, classical motif present in its other substrates such as β-catenin or IκB (*45, 46*). Therefore, we sought to characterize the interaction between GHR UbE motif and βTrCP in structural detail. NMR experiments revealed that a peptide of the UbE motif is essentially unstructured but adopts a residual structure when bound to the purified βTrCP. The UbE and βTrCP WD40 aminoacid residues involved in the interaction were mapped. Based on the NMR and mutagenesis data, a computational model was constructed, which shows that the interaction of βTrCP with GHR-UbE is unconventional.

We showed recently that GHR has in its cytosolic tail two motifs able to bind βTrCP (*da Silva Almeida AC*, manuscript submitted). Apart from the UbE motif, βTrCP binds to a sequence downstream, DSGRTS, which corresponds to a classical βTrCP binding motif. βTrCP interacts with the DSGRTS sequence in GHR with the same residues as it uses to interact with the DSGxxS motifs in β-catenin or IκB, namely Tyr244, Arg404, Arg447, and Tyr461. In an equivalent experiment, from these four residues, only Y244 and R447 were used by βTrCP to bind the UbE motif. We concluded that βTrCP binds to the DSGRTS sequence in a classical way, while the binding to the UbE motif was different. Moreover, while βTrCP binding to the UbE motif occurs both in presence and absence of GH stimulation, βTrCP binding to the DSGRTS sequence could only be measured in the absence of GH stimulation. Therefore, the focus of the present study was to characterize the potentially unconventional UbE-βTrCP interaction, important for both constitutive and GH-induced GHR endocytosis. For this purpose, all the experiments shown in this study were performed under conditions where the role of the DSGRTS sequence can be disregarded, since the assays were either in GH stimulated conditions, or short GHR tails or peptides without the DSGRTS sequence were used.

We expected the interaction of βTrCP with the UbE motif to be unconventional since the sequence of the UbE motif, DDSWVEFIELD, has little resemblance to the classical motif. The UbE motif is 11 amino acids long, while the classical motif is most of the times 6 amino acids long. Another difference is the fact that the UbE motif contains 3 acidic residues (Asp321, Glu326 and Asp331) instead of the 2 phosphorylated serine residues in the classical motif. Also the glycine residue characteristic in the classical motif is lacking in the UbE motif. Furthermore, the UbE motif is very unique since it has not been described in any other receptor or other protein so far. This study revealed that the UbE peptide is essentially unstructured, and adopts a residual structure when bound βTrCP. In this study a 22 amino acids long peptide was used. We cannot exclude that the length of the peptide used may have an influence on its structure. However, in the context of the full length GHR protein, the UbE motif is predicted to be unstructured, which would suggest that our NMR results may be extrapolated to the full length receptor. Another aspect to consider is that, physiologically, βTrCP binds a GHR dimer at the cell surface (*47*). We do not know at which extent the dimerization of GHR may influence the structure of the UbE motif. Additionally, βTrCP is also able to dimerize, due to a dimerization domain at its N-terminus (*48*). This may also have an influence on the structure adopted by the bound UbE motif. In the NMR studies a short form of βTrCP lacking the dimerization domain was used in order to facilitate its purification. Studies with the full length version of βTrCP would clarify if its dimerization may influence UbE motif structure. It is tempting to speculate that the residual structure of the UbE motif confers flexibility for the dynamic regulation of its interaction with βTrCP, such us by phosphorylation (see below).

Previous NMR studies have revealed that the structures of βTrCP-bound peptides containing $DSG(X)_{2+n}S$ motifs are characterized by an N-terminal loop followed by a large bend centered on the double phosphorylated motif (*25*). β-catenin exhibits an N-terminal domain with tendency to form turns followed by a bend and a C-terminal flexible part. The bound Vpu peptide shows a bend with

two turn regions on both sides. IκB also presents two turn regions on both sides of the bend. The ATF4 bound structure presents a well-defined turn like structure where a loop after the first turn is apparent. Importantly, the TRNOESY data revealed that the bound form of the UbE peptide is rather flexible, or partially unstructured. Nevertheless, when we performed docking of the ensemble of TRNOESY-derived UbE "structures" on βTrCP2 structure we obtained a model of the interaction. In the best scoring model, the bound UbE motif peptide showed a succession of turns in the N-terminus that formed a bend in the region before the residue Phe327, and a C-terminal part that remained extended. Further mutagenesis will be performed to verify the validity of the model. The bound structures of all the peptides, including the one of the UbE peptide, expose hydrophobic residues in the center that will form contacts with βTrCP binding channel.

From our *in vitro* binding assays three residues in the UbE seemed to be particularly important for βTrCP binding: Glu326, Phe327 and Asp331 (Fig. 4). Functional studies by Govers and collaborators have been performed in the past to evaluate the effect of mutations in the UbE motif on GHR endocytosis (*12*). In agreement with the present results, mutations in Glu326, Phe327, and Asp331 profoundly affected the rate of GHR endocytosis. Another residue revealed by Govers as important for GHR endocytosis was Ser323. In our *in vitro* binding assay, this residue did not seem as important for βTrCP binding. These results can be explained by our recent results showing that GH stimulation may trigger Ser323 phosphorylation, which increases the affinity of the UbE motif to βTrCP (*da Silva Almeida AC*, manuscript in preparation). On one hand, in the experiments by Govers, performed under GH stimulation, the phosphorylation of Ser323 is probably needed for full endocytosis capacity. On the other hand, the conditions of the *in vitro* binding assay mimic the situation of a non-phosphorylated UbE motif, where Ser323 seems to be less important for binding. The NMR experiments were performed with a non-phosphorylated UbE peptide. Based on the model of the UbE-βTrCP interaction, in the non-phosphorylated UbE peptide, Ser323 is not predicted to form contacts with βTrCP (table2 and Fig.2S, supplementary data). Future docking studies will be performed to evaluate the influence of Ser323 phosphorylation on its interactions with βTrCP. In fact, an extra negative charge brought by a phosphate group may interfere substantially with the UbE-βTrCP interaction. Interestingly, Trp324 in the vicinity of Ser323 forms cation-pi interactions with Arg258 and Lys241 that would be most likely affected by a phosphate group in Ser323 (Fig. 2S). Furthermore, βTrCP binds to the classical $DSG(X)_{2+n}S$ motif in its substrates only when both serines are phosphorylated. It is interesting to realize that although the UbE motif is so different, the affinity of its interaction with βTrCP is also influenced by a phosphorylation event.

Based on the best scoring model of the interaction, a map of the interactions necessary to maintain the UbE-βTrCP interaction was drawn (Table 4), which include hydrogen bonds, hydrophobic and electrostatic interactions, as well as cation-pi interactions. The same network of interactions also occurs between βTrCP and substrates containing $DSG(X)_{2+n}S$ motifs, such as βcatenin, Vpu, IκB and ATF4. β-catenin binds to the top face of the βTrCP WD40 domain, where the phosphorylated serine establishes hydrogen bonds (table 4, grey squares) and electrostatic interactions with residues located mainly within W1-W2 and W4-W5 domains. Additionally, Gly34 and Ile35 make hydrophobic interactions with residues in a hydrophobic pocket (see table 4, black squares). The binding of Vpu is marked by a dominant negative potential generated by the five aspartic and glutamic acid residues, increased by the phosphorylated Ser52 (pSer52) and Ser56 (pSer56). It has been suggested that the main chain of Ile46 and Leu 45 lies in close proximity to a hydrophobic pocket. Glu57 and Glu59 form similar hydrogen bonds with βTrCP as pSer33 of β-Cat. In the case of IκB binding, the phosphorylated Ser32 (pS32) makes the similar interactions as pSer33 in β-catenin (table 4, grey squares). Apart from residues contained within the known DpSGLDpS, other residues in its close proximity enhance the interaction of IκBα with βTrCP (not shown). The importance of hydrophobic interactions in the IκBα-βTrCP interaction is not clearly stated in literature. The S-turn like conformation of the ATF4 peptide allows the side chain of Ile221 to insert into the narrow central channel of βTrCP, where it makes hydrophobic interactions with a hydrophobic pocket (Table4, black squares). Interestingly, Glu226 in ATF4 has the same interaction with Arg431, Gly432 and Ser448, as the second phosphorylated serine (pS37) of β-catenin (*25*). Remarkably, in the case of the UbE motif, most of the contacts are formed by Glu326 which establishes extensive hydrogen bonds with several residues located within blade W1-W3 of βTrCP2 WD40 domain (Tyr244, Arg258, Ser282, Ser298, and Lys338). Similar contacts are formed between βTrCP1 and the first phosphorylated serine in IκB

(pS32) and ATF4 (pS219) (*25*). This suggests that the interactions of βTrCP with the UbE and $DSG(X)_{2+n}S$ motifs share some features, where the negatively charged Glu326 residue replaces the role of the phosphorylated serine in the other substrates. Additionally, hydrophobic interactions play a very important role in the binding of UbE to βTrCP as well, as it has been described for βTrCP interactions with $DSG(X)_{2+n}S$ containing peptides. Phe327 is placed in the central pocket of βTrCP where in forms hydrophobic interaction with Tyr244 and Leu324 (Fig. 7). Leu324 (Leu351 in βTrCP1) is also used to interact with β-catenin and ATF4, specifically with Gly34 and Ile221, respectively, which are also inserted in the βTrCP central channel. However, both Gly34 (in β-catenin) and Ile221 (in ATF4) form extra hydrophobic interactions with Asn394 and Ala434 in βTrCP, which do not make contacts with Phe327 (in the UbE). Two more residues in the UbE motif form hydrophobic interactions with βTrCP: Ile328 and Leu330. These residues interact with Ala364 and Ala365, which do not lie in βTrCP central chain. This characteristic is specific for the case of the UbE motif. Another interesting characteristic of the βTrCP hydrophobic binding pocket for the UbE motif is the fact that Arg447 in βTrCP form a cation-pi interaction with Phe327 (Fig. 7). Accordingly, Arg447 was revealed as a very important residue in the UbE- βTrCP interaction in the binding assays (Fig. 4B). Based on this we conclude that the Arg447-Phe327 contact is very important for the stabilization of the UbE-βTrCP interaction. The βTrCP residue Arg447 (Arg474 in βTrCP1) was also described as essential for interacting with $DSG(X)_{2+n}S$ containing substrates, particularly with β-catenin and ATF4, by forming hydrogen bonds or hydrophobic interactions with Gly34 and Ile221, respectively (Table 4). Therefore, we conclude that WD40 repeats domain in βTrCP is able to accommodate very different substrates through similar principles. In particular, an extensive network of hydrogen bonds and electrostatic interactions is formed, and certain residues of the interaction motif of the substrate are placed into a hydrophobic pocket in βTrCP. We show in this study that the binding pocket for UbE in βTrCP has some unconventional characteristics in relation to other βTrCP-substrate interactions. This makes the UbE-βTrCP interaction a promising target for drug design. The inhibition of this interaction would result in GHR endocytosis inhibition, increase in the GHR levels, and ultimately, improvement of the GH sensitivity of cells. This would have therapeutic value for patients with GH insensitivity, such as cancer patients suffering from cachexia. Future modeling studies will evaluate the possibility of designing compounds specifically targeting the interaction of βTrCP with UbE without affecting the interaction of βTrCP with other substrates.

GH signalling is involved in a plethora of physiological processes. The characterization of the UbE-βTrCP interaction, reported in this study, opens new possibilities for designing strategies that allow the modulation of GH sensitivity of cells.

Acknowledgments

We thank all members of the GHR group. We thank Alex Faesen and Prof. Titia Sixma for the help with the purification of βTrCP/Skp1 complex, and Adrien Melquiond for the critical advises on the docking. This research was supported by the European Network of Excellence, Rubicon "Role of ubiquitin and ubiquitin-like modifiers in cellular regulation" (Grant LSHG-CT-2005-018683), and the Marie Curie network, "UbiRegulators", (Grant MRTN-CT-2006-034555).

References

1. Lanning NJ, Carter-Su C 2006 Recent advances in growth hormone signaling. Rev Endocr Metab Disord 7:225-235
2. Argetsinger LS, Campbell GS, Yang X, Witthuhn BA, Silvennoinen O, Ihle JN, Carter-Su C 1993 Identification of JAK2 as a growth hormone receptor-associated tyrosine kinase. Cell 74:237-244
3. Frank SJ 2001 Growth hormone signalling and its regulation: preventing too much of a good thing. Growth Horm IGF Res 11:201-212
4. Waters MJ, Barclay JL 2007 Does growth hormone drive breast and other cancers? Endocrinology 148:4533-4535

5. Kleinberg DL, Wood TL, Furth PA, Lee AV 2009 Growth hormone and insulin-like growth factor-I in the transition from normal mammary development to preneoplastic mammary lesions. Endocr Rev 30:51-74
6. von Laue S, Ross RJ 2000 Inflammatory cytokines and acquired growth hormone resistance. Growth Horm IGF Res 10 Suppl B:S9-14
7. Crown AL, Cottle K, Lightman SL, Falk S, Mohamed-Ali V, Armstrong L, Millar AB, Holly JM 2002 What is the role of the insulin-like growth factor system in the pathophysiology of cancer cachexia, and how is it regulated? Clin Endocrinol (Oxf) 56:723-733
8. Tisdale MJ 2009 Mechanisms of cancer cachexia. Physiol Rev 89:381-410
9. Saini A, Al-Shanti N, Stewart CE 2006 Waste management - cytokines, growth factors and cachexia. Cytokine Growth Factor Rev 17:475-486
10. Strous GJ, van Kerkhof P 2002 The ubiquitin-proteasome pathway and the regulation of growth hormone receptor availability. Mol Cell Endocrinol 197:143-151
11. Strous GJ, van Kerkhof P, Govers R, Ciechanover A, Schwartz AL 1996 The ubiquitin conjugation system is required for ligand-induced endocytosis and degradation of the growth hormone receptor. Embo J 15:3806-3812
12. Govers R, ten Broeke T, van Kerkhof P, Schwartz AL, Strous GJ 1999 Identification of a novel ubiquitin conjugation motif, required for ligand-induced internalization of the growth hormone receptor. Embo J 18:28-36
13. van Kerkhof P, Putters J, Strous GJ 2007 The ubiquitin ligase SCF(betaTrCP) regulates the degradation of the growth hormone receptor. J Biol Chem 282:20475-20483
14. Deshaies RJ 1999 SCF and Cullin/Ring H2-based ubiquitin ligases. Annu Rev Cell Dev Biol 15:435-467
15. Petroski MD, Deshaies RJ 2005 Function and regulation of cullin-RING ubiquitin ligases. Nat Rev Mol Cell Biol 6:9-20
16. Kumar KG, Tang W, Ravindranath AK, Clark WA, Croze E, Fuchs SY 2003 SCF(HOS) ubiquitin ligase mediates the ligand-induced down-regulation of the interferon-alpha receptor. Embo J 22:5480-5490
17. Meyer L, Deau B, Forejtnikova H, Dumenil D, Margottin-Goguet F, Lacombe C, Mayeux P, Verdier F 2007 beta-Trcp mediates ubiquitination and degradation of the erythropoietin receptor and controls cell proliferation. Blood 109:5215-5222
18. Li Y, Kumar KG, Tang W, Spiegelman VS, Fuchs SY 2004 Negative regulation of prolactin receptor stability and signaling mediated by SCF(beta-TrCP) E3 ubiquitin ligase. Mol Cell Biol 24:4038-4048
19. Wu G, Xu G, Schulman BA, Jeffrey PD, Harper JW, Pavletich NP 2003 Structure of a beta-TrCP1-Skp1-beta-catenin complex: destruction motif binding and lysine specificity of the SCF(beta-TrCP1) ubiquitin ligase. Mol Cell 11:1445-1456
20. Megy S, Bertho G, Gharbi-Benarous J, Evrard-Todeschi N, Coadou G, Segeral E, Iehle C, Quemeneur E, Benarous R, Girault JP 2005 STD and TRNOESY NMR studies on the conformation of the oncogenic protein beta-catenin containing the phosphorylated motif DpSGXXpS bound to the beta-TrCP protein. J Biol Chem 280:29107-29116
21. Pons J, Evrard-Todeschi N, Bertho G, Gharbi-Benarous J, Tanchou V, Benarous R, Girault JP 2008 Transfer-NMR and docking studies identify the binding of the peptide derived from activating transcription factor 4 to protein ubiquitin ligase beta-TrCP. Competition STD-NMR with beta-catenin. Biochemistry 47:14-29
22. Pons J, Evrard-Todeschi N, Bertho G, Gharbi-Benarous J, Sonois V, Benarous R, Girault JP 2007 Structural studies on 24P-IkappaBalpha peptide derived from a human IkappaB-alpha protein related to the inhibition of the activity of the transcription factor NF-kappaB. Biochemistry 46:2958-2972
23. Coadou G, Gharbi-Benarous J, Megy S, Bertho G, Evrard-Todeschi N, Segeral E, Benarous R, Girault JP 2003 NMR studies of the phosphorylation motif of the HIV-1 protein Vpu bound to the F-box protein beta-TrCP. Biochemistry 42:14741-14751
24. Pons J, Evrard-Todeschi N, Bertho G, Gharbi-Benarous J, Benarous R, Girault JP 2007 Phosphorylation-dependent structure of ATF4 peptides derived from a human ATF4 protein, a member of the family of transcription factors. Peptides 28:2253-2267

25. Evrard-Todeschi N, Pons J, Gharbi-Benarous J, Bertho G, Benarous R, Girault JP 2008 Structure of the complex between phosphorylated substrates and the SCF beta-TrCP ubiquitin ligase receptor: a combined NMR, molecular modeling, and docking approach. J Chem Inf Model 48:2350-2361
26. Putters J, da Silva Almeida AC, van Kerkhof P, van Rossum AG, Gracanin A, Strous GJ 2011 Jak2 is a negative regulator of ubiquitin-dependent endocytosis of the growth hormone receptor. PLoS One 6:e14676
27. Fellinger K, Leonhardt H, Spada F 2008 A mutagenesis strategy combining systematic alanine scanning with larger mutations to study protein interactions. Anal Biochem 373:176-178
28. Schantl JA, Roza M, De Jong AP, Strous GJ 2003 Small glutamine-rich tetratricopeptide repeat-containing protein (SGT) interacts with the ubiquitin-dependent endocytosis (UbE) motif of the growth hormone receptor. Biochem J 373:855-863
29. Vranken W, Boucher W, Stevens T, Fogh R, Pajon A, Llinas M, Ulrich E, Markley L, Ionides J, Laue E 2005 The CCPN Data Model for NMR Spectroscopy: Development of a Software Pipeline. Proteins 59:687-696
30. Wishart D, Sykes B, Richards F 1992 The Chemical Shift Index: A Fast and Simple Method for the Assignment of Protein Secondary Structure through NMR Spectroscopy. Biochemistry 31:1647-1651
31. Herrmann T, Guntert P, Wuthrich K 2002 Protein NMR structure determination with automated NOE assignment using the new software CANDID and the torsion angle dynamics algorithm DYANA. J Mol Biol 319:209-227
32. Bax A, Davis D 1985 MLEV-17-based two-dimensional homonuclear magnetization transfer spectroscopy. J Magn Reson 65:355-360
33. Clore A, Gronenborn A 1982 Theory and applications of the transferred nuclear overhauser effect to the study of the conformations of small ligands bound to proteins. J Magn Reson 48:402-417
34. Clore G, Gronenborn A 1983 Theory of the Time Dependent Transferred Nuclear Overhauser Effect: Applications to Structural Analysis of Ligand-Protein Complexes in Solution. J Magn Reson 53:423-442
35. Bax A, Griffey R, Hawkins B 1983 Correlation Of Proton And N-15 Chemical-Shifts By Multiple Quantum NMR. J Magn Reson 55
36. Sklenar V, Piotto M, Leppik, Saudek VR 1993 Gradient-Tailored Water Suppression for 1H-15N HSQC Experiments Optimized to Retain Full Sensitivity. J Magn Reson 102:241-245
37. Mayer M, Meyer B 2001 Group epitope mapping by saturation transfer difference NMR to identify segments of a ligand in direct contact with a protein receptor. J Am Chem Soc 123:6108-6117
38. Fiser A, Sali A 2003 Modeller: generation and refinement of homology-based protein structure models. Methods Enzymol 374:461-491
39. Sali A, Blundell TL 1993 Comparative protein modelling by satisfaction of spatial restraints. J Mol Biol 234:779-815
40. de Vries SJ, van Dijk M, Bonvin AM 2010 The HADDOCK web server for data-driven biomolecular docking. Nat Protoc 5:883-897
41. Frescas D, Pagano M 2008 Deregulated proteolysis by the F-box proteins SKP2 and beta-TrCP: tipping the scales of cancer. Nat Rev Cancer 8:438-449
42. van Kerkhof P, Govers R, Alves dos Santos CM, Strous GJ 2000 Endocytosis and degradation of the growth hormone receptor are proteasome-dependent. J Biol Chem 275:1575-1580
43. Gaudet R, Bohm A, Sigler PB 1996 Crystal structure at 2.4 angstroms resolution of the complex of transducin betagamma and its regulator, phosducin. Cell 87:577-588
44. Tina KG, Bhadra R, Srinivasan N 2007 PIC: Protein Interactions Calculator. Nucleic Acids Res 35:W473-476
45. Latres E, Chiaur DS, Pagano M 1999 The human F box protein beta-Trcp associates with the Cul1/Skp1 complex and regulates the stability of beta-catenin. Oncogene 18:849-854
46. Winston JT, Strack P, Beer-Romero P, Chu CY, Elledge SJ, Harper JW 1999 The SCFbeta-TRCP-ubiquitin ligase complex associates specifically with phosphorylated destruction motifs in IkappaBalpha and beta-catenin and stimulates IkappaBalpha ubiquitination in vitro. Genes Dev 13:270-283

47. Gent J, van Kerkhof P, Roza M, Bu G, Strous GJ 2002 Ligand-independent growth hormone receptor dimerization occurs in the endoplasmic reticulum and is required for ubiquitin system-dependent endocytosis. Proc Natl Acad Sci U S A 99:9858-9863
48. Suzuki H, Chiba T, Suzuki T, Fujita T, Ikenoue T, Omata M, Furuichi K, Shikama H, Tanaka K 2000 Homodimer of two F-box proteins betaTrCP1 or betaTrCP2 binds to IkappaBalpha for signal-dependent ubiquitination. J Biol Chem 275:2877-2884

Supplementary data

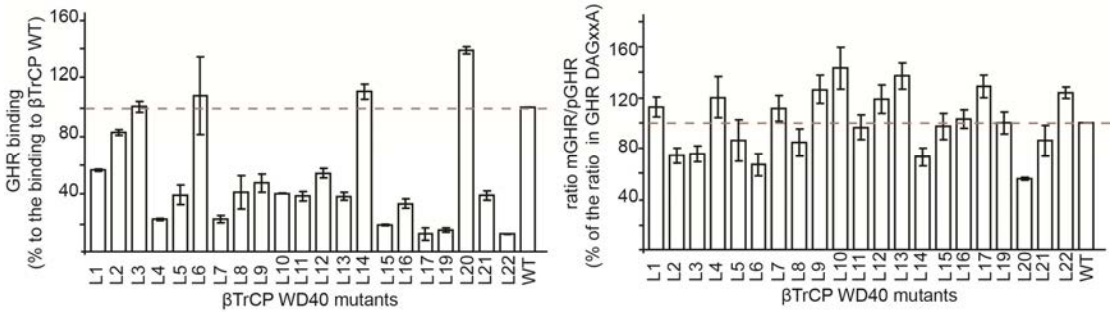

Blade			Triple mutation	mGHR:pGHR	GHR binding	Single mutation
W1	strand A	L1	243VYC	++	-	G242, Y244
W1	strand A	L2	246LQY	-	+	
W1	Loop BC	L3	258RDN	-	+	R258
W2	strand A	L4	283VLC	++	--	S282
W2	strand A	L5	286LQY	-	-	
W2	Loop BC	L6	298SDS	-	+	S298
W3	strand A	L7	323VLH	++	--	
W3	strand A	L8	326LRF	-	-	
W3	Loop BC	L9	338KDR	++	-	
W4	strand A	L10	366VNV	++	-	
W4	strand A	L11	369VDF	+	-	
W4	Loop BC	L12	381GDR	++	-	
W5	strand A	L13	404RGI	++	-	R404
W5	strand A	L14	407ACL	-	+	
W5	strand A	L15	410QYR	-	-	
W5	Loop BC	L16	421SDN	-	-	S421
W6	strand A	L17	446VRC	++	-	L445, R447
W6	strand A	L18(*)	449IRF	-	-	
W6	Loop BC	L19	461YDG	-	-	Y461
W7	strand A	L20	495VFR	-	+	R494
W7	strand A	L21	498LQF	-	-	
W7	Loop BC	L22	510HDD	++	--	

(*) This mutant was not expressed.

Fig. 1S. Summary of the effects of the triple mutations in βTrCP2 on GHR binding and degradation.
HEK293-TR cells were transiently co-transfected with GHR DAGxxA mutant together with Flag-βTrCP WT or Flag-βTrCP containing triple mutations to alanine in the WD40 domain. The subsequent experiment was performed as in 4B. The western blotting performed to analyse the samples are not shown. The quantification of GHR binding was done as described in 4B. The stabilization of mature GHR was analysed in the total cell lysates, quantified by calculating the ratio GHR mature:precursor, and expressed as a percentage of the ratio of GHR DAGxxA co-transfected with Flag-βTrCP WT. In the table, the descriptions of each of the Flag-βTrCP mutants are indicated: colored in red are the characteristics corresponding to a negative impact in the GHR-βTrCP interaction, and in green are the ones corresponding to neutral or positive impact on GHR-βTrCP; in the last column of the table, the single mutants contained in, or in very close proximity to, the triple mutants of the same row are indicated.

Table S1: Chemical ^{1}H, ^{15}N and ^{13}C chemical shifts of unbound UbE motif peptide at 278K

	H	N	N_ε	H_α	H_β	H_γ	H_δ	H_ε	H_ζ	H_η	C_α	C_β	C_γ	C_δ	C_ε	C_ζ	C_η	
1 Tyr		126.96		4.47	3.00 2.88		7.10	6.81			58.20	38.66		133.18	118.11			H* 8.40
2 Lys	8.13	126.61		4.52	1.59 1.72	1.35 1.36	1.65 1.65	2.96 2.96			53.22	32.90	24.11	28.95	41.86			
3 Pro				4.27	2.27 1.84	1.99 1.99	3.58 3.52				62.76	31.85	27.06	50.34				
4 Glu	8.63	120.68		4.18	1.88 1.88	2.22 2.08					56.30	30.10	35.84					
5 Phe	8.33	121.16		4.58	3.01 3.01		7.18	7.30	7.20		57.44	39.57		131.75	129.96	124.63		
6 His	8.39	122.01		4.61	3.16 3.02		7.08	8.39			54.92	29.59		119.97	136.31			
7 Ser	8.51	121.42		4.34	3.84 3.92						58.27	63.50						
8 Asp	8.55	122.25		4.68	2.78 2.72						54.12	40.91						
9 Asp	8.41	120.74		4.63	2.67 2.67						53.99	40.59						
10 Ser	8.40	115.66		4.39	3.89 3.89						58.79	63.51						
11 Trp	8.11	123.09	129.52	4.62	3.28 3.28		7.24	7.55 10.20	7.11 7.46	7.20	54.65	29.19		127.19	120.90	114.57	127.16	
12 Val	7.66	123.36		3.86	1.83	0.75 0.75					61.64	32.99	20.22 20.78					
13 Glu	8.20	124.25		3.99	1.86 1.82	2.20 2.08					56.27	30.12	35.83					
14 Phe	8.33	122.38		4.58	3.04 3.04		7.21	7.32	7.11		57.43	39.51		131.84	131.48	122.01		
15 Ile	8.01	124.83		4.06	1.72	1.42 0.83 1.11	0.83				60.32	38.84	26.98 17.00	12.52				
16 Glu	8.49	125.69		4.21	1.92 2.03	2.29 2.29					56.06	30.04	36.03					
17 Leu	8.43	124.36		4.34	1.65 1.56	1.66	0.87 0.95				54.68	42.58	26.70	24.78 23.12				
18 Asp	8.59	122.01		4.65	2.75 2.59						49.45	40.98						
19 Ile	8.20	120.62		4.20	1.91	1.19 0.92 1.44	0.89				60.88	38.89	17.34 26.79	12.99				
20 Asp	8.53	124.18		4.65	2.70 2.59						54.05	40.71						
21 Glu	8.33	122.58		4.61	1.94 2.06	2.30 2.30					54.01	29.66	35.56					
22 Pro				4.39	1.97 2.33	2.06 2.06	3.82 3.74				63.09	32.10	27.11	50.45				

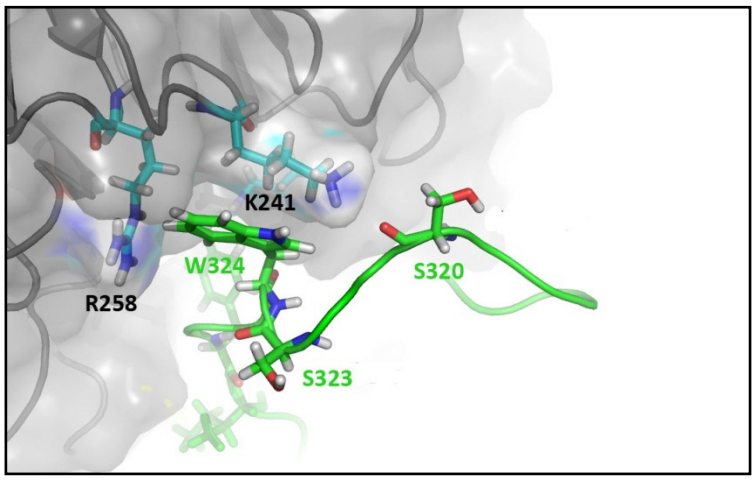

Fig. 2S. Ser323 position in the lowest HADDOCK scoring UbE-βTrCP2 complex. βTrCP2 is shown in grey (residue numbers in black) and the UbE motif peptide in green (residue numbers in green). In this model the non-phosphorylated S323 residue does not form close contacts with βTrCP2. Note that the UbE motif Trp324 residue forms a cation-Pi interaction with Lys241 and Arg258 in βTrCP2, in the proximity of Ser323. It could be that phosphorylation of Ser323 displaces the Trp324 interaction with Lys241 and/or Arg258.

Growth hormone receptor endocytosis and degradation are regulated by phosphorylation of serine 323 in the ubiquitin-dependent endocytosis motif

4

Ana C. da Silva Almeida[1,2], Agnes G S H van Rossum[1,2], Ger J Strous[1]

[1] Department of Cell Biology and Institute of Biomembranes, University Medical Center Utrecht, Heidelberglaan 100, 3584 CX Utrecht, The Netherlands

[2] Drug Discovery Factory BV, Albrechtlaan 14A, 1404 AK Bussum, The Netherlands

(Manuscript in preparation)

Abstract

Growth hormone (GH) is an important regulator of growth and metabolism. The duration of GH signaling is tightly controlled at several levels. In this way cells avoid the potential detrimental effects resulting from too high/low GH signaling. At steady state (in the absence of GH), GH receptor (GHR) has a half-life of approximately 60 min, mainly due to endocytosis and lysosomal degradation. Upon activation by GH the degradation is accelerated. In both cases, the endocytosis and degradation of GHR depend on the E3 ligase SCF(βTrCP), which is recruited to the ubiquitin-dependent endocytosis motif and mediates the ubiquitination of yet unknown factors. In this study we report that phosphorylation of S323 in the UbE motif considerably increases the affinity for SCF(βTrCP). This phosphorylation event is triggered by GH. Mutation of the S323 to a phosphomimetic residue (S323D) increased GHR endocytosis and degradation considerably. This finding provides a novel mechanism to regulate GHR endocytosis, which enables an efficient way for GH (de)sensitization of cells.

Introduction

Growth hormone (GH) is a major growth-promoting factor and metabolic regulator (*1*). GH signaling is triggered when this 22 kDa peptide binds to the GH receptor (GHR), a protein of 620 aminoacids expressed in all cells of the body, and member of the class 1 superfamily of cytokines receptors. A model of GHR activation has been presented that described how asymmetric binding of GH causes a rotation of the dimeric GHR tails (*2*). Due to the rotation, two JAK2 kinases, associated to the box-1 of the receptors, are brought in close proximity, which results in their cross phosphorylation and, ultimately, in GHR phosphorylation at multiple tyrosine residues (*3*). Downstream GH actions occur mainly through the activation of the signal transducer and activator of transcription 5 (STAT5). Upon its phosphorylation by JAK2, STAT5 dimerizes, migrates to the nucleus where it specifically binds to target genes and activates transcription (*4*). The mitogen activated protein kinase (MAPK) and phosphatidylinositol 3'-kinase (PI3K) pathways are also activated by GH (*1*).

GH is released by the anterior lobe of the pituitary gland in a pulsatile pattern, but the physiological importance and consequences are not completely clear (*5*). The pattern of GH secretion differs in male and female rats, characterized in males by abrupt peaks with a periodicity of 3-4 hours between peaks, and in females by a nearly continuous secretion pattern (*6*).This leads to continuous cycles of desensitization and re-sensitization of GH signaling. Differences in sex-specific gene expression in the liver have been attributed to this dimorphic pattern of GH release (*7*).

The duration of GHR signaling needs to be very tightly regulated. Prolonged signaling has been associated with development of certain cancers (*8*). Several levels of regulation exist. The suppressors of cytokine signaling (SOCS) proteins family suppress GH signaling by several mechanisms, including inhibition of JAK2 activity or STAT5 binding to GHR(*9*). Another level of regulation is through protein tyrosine phosphatases (PTPs) (*9, 10*). Endocytosis is an early step towards the termination of GH signaling. GHR endocytosis although occurring constitutively, is accelerated in presence of GH (*11, 12*).

The endocytosis of GHR depends on a functional ubiquitination system that acts via the "ubiquitin-dependent endocytosis motif" (UbE) in the cytoplasmic tail of the receptor (*13*). This motif works as a recruitment platform for βTrCP, the F-box substrate recognition subunit of SCF(βTrCP) E3 ligase, necessary for GHR endocytosis (*14*). Generally, SCF(βTrCP) recognizes the classical DSGxxS motif in its substrates (*15*), including receptors homologous to GHR, such as prolactin receptor (PRLR)(*16*), interferon-α receptor (IFNAR)(*17*), and erythropoietin receptor (EpoR)(*18*). In these receptors, βTrCP binds only when the serines residues in the DSGxxS motif are phosphorylated upon ligand binding , which leads to their endocytosis and signal termination. Recently, we reported that besides the UbE motif, GHR contains a constitutively phosphorylated DSGxxS motif able to bind βTrCP. However, the function of the DSGxxS motif in GHR is restricted to steady state conditions, in the absence of GH stimulation (*da Silva Almeida AC, submitted manuscript*). Therefore, in contrast with other cytokine receptor family members, GHR DSGxxS motif does not seem to contribute to signal termination. This role is carried out by the UbE motif, important for both steady state and GH-induced endocytosis (*da Silva Almeida AC, submitted manuscript*)(*19*). Since the regulation of βTrCP-substrates interactions involves serine phosphorylation, we evaluated the potential role of the UbE serine phosphorylation (S323) as a modulator of UbE-βTrCP interaction.

In this study we present evidence that GH stimulation triggers phosphorylation of S323 in the GHR UbE motif, which results in increased affinity for βTrCP binding to the UbE and consequently, in faster endocytosis. S323 phosphorylation might constitute a very efficient mechanism for signal termination after GH stimulation. In addition, S323 might also be phosphorylated by other stimuli, and work as a target where several pathways converge to regulate GHR endocytosis rate and GH sensitivity of the cells.

Materials and methods

Reagents and DNA constructs

Anti-poly-His monoclonal antibody was purchased from Sigma (Saint Louis, MO, USA). Anti-sera against residues 327-493 (anti-GHR (B)) and residues 271–318 of GHR (anti-GHR (T)), were raised in rabbits (*20*) (*21*). Anti-GST antibody was raised in rabbit against GST peptides (*20*). Monoclonal antibody against ubiquitin (clone FK2) was purchased from Biomol (Raamsdonksveer, The Netherlands), and anti-actin (Clone C4) was from MP Biomedicals Inc (Amsterdam, The Netherlands). Goat anti-mouse IgG Alexa-680 was from Molecular Probes (Eugene, OR, USA), and goat anti-rabbit IgG IRDye800 from Rockland Immunochemicals Inc (Gilbertsville, PA, USA). The primers were purchased from Sigma. The peptides were chemically synthesized by Pepscan (Lelystad, The Netherlands). The sequence of the UbE peptide (fragment 314-335) was 22 amino acids long: Acetyl-YKPEFHSDDSWVEFIELDIDEP-amide and the peptide P-UbE had the same sequencebut with a phosphate group attached to the S323. Glutathione (GSH)-beads were purchased from Amersham Biosciences (Freiburg, Germany). Protein A-beads were purchased from Repligen (Waltham, MA, USA). Human GH was a kind gift from Eli Lilly Research Labs (Indianapolis, IN, USA). Biotinylated-GH (biotin-GH) was made according to the manufacturer's protocol, Pierce. Cycloheximide and the CK2 inhibitor 4,5,6,7-tetrabromobenxotriazole (TBB) were purchased from Sigma. Full-length rabbit GHR cDNA in pcDNA3 has been previously described (*20*). The mutations in the UbE motif were inserted with Quick Change mutagenesis kit from Stratagene (Santa Clara, CA, USA). GHR S323A and F323A pcDNA3 constructs were generated as previously described (*13*). GHR S323D was generated with the forward primer 5'GAATTCTACAATGATGACGATTGGGTTGAATTCATCG 3' and the reverse primer 3'CTTAAGATGTTACTACTGCTAACCCAACTTAAGTAGC 5', using GHR WT as a template. The Flag-tagged wild type mouse βTrCP2 (Flag-βTrCP) construct was a generous gift from Prof. Carter-Su (University of Michigan, Ann Arbor).

Cell culture and transfections

Culture media, fetal calf serum and antibiotics for tissue culture were purchased from Gibco (Invitrogen, Groningen, The Netherlands). Human embryonic kidney 293 (HEK293) cells, stably expressing the Tetracycline Repressor (HEK293-TR), were a gift from Dr. Madelon Maurice (University Medical Centre Utrecht, The Netherlands). HEK293-TR cells were grown in Dulbecco's modified Eagle's medium (DMEM) supplemented with 10% fetal calf serum, 100 units/ml penicillin, 0.1 mg/ml streptomycin and 12 μg/ml Blasticidin S (MP Biomedicals). U2OS cell lines stably expressing GHR WT, and the mutants S323A and S323D were grown in DMEM supplemented with 10% fetal calf serum, 100 units/ml penicillin, 0.1 mg/ml streptomycin, and either with 150 μg/ml hygromycin (GHR WT), or 600 μg/ml Geneticin (G418) (GHR S323A and S323D). Cells were grown at 37°C with 5.0% CO_2. Twice a week the cells were washed with phosphate-buffered saline (PBS), detached from the flask with trypsin-EDTA (Invitrogen) diluted in fresh growth medium, and split into new culture flasks. βTrCP silencing using the "combi probe" was performed as previously described (*14*). As a control, a random siRNA from Ambion (Austin, Texas, USA) was used. U20S cells stably expressing GHR WT were transfected with small interfering RNA (siRNA) using Lipofectamine-2000 (Invitrogen) according to the manufacturer's protocol; 3 days after transfections the cells were stimulated with GH and used in western blotting experiments. For cycloheximide treatment, ^{125}I-GH uptake, GH stimulation and βTrCP silencing experiments cells were culture in 12-wells plates. DNA transfections were performed using FuGene 6 (Roche, Applied Sciences, Almere, The Netherlands). Seventy percent confluent cultures in 6-wells plates were transfected with 1 μg of DNA, according to the manufacturer's protocol. Twenty four hours after transfection, the cells were used for biotin-GH pull down experiments or co-immunoprecipitations. GH stimulation was performed by adding 180 ng/ml human GH to the cells. When indicated cells were treated with 20 μg/ml cycloheximide. 4,5,6,7-tetrabromobenxotriazole (TBB) (dissolved in DMSO in a concentration of 20 mM) was added to the cells in a final concentration of 75 μM.

Protein expression and purification

His-SF-βTrCP/His-Skp1ΔΔ was purified from Sf9 cells co-infected with the respective virus, with a His-Trap HP column (GE Healthcare, Hoevelaken, The Netherlands), followed by a gel filtration in a S200 column, with an Akta purifier (GE Healthcare). The procedure was previously described in detail *(da Silva Almeida AC, manuscript in preparation)*. GST tagged GHR tails (residues 270 to 339) from WT, GHR mutants S323A and S323D, and GHR WT tails (residues 270-334, including UbE) were expressed in *E. coli* (strain BL21). Protein synthesis was induced by isopropyl-1-thio-β-D-galactopyranoside (IPTG). The GST fusion proteins were purified with Glutathione (GSH)-beads (Amersham Biosciences) by standard protocol previously described (*22*).

In vitro binding assays

GST-GHR WT (270-339), GHR mutants S323A or S323D were dissolved in PBS supplemented with 1% BSA and protease inhibitors (1 mM PMSF, 10 µg/ml aprotinin, 10 µg/ml leupeptine) and incubated with GSH beads for 2 hours at 4^0C (10 µg GST fusion proteins were used for saturation of 25 µl of GSH beads). The beads were washed twice with the same buffer and twice with binding buffer (50 mM Tris pH8, 100 mM NaCl, 0.1 % Triton X-100, 0.1%BSA, 1 mM PMSF, 10 µg/ml aprotinin, 10 µg/ml leupeptine). 1 µg His-SF-βTrCP2/His-Skp1ΔΔ complex was then incubated for 2 hours with the GSH beads coupled to GST-GHR fusion proteins in the binding buffer at 4^0C. The beads were washed twice with binding buffer and twice with 0.1 X PBS. In case of competition with peptides, the beads were incubated for 2 more hours with increasing concentrations of the 22 amino acid-long UbE un-phosphorylated (UbE) or phosphorylated in S323 (P-UbE) peptides diluted in binding buffer. GHR WT (270-339) tails, resulting from the thrombin cleavage of the GST tag, were also used in competition assays. The beads were washed twice with binding buffer and twice with 0.1 X PBS and boiled in sample buffer, run on SDS-PAGE and immunoblotted with anti-GST and anti-His antibodies.

Cell lysis, biotin-GH pull downs and immunoprecipitations

For analysis of total cell lysates, cells were lysed for 20 minutes in cold lysis buffer (1% Triton X-100, 1 mM EDTA, 100 mM NaF, 1 mM Na_3VO_4, 1 mM PMSF, 10 µg/ml aprotinin, and 10 µg/ml Leupeptine, in PBS). After 5 min centrifugation at maximum speed at 4°C, the supernatant was analysed by western blotting.

For pull down experiments, biotin-GH (180 ng/ml) was added to the medium of the transfected HEK293-TR cells in the incubator, at 37°C, for 10 min. The cells were washed three times with PBS, and lysed with cold lysis buffer (1% Triton X-100, 1 mM EDTA, 1 mM PMSF, 10 µg/ml aprotinin, 10 µg/ml Leupeptine, 1 mM Na_3VO_4 and 100 mM NaF in PBS) for 20 minutes. After 5 min centrifugation at maximum speed at 4°C, the supernatant was incubated for 1 h with 25 µl streptavidin beads at 4°C. Beads were boiled and subjected to SDS-PAGE, and western blotting.

For co-immunoprecipitation experiments, transfected HEK293-TR were stimulated for 30 min with GH, and lysed with cold lysis buffer, as described above. The supernatants were incubated with 7.5 µl anti-GHR (T) antibody for 2 hours, followed by incubation with 25 µl protein A beads. Immunoprecipitates were subjected to SDS-PAGE and western blotting.

For ubiquination experiments U2OS cells stably expressing GHR WT, S323A or S323D mutants were lysed in 1% Triton X-100 with inhibitors (1 mM EDTA, 1 mM PMSF, 10 µg/ml aprotinin, 10 µg/ml leupeptin, 10 mM NEM, 1 mM Na_3VO_4 and 100 mM NaF). The cell lysates were centrifuged at maximum speed, for 5 min, at 4°C, and the supernatants were used for GHR isolation with anti-GHR antibody (anti-T) and protein A-beads, in 1% Triton X-100, 0.5% SDS, 0.25% sodium deoxycholate, 0.5% BSA and inhibitors. Immunoprecipitates were subjected to SDS-PAGE and western blotting.

Immuno Blotting

Following SDS-PAGE, proteins were transferred to an Immobilion-FL PVDF membrane (Millipore, Amsterdam, The Netherlands). The membranes were blocked with Odyssey blocking buffer (Li-Cor Biosciences, Lincoln, NE, USA) diluted 1:1 with PBS for 1 hour at room temperature. The blots were incubated with the indicated primary antibodies for 1.5 hour, and after washing in PBS 0.1% Tween-20, membranes were incubated for 1 hour with secondary antibody. The detection and

analysis of the immunoblots was performed with an Odyssey infrared imaging system (Li-Cor Biosciences, Lincoln, Nebraska).

^{125}I binding and internalization

^{125}I-Human GH was prepared using chloramine T (*20*). For internalization experiments, U2OS cells stably expressing GHR WT, S323A or S323D mutants, grown in 12-well plates, were washed with 1 ml of minimal essential medium supplemented with 20 mM Hepes pH7.4, and 0.1% bovine serum albumin, and put on ice. ^{125}I-GH (180 ng/ml in DMEM/Hepes/0.1% bovine serum albumin) was added to the cells. After 2h binding on ice, cells were placed at 37ºC for 15 min, to allow receptor endocytosis. Cells were then washed once with 2 ml of PBS-c (PBS with 0.135g/liter $CaCl_2$ and 0.1 g/liter $MgCl_2$).

Cell surface ^{125}I-GH was removed by treating the cells twice with 0.75 ml acid wash (0.15 M NaCl, 50 mM glycine, 0.1% bovine serum albumin, pH 2.5) for 5 min on ice. Acid wash was collected in counting tubes, and radioactivity was measured using a LKB counter. Cells were solubilized overnight in 1 N NaOH. Internalized ^{125}I-GH was determined by measuring the radioactivity in the collected NaOH fraction. Unspecific counts were determined by incubating the cells with ^{125}I-GH together with excess unlabeled GH (9 μg/ml).

Biacore measurements

Surface plasmon resonance (SPR) was performed on a Biacore T-100 (GE Healthcare), with His-SF-βTrCP/His-Skp1ΔΔ coupled to a CM5 chip using –NH2 coupling. The affinities of UbE and P-UbE peptides in phosphate buffer 50 mM pH7.2, 200 mM NaCl, 5% Glycerol and 5 mM β-Mercaptoethanol, were compared. 9% dimethylformamide (DMF) was added in the case of the UbE peptide to help the dissolution of the peptide. The specific association of the peptides to the chip results in increasing SPR signal, expressed in response units (RU), followed by a dissociation curve. Data were processed using Bia Evaluation (GE Healthcare) and GraphPad Prism5.

Results

GHR UbE motif with phosphorylated S323 binds βTrCP with higher affinity

Whereas serine phosphorylation in the degron DSGxxS is required for binding βTrCP (*15*), binding of βTrCP to UbE motif (DDSWVEFIELD) can occur without a phosphorylation event (*da Silva Almeida, manuscript in preparation*). However, serine phosphorylation in the UbE motif (S323) might influence the UbE-βTrCP interaction. To investigate this possibility we performed *in vitro* competition studies with increasing concentrations of phosphorylated (P-UbE) or unphosphorylated (UbE) UbE peptides (Fig. 1A). Surprisingly, P-UbE peptide competed the interaction between βTrCP and GST-GHR tail containing the UbE motif (GST-GHR+UbE) approximately 100 times more efficiently than the UbE. In addition, "Surface Plasmon Resonance" measurements were performed to obtain more quantitative data (Fig. 1B). The purified His-SF-βTrCP/His-Skp1ΔΔ complex was coupled to the gold surface of the chip, and the UbE peptides in solution were injected. The response units (RU) in equilibrium, obtained at a certain concentration of peptide were plotted (Fig. 1B). Due to

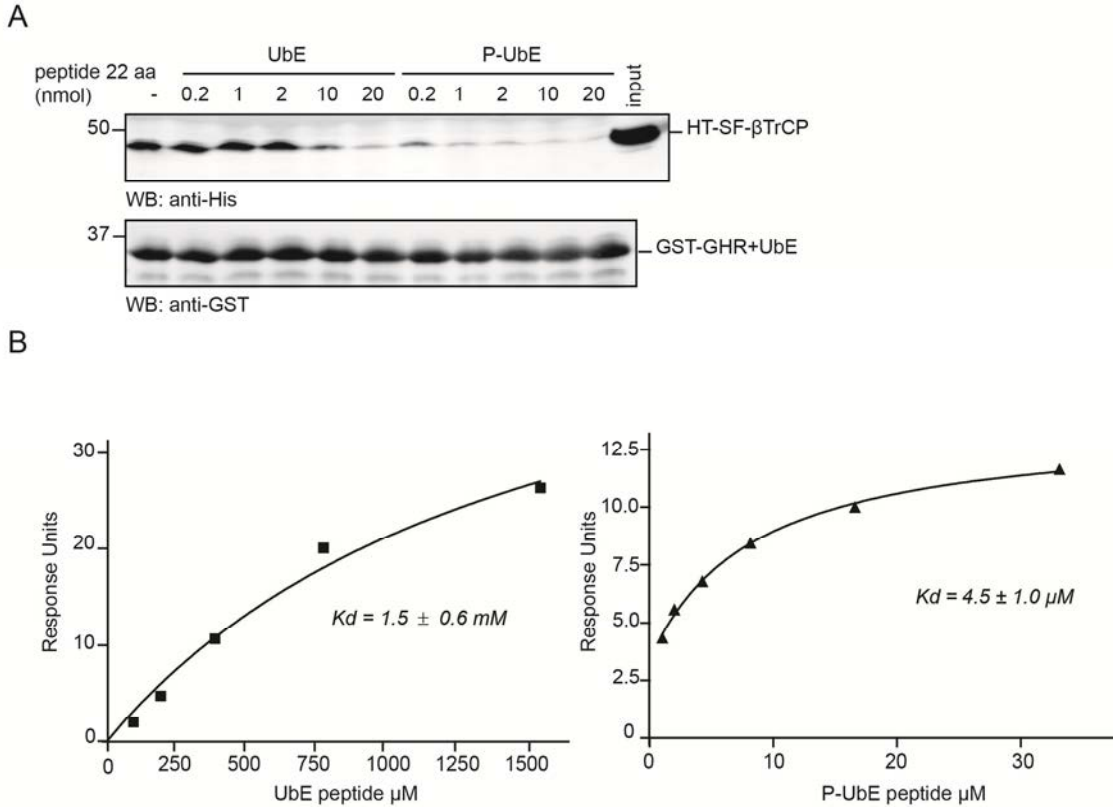

Fig. 1: GHR UbE motif with phosphorylated S323 binds βTrCP with higher βTrCP
(A) GST-GHR 270-334 tails containing the UbE motif (GST-GHR+UbE) were coupled to glutathione beads, followed by binding to purified βTrCP/Skp1 complex (His-SF-βTrCP/His-Skp1ΔΔ) for 2 hours. UbE and P-UbE peptides were then added in increasing amounts (0.2, 1, 2, 10, 20 nmol) to compete for βTrCP binding. The samples were analyzed by western blotting with anti-His and anti-GST antibodies. His-SF-βTrCP/His-Skp1ΔΔ input is shown (lane 12). These data are representative of three independent experiments. **(B)** Fitting binding curves for the interaction of the UbE and P-UbE with His-SF-βTrCP2/His-Skp1ΔΔ at equilibrium, obtained with Surface Plasmon Resonance (SPR).

poor solubility of the peptide, the maximal possible UbE peptide concentration was not high enough to reach saturation in the binding curve. Addition of DMF increased the solubility of the UbE peptide whereas DMF was not necessary to dissolve the P-UbE peptide. DMF did not have an effect by itself in GHR-UbE-βTrCP binding affinity (Supplementary data, Fig. 1). The binding affinities of the βTrCP-UbE interaction (Kd) were estimated at 1.5±0.6 mM for the UbE peptide, and 4.5±1 μM for the P-UbE peptides. We conclude that phosphorylation of the S323 in the GHR UbE motif results in a substantial increase in the affinity for βTrCP.

Phosphomimetic GHR S323D mutant and βTrCP binding

To investigate the role of serine phosphorylation in the UbE motif further, the S323 was mutated to aspartic acid (S323D) and we asked whether this mutation mimicked phosphorylation. As a control we mutated the S323 to alanine (S323A). In Fig. 2A, beads coupled to GST-GHR tails WT, S323A or S323D mutants were allowed to bind increasing amounts of purified His-SF-βTrCP/His-Skp1ΔΔ complex. No clear differences in βTrCP binding could be detected between the three forms of GST-GHR tails. As expected, GST-GHR WT and S323A mutant bound βTrCP with similar affinities, since both GST-GHR tails where expressed in *E.coli,* where the appropriate enzymes are lacking. However, if S323D worked as a phosphomimetic it should bind better to βTrCP/Skp complex. These results are indicative of very poor phosphomimetic abilities of the S323D mutant. To compare more directly binding affinities, competition assays were performed. βTrCP was bound to GST-GHR WT or S323, and then increasing amounts of GHR tails WT (from which the GST tag has been removed) were added to compete for βTrCP binding (Fig, 2B). The addition of 2 nmoles of GHR tails resulted in a decrease binding to βTrCP of 26%, 20%, and 48% of the initial βTrCP binding, for GST-GHR WT, S323A and S323D, respectively. This indicates a slightly higher binding affinity for the GST-GHR S323D to βTrCP compared to S323A mutant or GHR WT. Subsequently, the binding efficiency of the phosphomimetic GHR S323D mutant to βTrCP was analyzed in the context of the full length receptor. GHR complexes were pulled with biotin-GH from the cell surface of HEK293-TR cells transiently expressing GHR WT, S323A, S323D or F327A mutants together with Flag-βTrCP. Previously, we showed that theF327A mutation reduces βTrCP binding (*13*), and therefore it was used as a control of the assay. The GHR S323A mutant bound about 20% less Flag-βTrCP compared to the GHR WT. GHR S323D mutant bound Flag-βTrCP more efficiently that the S323A mutant, but as efficient as GHR WT (Fig. 2C, quantified in Fig. 2D). Similar results were obtained in co-immunoprecipitation experiments (Fig. 2E, quantified in Fig. 2F). These results show that GHR S323D might work as a phosphomimetic *in vivo*. Furthermore, under those experimental conditions, GHR WT seems to be phosphorylated at S323.

Taken together, we conclude that *in vitro,* in short GHR tails, the S323D mutant mimics very poorly a phosphorylation event that results in increased βTrCP binding affinity. In cells, full length GHR S323D might work as a phosphomimetic, resulting in a more efficient βTrCP binding than S323A.

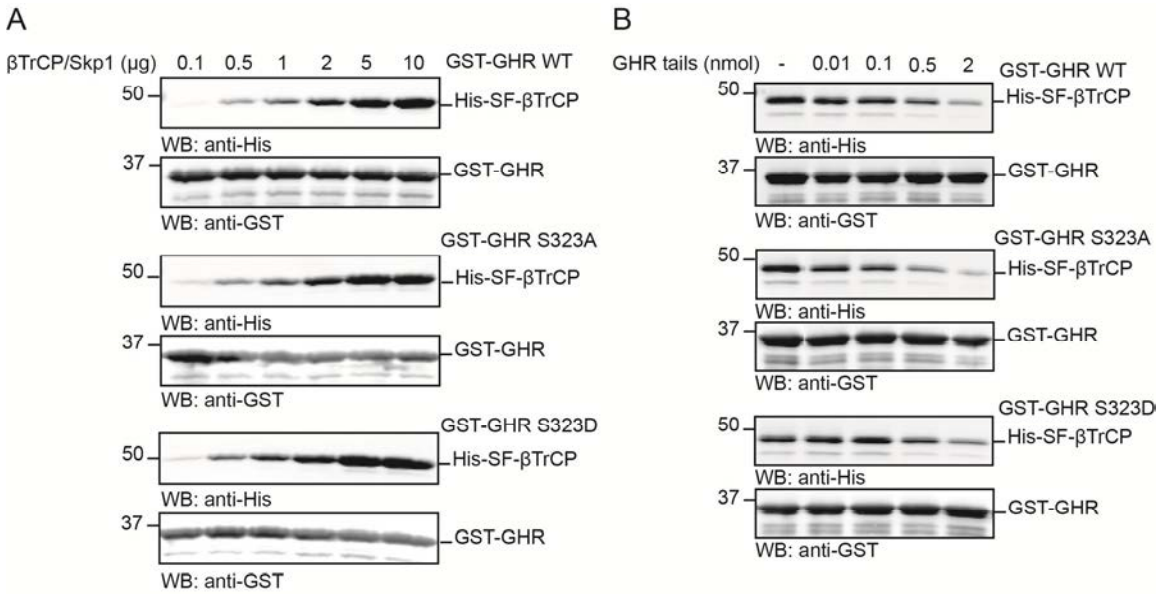

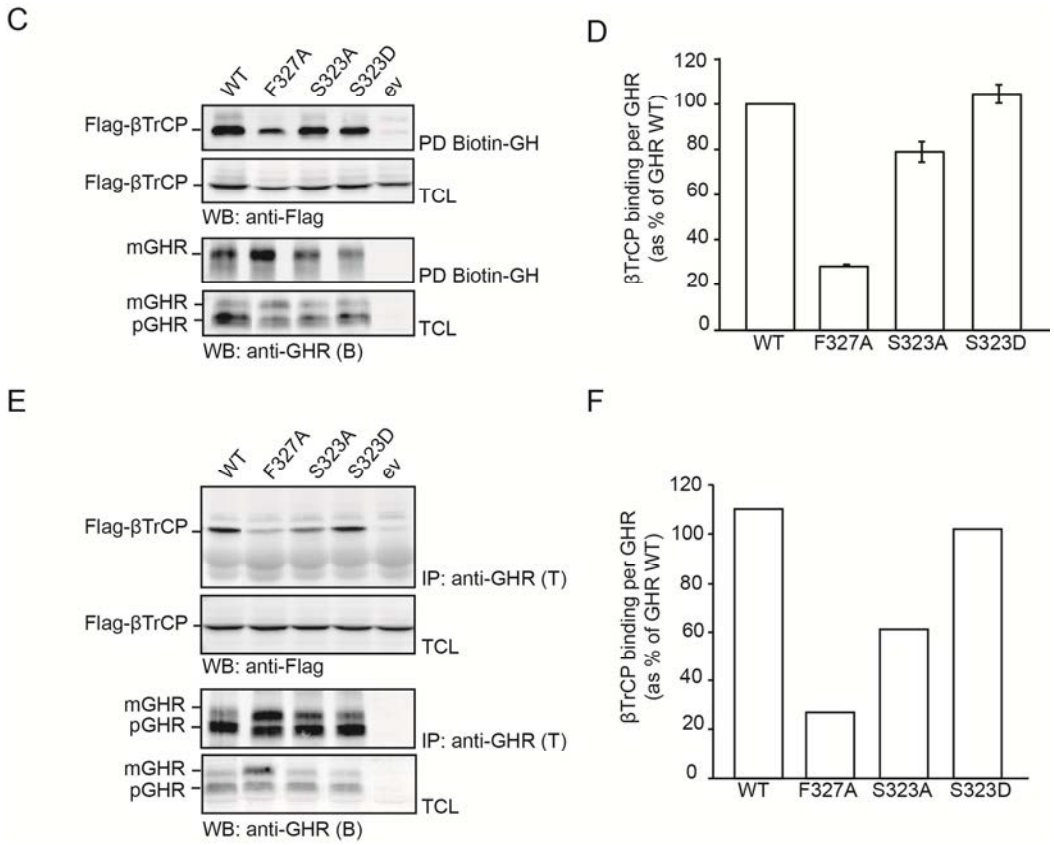

Fig. 2: Phosphomimetic GHR S323D mutant and βTrCP binding

(A) GST-GHRWT tails (270-339), S323A, and S323D mutants were coupled to glutathione beads, and then, allowed to bind the indicated increasing amounts of purified βTrCP/Skp1 complex (His-SF-βTrCP/His-Skp1ΔΔ). The samples were analyzed by western blotting with anti-His and anti-GST antibodies. **(B)** GST-GHR WT tails (270-339), S323A, and S323D mutants were coupled to glutathione beads and allowed to bind the indicated increasing amounts purified βTrCP/Skp1 complex (His-SF-βTrCP/His-Skp1ΔΔ). GHR WT tails (270-339) without GST tag, were added in increasing amounts to compete for βTrCP binding. The samples were analyzed by western blotting with anti-His and anti-GST antibodies. **(C)** HEK293-TR cells were transfected with GHR WT, F327A, S323A, S323D, and co-transfected with Flag-βTrCP. 180 ng/ml biotin-GH was added for 10 min at 37^{o}C. After lysis, GHR complexes were pulled from the cell surface using streptavidin beads. The samples were subjected to western blotting and detected with anti-GHR (B) and anti-Flag (for Flag-βTrCP detection) antibodies. Note that only mature GHR is detected in the PD samples. Aliquots of cell lysates were also analyzed by western blotting with the same antibodies. mGHR, mature GHR; pGHR, precursor GHR in the endoplasmic reticulum; PD, pull down; TCL, total cell lysates; ev, empty vector. **(D)** Quantification of 2C. The effect of each GHR mutant was expressed as amount of βTrCP binding per GHR in percentage of the WT. The data represent the mean of three independent experiments ± SEM. **(E)** HEK293-TR cells were transfected with GHR WT, F327A, S323A, S323D mutants, and co-transfected with Flag-βTrCP. 180 ng/ml GH was added for 30 min, lysed and subjected to co-immunoprecipitation with anti-GHR (T) antibody. The samples analyzed by western blotting with anti-GHR (B) and anti-Flag (for Flag-βTrCP detection) antibodies. Aliquots of cell lysates were also analyzed by western blotting with the same antibodies. mGHR, mature GHR; pGHR, precursor GHR in the endoplasmic reticulum; IP, immunoprecipitation; TCL, total cell lysates; ev, empty vector**.(F)** Quantification of 2E. The effect of each GHR mutant was expressed as amount of βTrCP binding per GHR in percentage of the WT. The data represent one experiment.

GHR S323 phosphomimetic mutant accelerates GHR degradation

The recruitment of SCF(βTrCP) to the UbE motif of GHR is necessary for its endocytosis (*14*). Because S323 phosphorylation results in an increased affinity of the GHR UbE- βTrCP interaction, we expect that UbE phosphorylation will cause faster GHR endocytosis/degradation. To investigate the involvement of amino acid S323 on basal GHR degradation, U2OS cells stably expressing GHR WT, S323A and S323D mutants were treated with cycloheximide for different time periods, and the decrease of GHR was quantitated (Fig. 3). GHR WT and S323A mutant were degraded at the same rate, while the degradation of the phosphomimetic GHR S323D was 1.5 times faster. Thus, we conclude that the S323D mutant GHR has 1.5 times shorter half-life than the WT and the S323A

mutant, and that S323 does not contribute to the basal degradation of the receptor. This suggests that when GHR is phosphorylated at S323 (as mimicked with S323D mutant) its degradation is accelerated. The half life time of the S323A mutant is comparable to GHR WT, indicating that basal GHR degradation occurs independently of the S323 phosphorylation event.

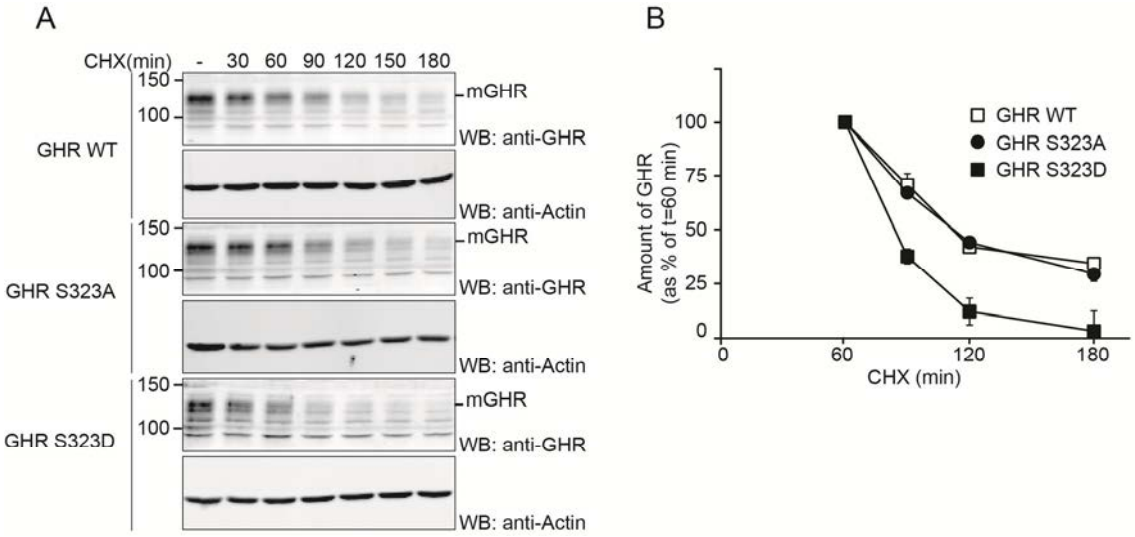

Fig. 3: GHR S323 phosphomimetic mutant accelerates GHR degradation.
(A) U2OS cell lines stably expressing GHR WT, S323A or S323D mutant were subjected to cycloheximide treatment (C=20µg/ml) treatment for the different indicated time points (30, 60, 90, 120, 150 or 180 min). The cells were lysed and equal amounts of total cell lysates were analyzed by western blotting, using anti-GHR (B). CHX, cycloheximide; mGHR, mature GHR. **(B)** Quantification of 3A.The total amount of GHRs was determined, corrected for actin, and expressed in relation to the amount of receptor at t=60 min of cycloheximide treatment, which was set at 100%, to avoid the contribution from the precursor form of GHR. The data represent the mean of two independent experiments ± SEM.

GH stimulates GHR endocytosis and degradation via potential phosphorylation of S323

As S323 is most likely not phosphorylated under basal conditions, the potential phosphorylation of this residue might be triggered by certain stimuli. In PRLR, IFNAR and EPOR the DSGxxS motif becomes phosphorylated after stimulation with the ligand (*16-18*). Since DSGRTS in GHR is probably constitutively phosphorylated, independently on GH stimulation *(da Silva Almeida, manuscript submitted*), we hypothesized that GH binding might act as a trigger for the phosphorylation of S323 in the UbE motif. To investigate this, the rate of ^{125}I-GH internalization in U2OS cells stably expressing GHR WT, S323A and S323D was compared. GH-induced endocytosis of the GHR S323A mutant has been previously tested by Govers et al, and was found to be substantially inhibited in both Cy3-GH and ^{125}I-GH uptake assays (*13*). In agreement with Govers, we found similar results in ^{125}I-GH uptake experiment, in which the endocytosis was 50 % less efficient than the WT. The rate of ^{125}I-GH internalization of the S323D mutant was comparable with GHR WT, indicating that the GHR WT is nearly completely phosphorylated at S323 by GH stimulation. Next, we investigated whether stimulation of cells with increasing concentrations of GH might accelerate GHR endocytosis/degradation through S323 phosphorylation. The amount of GHR WT reduced when cells were stimulated with increasing GH concentrations, and more clearly with 150 and 300 ng/ml (Fig. 4B, 1st panel). GH stimulation did not affect the endocytosis/degradation for the GHR S323A mutant (Fig. 4B, 3rd panel). Taken together the results indicate that GH stimulation triggers S323 phosphorylation, which results in faster GHR endocytosis.

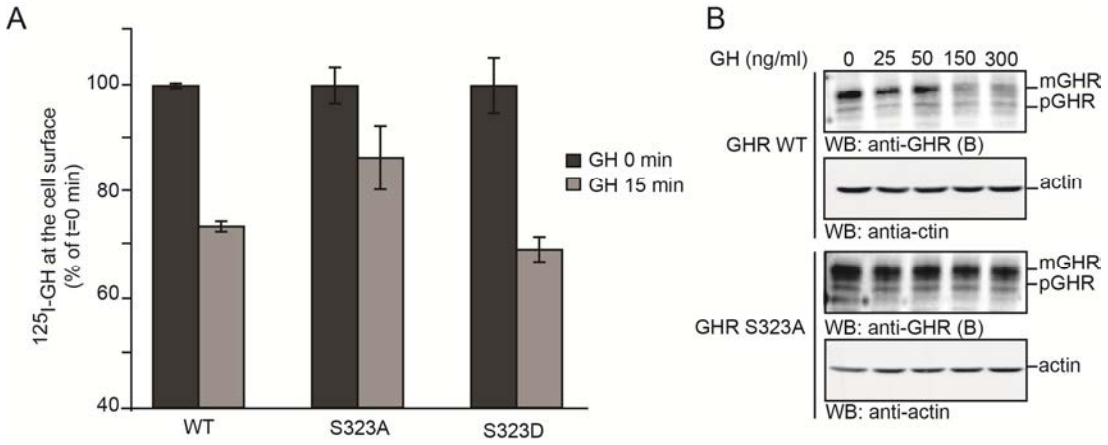

Fig. 4: GH stimulates GHR endocytosis and degradation via potential phosphorylation of S323
(A) U2OS cells stably expressing GHR WT, S323A, and S323D were incubated on ice for 2 hours with 180 ng/ml ^{125}I-GH (saturating amounts), and then placed at 37^{o}C for 15 min, or not (time(t)=0 min), in order to allow internalization to occur. The amount of ^{125}I-GH at the cell surface at t=0 min stimulation was set at 100%, and the cell surface ^{125}I-GH at t= 15 min was expressed as percentage of t=0 min. The data represent the mean of four independent measurements ±SEM. **(B)** U2OS cells stably expressing GHR WT, S323A were incubated for 30 min with the indicated concentrations of GH. The cells were lysed, and equal amounts of total cell lysates were analyzed by western blotting, using anti-GHR (B) and anti-actin antibodies. mGHR, mature GHR; pGHR, precursor GHR in endoplasmic reticulum. These data are representative of two independent experiments.

S323 phosphorylation is necessary for GH-induced, βTrCP-mediated GHR ubiquitination and degradation

The results reported so far support a scenario wherein S323 phosphorylation in the UbE motif increases the affinity for βTrCP. Likely, GH-induced downregulation of GHR S323A is slower than in GHR WT due to ineffective βTrCP function. To investigate whether GH-induced degradation of mature GHR requires the action of βTrCP, a GH stimulation time curve was performed in cells where βTrCP was silenced (Fig. 5A, right panel). Due to unavailability of a good anti-βTrCP antibody able to detect endogenous βTrCP, the silencing efficiency was confirmed indirectly by looking at the strong accumulation of mature GHR in βTrCP-silenced cells (Fig. 5A, right panel), compared to cells silenced with a control probe (Fig. 5A, left panel) (*14*). GHR receptor amounts remained constant with time of GH stimulation in the cells silenced for βTrCP, showing that βTrCP is necessary for the GH-induced downregulation of GHR WT. SCF(βTrCP) mediates ubiquitination events necessary for GHR endocytosis (*14, 19*). Ubiquitination of the GHR itself, although not required, precedes its endocytosis as was previously shown by clathrin heavy chain gene silencing (*23*). Therefore, GHR ubiquitination can be used as a measure of SCF(βTrCP) activity and GHR endocytosis. To investigate whether S323 in the UbE contributes to GH-induced GHR ubiquitination, U2OS WT and S323A mutant cell lines were used. GH stimulation caused a substantial increase in the ubiquitination of GHR WT, reflecting an increase in GHR endocytosis rate (Fig. 5B, compare lane 1 with lane 2). For the GHR S323A mutant, this increase in GHR ubiquitination was very minor (Fig. 5B, compare lane 3 with lane 4), correlating with decreased GH-induced receptor endocytosis (Fig. 4A). At the basal state, the ubiquitination of the GHR WT and S323A were comparable, in agreement with previous results, which showed that βTrCP binds to S323A mutant and GHR WT equally, in basal conditions (*da Silva Almeida, manuscript in preparation*). We conclude that GH stimulation acts via S323 to increase the affinity of GHR-βTrCP interaction, and consequently increase GHR ubiquitination and endocytosis rate.

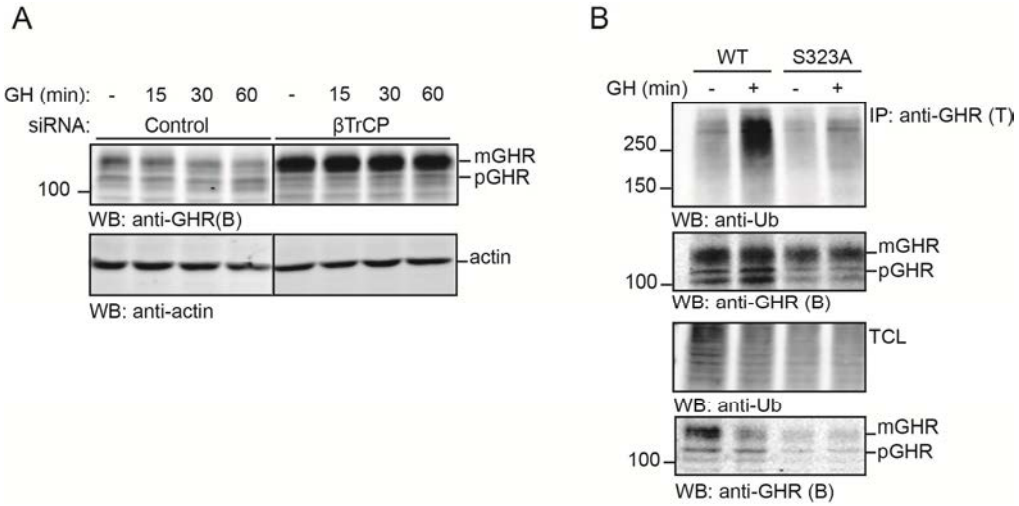

Figure5. S323 phosphorylation is necessary for GH-induced, βTrCP-mediated GHR ubiquitination and downregulation
(A) U2OS cells stably expressing GHR WT were transfected with siRNA as indicated to silence βTrCP; a random siRNA was applied as a control. Cells were incubated for the indicated time points (0, 10, 20, 30, 60 min) with 180 ng/ml GH, and lysed. Equal amounts of total cell lysates were analyzed by western blotting, using anti-GHR (B) and anti-actin antibodies. mGHR, mature GHR; pGHR, precursor GHR in endoplasmic reticulum. This data is representative of two independent experiments.**(B)** GHRs were isolated by immunoprecipitation, with anti-T antibody, from U2OS cells stably expressing GHR WT and S323A mutants, stimulated or not for 15 min at 37°C with180 ng/ml GH. The immunoprecipitations were performed under denaturating conditions, to guarantee that ubiquitination signal is coming only from the GHR. The samples were subjected to western blotting and detected for Ubiquitin (with FK2 antibody: anti-Ub) and GHR (anti-GHR(B)). Aliquots of cell lysates were analyzed by western blotting with the same antibodies. mGHR, mature GHR; pGHR, precursor GHR in the endoplasmic reticulum; TCL, Total cell lysates; IP, immunoprecipitations. These data are representative of three independent experiments.

Discussion

In the present study we describe a potentially very important feature of the UbE motif, by which the endocytosis of GHR can be regulated. We showed that GH binding induces the phosphorylation of S323 in the UbE motif that results in enhanced βTrCP affinity to the UbE motif and accelerated GHR endocytosis.

Recently, we presented evidence for a model wherein the basal binding of JAK2 to GHR inhibits its endocytosis until GH stimulation triggers JAK2 detachment from GHR. The receptor is then allowed to endocytose through SCF(βTrCP)-mediated ubiquitination of yet unknown factors (*19*). The phosphorylation of S323 in the UbE motif might occur only after JAK2 disassociation, or vice-versa, S323 phosphorylation might facilitate JAK2 release. The later scenario would implicate that other signaling pathways could influence GHR endocytosis rate as well. Under basal conditions, in the absence of GH, βTrCP binds to two motifs in GHR, UbE and DSGxxS, and both contribute to GHR endocytosis/degradation (*da Silva Almeida AC*, manuscript submitted). Upon GH stimulation, the role of the DSGxxS motif becomes redundant. An explanation could be that GH stimulation triggers S323 phosphorylation, resulting in higher affinity of βTrCP to the UbE motif. This supports the predominant role of the UbE motif in GH-induced GHR endocytosis.

The induction of S323 phosphorylation is potentially important in GH signaling termination by increasing the rate of GHR endocytosis, in order to reset the cells for another round of full signaling activation. In fact, full STAT5 activation in males depends on the pulsatile secretion of GH (*24*) (*25*). Interestingly, the deactivation of STAT5 was suggested to need proteasomal action and to depend on a serine/threonine phosphorylation reaction (*26*). Continuous GH stimulation (characteristic of females) reduces the levels of activated STAT5 (*25*). Therefore, an interval between pulses (~2.5-3 hours) is necessary to reestablish the full responsiveness of the cells for another pulse of GH (*25*), as it happens in males. The regulation of GHR levels by repeated GH stimulation has been suggested as the mechanism determining GH responsiveness via the JAK2/STAT5 pathway (*27*). Presumably, GH -

induced S323 phosphorylation (and JAK2 release from GHR (*19*)) might be involved in this mechanism.

The kinase responsible for S323 phosphorylation is likely activated in the crossroads of the GH signaling pathways. JAK2 has been regarded as the major effector kinase in GH signaling (*9*). However, recent evidence supports that Src family kinases (SFKs) are also directly activated by GH, independently of JAK2 activation (*28, 29*). The activation of SFKs by GH was shown to activate extracellular signal-regulated kinase 1 and 2 (ERK1 and 2), through the phospholipase Cγ-Ras pathway (*29*). Future studies are needed to establish which of these signaling pathways mediate the induction of S323 phosphorylation by GH. These studies are hampered by the fact that no antibodies against phosphorylated S323 are available. In addition, efforts to use mass spectrometry analysis of GHRs pulled from surface of cells stimulated with GH failed to identify peptides containing the residue S323 neither in trypsin, nor in elastase and V8 digests (data not shown).

In addition to GH, other stimuli/stressors or signaling pathways may trigger S323 phosphorylation via the yet unknown specific kinase. There is evidence that insulin is able to modulate the biological action of GH (*30-32*), namely by reducing GHR availability at the cell surface (*31*). Additional evidence comes from a study of Shaonin Ji and coworkers, who showed that continuous insulin treatment in rat hepatoma cells reduced GHR levels and GH-induced phosphorylation of JAK2 and STAT5B (*33*). Short-term insulin pretreatment has been reported to enhance GH-induced MEK/ERK phosphorylation (*34*). In addition, PI-3 kinase pathways have also been suggested to mediate the insulin effects on the subcellular distribution of GHRs, in particular the decrease in the amount of GHRs at the cell surface (*31*). These pathways may act by influencing S323 phosphorylation status. Further experiments need to be performed to investigate the potential involvement of insulin signaling in the regulation of GHR endocytosis, particularly in S323 phosphorylation. Other stressors have been associated with low GHR levels, such as pro-inflammatory cytokines ("tumour necrosis factor α" (TNF-α), "interleukin 6" (IL-6) and "interleukin 1"(IL-1)(*35*)), glucocorticoids (*36-38*), among others. Further studies are needed to examine whether these stimuli may increase GHR endocytosis through S323 phosphorylation to shut off energy-consuming (GH-induced) anabolic actions. Therefore, the fast downregulation of GHR cellular levels under stress would be a way to ensure that the available energy is principally used by the organisms to cope with stressful situations.

The kinase responsible for S323 phosphorylation is not known yet. S323 is contained in a minimal consensus site for CK2 phosphorylation, which has been identified to be S-X-X-Acidic. The acidic residue may be glutamate, aspartate, or phosphorylated serine and tyrosine: in case of S323 this sequence is S^{323}WVE (*39*). Preliminary studies on the evaluation of a potential role for CK2 in S323 phosphorylation, by using the CK2 inhibitor 4,5,6,7-tetra-bromo-benxotriazole (TBB) (*40*), revealed that CK2 is a promising target. Future studies will be performed to verify this possibility. CK2 has a broad specificity, and it plays key roles in several physiological and pathological processes(*41*). Although CK2 has been regarded for a long time a constitutively active enzyme, recent reports about its regulation brought controversy within the CK2 field (*42*). It has become apparent that the regulation of CK2 involves regulated expression, assembly and subcellular localization, post-translational modifications, and regulatory interactions with molecules and proteins (*42, 43*). Interestingly, there are reports of increased CK2 activation by insulin, EGF, IGF-1(*44, 45*) and TNF (*46*). EGF-activated ERK2 binds directly CK2α enhancing its activity (*47*). TNFα-induced activation of CK2 was also related to ERK1/2 activity (*46*). It is interesting to evaluate whether CK2 can be activated by GH. Other stressors or pathways that activate ERK1/2 may result in increased activity of CK2 towards S323 in GHR, resulting in increased GHR endocytosis. Future studies will elucidate this hypothesis.

This study represents a new additional mechanism used by the cells to regulate and/or terminate GH signaling. Precise regulation of GH signaling, including its downregulation, is vitally important for proper body growth and metabolism. GHR endocytosis can be quickly increased via a phosphorylation event in S323, which confirms the versatility of this process as a regulatable mechanism for fast GH signaling desensitization. Other stressors may also act on S323 to accelerate GHR endocytosis. The kinase involved in S323 phosphorylation may represents a new possible target for drug discovery against conditions of GH insensitivity or cancers related to excessive GH signaling.

Acknowledgements

We thank all members of the GHR group. We thank Alex Faesen for the help with the surface plasmon resonance experiments. This research was supported by the European Network of Excellence, Rubicon "Role of ubiquitin and ubiquitin-like modifiers in cellular regulation" (Grant LSHG-CT-2005-018683), and the Marie Curie network, "UbiRegulators", (Grant MRTN-CT-2006-034555).

References

1. Birzniece, V., Sata, A., and Ho, K. K. (2009) Growth hormone receptor modulators, *Rev Endocr Metab Disord 10*, 145-156.
2. Brown, R. J., Adams, J. J., Pelekanos, R. A., Wan, Y., McKinstry, W. J., Palethorpe, K., Seeber, R. M., Monks, T. A., Eidne, K. A., Parker, M. W., and Waters, M. J. (2005) Model for growth hormone receptor activation based on subunit rotation within a receptor dimer, *Nat Struct Mol Biol 12*, 814-821.
3. Hansen, L. H., Wang, X., Kopchick, J. J., Bouchelouche, P., Nielsen, J. H., Galsgaard, E. D., and Billestrup, N. (1996) Identification of tyrosine residues in the intracellular domain of the growth hormone receptor required for transcriptional signaling and Stat5 activation, *J Biol Chem 271*, 12669-12673.
4. Ihle, J. N. (1996) STATs: signal transducers and activators of transcription, *Cell 84*, 331-334.
5. Schwartz, J. (2001) Editorial: pulsatile hormone patterns governing transcription factor function. Physiology of episodic GH secretion, *Endocrinology 142*, 4595-4598.
6. Tannenbaum, G. S., and Martin, J. B. (1976) Evidence for an endogenous ultradian rhythm governing growth hormone secretion in the rat, *Endocrinology 98*, 562-570.
7. Rinn, J. L., and Snyder, M. (2005) Sexual dimorphism in mammalian gene expression, *Trends Genet 21*, 298-305.
8. Waters, M. J., and Barclay, J. L. (2007) Does growth hormone drive breast and other cancers?, *Endocrinology 148*, 4533-4535.
9. Lanning, N. J., and Carter-Su, C. (2006) Recent advances in growth hormone signaling, *Rev Endocr Metab Disord 7*, 225-235.
10. Hackett, R. H., Wang, Y. D., Sweitzer, S., Feldman, G., Wood, W. I., and Larner, A. C. (1997) Mapping of a cytoplasmic domain of the human growth hormone receptor that regulates rates of inactivation of Jak2 and Stat proteins, *J Biol Chem 272*, 11128-11132.
11. Murphy, L. J., and Lazarus, L. (1984) The mouse fibroblast growth hormone receptor: ligand processing and receptor modulation and turnover, *Endocrinology 115*, 1625-1632.
12. Gorin, E., and Goodman, H. M. (1985) Turnover of growth hormone receptors in rat adipocytes, *Endocrinology 116*, 1796-1805.
13. Govers, R., ten Broeke, T., van Kerkhof, P., Schwartz, A. L., and Strous, G. J. (1999) Identification of a novel ubiquitin conjugation motif, required for ligand-induced internalization of the growth hormone receptor, *EMBO J 18*, 28-36.
14. van Kerkhof, P., Putters, J., and Strous, G. J. (2007) The ubiquitin ligase SCF(betaTrCP) regulates the degradation of the growth hormone receptor, *J Biol Chem 282*, 20475-20483.
15. Frescas, D., and Pagano, M. (2008) Deregulated proteolysis by the F-box proteins SKP2 and beta-TrCP: tipping the scales of cancer, *Nat Rev Cancer 8*, 438-449.
16. Li, Y., Kumar, K. G., Tang, W., Spiegelman, V. S., and Fuchs, S. Y. (2004) Negative regulation of prolactin receptor stability and signaling mediated by SCF(beta-TrCP) E3 ubiquitin ligase, *Mol Cell Biol 24*, 4038-4048.
17. Kumar, K. G., Tang, W., Ravindranath, A. K., Clark, W. A., Croze, E., and Fuchs, S. Y. (2003) SCF(HOS) ubiquitin ligase mediates the ligand-induced down-regulation of the interferon-alpha receptor, *EMBO J 22*, 5480-5490.
18. Meyer, L., Deau, B., Forejtnikova, H., Dumenil, D., Margottin-Goguet, F., Lacombe, C., Mayeux, P., and Verdier, F. (2007) beta-Trcp mediates ubiquitination and degradation of the erythropoietin receptor and controls cell proliferation, *Blood 109*, 5215-5222.

19. Putters, J., da Silva Almeida, A. C., van Kerkhof, P., van Rossum, A. G., Gracanin, A., and Strous, G. J. (2011) Jak2 is a negative regulator of ubiquitin-dependent endocytosis of the growth hormone receptor, *PLoS One 6*, e14676.
20. Strous, G. J., van Kerkhof, P., Govers, R., Ciechanover, A., and Schwartz, A. L. (1996) The ubiquitin conjugation system is required for ligand-induced endocytosis and degradation of the growth hormone receptor, *Embo J 15*, 3806-3812.
21. van Kerkhof, P., Govers, R., Alves dos Santos, C. M., and Strous, G. J. (2000) Endocytosis and degradation of the growth hormone receptor are proteasome-dependent, *J Biol Chem 275*, 1575-1580.
22. Schantl, J. A., Roza, M., De Jong, A. P., and Strous, G. J. (2003) Small glutamine-rich tetratricopeptide repeat-containing protein (SGT) interacts with the ubiquitin-dependent endocytosis (UbE) motif of the growth hormone receptor, *Biochem J 373*, 855-863.
23. Sachse, M., van Kerkhof, P., Strous, G. J., and Klumperman, J. (2001) The ubiquitin-dependent endocytosis motif is required for efficient incorporation of growth hormone receptor in clathrin-coated pits, but not clathrin-coated lattices, *J Cell Sci 114*, 3943-3952.
24. Waxman, D. J., Ram, P. A., Park, S. H., and Choi, H. K. (1995) Intermittent plasma growth hormone triggers tyrosine phosphorylation and nuclear translocation of a liver-expressed, Stat 5-related DNA binding protein. Proposed role as an intracellular regulator of male-specific liver gene transcription, *J Biol Chem 270*, 13262-13270.
25. Gebert, C. A., Park, S. H., and Waxman, D. J. (1997) Regulation of signal transducer and activator of transcription (STAT) 5b activation by the temporal pattern of growth hormone stimulation, *Mol Endocrinol 11*, 400-414.
26. Gebert, C. A., Park, S. H., and Waxman, D. J. (1999) Termination of growth hormone pulse-induced STAT5b signaling, *Mol Endocrinol 13*, 38-56.
27. Ji, S., Frank, S. J., and Messina, J. L. (2002) Growth hormone-induced differential desensitization of STAT5, ERK, and Akt phosphorylation, *J Biol Chem 277*, 28384-28393.
28. Barclay, J. L., Kerr, L. M., Arthur, L., Rowland, J. E., Nelson, C. N., Ishikawa, M., d'Aniello, E. M., White, M., Noakes, P. G., and Waters, M. J. (2010) In vivo targeting of the growth hormone receptor (GHR) Box1 sequence demonstrates that the GHR does not signal exclusively through JAK2, *Mol Endocrinol 24*, 204-217.
29. Rowlinson, S. W., Yoshizato, H., Barclay, J. L., Brooks, A. J., Behncken, S. N., Kerr, L. M., Millard, K., Palethorpe, K., Nielsen, K., Clyde-Smith, J., Hancock, J. F., and Waters, M. J. (2008) An agonist-induced conformational change in the growth hormone receptor determines the choice of signalling pathway, *Nat Cell Biol 10*, 740-747.
30. Bennett, W. L., Keeton, A. B., Ji, S., Xu, J., and Messina, J. L. (2007) Insulin regulation of growth hormone receptor gene expression: involvement of both the PI-3 kinase and MEK/ERK signaling pathways, *Endocrine 32*, 219-226.
31. Leung, K. C., Doyle, N., Ballesteros, M., Waters, M. J., and Ho, K. K. (2000) Insulin regulation of human hepatic growth hormone receptors: divergent effects on biosynthesis and surface translocation, *J Clin Endocrinol Metab 85*, 4712-4720.
32. Menon, R. K., Stephan, D. A., Rao, R. H., Shen-Orr, Z., Downs, L. S., Jr., Roberts, C. T., Jr., LeRoith, D., and Sperling, M. A. (1994) Tissue-specific regulation of the growth hormone receptor gene in streptozocin-induced diabetes in the rat, *J Endocrinol 142*, 453-462.
33. Ji, S., Guan, R., Frank, S. J., and Messina, J. L. (1999) Insulin inhibits growth hormone signaling via the growth hormone receptor/JAK2/STAT5B pathway, *J Biol Chem 274*, 13434-13442.
34. Xu, J., Keeton, A. B., Franklin, J. L., Li, X., Venable, D. Y., Frank, S. J., and Messina, J. L. (2006) Insulin enhances growth hormone induction of the MEK/ERK signaling pathway, *J Biol Chem 281*, 982-992.
35. Wang, P., Li, N., Li, J. S., and Li, W. Q. (2002) The role of endotoxin, TNF-alpha, and IL-6 in inducing the state of growth hormone insensitivity, *World J Gastroenterol 8*, 531-536.
36. Beauloye, V., Ketelslegers, J. M., Moreau, B., and Thissen, J. P. (1999) Dexamethasone inhibits both growth hormone (GH)-induction of insulin-like growth factor-I (IGF-I) mRNA and GH receptor (GHR) mRNA levels in rat primary cultured hepatocytes, *Growth Horm IGF Res 9*, 205-211.
37. King, A. P., and Carter-Su, C. (1995) Dexamethasone-induced antagonism of growth hormone (GH) action by down-regulation of GH binding in 3T3-F442A fibroblasts, *Endocrinology 136*, 4796-4803.

38. Jux, C., Leiber, K., Hugel, U., Blum, W., Ohlsson, C., Klaus, G., and Mehls, O. (1998) Dexamethasone impairs growth hormone (GH)-stimulated growth by suppression of local insulin-like growth factor (IGF)-I production and expression of GH- and IGF-I-receptor in cultured rat chondrocytes, *Endocrinology 139*, 3296-3305.
39. Pinna, L. A. (1990) Casein kinase 2: an 'eminence grise' in cellular regulation?, *Biochim Biophys Acta 1054*, 267-284.
40. Szyszka, R., Grankowski, N., Felczak, K., and Shugar, D. (1995) Halogenated benzimidazoles and benzotriazoles as selective inhibitors of protein kinases CK I and CK II from Saccharomyces cerevisiae and other sources, *Biochem Biophys Res Commun 208*, 418-424.
41. Meggio, F., and Pinna, L. A. (2003) One-thousand-and-one substrates of protein kinase CK2?, *FASEB J 17*, 349-368.
42. Litchfield, D. W. (2003) Protein kinase CK2: structure, regulation and role in cellular decisions of life and death, *Biochem J 369*, 1-15.
43. Montenarh, M. (2010) Cellular regulators of protein kinase CK2, *Cell Tissue Res 342*, 139-146.
44. Sommercorn, J., Mulligan, J. A., Lozeman, F. J., and Krebs, E. G. (1987) Activation of casein kinase II in response to insulin and to epidermal growth factor, *Proc Natl Acad Sci U S A 84*, 8834-8838.
45. Klarlund, J. K., and Czech, M. P. (1988) Insulin-like growth factor I and insulin rapidly increase casein kinase II activity in BALB/c 3T3 fibroblasts, *J Biol Chem 263*, 15872-15875.
46. Van Lint, J., Agostinis, P., Vandevoorde, V., Haegeman, G., Fiers, W., Merlevede, W., and Vandenheede, J. R. (1992) Tumor necrosis factor stimulates multiple serine/threonine protein kinases in Swiss 3T3 and L929 cells. Implication of casein kinase-2 and extracellular signal-regulated kinases in the tumor necrosis factor signal transduction pathway, *J Biol Chem 267*, 25916-25921.
47. Ji, H., Wang, J., Nika, H., Hawke, D., Keezer, S., Ge, Q., Fang, B., Fang, X., Fang, D., Litchfield, D. W., Aldape, K., and Lu, Z. (2009) EGF-induced ERK activation promotes CK2-mediated disassociation of alpha-Catenin from beta-Catenin and transactivation of beta-Catenin, *Mol Cell 36*, 547-559.

Supplementary data

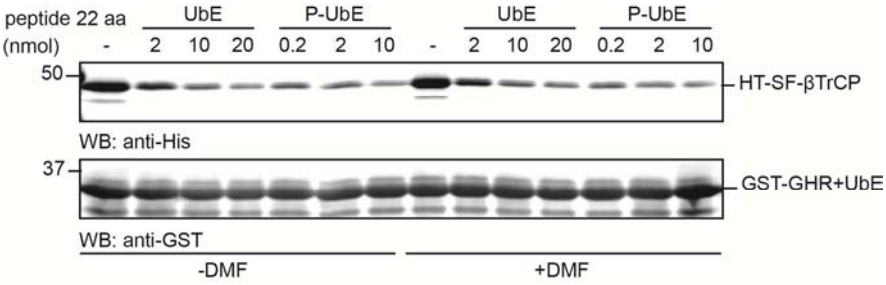

Supplementary Fig. 1. DMF does not affect the binding affinity of the UbE peptides to βTrCP.
Glutathione beads were saturated with GST-GHR 270-334 tails containing the UbE motif (GST-GHR+UbE), followed by binding to purified βTrCP/Skp1complex (His-SF-βTrCP/His-Skp1ΔΔ). UbE and P-UbE peptides, dissolved in a buffer containing (+) or not (-) 9% Dimethylformamide **(**DMF), were added in increasing amounts (0.2, 1, 2, 10, 20 nmol) to compete for βTrCP binding. The samples were analyzed by western blotting with anti-His and anti-GST antibodies. These data are representative of two independent experiments.

A high-throughput small molecule screen targeted to the growth hormone receptor – βTrCP interaction

5

Ana C. da Silva Almeida[1,2], Daphne Lelieveld[1], Peter van Kerkhof[1], Henk Viëtor[2], Peter Maas[3], Adri Slob[4], Jan A. Mol[4], Ger J Strous[1], Agnes G S H van Rossum[1,2]

[1] Department of Cell Biology and Institute of Biomembranes, University Medical Center Utrecht, Heidelberglaan 100, 3584 CX Utrecht, The Netherlands

[2] Drug Discovery Factory BV, Albrechtlaan 14A, 1404 AK Bussum, The Netherlands

[3]Compound Handling B.V. (Specs), Kluyverweg 6, 2629 HT, Delft, The Netherlands.

[4]Department of Clinical Sciences of Companion Animals, Faculty of Veterinary Medicine, Utrecht University, Yalelaan 198, Utrecht, The Netherlands

(Manuscript in preparation)

Abstract

Cachexia is a syndrome characterized by extensive body weight loss and metabolic abnormalities. There are reports of growth hormone (GH) resistance in cachexia patients, probably due to a decreased level of GH receptors (GHRs).In this study we show for the first time that in tumor-bearing mice suffering from cachexia the GHR mRNA expression in the liver is 2.5 times lower and GHR protein level 9 times lower than in control mice, indicating that cachexia is associated with decreased GHR levels. In this study we aim to discover small drugs, which improve the GH sensitivity of cells by reducing GHR degradation, and consequently increase the number of GHRs. GHR interacts via its UbE motif with βTrCP (the substrate recognizing factor of the E3 ligase SCF(βTrCP)). This interaction is essential for GHR endocytosis and degradation. The UbE motif (DDSWVEFIELDIDD) differs from the canonical motif (DSGxxS) in other βTrCP substrates and is, therefore, a specific target for drug discovery. We developed a high throughput screening assay based on the molecular interaction between GHR and βTrCP. From a 40,000-compound library 26 compounds were identified that specifically inhibited the interaction between βTrCP and the GHR-UbE motif. Six compounds blocked GHR endocytosis. From the four most potent hits 352 analogous compounds were selected and tested in the same high throughput screening and cell based assays. Three most prominent compounds were tested in mice. One compound showed accumulation of GHR levels in mouse liver lysates and increased GH signaling. In conclusion, we developed a robust screenings route that includes a simple molecular-based high throughput screening, several cell based assays and a mouse model to find potential lead compounds for future therapeutic use in cachexia.

Introduction

Loss of lean body mass and muscle wasting (cachexia) are common features of many disease states including congestive heart failure (CHF), chronic renal failure, eating disorders, renal tubular defects, diabetes, uremia, burn injuries, sepsis, AIDS and cancer. Cachexia is a complicated syndrome, regulated by different, mostly pro-inflammatory, mediators like cytokines, catabolic hormones and prostaglandins that are synthesized in response to disease, infection or malignant tumors (1-3). Cancer cachexia implies marked muscle wasting and atrophy associated with tumor load (4, 5). This condition lowers responsiveness to treatment, contributing to an unfavorable prognosis and poor quality of life. Several mediators of muscle wasting have been identified including immune and tumor-derived cytokines such as tumor necrosis factor (TNFα), interleukin (IL)1, IFNγ and IL6 (6). Most of these pathways mediate their effects by reducing the rate of protein synthesis at the level of protein translation or RNA content and by stimulating protein catabolism through the activation of the ubiquitin-proteasome pathway accompanied by induction of the ubiquitin E3 atrophy markers, muscle RING finger- 1 (MURF1 or TRI63) and muscle atrophy F-Box (known as MAFbx, atrogin-1; official symbol FBX32) (7). The heterogeneity of these factors and their potentially synergistic mode of action have rendered their study a real challenge with little clinical benefit until now: effective treatment of the cachectic syndrome is still lacking.

Acquired growth hormone (GH) resistance, characterized by elevated concentrations of GH and decreased concentrations of GH binding protein and IGF-I, is a feature of severe illness, in particular in cachexia patients (8, 9). The underlying causes and mechanisms are elusive. The reduction in circulating IGF-1, characteristic of GH resistance conditions, is probably due to diminished production in the liver. Since GH, which normally stimulates IGF-1 production, is present in excess, mechanisms related to the GHR or GH signaling are most likely the cause of low IGF-1 levels in blood circulation. It is impossible to study the GHR levels in livers of patients in catabolic states directly. The GH binding protein (GHBP) levels in circulation have been used as an indication of GHR levels in cells. Patients with GH resistance have a reduced GHBP level compared to controls (10-12), suggesting decreased GHR levels as the cause of cachexia.

GH regulates somatic growth, cellular metabolism and body composition. Responses to GH are mediated by the GH receptor (GHR). GHR signaling via JAK2 kinase involves the role of at least three major pathways, STATs, MAPK, and PI3-kinase/AKT (13). GHR signaling results in expression of genes involved in anabolic processes including increased protein synthesis, lipid degradation, immune function, muscle mass, bone turnover, and tooth development (14). The expression of GHR at the cell surface can be regulated by modifying receptor synthesis, shedding, or endocytosis (15). Previously, we have shown that the SCF(βTrCP) E3 ligase complex drives endocytosis and degradation of the GHRs (16). βTrCP is the substrate recognition subunit of the SCF complex that via its WD40 domain binds to a DSGxxS motif in proteins such as β-catenin, IκB, IFNAR1 and prolactin receptor in which the serines are phosphorylated (17). We have shown that βTrCP binds unconventionally to the UbE motif (DDSWVEFIELDIDD) of GHR (*da Silva Almeida, manuscript in preparation*). This interaction is essential for GHR endocytosis and degradation because mutations in the UbE motif cause a dramatic drop in endocytosis and lysosomal degradation, rendering the cells GH-sensitive (18).

In this study, we report a decrease in mRNA and protein levels of GHR in livers of tumor-bearing mice suffering from weight loss. Our aim is to use the unique GHR-βTrCP interaction as a target to discover drugs that increase GHRs at the surface of cells, and consequently improve their GH sensitivity. The approach is to reduce the endocytosis of the GHR by drugs that specifically interfere with the interaction of the GHR-UbE motif with the βTrCP-WD40 domain. Small molecules, selectively inhibiting the GHR-βTrCP interaction, are currently lacking. We developed a novel molecular based high-throughput screen (HTS) in 96-well plate format in which fluorescently labeled recombinant βTrCP is allowed to bind GST-tagged GHR-UbE peptide in the presences of compounds. Using this assay we have screened 39.684 small

molecules and identified 26 (0.066%) compounds that consistently decreased the GHR-βTrCP interaction more than 50% compared to DMSO control. From these compounds, six blocked the GHR endocytosis in U2OS cells. From the four most potent hit compounds, 352 analogues compounds were selected and tested in both the HTS and in cell based assays. Combining chemical clustering analyses with results of the cell based assays; we identified potential lead compounds for development into potential therapeutics against cachexia. We selected three most prominent lead compounds and tested them in mice. One compound increased GHR levels in mouse liver.

Materials and methods

Mice and tissue preparation.

Animal care and experiments were performed in accordance with legislation on animal experiments as determined by the Dutch Veterinary Inspection. For cachexia experiments, seven weeks old CD2F1 (Balb/c x DBA/2) male mice, purchased from Harlan (Horst, The Netherlands), were subcutaneously injected with $5x10^5$ colon C26 cells in 0.1 x PBS or with PBS alone for the control mice. Every day, mice were weighted and tumor size was measured to monitor weight loss. After 20 days, mice were sacrificed by anesthesia with isofluraan, and livers and tumors were taken out, weighted and snap frozen in liquid nitrogen and stored at -80°C for further analysis. Carcass weight was calculated as mouse weight minus tumor.

For compound experiments, seven weeks old C57BL/6J female mice, purchased from Harlan (Horst, The Netherlands), were intraperitoneally injected with 5 mg/kg compound in 5% cremophor EL solution diluted in PBS or with 5% cremophor/PBS as a control. Some mice were additionally intraperitoneally injected with 1.5 mg/kg human GH in PBS (0.1 M NaPi, pH 8.0, 150 mM NaCl) or PBS as a control. After treatment with compound only or compound followed by 15 minutes GH stimulation, mice were sacrificed by cervical dislocation and liver and muscle tissue were snap frozen in liquid nitrogen and stored at -80°C for further analysis.

Real time PCR

From liver biopsies of 5 control mice and 5 tumor bearing mice 25 mg liver was used for RNA isolation using the RNeasy mini kit (Qiagen) according to the manufacturer's instructions. Synthesis of cDNA was performed with 200 ng total RNA using the iScript cDNA Synthesis Kit (Biorad), according to the manufacturer's instructions. Real-time PCR based on the high-affinity double stranded DNA-binding dye SYBR green I was performed in triplicate in a spectrofluorimetric thermal cycler (iCycler; BioRad, Hercules, CA, USA). Data were collected and analyzed with the provided application software. β-actin, glyceraldehydephosphate dehydrogenase (GADPH), hypoxanthine-guanine phosphoribosyltransferase (HPRT), beta-2-microglobulin (B2M), and ribosomal protein S19 (RPS19) were housekeeping genes used as endogenous references. For each real-time reaction, 10ng cDNA was used in a reaction volume of 24µl containing 1× iQ SYBR Green Supermix (BioRad), 20 pmol forward primer, and 20 pmol reverse primer. Primer pairs previously validated in literature were used (Table 1).The PCR conditions were the following: 3 min at 95°C followed by 40 cycles of 10 s at 95°C, 30 s at the primer specific annealing temperature (Table 1), and 30s at 72°C. Melt curves (iCycler) and agarose gel electrophoresis were used to examine each sample for purity and standard sequencing procedures (ABI PRISM 310 Genetic Analyzer; Applied Biosystems, Foster City, CA, USA) were used to verify the analytical specificity of the PCR products. The individual melting curves proved that a single, unique product was amplified. For each experimental sample, the amount of target (GHR1, GHR2, and GHR3), with β-actin, GAPDH, HPRT, B2M and RPS19 as endogenous references, was determined from the appropriate standard curve. Data were analyzed using REST-XL (pair wise fixed reallocation and randomization test) software (19) estimating a relative normalized fold change in gene expression between the groups.

Table 1: Primer pairs used in the PCR amplification of cDNA generated from total mRNA in the various liver biopsies

Gene	Primer (5'-3')	Exon	Amplicon length (bp)	Annealing temperatures (°C)
GHR1	F: GATTTTACCCCCAGTCCCAGTTC R: GACCCTTCAGTCTTCTCATCCACA	9 10	198	60
GHR2	F: GGTGAGATCCAGACAACGGA R:TCACCTCCTCCAACTTCCCT	8 11	284	60
GHR3	F: ACAGTGCCTACTTTTGTGAGTC R: GTAGTGGTAAGGCTTTCTGTGG	11 11	133	62
HPRT	F: GCTGGTGAAAAGGACCTC R: CACAGGACTAGAACACCTGC	7 9	248	60
GADPH	F: GGTGAAGGTCGGTGTGAACG R: CTCGCTCCTGGAAGATGGTG	2 3	233	60
βActin	F: TGCGTGACATCAAAGAGAAG R: GATGCCACAGGATTCCATAC	4 5	197	60
B2M	F: TTCTGGTGCTTGTCTCACTGA R: CAGTATGTTCGGCTTCCCATTC	1 2	104	64
RPS19	F: CAGCAGGAGTTCGTCAGAGC R: CACCCATTCGGGGACTTTCA	2 3	172	56

Compound library and robotics

The compound library was provided by SPECS B.V. (Delft, The Netherlands). This library is composed of ~ 40.000 small molecular compounds stored in dimethyl sulfoxide (DMSO) at 10 mM per compound in 96-well plates at −20°C. Before use, all compound plates were equilibrated to room temperature and each compounds plate was diluted in a well-to-well manner to a user stock of 2 mM compound in DMSO, 80 compounds per plate. The dilution plates were stored at −20°C and equilibrated to room temperature before use in the HTS. Compounds dilutions and transfer handlings during the HTS were all operated by Biomek®FX Laboratory Automated Microplate Pipetting Worksystems (Beckman Coulter, Inc.) at room temperature. A multi-channel pod, which is based on air displacement technology was used to accurately and precisely aspirate and dispense very small volumes of solvent simultaneously to 96-positions. Reagents were transferred using Beckman Coulter AP250 pipet tips (#717251) with a volume range of 1–220 µl. All solutions were aqueous except the compounds which were dissolved in DMSO.

HTS assay

GST-tagged GHR-UbE peptides (GST-GHR(271-334), production procedure see below) were coated to Nunc 96-wells plates (#439454) in wells 1-88 and GST-tagged GHR peptide without UbE motif (GST-GHR(271-318)) in wells 89-96 in 20 mM Tris-HCl, pH 8.0 overnight at 4°C. The wells were saturated with GST-GHR-UbE peptide and retained approximately 2 ng, which was obtained by adding 100 µl of a solution of 0.8 µg/ul per well. Next, nonspecific sites were blocked with 100 µl of blocking solution (20 mM Tris-HCl, pH 8.0 supplemented with 0.2% BSA) for 30 minutes at 4°C. The wells were washed 3 times with TBS-T buffer (50 mM Tris-HCl, pH 8.0, 138 mM NaCl, 0.05% Tween-20) to remove the excess of unbound GST-GHR peptides. Then, 50 µl of 0.1% BSA in TBS-T buffer is added to the wells followed by 2 µl of compounds from dilution plates (2 mM stock), and 50 µl of 0.1% BSA in TBS-T buffer containing 100 ng Dylight800 labeled His-tagged βTrCP2/Skp1ΔΔ complex (1 µg/ml). The final concentration was 40 µM compound and 2% DMSO. The plates were incubated at 4°C for 1.5 hours. Next, the wells were washed 4 times with TBS-T and once with Milli Q water to remove the excess of unbound Dylight800 labeled βTrCP2/Skp1ΔΔ complex. Plates were dried in the vacuum dryer for 20 minutes. Plates were scanned by an Odyssey Imaging System (Li-Cor Biosciences). Compounds that decreased the control value more than 50% (threshold) were scored as effective in the initial singlicate

screen. Those hits were collected from the original library stock and grouped in new stock plates, re-screened at 40 µM in duplicate, and in singlicate at 20 µM and 10 µM concentrations. From the best 4 hits, 352 analogues compounds were selected and screened at 40 µM in duplicate and in singlicate at 20 µM and 10 µM concentrations.

HTS assay evaluation and validation

For the validation of the assay, each 96-wells plate contained two columns with 8 control wells, 8 of DMSO on GST-GHR(271-334) with UbE peptide ($Mean_S$) and 8 on GST-GHR(271-318) without UbE peptide ($Mean_B$). All control wells were treated with 2% DMSO and used to calculate Z'-value for each plate and to normalize the data per plate. All data were analyzed for the determination of Z'-value, S/B (signal-to-background) ratio and percent inhibition for each assayed compounds (20). Results were expressed as percent inhibition compared to DMSO control, where 0% inhibition is [$Mean_S$-$Mean_B$] and 100% inhibition is [$Mean_B$-$Mean_B$]. Hits were defined as values lower than 50% fluorescent signal of [$Mean_S$- $Mean_B$]. Statistical calculations of Z'-values were made as follows: $Z' = 1–((3xStdDev_S+ 3xStdDev_B)/|Mean_S – Mean_B|)$. Here $Mean_S$ is the mean fluorescent signals of the DMSO controls on GST-GHR(271-334) with UbE peptide, $StdDev_S$ is the standard deviation of the DMSO controls on GST-GHR(271-334) peptide, $Mean_B$ is the mean fluorescent signals of the DMSO controls on GST-GHR(271-318) peptide without UbE motif, and $StdDev_B$ is the standard deviation of the DMSO controls on GST-GHR(271-318) peptide without UbE motif. $S/B = Mean_S/Mean_B$. For DMSO 96-well control plates the Z'-values was 0.7 and the S/B was 15. The assay variability was measured throughout the screenings and the Z'-values varied from 0.3 till 0.7 and the S/B varied from 6 till 16.

Production of GST-GHR fusion proteins

pGEX-GHR plasmids were used to express GST-GHR(271-334) and GST-GHR(271-318) fusion proteins in Escherichia coli (strain BL21) (21). The synthesis of recombinant proteins was induced by 0.5 mM isopropyl β-D-1-thiogalactopyranoside (IPTG). GST fusion proteins were purified with GSH-Sepharose beads (Amersham Pharmacia Biotech, Roosendaal, The Netherlands) by the procedure recommended by the manufacturer. Purified protein was aliquoted, freeze dried and stored at -20°C until further use.

Expression, purification and labeling of βTrCP2/Skp1ΔΔ complex

βTrCP2 cDNA N-terminally fused with a flag tag cloned in pcDNA3 was a generous gift from Tomoki Chiba, Tokyo Metropolitan Institute of Medical Science, Tokyo, Japan. A short part of βTrCP2 (114-542, including Skp1 binding domain, but excluding dimerization domain) was cloned into pFastBac-HT-B Baculoviral vector with a HIS-tag (Invitrogen, Groningen, The Netherlands). Skp1ΔΔ, lacking unstructured loops of amino acids 38-43 and 71-82 in the pAcSG2 vector, was a generous gift from Brenda Shulman, St. Jude Children's Research Hospital, Memphis, USA. Skp1ΔΔ was cloned into pFastBac-HT-B (with HIS tag). The primers were purchased from Sigma-Genosys. The generation of the baculovirus for HIS-βTrCP2 (114-542) and HIS-SKP1ΔΔ was performed according to the manufacturers of the Bac-to-Bac® Baculovirus expression system (Invitrogen, Groningen, The Netherlands). For expression of high amounts of functional HIS-βTrCP2 (114-542) protein, co-expression with HIS-Skp1ΔΔ in a virus ratio 4:1 was needed to stabilize the βTrCP2 protein. Infected SF9 cells were lysed in 50 mM NaH_2PO_4, pH 8, 200 mM NaCl, 5 mM β-mercaptoethanol, 5% glycerol, 20 mM imidazole, 1 mM PMSF, 10 µg/ml leupeptine, 10 µg/ml aprotinine. After sonication, the cells were centrifugated for 60 minutes at 30,000 rpm at 4^0C. For purification, the lysates were loaded on a HIS-trap column connected to an Äkta Explorer high-performance liquid chromatography (HPLC) (GE Healthcare, Hoevelaken, The Netherlands), followed by a gel filtration column (for more details see materials and methods of *da Silva Almeida AC (manuscript in preparation*). The activity of the HIS-βTrCP2 (114-542) - HIS-Skp1ΔΔ complex was determined by showing specific binding to GST-GHR(271-334) and not to GST-GHR(271-318) fusion proteins. The purified and concentrated βTrCP2 (114-542) - HIS-Skp1ΔΔ complex was labeled with a DyLight800 labeling kit form Thermo scientific (# 46422, Breda, The Netherlands)

according to the manufacturer's instructions. After confirming the specific activity of the labeled complex by binding experiments to GST-GHR(271-334), the fluorescent HIS-βTrCP2(114-542)- HIS-Skp1ΔΔ protein complex was aliquoted and frozen with liquid nitrogen and stored in the -80°C until further use for the HTP screen.

Antibodies and materials

Anti-GHR(anti-B6) antibody was raised against amino acids 327–493 of the cytosolic tail of the rabbit GHR (22). Rabbit polyclonal against STAT5b (C17) was from Santa Cruz Biotechnologies Inc (Santa Cruz, CA, USA) and monoclonal antibody against phosphorylated MAPK (M9692) was from Sigma, (Saint Louis, Missouri, USA). Monoclonal against actin (C4) was from MP Biomedicals, and monoclonal antibody against the extracellular domain of the GHR (Mab5) was purchased from AGEN (Acacia Ridge, Australia). Goat anti-mouse IgG Alexa 680 from Molecular Probes, and goat anti-rabbit IgG IRDye800 from Rockland Immunochemicals Inc. (Gilbertsville, PA, USA). Streptavidin beads were purchased from Pierce (Rockford, IL, USA). Human GH was a kind gift of Eli Lilly Research Labs (Indianapolis, IN, U.S.A.). Biotinylated GH (biotin-GH) was made according to the manufacturer's instructions from Pierce (Rockland, IL, USA). MG132 (carbobenzoxy-L-leucyl-L-Leucyl-L-Leucinal) was from Calbiochem (San Diego, CA, USA) and GM6001 (N-[(2R)-2-(hydroxamidocarbonylmethyl)-4-methylpentanoyl]-L-tryptophan methylamide) was from Calbiochem (Darmstadt, Germany).

Cell culture

Culture media, foetal calf serum and antibiotics for tissue culture were purchased from Gibco (Invitrogen, Groningen, The Netherlands). U2OS cells stably expressing the wild type rabbit GHR (U2OS-wtGHR) were grown in Dulbecco's modified Eagle's medium (DMEM #41966,) supplemented with 10% fetal calf serum, 100 units/ml penicillin, 0.1 mg/ml streptomycin. Mouse 3T3-F442A preadipocytes expressing endogenous GHR, were grown in DMEM supplemented with 5% FCS and pen/strep. Human embryonic kidney 293 (HEK293) cells, stably expressing the Tet-repressor (HEK293-TR), a gift from Dr. Madelon Maurice, University Medical Center Utrecht, Utrecht, The Netherlands,, were grown in DMEM supplemented with 10% FCS and Pen/Strep, and 12 µg/ml Blasticidin-S (MP Biomedicals). HEK293-TR cells stably expressing the wild type rabbit GHR (HEK-wtGHR) were grown in the same medium as HEK293-TR cells but supplemented with 600 µg/ml Geneticin (G418). All cells used were grown at 37°C with 5% CO_2. Twice a week, cells were washed with phosphate-buffered saline (PBS), detached from the flask with trypsin-EDTA, diluted in fresh growth medium, and split into new culture flasks.

Confocal Microscopy

Cy3-GH was prepared using a Fluorolink-Cy3 label kit according to the supplier's instructions (Amersham Biosciences, Roosendaal, The Netherlands). U2OS cells stably expressing the wild type rabbit GHR (U2OS-wtGHR) were grown in 24-wells plates on glass coverslips until 70% confluence. Then medium was replaced with medium containing either 20 µM compound or DMSO or MG132/GM6001 for 3 or 18 hours in DMEM without FCS. Then, the cells were incubated for 30 minutes at 37°C with Cy3-GH (540 ng/ml) and Alexa488-labeled transferrin (1.6 µg/ml) (Molecular Probes). Cells were washed with PBS to remove unbound label and fixed for 30 minutes at room temperature in 3% paraformaldehyde in PBS, pH 7.4. After fixation, coverslips were embedded in Mowiol, and confocal laser-scanning microscopy was performed using a Leica TCS 4D system.

Cell lysis and biotin-GH pull down

HEK293-TR-wtGHR and 3T3-F442A cells were stimulated respectively for 5 minutes with 180 ng/ml GH or 3 minutes with 10 ng/ml GH. Medium was aspirated and the cells were lysed 15 minutes on ice in 100 µl cold lysis buffer (1% Triton X-100, 1 mM EDTA, 1mM PMSF, 10 µg/ml aprotinin, 10 µg/ml leupeptin, 1 mM Na_3VO_4 and 5 mM NaF in PBS). The cells were scraped and cell lysates were centrifuged for 10 minutes at 16.000xg at 4°C to pellet the nuclei. Post-nuclear supernatants were mixed

with Laemmli sample buffer containing dithiothreitol and boiled for 5 minutes. Lysates were subjected to reducing 7.5% SDS-PAGE.

Pieces of snap frozen mouse livers were dounced on ice in 1.5 ml RIPA buffer (20 mM Tris-HCl pH 7.4, 150 mM NaCL, 0.5% NP-40, 2 mM EDTA, 1 mM PMSF, 10 µg/ml aprotinin, 10 µg/ml leupeptin, 1 mM Na_3VO_4, 5 mM NaF and 1 tablet of complete protease inhibitors (Roche, Mannheim, Germany) and allowed to spin end-over-end for 45 minutes at 4°C. Small differences in lysis times between samples resulted in some variations in the amount of pulled GHR. In the interpretation of the results (particularly in Fig.8) this aspect was taken into consideration. After 10 minutes centrifugation at 16000xg speed at 4°C, the protein concentration in the supernatant was determined by the BCA™ protein assay kit (Pierce, Rockford, IL, USA). For one pull down, 2 mg of protein lysate were used in 2 ml RIPA buffer and supplemented with 3 µg biotin-GH, and allowed to bind GHR for 100 minutes. Then, 50 µl streptavidin beads were added for 45 minutes. The pull downs were washed twice with the same RIPA buffer and twice with 10-fold diluted PBS. Beads were mixed with Laemmli sample buffer containing dithiothreitol and boiled for 5 minutes, and the biotin-GH-GHR complexes were subjected to 7.5% SDS-PAGE.

Immunoblotting

After SDS-PAGE, proteins were transferred to an Immobilon-FL PVDF membrane (Millipore, Amsterdam Zuid-Oost, The Netherlands). The membranes were blocked with Odyssey buffer (Li-Cor Biosciences, Lincoln, NE, USA) diluted 1:1 with PBS for 2 hours at room temperature. Specific detection was performed by probing the membranes with the indicated primary antibodies for 1.5 hours at RT or overnight at 4°C and secondary antibodies for 1 hour at RT in Odyssey buffer diluted 1:1 in PBS supplemented with 0.1% Tween-20. Membranes were washed in Tris-buffered saline with Tween-20 (TBST; 50 mM Tris pH 7.5, 150 mM NaCl, 0.05% Tween-20). Detection was performed with an Odyssey infrared imaging sysem (Li-Cor Biosciences).

Luciferase assays

HEK293T cells were seeded at a density of 1.5×10^5 cells/well in 24-wells plates in RPMI-1640 (#52400), Invitrogen) supplemented with 10% fetal calf serum, 100 units/ml penicillin, and 0.1 mg/ml streptomycin. Transfections were performed using FuGENE6 reagent and (Roche, Mannheim, Germany) according to the manufacturer's instructions. The next day, 40% confluent wells were co-transfected with 215 ng pcDNA3 empty vector combined with 5 ng pTK Renilla vector (internal standard) + 30 ng TOP (Tcf Optimal operator) or FOP (Far from Optimal mutated operator) vector of vectors. Per condition, TOP and FOP were taken in duplicates. After 36 hs the transfection medium was replaced by RPMI medium containing 20 µM compound, or DMSO. The positive control, Wnt3a conditioned medium, was diluted 1:1 in RPMI medium. The luciferase assay was performed after 20 h compound incubation. Medium was aspirated and cells were lysed in 100 µl of Passive Lysis Buffer (PLB) from DUAL luciferase Reporter Assay (Promega Benelux. Leiden, The Netherlands) for 20 minutes at room temperature. 20 µl of each lysate was measured in a Lumat LB9507 luminometer with a dual injector (Berthold technologies) programmed for this assay (background injection 1 (50 µl), 2 s delay, 10 s measurement, injection 2 (50 µl), 2 s delay, 10 s measurement). The Luciferase reporter gene activity was normalized to the Renilla Luciferase activity. The values represent the mean ±SD of a duplicate transfection. The data shown are representative of two independent experiments.

Results

1. Tumor-bearing mice suffering from cachexia have decreased levels of GHR

To investigate whether decreased GHR levels in the liver correlate with the development of cachexia, GHR levels in livers from control and tumor-bearing mice were compared. Cachexia is induced in cancer by chronic presence of catabolic factors, like inflammatory cytokines and corticosteroids. An established mouse tumor model for cancer cachexia was used in which colon C26 adenocarcinoma cells were subcutaneously injected (23-25). After 20 days, mice were sacrificed and livers were snap-frozen. Detectable amounts of endogenous mouse mature GHR could be isolated with biotin-GH from liver lysates (Fig. 1A, control mice 1 to 5). Tumor-bearing mice, suffering from cachexia, as examined by decreased carcass weight, showed 9 times less GHR compared to control mice (Fig. 1A, mice 6 to 9, quantified in 1B). Mouse 10, although having a tumor of similar size as the other mice, did not show decreased carcass weight at the time of sacrifice. No decrease in GHR levels was seen in the liver of this mouse (Fig 1A, quantified in 1B). In summary, the level of GHR in liver lysates decreases 9-fold in mice suffering from cancer-induced cachexia, but not in a mouse bearing a tumor with no weight-loss. Therefore, the level of GHR seems to correlate with the development of cachexia.

To investigate whether the decreased GHR protein levels were caused by decreased GHR mRNA levels, real-time (RT) PCR analysis on liver biopsies was performed. Three different sets of primers were used for mouse GHR amplification (GHR 1, 2 and 3), and five housekeeping genes were used as standard controls (HPRT, GAPDH, β-actin, β-2-microglobulin, RPS19). The GHR mRNA levels in the tumor-bearing mice (mice 6 to 9) were 2.5-fold lower compared to control mice (mice 1 to 5), which were set at 1, for all three GHR primer sets (Table 2). In mouse 10, bearing a tumor with no sign of cachexia, the GHR mRNA levels did not significantly differ from control mice (data not shown). Taken together, these results show that both mRNA and protein GHR levels, are significantly down-regulated in cancer induced cachexia, but not in a tumor-bearing mice not suffering from cachexia. These results indicate that GHR levels are down-regulated in cachexia.

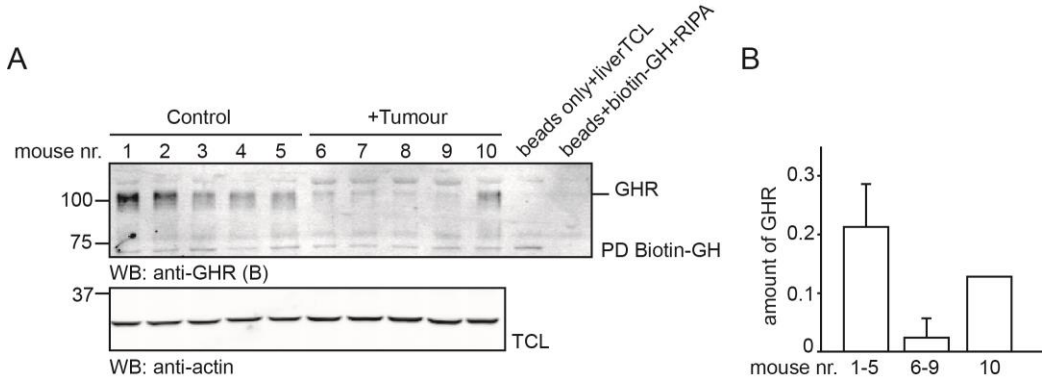

Fig. 1: Tumor- bearing mice suffering from cachexia have decreased levels of GHR

(A) Liver biopsies from five wild type CD2F1 (Balb/c x DBA/2) male mice (1-5) and from five tumor-bearing mice (6-10) were lysed and biotin-GH pull downs (PD biotin-GH) were performed. The samples were analyzed by western blotting with anti-GHR (B) antibody. The total cell lysates were analyzed with anti-actin antibody, to confirm that the same amount of lysates was used for each pull down. Note that mice 6-9 suffered from weight loss while mouse 10 did not. **(B)** The amount of GHR was quantified, corrected for actin and represented in the graph. PD, pull down; TCL, total cell lysates.

Table 2

Nomalized target values of GHR gene expression determined by real-time polymerase chain reaction (PCR) in liver biopsies

	Tumours(*)		
	GHR1	GHR2	GHR3
Mean factor	0.355	0.409	0.457
Range (S.E.)	0.213-0.587	0.318-0.549	0.361-0.576
p	0.006	0.007	0.006

(*) Mice without tumours were used as controls
Data from mouse 10 was not included in the analysis

Table 2: Normalized target values of GHR gene expression determined by real-time polymerase chain reaction (PCR) in liver biopsies. The same livers used in the GHR PD (Fig. 1) were used for RNA extraction, cDNA amplification and real time PCR analysis, except mouse 10. β-actin, GAPDH, HPRT, β2M and RPS19 were used as endogenous references. The data was normalized with the values obtained for tumor free mice (control mice). The mean factor indicates the fraction of mRNA expression compared to control mice, which is set to 1. Three primers pairs were used for GHR mRNA RT-PCR as indicated with GHR1, GHR2, GHR3.

2. Establishment of HTS to identify inhibitors of GHR-βTrCP2 interaction.

In order to find lead compounds for therapeutic use against cachexia, we developed and validated a molecular based HTS to identify small molecule compounds that can inhibit the GHR-βTrCP interaction. With this novel molecular based HTS assay a compound library of 39.684 compounds was screened in singlicate at 40 µM (Fig. 2A). Fluorescently labeled HIS-tagged short form of βTrCP2 protein (HIS-βTrCP2 (144-542) in complex with HIS-Skp1ΔΔ was allowed to bind to the GST-tagged GHR-UbE peptide (GST-GHR (271-334)) in the presents of DMSO or compounds. The wells were saturated with GST-GHR peptides and retained approximately 2 ng. The half maximal concentration of Dylight800 labeled HIS-βTrCP2/HIS-Skp1ΔΔ complex was determined at 1 µg/ml and used to select for compounds that either decrease or increase the GHR-βTrCP interaction. Hits were defined as the values lower than 50% fluorescent signal, which is the mean of the positive controls (DMSO on GST-GHR (271-334)) minus the mean of the negative controls (DMSO on GST-GHR (271-318)). 911 compounds were identified that decreased the signal (a hit rate of 2.3%). The results of a representative plate carrying one such inhibitory compound is displayed in Fig. 2B. Re-screening of the 911 compounds in duplicate at 40 µM and at two lower concentrations (20 µM and 10 µM) reduced the hit count to 30 compounds (0.075%) that consistently decreased the signal (22 compounds in all 3 concentrations). Four of the 30 compounds appeared false positives because they quenched the fluorescent signal as determined by combining fluorescent βTrCP with the compound in the absence of GST-GHR-UbE peptide (Fig. 2C). None of the compounds were auto-fluorescent. In conclusion, 26 compounds (0.066%) were selected that decreased the GHR-UbE interaction with βTrCP2.

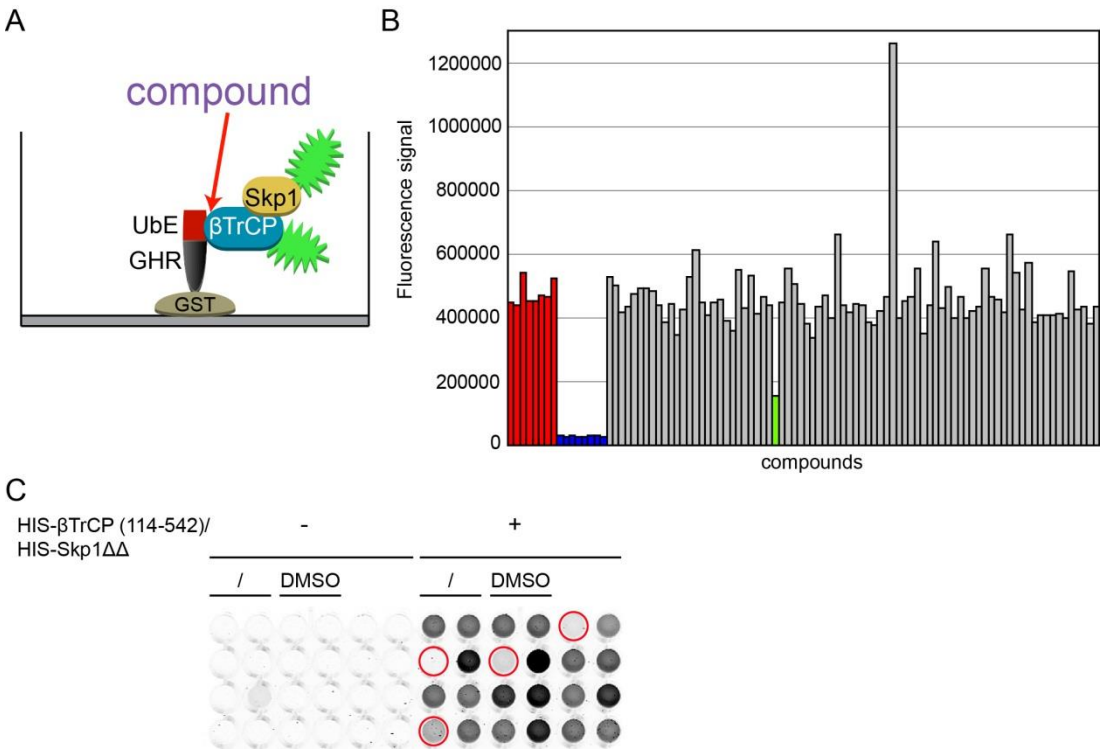

Fig. 2: Schematic representation of the design of the molecular based HTS. (A) GST-tagged GHR-UbE peptide was bound to 96-wells plates and allowed to bind purified fluorescently labeled HIS-βTrCP2(114-542)/HIS-Skp1ΔΔ in the presence of DMSO or compounds. After washing the wells, the fluorescence was measured using an Odyssey imaging system. **(B)** Representative assay result from the HTS. The data illustrate the results from one 96-wells plate. The red bars are an 8-plo of the DMSO controls on GHR with UbE peptide ($Mean_S$) and the blue bars are an 8-plo of DMSO on GHR-peptide without UbE ($Mean_B$). The S/B ratio [$Mean_S/Mean_B$] in this particular experiment is 16 and the Z'-values is 0.74. In this experiment one compound was selected that decreased (green bar) and one compound likely increased the GHR-βTrCP2 interaction. **(C)** Representative experiment to test auto fluorescence of compounds (wells 3-24) and their ability to quench fluorescently labeled HIS-βTrCP(114-542)/HIS-Skp1ΔΔ complex. The fluorescent signal of the compound in TBST/0.1% BSA was measured in the absence (left panel) or presence (right panel) of dylight800 fluorescently labeled HIS-βTrCP(114-542)/HIS-Skp1ΔΔ complex. Four compounds (red circles) quenched the fluorescent signal. DMSO was taken as control.

3. Identification of compounds that inhibit GHR endocytosis in human U2OS cells.

The 26 compounds were tested for their ability to inhibit GHR endocytosis. For this assay, GHR-expressing U2OS cells were used because of their excellent morphology in microscopic screens. Compounds were tested at 2 µM and 20 µM concentrations. After a 3 hours compound treatment, Cy3-labeled GH and Alexa488-transferrin were added for 30 minutes. Compounds that either affected the transferrin endocytosis route, showed precipitates or affected cell morphology were discarded. At 2 µM concentration, none of the compounds inhibited GHR endocytosis. At 20 µM-concentration, 6 compounds inhibited GHR endocytosis (although to a different extent) as seen by an increase of Cy3-GH labeling at the plasma membrane, while transferrin uptake remained intact (Fig. 3): 175D3, 368A5, 472B7, 320C6, 495D5 and 387D9. In conclusion, six compounds inhibited GHR endocytosis in human U2OS cells, while there was no effect on the general clathrin-mediated endocytosis as measured with transferrin.

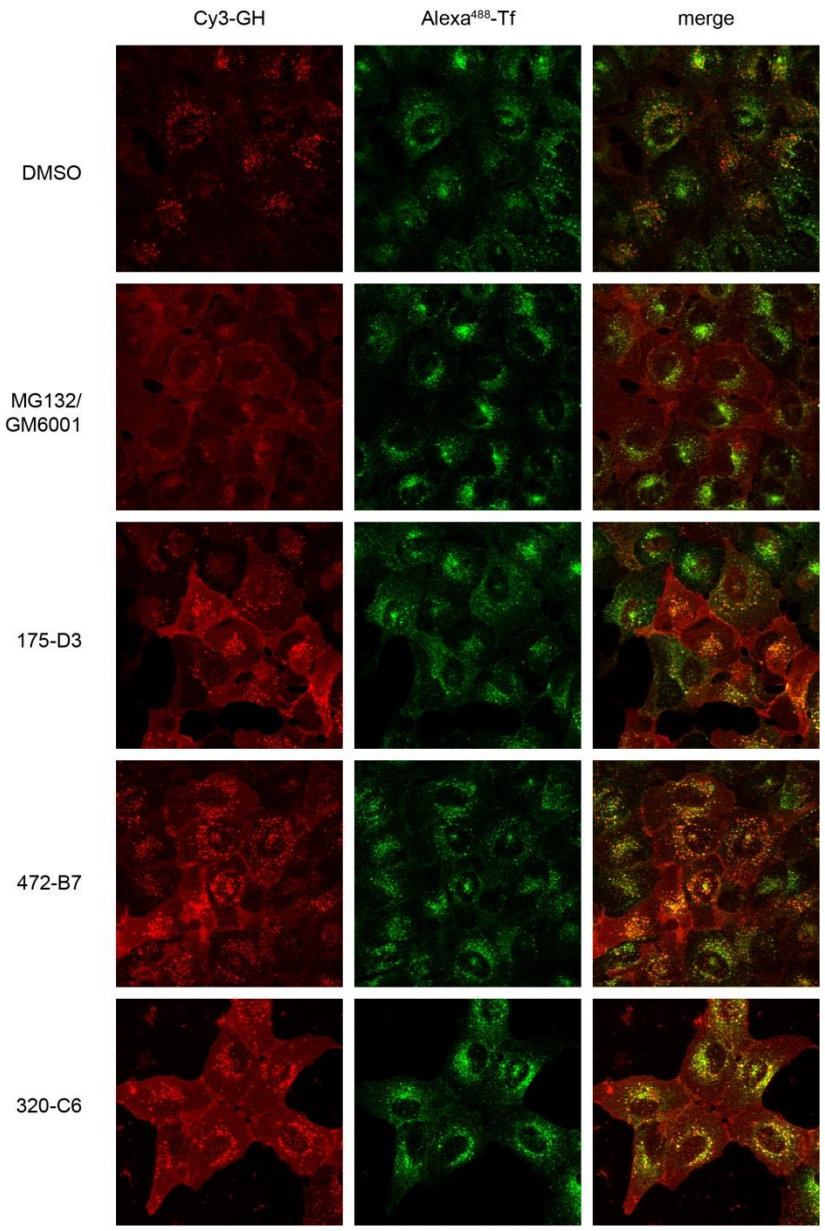

Fig. 3: Identification of small molecule compounds that inhibit GHR endocytosis in human U2OS cells. U2OS cells expressing GHR, treated with 20 µM compound or DMSO as a negative control, were incubated for 30 minutes with Cy3-labeled GH (Cy3-GH) and Alexa488-transferrin (Alexa^{488}-Tf), and fixed in formaldehyde. As a positive control of the phenotype of GHR accumulation at the plasma membrane, 20 µM of inhibitor MG132 together with 20 µM TACE inhibitor GM6001 was used to inhibit proteasomal degradation and GHR shedding activity. Representative pictures were taken. Fluorescence was visualized with a confocal microscope. The results shown are from two out of six compounds that inhibit GHR endocytosis.

4. The compounds act specifically on GHR-UbE interaction

Because βTrCP is involved in many different regulatory systems, it is important that compounds that inhibit GHR endocytosis target specifically the interaction with GHR rather than affecting the binding properties of βTrCP to other substrates. A well-known reported βTrCP substrate is β-catenin, a central component of the WNT signaling pathway, containing a classical DSGxxS motif to bind to βTrCP. We used a WNT signaling TOP/FOP dual luciferase reporter assay (26) to investigate if compounds affect

βTrCP-βcatenin interaction. Binding of Wnt3A to Frizzled and Lrp5/6 co-receptors leads to inhibition of βTrCP-mediated degradation of βcatenin, allowing β-catenin to enter the nucleus and turn on gene transcription (27). The activation of gene transcription by βcatenin can be measured with this TOP/FOP luciferase assay. Compounds that disturb βTrCP binding pocket in general will inhibit βTrCP-βcatenin interaction resulting in its nuclear translocation and gene transcription. None of the 5 compounds tested resulted in activation of the luciferase activity, indicating that they do not affect the β-catenin-βTrCP interaction (Fig. 4). From compound 387D9 insufficient material was available to perform this test. In conclusion, the selected compounds did not interfere with WNT signaling, indicating that the interaction of βTrCP with one of its classical substrates, β-catenin is not affected, and suggesting that these compounds act specifically at the βTrCP-GHR interaction.

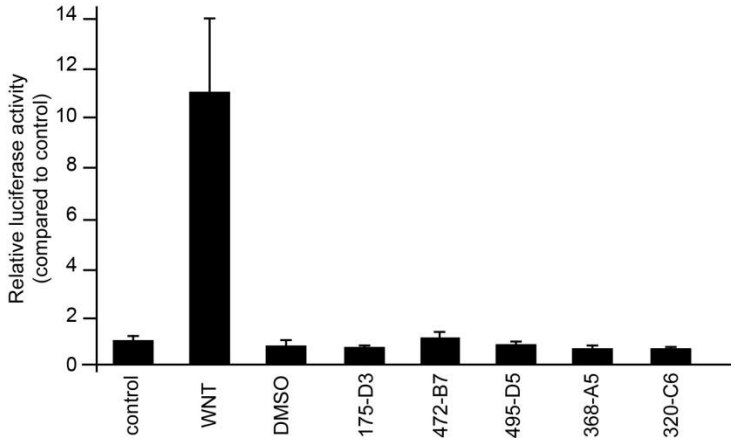

Fig. 4. Compounds act specifically on GHR-UbE interaction. HEK293-TR cells were transfected with TOP (Tcf Optimal) operator or FOP (Far from Optimal) mutated operator and pTk-Renilla (internal standard) and incubated for 20 hours with 20 μM compound. WNT3a conditioned medium was taken as positive control, and DMSO as control for compounds incubation. The Luciferase reporter gene activity was normalized to Renilla Luciferase activity. The values represent the mean ±SD of a duplicate transfection. Data are representative of two experiments.

5. Effect of compounds on GH sensitivity of cells.

Next, the six compounds were tested for their ability to increase GH sensitivity of cells in HEK293-TR cells stably expressing rabbit GHR. HEK293-TR-GHR cells were incubated for 3 or 20 hours with 20 μM compound. Then cells were stimulated with180 ng/ml GH for 5 minutes to obtain 50% activation of STAT5b. The compounds 472B7, 495D5 and 320C6 inhibited GHR endocytosis significantly. The strongest effects were obtained after 20 hours of compound incubation (Fig. 5A, quantified in 5B). The accumulation of GHR, upon treatment with these compounds, did not correlate with increase of MAPK and STAT5 activation (Supplementary data, Fig. S1). In a STAT5b luciferase assay on HEK293-TR-GHR, only the compound 472B7 showed a slight increase of GH induced STAT5b activation (data not shown). The lack of correlation between GHR levels and GH signaling activation is very likely due to the fact that the used cell systems, in the conditions of the experiment, do not have enough extra signaling capacity to respond to increased GHR levels. In conclusion, compounds 472B7, 495D5, 320C6 were selected for further chemical evaluation, as they were able to interfere with the βTrCP-GHR interaction in vitro, and be effective in causing GHR endocytosis inhibition in cells. Although no sufficient material was available from compound 387D9 to perform all experiments, we decided to take this compound along as a representative of another structural class.

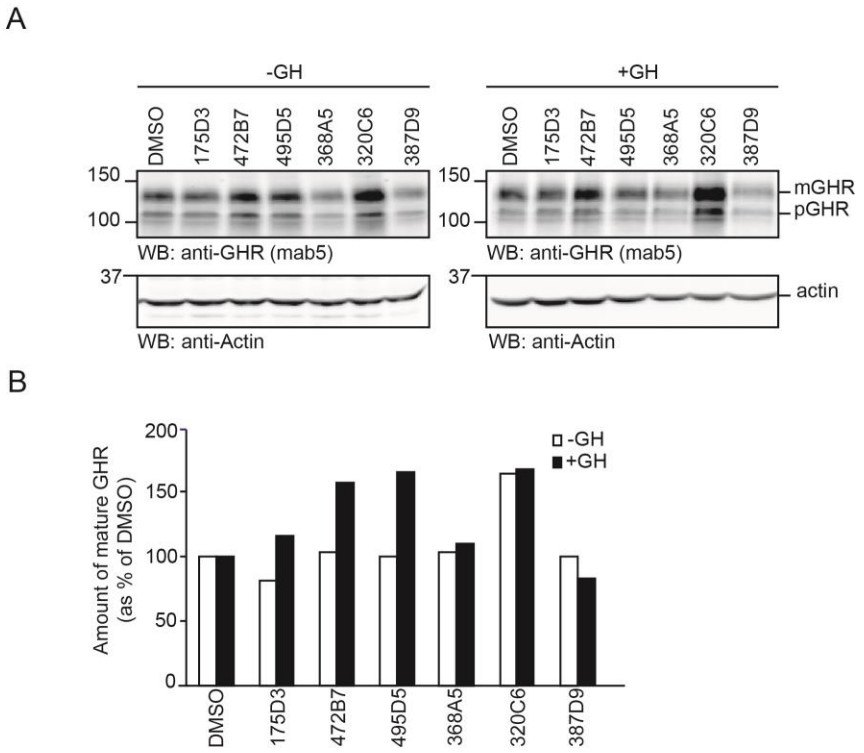

Fig. 5. Effect of compounds on GH sensitivity of cells. (A) HEK293-TR cells stably expressing GHR were incubated 20 hours with 20 µM compound and stimulated 5 minutes with 180 ng/ml hGH. Cells were lysed and total cell lysates were put on SDS-PAGE gel. Blots were detected for GHR (MAb5) and phosphorylated MAPK, total STAT5b, and actin for loading control. **(B)** The amount of mature GHR was corrected for actin and represented in a graph as percentage of the DMSO treatment situation.

6. HTS of chemical analogues of hit compounds.

After hit compound identification, we selected 352 structural analogues of the compounds 472B7, 495D5, 320C6 and 387D9. Screening of these selected analogues in the HTS was performed in singlicate at 10 and 20 µM and in duplicate at 40 µM. This resulted in 44 compounds that decreased the signal more than 50% compared to DMSO control (hit rate of 12.8%) including 3 of the initial hits (495D5, 320C6 and 387D9) (see Table S3, supplementary data). All 44 analogues were true positives, because they neither quenched the fluorescent signal nor showed auto fluorescence (data not shown).

7. Validation of analogues hit compounds in cell based assays.

All 44 analogues hit compounds were tested for their ability to inhibit GHR endocytosis (for summary of the results see Table 1S, supplementary data). Two main criteria were considered to evaluate the effectiveness of the compounds: (1) Cy3-GH uptake inhibition by U20S cells after 3 or 18 hours compound treatment; (2) accumulation of GHR in HEK293-TR-GHR cells after 18 hours compound treatment (representative example in Fig. 6). Compounds that showed precipitates or affected cell morphology were discarded. Six compounds (10, 12, 16, 25, 28, and 39) inhibited GHR endocytosis in both U2OS and HEK293-TR-GHR cells. In addition, an effective compound should show a dose-response effect. Therefore, the effect of 5 compounds (10, 12, 16, 25, 39) on GHR stabilization in HEK293-TR-GHR cells was tested at 6 concentrations (0.5, 1, 2.5, 5, 10, 20 µM) and compared to corresponding DMSO concentrations. Compound 10 (Fig. 7A, quantified in 7B) and to a lesser extent also compound 12 (Fig. 7C, quantified in 7D) showed a concentration dependent effect on GHR stabilization. None of the 9 analogue compounds tested (6, 10, 11, 12, 16, 23, 25, 28, 29) induced WNT signaling, as evaluated with

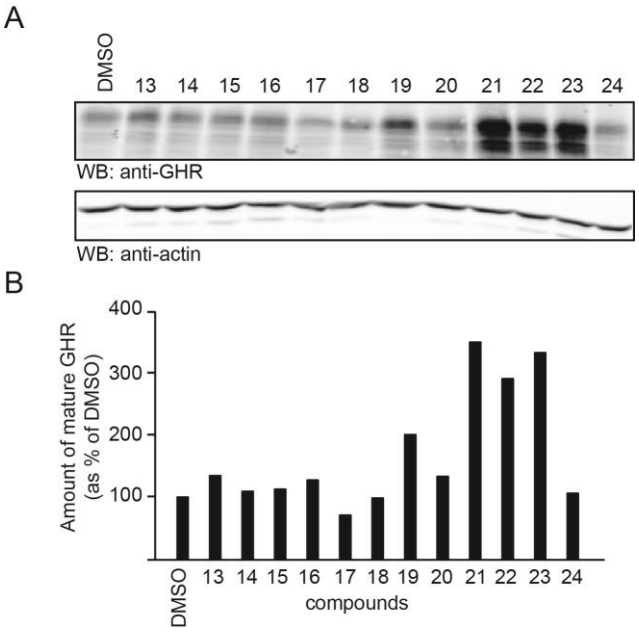

Fig. 6. Effect of analogous hit compounds on GH sensitivity of cells. (A) HEK293-TR cells stably expressing GHR were incubated 18 hours with 20 µM compound and stimulated 5 minutes with 180 ng/ml hGH. Cells were lysed and total cell lysates were put on SDS-PAGE gel. Blots were detected for GHR (Mab5) and actin for loading control. The screen performed with all 44 compounds was performed once. The figure shows a representative part of the screen. **(B)** The amount of mature GHR was corrected for actin and represented in a graph as percentage of the DMSO treatment situation. Data are representative of two experiments.

the TOP/FOP luciferase reporter assay, suggesting that they act rather specifically on the UbE-βTrCP interaction (Fig 7E). In conclusion, compound 10 and 12 were acting most positively in all tested assays. The 44 analogues compounds were structurally clustered in 4 classes: class 1 (33 compounds), class 2 (7 compounds), class 4 (1 compound), class 5 (3 compounds) (see Table S1). Compounds 10 and 12 belong to structure class I, while compound 16 (495D5) belongs to structure class 4. Because compounds 10 and 12 were the most promising hits, they were tested in mice. Although compound 16 did not show a concentration dependent effect on GHR stabilization in HEK293-TR-GHR cells, we tested it in mice as a representative of another structural class.

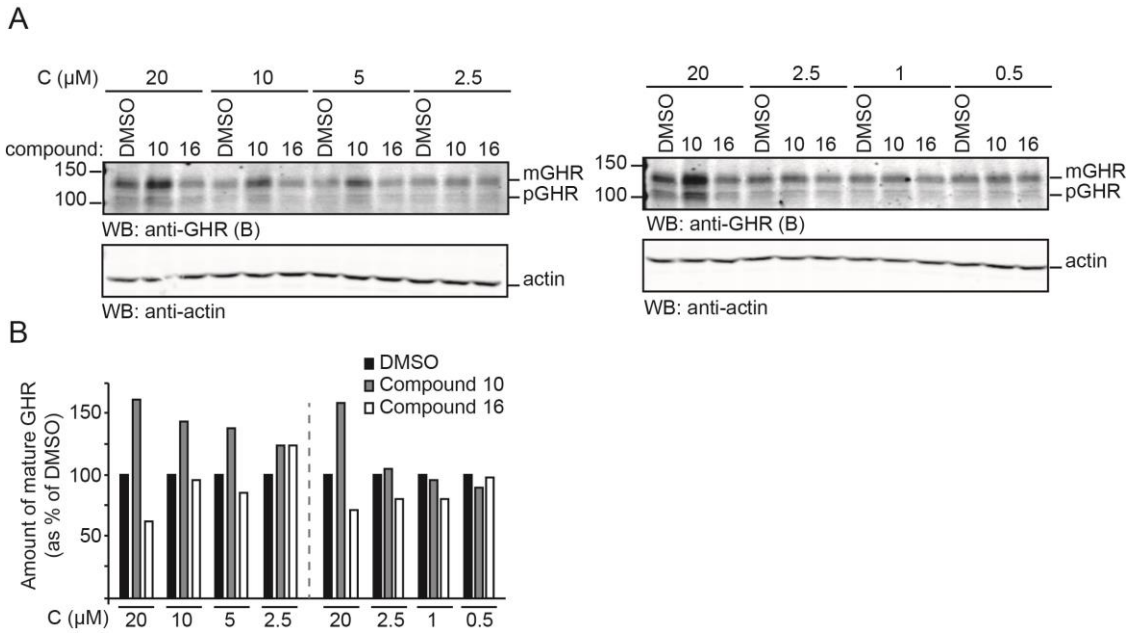

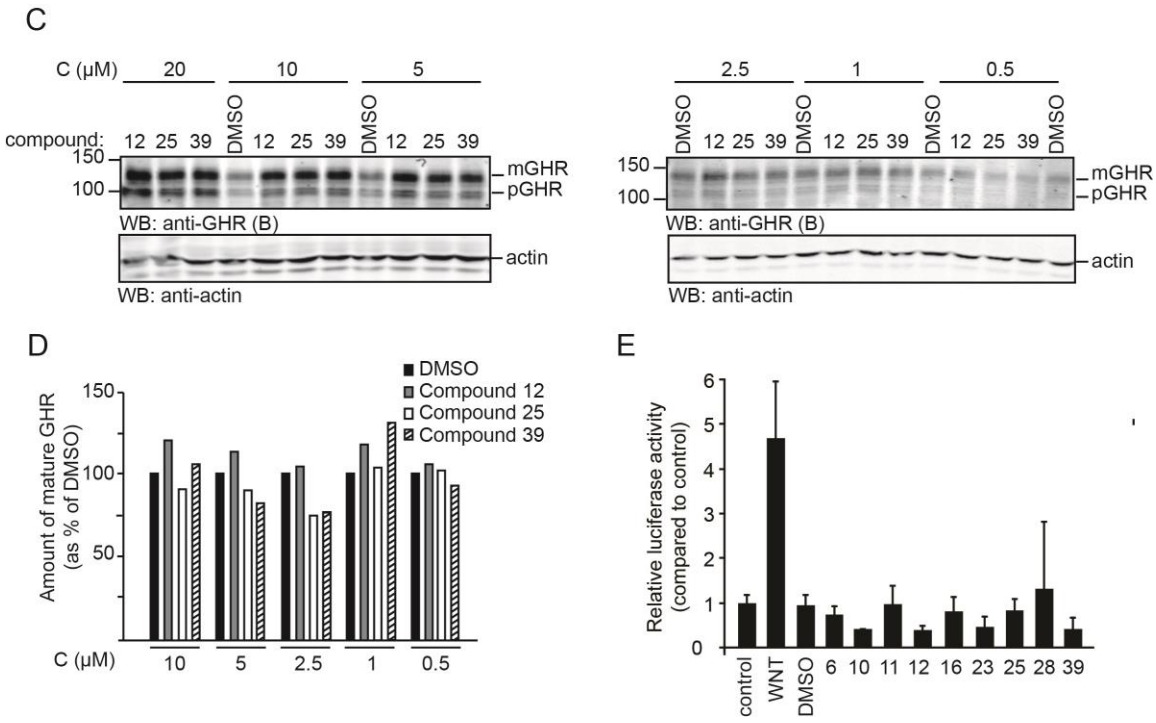

Fig. 7. Concentration dependent effect of analogous hit compounds 10 and 12, but not 16, 25 and 39 on GH sensitivity. (**A) (C)** HEK293-TR cells stably expressing GHR were incubated 18 hours with indicated concentration of compound and stimulated 5 minutes with 180 ng/ml hGH. Cells were lysed and total cell lysates were put on SDS-PAGE gel. Blots detected for GHR and actin for loading control. The screen was performed once**. (B)(D)** Quantification of the effect of the compounds shown in 7A and 7C, respectively, represented in the graph as the amount of mature GHR corrected for actin, and expressed as percentage of the DMSO treatment situation. **(E)** TOP/FOP dual luciferase reporter assay suggests that the 9 analogue compounds tested do not act on βTrCP interaction with βcatenin. The assay was performed as in Fig.4. The values represent the mean ±SD of a duplicate transfection. Data are representative of two experiments.

8. Effect of hit compounds on GHR stabilization and GH signaling in mice.

This challenging project was started to find potential lead compounds for future therapeutic development against cachexia. We succeeded in developing a simple molecular based HTS and identified compounds that specifically disrupt the interaction between GHR-UbE and βTrCP. Consequently, these compounds, provided they can effectively cross the plasma membrane, are expected to interfere specifically with GHR endocytosis. Indeed, several of these compounds specifically inhibited GHR endocytosis in two different cell lines (U2OS and HEK293), tested in two different assays (Cy3-GH uptake and mature GHR stabilization). Three compounds (10, 12 16) also showed increased GH-induced MAPK activation. The next step in the drug discovery route was to test whether compounds able to inhibit GHR endocytosis in cells can also stabilize GHR in mice. Our primary parameter was the amount of GHR protein per gram liver after isolation of using biotin-GH (Fig. 8). As the half-life of GHR in liver is relatively short (28-31) mice were treated for 4 hours with the compounds, i.e. 3 times the half-life of the GHR. C57BL/6J female mice of 7 weeks old were intraperitoneally (i.p.) injected with compound solution (5 mg/kg) or vehicle. Biotin-GH pull downs were performed in liver lysates and the amounts of GHR were quantitated. From the injected compounds (10, 12 and 16), only compound 10 stabilized the mature GHR in mice livers (40% more than control) (Fig. 8A, lane 9-12; for compound 12 and 16 data not shown). Some mice were also stimulated with human GH (1.5 mg/kg) via i.p. injection for 15 minutes to test the effects of the compounds on signaling events. 15 minutes of GH treatment was chosen, because

then STAT5b activation was half maximal and an increase in GH-induced STAT5b activation due to the inhibitory effect of the compound on GHR endocytosis could be detected. In mice treated with GH endogenous mature GHR could not be pulled down from the liver lysates, because the GHRs were occupied and in complex with the i.p. injected hGH (Fig.8A, lane 4, 7 and 8). Apparently, GH was not injected appropriately in mouse nr.3, since no STAT5 activation was detected (Fig. 8B, 1st panel, lane 3), and GHR could be pulled down with biotin-GH (Fig. 8A, lane 3). This indicates that the band at the height of 100 kDa represents the mature mouse GHR. Moreover, GH stimulation in mice treated with compound 10 resulted in increased STAT5 activation, accessed by a higher ratio pSTAT5:STAT5, when compared to control mice (Fig. 8B, cf. lanes 7 and 8 to lane 4). The MAPK was hardly activated upon 1.5 mg/kg GH stimulation (data not shown). In conclusion, we developed a simple mouse model to test potential lead compounds for their ability to stabilize GHR expression in vivo. Compound 10 is a promising hit but the results need to be validated with a higher number of animals. Ultimately, this compound needs to be tested in a cancer cachexia mouse model, in order to test its effectiveness in reducing cancer-induced cachexia.

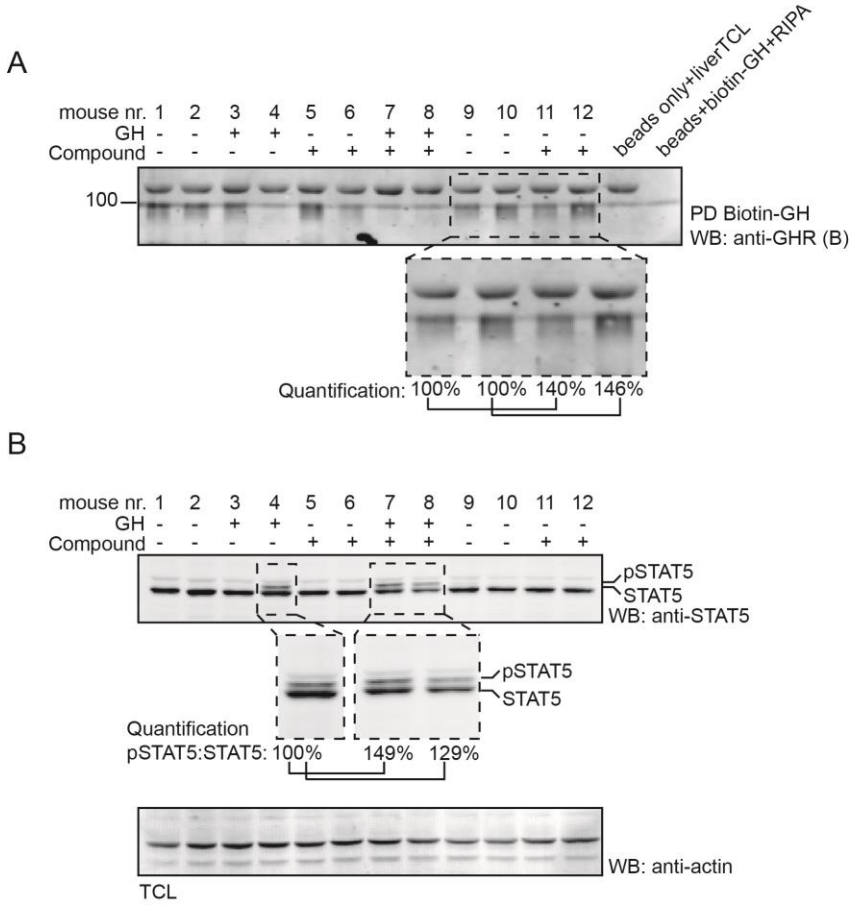

Fig. 8. Effect of hit compounds on GHR stabilization and GH signalling in mice. A) C57BL/6J female mice of 7 weeks old were intraperitoneally injected with 5 mg/kg compound in 5% Cremophor EL/PBS solution or with vehicle (5% Cremophor EL/PBS). After 4 hours, mice were sacrificed and livers were snap frozen. Liver biopsies were lysed and biotin-GH pull downs (PD) were run in SDS-PAGE gel, and analyzed by western blotting with anti-GHR (B) antibody. **B)** After 4 hours of intraperitoneal (i.p.) injection with compounds, some mice were treated with human GH via i.p. injection for 15 minutes. The mice were sacrificed and livers were snap frozen. Liver biopsies were lysed and analyzed by western blotting, with anti-STAT5b, anti-P-MAPK and anti-actin antibodies. Note that due to experimental reasons, the amount of GHR in lane 9 should be compared to lane 11, and lane 10 to lane 12. PD, pull down; TCL, total cell lysates.

Discussion

Our report represents the starting point of a series of ongoing studies that aimed to identify bioactive, potent, and selective inhibitors of GHR-βTrCP interaction that stabilize GHR levels at the plasma membrane and increase GH sensitivity. Since acquired GH resistance is a feature in cachexia patients, our goal is that such inhibitors eventually will result in a novel, medical treatment for patients suffering from cachexia. An important feature of our novel HTS assay is that it is based on a molecular model that underlies the cellular regulation of GHR degradation and, consequently, the pathology of cachexia in mice and man.

The mechanism responsible for GH resistance in cachexia has been discussed for long (9). Although malnutrition has also been suggested as a possible cause for GH resistance in cachexia states, it appears that adequate nutritional support of the patients did not subvert the GH resistance phenotype (32). Also changes in the half-life of IGF-1 or levels of IGF binding protein (IGFBP)(33), or most likely changes in the synthesis of hepatic IGF-1(34) have been suggested as the cause of GH resistance in cachexia. Because high GH serum levels are combined with reduced circulating IGF-1 levels in cachexia patients, either lack of GHR or defects in its signaling pathways are the primary cause of GH resistance. Importantly, this phenotype is accompanied by increase in inflammatory cytokines levels. There are studies reporting negative impact of some cytokines, such as TNFα, IL-1 and IL-6, in GH actions (35-37). Therefore, it has been suggested that GH resistance occurs as a consequence of inflammation. Paradoxically, anti- inflammatory factors like glucocorticoids have been reported to inhibit GH actions (38). It remains unclear what is the pathophysiological mechanism of cachexia syndrome. In this study, we show for the first time that in tumor-bearing mice suffering from cachexia GHR protein levels in the liver are is 9 times lower indicating that decreased GHR levels are associated with cachexia conditions (Fig.1). Since cachexia and GH resistance seem to be multifactorial in origin several treatments need probably to be applied in parallel to achieve successful therapeutic results. In fact, strategies to interfere with cytokine synthesis or activity, developed in the last years, failed to improve cachexia (39). Combination of these agents with compounds that reverse the GHR resistance phenotype, as resulting from our HTS screening, might constitute an improvement in the effectiveness of cachexia treatment.

The sensitivity of cells to GH is mainly determined by the amount of GHRs at the cell surface, which represents a balance of two processes: GHR synthesis and degradation. On one hand, mice suffering from cachexia have 2.5 less GHR mRNA in their livers when compared to control mice. On the other hand, GHR protein levels are down regulated 9 times in the livers of these cachectic mice. It is difficult to predict at which extent a reduction in GHR mRNA levels affects GHR protein levels. Therefore, the GH resistance phenotype occurring in cachexia patients could be caused by a combination of two factors: reduced GHR mRNA expression and accelerated degradation of GHR protein. It is unclear which of these two factors is dominant. In the present study, we targeted the GHR degradation process. $SCF^{\beta TrCP}$ is one of the main regulators of GHR degradation. βTrCP interacts with the GHR UbE motif in an unconventional manner (*da Silva Almeida AC, manuscript in preparation*). This makes the interaction UbE-βTrCP a very promising target for compounds that by inhibiting this interaction block GHR degradation, increase GHR levels, and consequently the sensitivity of the cells to GH.

In our initial HTS screens of ~40,000 compounds, 26 inhibitors were identified that inhibited the GHR-βTrCP interaction. Compounds that are able to enter the cells are expected to inhibit GHR endocytosis. Four compounds were effective in doing so. 352 analogues from these compounds were selected and tested in the same HTS and cell based assays. From this analogues compound 10 was the most potent inhibitor in all assays. Furthermore, compound 10 treatment stabilized the mature GHR in mice livers for about 40%, indicating that this drug is sufficiently stable in circulation. However, further detailed investigation is needed: expanding the study to a bigger population of animals, determination of pharmacokinetics parameters *in vitro* and *in vivo*, bioavaibility and toxicology testing, among others. At this stage the effective concentration (EC50) of compound 10 (in µM range) is too high for therapeutic use in humans. Further optimization of the compound by chemical modification may improve its effectiveness, in order to reach an EC50 at nm range. We are currently working on the structural

characterization of the UbE-βTrCP interaction using NMR techniques (*da Silva Almeida AC, manuscript in preparation*). This will provide us with structural insights that will facilitate the design of effective drugs, potentially analogues of compound 10, able to inhibit this interaction.

To evaluate the effects of the compounds, besides analyzing GHR stabilization at the plasma membrane we also tried to evaluate the activation of GH signaling, in particular GH-induced STAT5b and MAPK activation. GH-induced STAT5 activation is critical for GH-induced IGF-1 expression and body growth (40). GH-dependent MAPK activation has been implicated in cell differentiation and proliferation. We were unable to detect increased STAT5b activation correlating with the compound-mediated accumulation of GHR in cells In some cases, increased MAPK activation correlated with increased GHR levels, but not for all the compounds (Fig. S1 and S2). Probably, the cell systems and experimental conditions used were not sensitive enough for evaluating the effects of the compounds in GH signaling. The extent of GH signaling does not depend exclusively on GHR levels. On one hand, GHR signaling is dependent on the cell type and the height and duration of the GH peak. We showed that in 3T3-F442A cells, a low concentration of GH (10 ng/ml) during a short time (3 minutes) results in 50% STAT5b activation, while in HEK293-TR-GHR cells, overexpressing GHR, 5 minutes stimulation of 180 ng/ml is optimal to get 50% STAT5b activation. On the other hand, the signaling machinery in the used cell systems may be the limiting factor for their signaling capacity. In this case, after GH binding, the extra amount of GHRs (on top of the normal) may not have sufficient downstream signaling molecules available (as Jak2 or STAT5b) to effectively trigger signaling. The optimal cell model for studying the effects of the compounds on GH signaling would be one where the limiting factor is the amount of GHR, as probably occurs in cachexia. Therefore, the selection of the potential compounds, from the cell based assays, for the treatment of cachexia was primarily based on GHR endocytosis inhibition and GHR accumulation, instead of downstream signaling events. For the same reasons, the mouse model used may constitute a limitation to the sensitivity of the drugs validation *in vivo*, since we were trying to increase the GHR levels in the liver on top of the normal endogenous GHR levels. Preferably, the compounds should be tested in mouse models that mimic the cachectic situation, particularly in terms of GHR levels. Mouse models for cancer cachexia have been broadly used for the understanding of the syndrome (41). As shown in this study, GHR levels are extensively lower than in wild type mice, indicating that this mouse model is ideal to test potential lead compounds. However, the generation of these models implies implanting tumor cells to create large tumours, which represents a difficult and time consuming procedure, which is harmfull for the animals. Dexamethasone (synthetic glucocorticoid) has been shown to decrease GHR mRNA levels and inhibit GH induction of IGF-1 (42). A easier mouse model for cachexia could be normal mice treated with dexamethasone. This is under current investigation. Ultimately, when testing the compounds in mice, if using an appropriate mouse model, we expect the positive compounds to have an effect on GH-induced gene expression in the liver and on the IGF-I levels in the blood. We expect that in cachexia patients, our drug will increase the number of the limiting GHRs, and that the normal systemic GH pulses are then sufficient to generate extra JAK/STAT signaling.

In conclusion, we developed a robust screenings route that includes a simple molecular based HTS assay, several cell based assays and a mouse model to discover drugs that inhibit GHR endocytosis. The potential hits found in this study could represent leads for drugs against cachexia, and can then be tested in our mouse model for cancer-induced cachexia. The successful development of a novel anti-cachexia drug would have a significant impact on the quality of life of millions of patients suffering from cachexia. But in addition, since GH actions are involved in overweight, obesity, insulin resistance, aging and mental retardation, this novel drug might have a tremendous worldwide impact on society, the health and economic system.

Acknowledgements

We thank Carin Zwartjes, Marcel Roza and Mariska Mulderij for their contribution to the HTP screening. We thank all members of the GHR group and René Scriwanek and Marc van Peski for assistance with the figures. We thank Madelon Maurice for the generous gift of the HEK293-TR cells and use of the Wnt TOP/FOP luciferase assay. This research was supported by the European Network of Excellence, Rubicon "Role of ubiquitin and ubiquitin-like modifiers in cellular regulation" (Grant LSHG-CT-2005-018683), the U-balance project of 'Senter Innovatiesubsidie samenwerkingsprojecten' from SenterNovem "Drug discovery in growth hormone metabolism' (Projectnumber ISO43051), and the Marie Curie network, "UbiRegulators", (Grant MRTN-CT-2006-034555).

References

1. Moses AG, Maingay J, Sangster K, Fearon KC, Ross JA 2009 Pro-inflammatory cytokine release by peripheral blood mononuclear cells from patients with advanced pancreatic cancer: relationship to acute phase response and survival. Oncol Rep 21:1091-1095
2. Tisdale MJ 2008 Catabolic mediators of cancer cachexia. Curr Opin Support Palliat Care 2:256-261
3. Pajak B, Orzechowska S, Pijet B, Pijet M, Pogorzelska A, Gajkowska B, Orzechowski A 2008 Crossroads of cytokine signaling--the chase to stop muscle cachexia. J Physiol Pharmacol 59 Suppl 9:251-264
4. Morley JE, Thomas DR, Wilson MM 2006 Cachexia: pathophysiology and clinical relevance. Am J Clin Nutr 83:735-743
5. Tisdale MJ 2009 Mechanisms of cancer cachexia. Physiol Rev 89:381-410
6. Argiles JM, Busquets S, Toledo M, Lopez-Soriano FJ 2009 The role of cytokines in cancer cachexia. Curr Opin Support Palliat Care 3:263-268
7. Tisdale MJ 2005 The ubiquitin-proteasome pathway as a therapeutic target for muscle wasting. J Support Oncol 3:209-217
8. Anker SD, Volterrani M, Pflaum CD, Strasburger CJ, Osterziel KJ, Doehner W, Ranke MB, Poole-Wilson PA, Giustina A, Dietz R, Coats AJ 2001 Acquired growth hormone resistance in patients with chronic heart failure: implications for therapy with growth hormone. J Am Coll Cardiol 38:443-452
9. Jenkins RC, Ross RJ 1996 Acquired growth hormone resistance in catabolic states. Baillieres Clin Endocrinol Metab 10:411-419
10. Counts DR, Gwirtsman H, Carlsson LM, Lesem M, Cutler GB, Jr. 1992 The effect of anorexia nervosa and refeeding on growth hormone-binding protein, the insulin-like growth factors (IGFs), and the IGF-binding proteins. J Clin Endocrinol Metab 75:762-767
11. Menon RK, Arslanian S, May B, Cutfield WS, Sperling MA 1992 Diminished growth hormone-binding protein in children with insulin-dependent diabetes mellitus. J Clin Endocrinol Metab 74:934-938
12. Ross RJ, Miell JP, Holly JM, Maheshwari H, Norman M, Abdulla AF, Buchanan CR 1991 Levels of GH binding activity, IGFBP-1, insulin, blood glucose and cortisol in intensive care patients. Clin Endocrinol (Oxf) 35:361-367
13. Argetsinger LS, Carter-Su C 1996 Mechanism of signaling by growth hormone receptor. Physiol Rev 76:1089-1107
14. Waters MJ, Shang CA, Behncken SN, Tam SP, Li H, Shen B, Lobie PE 1999 Growth hormone as a cytokine. Clinical and Experimental Pharmacology and Physiology 26:760-764
15. Strous GJ, van Kerkhof P 2002 The ubiquitin-proteasome pathway and the regulation of growth hormone receptor availability. Mol Cell Endocrinol 197:143-151
16. van Kerkhof P, Putters J, Strous GJ 2007 The Ubiquitin Ligase SCF(betaTrCP) Regulates the Degradation of the Growth Hormone Receptor. J Biol Chem 282:20475-20483

17. Frescas D, Pagano M 2008 Deregulated proteolysis by the F-box proteins SKP2 and beta-TrCP: tipping the scales of cancer. Nat Rev Cancer 8:438-449
18. Govers R, ten Broeke T, van Kerkhof P, Schwartz AL, Strous GJ 1999 Identification of a novel ubiquitin conjugation motif, required for ligand-induced internalization of the growth hormone receptor. EMBO J 18:28-36.
19. Pfaffl MW, Horgan GW, Dempfle L 2002 Relative expression software tool (REST) for group-wise comparison and statistical analysis of relative expression results in real-time PCR. Nucleic Acids Res 30:e36
20. Zhang JH, Chung TD, Oldenburg KR 1999 A Simple Statistical Parameter for Use in Evaluation and Validation of High Throughput Screening Assays. J Biomol Screen 4:67-73
21. Schantl JA, Roza M, de Jong AP, Strous GJ 2003 Small glutamine-rich tetratricopeptide repeat-containing protein interacts with the ubiquitin-dependent endocytosis motif of the growth hormone receptor. Biochem J 373:855-863
22. Strous GJ, van Kerkhof P, Govers R, Ciechanover A, Schwartz AL 1996 The ubiquitin conjugation system is required for ligand-induced endocytosis and degradation of the growth hormone receptor. EMBO J 15:3806-3812
23. Tanaka Y, Eda H, Tanaka T, Udagawa T, Ishikawa T, Horii I, Ishitsuka H, Kataoka T, Taguchi T 1990 Experimental cancer cachexia induced by transplantable colon 26 adenocarcinoma in mice. Cancer Res 50:2290-2295
24. Samuels SE, Knowles AL, Tilignac T, Debiton E, Madelmont JC, Attaix D 2000 Protein metabolism in the small intestine during cancer cachexia and chemotherapy in mice. Cancer Res 60:4968-4974
25. Diffee GM, Kalfas K, Al-Majid S, McCarthy DO 2002 Altered expression of skeletal muscle myosin isoforms in cancer cachexia. Am J Physiol Cell Physiol 283:C1376-1382
26. Korinek V, Barker N, Morin PJ, van Wichen D, de Weger R, Kinzler KW, Vogelstein B, Clevers H 1997 Constitutive transcriptional activation by a beta-catenin-Tcf complex in APC-/- colon carcinoma. Science 275:1784-1787
27. Tauriello DV, Maurice MM 2010 The various roles of ubiquitin in Wnt pathway regulation. Cell Cycle 9:3700-3709
28. Murphy LJ, Lazarus L 1984 The mouse fibroblast growth hormone receptor: ligand processing and receptor modulation and turnover. Endocrinology 115:1625-1632
29. Baxter RC 1985 Measurement of growth hormone and prolactin receptor turnover in rat liver. Endocrinology 117:650-655
30. Gorin E, Goodman HM 1985 Turnover of growth hormone receptors in rat adipocytes. Endocrinology 116:1796-1805
31. Roupas P, Herington AC 1986 Growth hormone receptors in cultured adipocytes: a model to study receptor regulation. MolCell Endocrinol 47:81-90
32. Chwals WJ, Bistrian BR 1991 Role of exogenous growth hormone and insulin-like growth factor I in malnutrition and acute metabolic stress: a hypothesis. Crit Care Med 19:1317-1322
33. Bentham J, Rodriguez-Arnao J, Ross RJ 1993 Acquired growth hormone resistance in patients with hypercatabolism. Horm Res 40:87-91
34. Moats-Staats BM, Brady JL, Jr., Underwood LE, D'Ercole AJ 1989 Dietary protein restriction in artificially reared neonatal rats causes a reduction of insulin-like growth factor-I gene expression. Endocrinology 125:2368-2374
35. De Benedetti F, Alonzi T, Moretta A, Lazzaro D, Costa P, Poli V, Martini A, Ciliberto G, Fattori E 1997 Interleukin 6 causes growth impairment in transgenic mice through a decrease in insulin-like growth factor-I. A model for stunted growth in children with chronic inflammation. J Clin Invest 99:643-650
36. Thissen JP 2007 How proinflammatory cytokines may impair growth and cause muscle wasting. Horm Res 67 Suppl 1:64-70
37. Thissen JP, Verniers J 1997 Inhibition by interleukin-1 beta and tumor necrosis factor-alpha of the insulin-like growth factor I messenger ribonucleic acid response to growth hormone in rat hepatocyte primary culture. Endocrinology 138:1078-1084

38. Beauloye V, Ketelslegers JM, Moreau B, Thissen JP 1999 Dexamethasone inhibits both growth hormone (GH)-induction of insulin-like growth factor-I (IGF-I) mRNA and GH receptor (GHR) mRNA levels in rat primary cultured hepatocytes. Growth Hormone & IGF Research 9:205-211
39. Penna F, Minero VG, Costamagna D, Bonelli G, Baccino FM, Costelli P 2010 Anti-cytokine strategies for the treatment of cancer-related anorexia and cachexia. Expert Opin Biol Ther 10:1241-1250
40. Hwa V, Little B, Adiyaman P, Kofoed EM, Pratt KL, Ocal G, Berberoglu M, Rosenfeld RG 2005 Severe growth hormone insensitivity resulting from total absence of signal transducer and activator of transcription 5b. J Clin Endocrinol Metab 90:4260-4266
41. Emery PW 1999 Cachexia in experimental models. Nutrition 15:600-603
42. Beauloye V, Ketelslegers JM, Moreau B, Thissen JP 1999 Dexamethasone inhibits both growth hormone (GH)-induction of insulin-like growth factor-I (IGF-I) mRNA and GH receptor (GHR) mRNA levels in rat primary cultured hepatocytes. Growth Horm IGF Res 9:205-211

Supplementary data

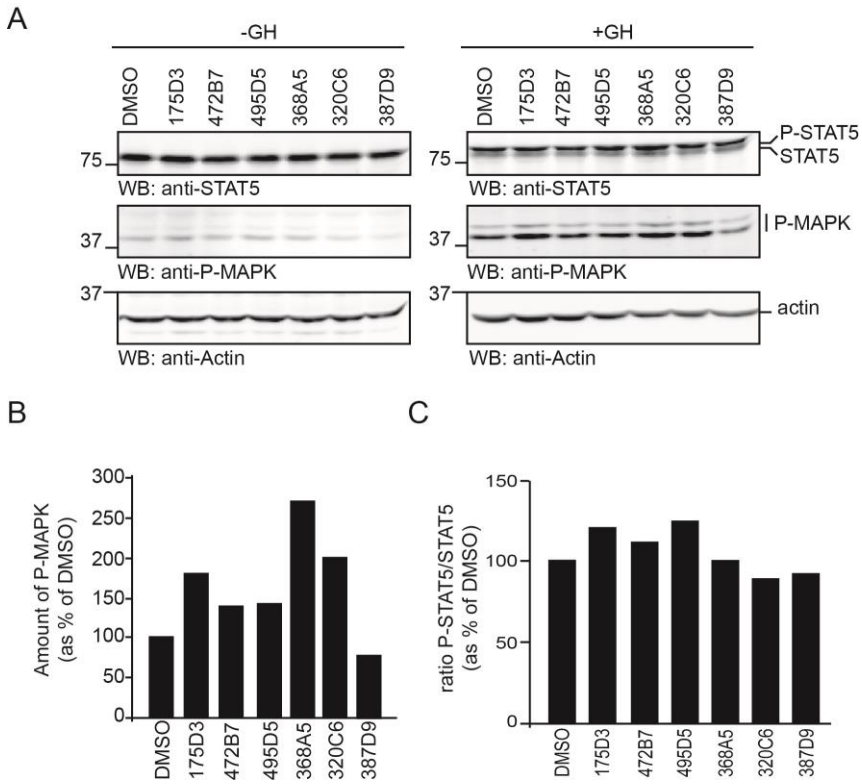

Fig. S1. Effect of compounds on GH sensitivity of cells. (A) HEK293-TR cells stably expressing GHR were incubated 20 hours with 20 µM compound and stimulated 5 minutes with 180 ng/ml hGH. Cells were lysed and total cell lysates were put on SDS-PAGE gel. Blots were detected for phosphorylated MAPK (P-MAPK), total STAT5b, and actin for loading control. **(B)** The amount of P-MAPK was corrected for actin and represented in a graph as percentage of the DMSO treatment situation. **(C)** The activation of STAT5 was quantified by determining the ratio between the upper band (P-STAT5) and the lower band (STAT5), and represented in a graph as percentage of the DMSO treatment situation. Data are representative of two experiments.

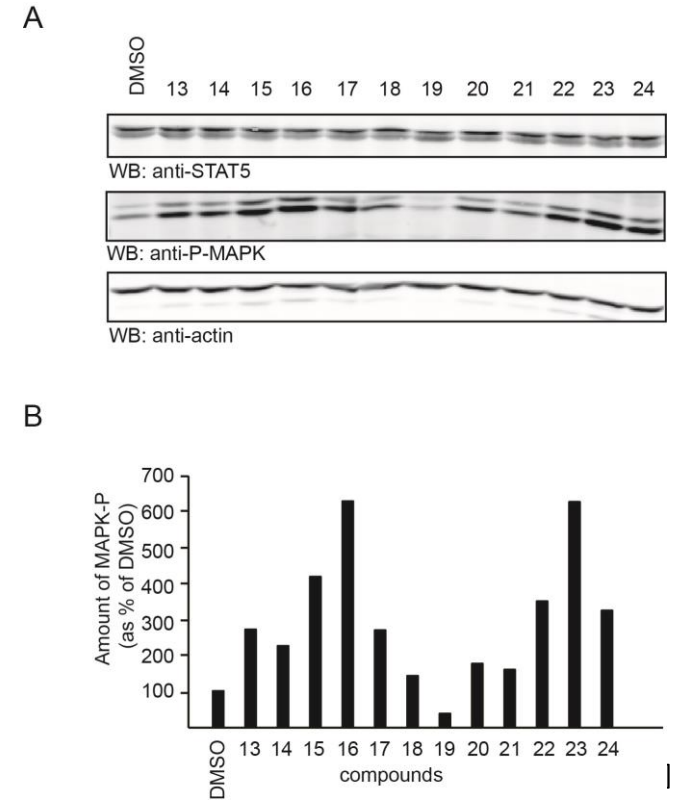

Fig. S2. Effect of analogous hit compounds on GH sensitivity of cells. (A) HEK293-TR cells stably expressing GHR were incubated 18 hours with 20 µM compound and stimulated 5 minutes with 180 ng/ml hGH. Cells were lysed and total cell lysates were put on SDS-PAGE gel. Blots were detected for phosphorylated MAPK (P-MAPK), total STAT5b, and actin for loading control. The screen performed with all 44 compounds was performed once. The figure shows a representative part of the screen. **(B)** The amount of P-MAPK was corrected for actin and represented in a graph as percentage of the DMSO treatment situation.

Table S1: Analogue compounds from primary hit compounds 495D9, 472B7, 320C6 and 387D9

Nr.	Struct. Class	HTP conc. Series (µM)				U20S cells Cy3-GH % endocytosis inhibition (20 µM, 3 h)	U20S cells Cy3-GH % endocytosis inhibition (20 µM, 18 h)	HEK-GHR GHR level (20µM, 18 h) (DMSO-100%)	HEK-MAPK activation (20µM, 18h) (DMSO-100%)	Remarks	Effect on 3T3 cells morphology
		40	40	20	10						
1	5	22	22	6	7	< 5%	nd	94	117		
2	2	20	17	18	29	< 5%	nd	126	79	Precipitates in U2OS (3h)	
3	1	41	65	24	25	< 5%	nd	89	32		
4	1	28	20	41	48	< 5%	nd	-	-	Detachment of Hek293-TR cells	
5	2	49	45	50	50	< 5%	< 5%	110	322		
6	1	9	6	26	14	< 5%	30-40%	172	88		
7 (387D9)	1	35	28	40	28	< 5%	-	186	53	Detachment of U2OS (19h)	
8	1	38	37	69	34	< 5%	< 5%	91	171		
9	1	43	39	51	41	< 20%	10%	93	129		
10	1	25	23	15	15	< 20%	60%	131	120		
11	1	13	10	15	15	< 10%	60%	118	36		
12	1	13	13	20	15	< 10%	40%	170	155		
13	1	43	34	53	51	< 5%	nd	121	303	Precipitates in U2OS (3h)	cells detached
14	1	69	39	47	41	< 5%	nd	96	257	Precipitates in U2OS (3h)	1/2 cells detached
15 (320C6)	5	35	36	9	10	< 10%	80-90%	99	475	Precipitates in U2OS (19h)	
16 (495D5)	4	6	3	11	11	< 10%	10%	132	606		
17	1	54	27	64	37	< 10%	20%	64	300		
18	1	95	46	70	37	< 20%	20%	94	149	Precipitates in U2OS (3+19h)	
19	1	27	26	27	20	< 5%	10%	131	41		
20	1	73	32	45	40	< 5%	< 5%	123	192	Precipitates in U2OS (19h)	
21	1	37	47	30	36	< 10%	10-20%	364	153	Precipitates in U2OS (3+19h)	
22	1	49	41	51	48	< 5%	< 5%	280	364		
23	1	47	11	46	37	< 10%	< 5%	372	562		
24	1	22	23	53	48	< 5%	< 5%	91	378		precip
25	1	12	17	14	11	< 10%	20-30%	184	42		
26	1	27	28	40	45	< 20%	30-40%	85	57	migratory cells in U2OS (19h) and precipitates (3h)	1/2 cells detached
27	1	50	39	37	35	< 10%	10%	90	43		1/3 cells detached
28	4	50	47	55	41	< 10%	20%	126	50		
29	2	35	31	48	44	< 20%	<5%,	220	82	Precipitates in U2OS (3+19h)	
30	2	44	33	63	44	< 5%	< 5%	96	62		precip
31	1	49	45	60	39	< 5%	< 5%	125	64		
32	1	36	27	37	27	< 5%	nd	98	50		

33	5	15	14	5	3	< 5%	50%	111	106		
34	1	48	35	43	38	< 5%	<5%	105	51	migratory cells in U2OS (19h) and precipitates (3h)	1/4 cells detached
35	1	75	42	49	46	< 5%	10-20%	165	32		
36	1	35	32	34	39	< 5%,	nd	57	79	Precipitates in U2OS (3h)	1/4 cells detached
37	1	22	15	58	86	< 10%	nd	105	48	Precipitates in U2OS (3h)	
38	1	42	42	60	60	< 20%	<5%	86	47	Precipitates in U2OS (3+19h)	1/2 cells detached
39	1	22	19	94	85	< 10%	10%	154	28		
41	1	40	43	67	58	< 5%	50%	188	80	Precipitates in U2OS (19h)	1/2 cells detached
42	1	85	149	48	33	< 5%	nd	93	40	Precipitates in U2OS (3h)	
43	2	62	51	48	41	< 5%	< 5%	133	109		changed morphology
44	1	116	83	48	47	< 5%	nd	62	30		
45	1	56	47	48	37	< 20%	5%	105	119	Precipitates in U2OS (19h)	precip

Table S1: Summary of results of 44 analogues compounds from the molecular based GHR-βTrCP HTS , Cy3-GH uptake in U2OS cells, GHR stabilization and MAPK activation in HEK293-TR-GHR cells. In the U2OS DMSO control always some cells (less than 5%) showed some plasma membrane staining of cy3-GH. The compounds were used at 20 µM concentration in U2OS en HEK293-TR-GHR experiments. In U2OS experiment, wells are marked grey, if they did show some inhibition of GHR endocytosis, but also showed precipitates or changes in cell morphology. nd, not done.

Study of growth hormone receptor endocytosis in living cells using bioluminescence resonance energy transfer (BRET).

6

Ana C. da Silva Almeida[1,2], Ger J Strous[1], Agnes G S H van Rossum[1,2]

[1] Department of Cell Biology and Institute of Biomembranes, University Medical Center Utrecht, Heidelberglaan 100, 3584 CX Utrecht, The Netherlands

[2] Drug Discovery Factory BV, Albrechtlaan 14A, 1404 AK Bussum, The Netherlands

(Manuscript in preparation)

Partially published in:

Putters J, da Silva Almeida AC, van Kerkhof P, van Rossum AG, Gracanin A, Strous GJ. JAK2 is a negative regulator of ubiquitin-dependent endocytosis of the growth hormone receptor. PLoS One 6: e14676, February 2011

Abstract

Bioluminescence resonance energy transfer (BRET) has been used successfully in the analysis of a substantial number of interactions in real time. In this study, BRET technology was used to study interactions important for the regulation of growth hormone receptor (GHR) endocytosis: the E3 ligase SCF(βTrCP) and the kinase JAK2. GHR is constitutively endocytosed through the action of the ubiquitin ligase SCF(βTrCP) bound to the UbE motif in the cytoplasmic tail of the receptor. Binding of JAK2 to box1 inhibits GHR endocytosis. Using BRET, we showed in living cells, in real time, that JAK2 is constitutively bound to GHR. Moreover, we show that GH stimulation results in decreased BRET signal from GHR-JAK2 interaction, consistent with GH-induced JAK2 release from GHR. GHR-βTrCP interaction was measured constitutively, and was not influenced by GH stimulation. The hypothesis that JAK2 and βTrCP compete for GHR binding could not be proven. Finally, the potential applications of the developed BRET assay, including its use as screening platforms for drug discovery are discussed.

Introduction

Analysis of protein-protein interaction *in vivo* is essential to understand the regulation of physiologic processes in the cells. There is a growing interest in the development of techniques that allow the assessment of the dynamics of the interactions in a certain spatiotemporal context. Resonance energy transfer techniques have become extensively used for this purpose, in particular fluorescence energy transfer (FRET) and bioluminescence energy transfer (BRET)(1).

BRET combines the attractive characteristics of FRET without the problems associated with fluorescence excitation, such as photobleaching, autofluorescence and simultaneous excitation of both donor and acceptor. BRET involves the transfer of energy from a donor enzyme (*Renilla* luciferase-RLUC) to a complementary acceptor fluorophore after the oxidation of a substrate, without need of external excitation (2). The substrate for RLUC, coelenterazine, is a hydrophobic molecule able to penetrate the cell membrane. The transfer of energy between the donor and acceptor is inversely proportional to the sixth power of the distance between the two molecules(3). The effective range of transfer is less than 10 nm, which is in the scale of the dimensions within macromolecular protein complexes, making BRET a suitable technique for analyzing these interactions. The proteins of interest need to be covalently fused to a "BRET tag", consisting either of a bioluminescent donor (a RLUC tag, 35 kD) or a fluorescent acceptor (most commonly a YFP tag, 27 kD)(2). The energy transfer occurs when the interaction of the proteins of interest brings the two "BRET tags" in close proximity (less than 10 nm).

BRET has been extensively used to study a wide range of protein interactions in real-time, in various cellular compartments, particularly ligand-induced regulation and oligomerization of G protein-coupled receptors (GPCRs) (4-7). The applications have also been extended to analyze the dynamic interactions involved in the regulation of the insulin receptor (IR) and fibroblast growth factor receptor (FGF-R) signaling in real time (8-10). Applications of BRET in imaging protein-protein interactions have also been described (11, 12). Brown *et al* used BRET to show in living cells that GHR is present as a pre-formed dimer at the cell surface. This demonstrates the potential of using this technology to analyze aspects of GHR physiology (13).

In this paper we used BRET to assess in living cells crucial interactions involved in the regulation of GHR endocytosis. GHR endocytosis provides a way of controlling the GH sensitivity of the cells. In the past we have described key players involved in this process. The ubiquitin-dependent endocytosis motif (UbE) in the cytoplasmic tail of the GHR (14) binds $SCF^{\beta TrCP}$, which is likely responsible for polyubiquitination events necessary for the endocytosis of the receptor (15). Recently, an important role of JAK2 in GHR endocytosis/degradation regulation has been reported (16, 17). The constitutive binding of JAK2 to the GHR stabilizes GHR at the cell surface by inhibiting its endocytosis. In our model JAK2 detachment from GHR precedes GHR endocytosis (17). Therefore, JAK2 and βTrCP have opposite regulatory roles: JAK2 prevents and βTrCP promotes GHR endocytosis. We used BRET technology to characterize and understand the interplay of these two interactors in real time.

In this study we describe the validation of the constructs of GHR, JAK2 and βTrCP fused to the "BRET tags", and the BRET assay development (Fig. 1). BRET data showed that JAK2 is constitutively bound to GHR and that GH stimulation decreased BRET signal from GHR-JAK2 interaction. This finding is in agreement with a scenario where GH induces JAK2 detachment from GHR. The GHR-βTrCP interaction was also measured constitutively but was not influenced by GH stimulation. The question whether JAK2 and βTrCP compete for GHR remained unanswered. We discuss the potential applications of our assay as a platform for drug screening to find compounds able to manipulate GH sensitivity of the cells.

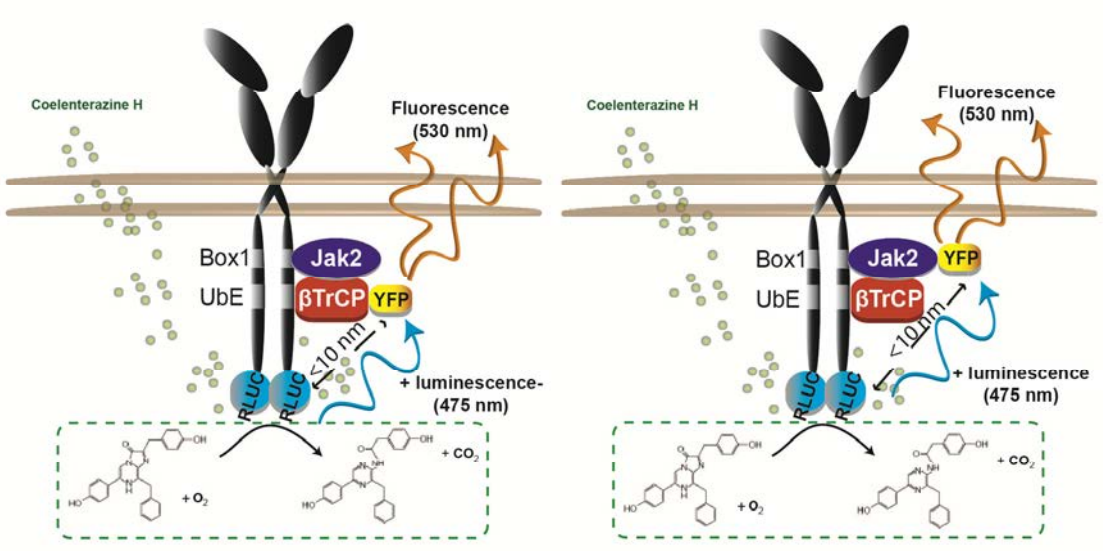

Fig. 1. Schematic representation of the experimental set up. GHR-JAK2 and GHR-βTrCP interactions were monitored using the BRET technology. Proteins need to be fused to BRET tags. When the donor tag (RLUC) oxidizes its cell permeable substrate coelenterazine H, luminescence (475 nm) is released, which is able to excite the acceptor tag (YFP), resulting in emission of fluorescence (530 nm). A plate reader is used to detect the two wavelengths (475 and 530 nm) simultaneously with high sensitivity. Both interactions, GHR-JAK2 and GHR-βTrCP, are well validated and therefore it should be possible to bring the donor and acceptor tags fused to these interaction partners in a distance of less than 10 nm to allow the transfer of energy to occur.

Materials and Methods

Reagents and DNA constructs. GHR antibodies recognizing the membrane-proximal amino acid residues 271–318 (anti-T) and 327-493 (anti-B), were raised in rabbit (18, 19). Anti-GFP antibody was purchased from Roche Applied Sciences (Woerden, The Netherlands), Anti-actin (Clone C4) from MP Biomedicals Inc, and Monoclonal anti-Flag (M2) from Sigma (Saint Louis, MO, USA). Polyclonal anti-JAK2 was described previously (20), as well as polyclonal anti-βTrCP1(15). Goat anti-mouse IgG Alexa 680 was from Molecular Probes, and goat anti-rabbit IgG IRDye800 from Rockland Immunochemicals Inc (Gilbertsville, PA, USA). Human GH was a kind gift from Eli Lilly Research Labs (Indianapolis, IN, USA). Protein A-beads were from Repligen (Waltham, MA, USA). ViviRen was purchased from Promega (Madison, WI, USA). Full-length rabbit GHR cDNA in pcDNA3 has been described before (19). The Flag-tagged wild type Jak2 constructs were generous gifts from Prof. Carter-Su (University of Michigan, Ann Arbor, USA). Jak2 (Y119E) and GHR F327A were generated using the Quickchange mutagenesis kit from Stratagene (Santa Clara, CA, USA). The Flag-tagged βTrCP2 in pcDNA3 were generous gifts of Prof. Tomoki Chiba (Tokyo Metropolitan Institute of Medical Science, Tokyo, Japan). The Renilla Luciferase (RLUC) expression vector was a kind gift from Prof. Bouvier (Université de Montrèal, Montrèal, Canada).

Constructs. For creating the RLUC-pcDNA3 construct we first amplified the RLUC coding region with the forward primer GATCGCGGCCGCATGACTTCGAAAGTTTATG and the reverse primer GATCTCTAGATTATTGTTCATTTTTGAGAACTCG. All primers were purchased from Sigma (Saint Louis, MO, USA). The RLUC fragment was then ligated into pcDNA3 (Invitrogen, Groningen, The Netherlands) using Not1 and Xba1 restriction sites. For creating the YFP-pcDNA3 construct the YFP sequence was first amplified from EYFP-N1 vector (Clontech, Mountain View, CA, USA), using the forward primer GATCGCGGCCGCATGGTGAGCAAGGGCG and the reverse primer GATCTCTAGATTACTTGTACAGCTCGTCC. The YFP fragment was then ligated into pcDNA3 using Not1 and Xba1 restriction sites. The same procedure was used to create GFP-pcDNA3 vector. GHR cDNA was amplified from GHR-pcDNA3 expression vector (21) with the forward primer, GATCGGTACCGCCACCATGGATCTCTGGCAG and the reverse primer GATCCCAGTGTGCTGGTGGCAAGATTTTGTTCAG. The obtained PCR product was cloned in

frame with the RLUC or YFP (and GFP) coding sequence in the previously generated RLUC-pcDNA3 vector or YFP /GFP-pcDNA3 vector, using Kpn1 and BstX1 restriction sites. Expression from these vectors results in C-terminally RLUC tagged GHR (GHR-RLUC) or C-terminally YFP/GFP tagged GHR (GHR-YFP/GFP). GHR F327A pcDNA3 construct was generated as described before (14), and it was cloned in the BRET vectors in the same way as for the WT GHR.
The RLUC-pcDNA4 construct was generated by ligating the RLUC fragment, amplified with the forward primer, GATCCTTAAGGCCACCATGACTTCGAAAG, and the reverse primer GATCGGTACCTTGTTCATTTTTGAGAACTCG, into the doxycycline inducible promoter pcDNA4/TO (Invitrogen) using Afl2 and Kpn1 restriction sites. To generate the YFP-pcDNA4, first the YFP sequence was amplified from EYFP-N1 vector, using the forward primer GATCCTTAAGGCCACCATGGTGAGCAAG, and the reverse primer, GATCGGTACCCTTGTACAGCTCGTCCATGC. The PCR product was then cloned into pcDNA4/TO using Afl2 and Kpn1 restriction sites. JAK2 (WT) and JAK2 (Y119E) were amplified from pcDNA3-flag-JAK2 (WT) and pcDNA3-Flag-JAK2 (Y119E) expression vectors, respectively, using the forward primer GATCGGATCCATGGGAAATGGCCTGCC and reverse primer GATCGCGGCCGCCTATACTGTCCCGGATTTGATCC. The obtained PCR products were cloned in frame with the RLUC and YFP coding sequence in the previously generated RLUC-pcDNA4 and YFP-pcDNA4 vector, using the restriction sites BamH1 and Not1. Expression from these vectors resulted in N-terminally RLUC tagged JAK2 (RLUC-JAK2 WT or RLUC-JAK2 Y119E) or in N-terminally YFP tagged JAK2 (YFP-JAK2 WT or YFP-JAK2 Y119E), respectively. βTrCP2 was amplified from pcDNA3-flag-βTrCP2 expression vector using the forward primer, GATCGGATCCATGGAGCCCGACTCGGTG, and the reverse primer, GATCGCGGCCGCTTATCTAGAGATGTAAGTGTATG. The obtained PCR product was cloned in frame with the RLUC and YFP coding sequences in the previously generated RLUC-pcDNA4 and YFP-pcDNA4vectors, respectively, using the restriction sites BamH1 and Not1.

Cell culture, transfections and stable generation of stable cell lines. HEK293 cells, stably expressing the Tetracycline Repressor (HEK293-TR), were a kind gift from Dr. Madelon Maurice (University Medical Centre Utrecht, Utrecht, The Netherlands). HEK293-TR cells were grown in Dulbecco's modified Eagle's medium (DMEM) supplemented with 10% fetal calf serum, 100 units/ml penicillin, 0.1 mg/ml streptomycin and 12 μg/ml Blasticidin S (MP Biomedicals). Twice a week the cells were washed with phosphate-buffered saline (PBS), detached from the flask with trypsin-EDTA (Invitrogen) diluted in fresh growth medium, and split into new culture flasks. DNA transfections were performed using FuGene 6 (Roche, Applied Sciences). Seventy percent confluent cultures in 6-wells plates were transfected with 1 μg of DNA, according to the manufacturer's protocol. After 24 hours the cells were used for expression/functionality tests, or trypsinized and seeded for BRET measurements.

For creating stable cell lines, HEK293-TR cells were transfected with GHR WT-RLUC-pcDNA3 or GHR F327A-RLUC construct using Fugene 6 (Roche, Applied Sciences, Almere, The Netherlands), according to the manufacturer's instructions. The selection of clones expressing GHR WT-RLUC or GHR F327A-RLUC was done using Geneticin (Invitrogen). Double stable cell lines expressing GHR-RLUC and YFP-JAK2 (WT or Y119E) were generated, by transfecting YFP-JAK2 (WT or Y119E)-pcDNA4 in the previously generated cell line expressing GHR-RLUC. For the selection of clones expressing GHR-RLUC together with YFP-JAK2 (WT or Y119E), zeocin (Invitrogen) was used. Double stable cell lines expressing GHR WT-RLUC or GHR F327A-RLUC together with YFP-βTrCP were generated, by transfecting YFP- βTrCP-pcDNA4 in the previously generated cell lines expressing GHR WT-RLUC or GHR F327A-RLUC. Zeocin was used for selection of the clones. The generated BRET cell lines were maintained in DMEM high glucose (4.5 g/l) (Invitrogen), supplemented with 10% FCS (Invitrogen), 100 U/ml penicillin (Invitrogen), 100 μg/ml streptomycin (Invitrogen), 600 μg/ml Geneticin (Invitrogen) and 100 μg/ml zeocin (Invitrogen). The expression of YFP-JAK2 and YFP- βTrCP was induced by addition of 1 μg/ml doxycycline (Clontech) 24 hours before the experiment.

BRET measurements. 24 hours prior to the measurements, cells were washed with PBS, and detached with trypsin-EDTA. $4x10^4$ cells were reseeded in DMEM phenol-red free medium (Gibco),

containing 10 % FCS, 100 U/ml penicillin, 100 µg/ml streptomycin per well of a 96-well plate (white cell culture plate Nunc cat. no. 136101, Roskilde, Denmark), in the presence or absence of doxycycline. Cells treated in the same way, were seeded $2x10^5$ per well in 24 wells plates and lysed 24 hours later to evaluate the expression levels of the BRETconstructs used. Before the BRET measurements, the culture medium was replaced by BRET assay buffer (PBS 0.1 % glucose, 25 mM Hepes, pH 7.4). 200 ng/ml human GH (hGH) was added to the wells 30 seconds before the measurement started for indicated periods of time. The substrate ViviRen (Promega) was then added to each well in a final concentration of 60 µM. Repeated readings at 475 nm and 535 nm (15 cycles, 0,5 seconds interval time, 15 seconds per reading), for donor and acceptor emission, respectively, were taken at 37°C with a Fluorstar Optima Fluorescence Plate Reader (BMG LABTECH). BRET signal was expressed in milliBRET Units, as defined previously (4). A BRET unit is the signal ratio 535/475 nm obtained when the donor and acceptor are expressed (in presence of doxycycline), subtracted from the ratio obtained under the same experimental conditions, when only the donor partner (fused to RLUC) is expressed (in absence of doxycycline). When indicated, two-way ANOVA was performed with the statistical program SPSS 15.0. The factors were compared in the presence/absence of GH and at the time periods after GH addition.

Confocal microscopy. Cy3-GH was prepared using a fluorolink-Cy3 label kit according to the manufacter's protocol (Amersham Biosciences, Roosendaal, The Netherlands). Transfected HEK293-TR cells, grown on coverslips, were incubated for 30 min with Cy3-GH (180ng/ml), washed with PBS and fixed for 30 min in 4% paraformaldehyde in PBS. After fixation, the cells were embedded in Mowiol, and confocal pictures were taken using LeicaTCS 4D system.

Cell lysis and immunoprecipitations. For GHR-JAK2 co-immunoprecipitations, cells were lysed in 20 mM Tris pH 8.0, 150 mM NaCl, 0.5% NP40, 1 mM PMSF, 10 µg/ml aprotinin, 10 µg/ml leupeptin. After 20 min, cell extracts were centrifuged for 5 min to separate nuclei. Supernatants were incubated for 2 hours with anti-GHR (anti-T) antibodies, after which they were incubated with protein A beads. To analyze the expression levels of the donor/acceptor BRET pairs, the same cells as the ones used in the BRET measurements were lysed in lysis buffer containing 1% Triton X-100, 1 mM EDTA, 1 mM PMSF, 10 µg/ml aprotinin, 10 µg/ml Leupeptine, 1 mM Na_3VO_4 and 100 mM NaF in PBS. The samples were subjected to SDS-PAGE, followed by the transfer of the proteins to an Immobilion-FL PVDF membrane (Millipore, Amsterdam, The Netherlands). The membranes were blocked with Odyssey blocking buffer (Li-Cor Biosciences, Lincoln, NE, USA) diluted two times with PBS for 1 hour at room temperature, followed by incubation with the indicated primary antibodies for 1 hour. After washing in PBS 0.1% Tween-20, membranes were incubated for 1 hour with secondary antibody. The detection and analysis of the immunoblots was performed with an Odyssey infrared imaging system (Li-Cor Biosciences, Lincoln, Nebraska).

Results

Expression test and validation of the BRET constructs

BRET measurements require the proteins of interest to be fused to the bioluminescent donor or fluorescent acceptor(2). "*Renilla* luciferase" (RLUC) was fused to the proteins of interest as donor tag, while "Yellow Fluorescent Protein" (YFP) was used as an acceptor tag. Fusing of the "BRET tags" must occur without compromising protein function. βTrCP and Jak2 (WT or Y119E mutant) were fused at their N-termini to YFP (YFP- βTrCP, YFP-Jak2 WT or Y119E) and RLUC (RLUC- βTrCP and RLUC-Jak2 WT or Y119E) tags, and cloned under the control of a doxycycline inducible promoter. Without doxycycline addition, transient transfection of the constructs in HEK293-TR cells resulted in a very low expression of βTrCP and JAK2 fusion proteins. Doxycycline addition induced a strong expression (Fig. 1A). GHR WT and F327A mutant were fused at their C-termini to RLUC (GHR WT/F327A-RLUC) and YFP (GHR WT/F327A-YFP), the tags faced the cytoplasm. In addition, a "Green Fluorescent Protein" (GFP) tagged GHR was created as a potentially useful tool. GHR fusion constructs were expressed at comparable amounts with the untagged GHR constructs when transiently expressed in HEK293-TR (Fig. 2B). In all cases, two major bands were visible, where the lower band represents the precursor form of the GHR in the endoplasmatic reticulum (ER) and the upper diffuse band representing the mature GHR protein at the cell surface. This indicates that the tagged GHR versions fold and mature properly. As the GHR F327A mutant does not efficiently endocytose due to impaired function of the UbE motif (14), the mature form of the GHR accumulates at the cell surface (Fig. 2B, compare lanes 1 and 2). GHR F327A-RLUC, –GFP, and –YFP also have an increased ratio mature:precursor when compared to their respective WT. This indicates that the tagged GHRs behave normal, particularly in terms of endocytosis regulation. In Fig. 2C, cells transfected with GHR WT internalized Cy3-GH normally, as seen by small punctae labeling inside the cells, indicating that GHR WT fusion proteins were efficiently endocytosed. GHR F327A mutant did not internalize and the bound Cy3-GH remained at the plasma membrane. As previously shown, endocytosis of GHR is dependent on the interaction of the UbE with βTrCP(15). The results in Fig. 2B and 2C show that the interaction of βTrCP with the GHR WT fusions is intact, while that with GHR F327A fusions is not, indicating that the fusion proteins function is preserved. Another aspect of the regulation of GHR is its interaction with JAK2. We recently reported that the interaction of JAK2 with GHR results in endocytosis inhibition (17). To validate the GHR fusion proteins for their functional interaction with JAK2, HEK293-TR cells were transiently co-transfected with the GHR fusion constructs together with Jak2. Jak2

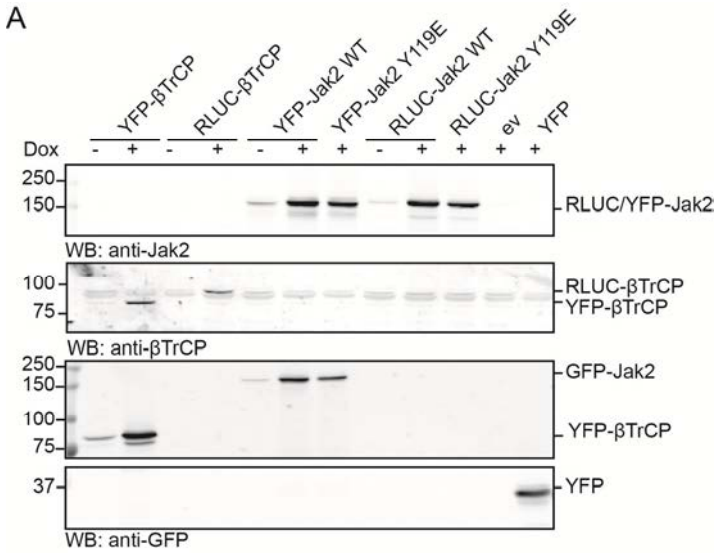

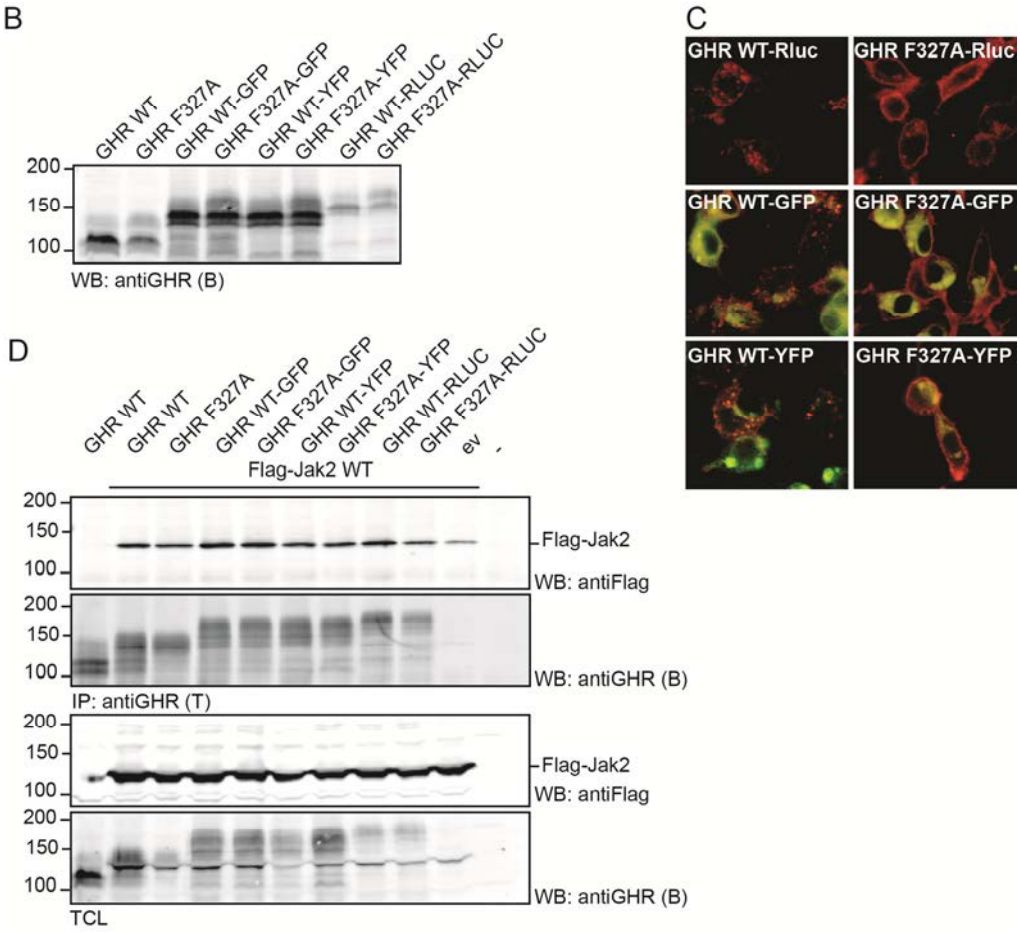

Fig. 2. Expression test and validation of the BRET constructs. (A) HEK293-TR cells were transiently transfected with the tagged forms of βTrCP (YFP-, RLUC-), JAK2 WT and JAK2 Y119E (YFP-, RLUC-), and pcDNA4-YFP. When indicated, the expression of the constructs was induced for 24 hours with doxycycline (Dox), and the cells were lysed. Equal aliquots from the total cell lysates were analyzed by western blotting (WB) with the indicated antibodies. ev, empty vector. **(B)** HEK293-TR cells were transiently transfected with untagged and tagged forms of GHR WT and GHR F327A (-GFP, -YFP and -RLUC). After 24 hours the cells were lysed, and equal aliquots of total cell lysates were analyzed by western blotting with anti-GHR (B). **(C)** HEK293-TR cells, cultured on coverslips, were transiently transfected with the tagged forms of GHR WT and F327A (-GFP, -YFP and -RLUC). After 24 hours the cells were incubated with Cy3-GH 180 ng/ml for 30 min at 37°C, and fixed in paraformaldehyde. Representative confocal pictures were taken. **(D)** HEK293-TR cells were transiently transfected with GHR WT, F327A, and the indicated tagged forms (-GFP, -YFP, -RLUC) together with Flag-tagged JAK2 (Flag-JAK2). GHR complexes were immunoprecipitated with anti-GHR (T). The immunoprecipitates were subjected to western blotting and detected with anti-Flag antibody (for Flag-JAK2 detection), and anti-GHR (B). Equal aliquots of total cell lysates (TCL) were also analyzed by western blotting with the same antibodies. ev, empty vector; IP, immunoprecipitations

overexpression resulted in the stabilization of mature GHR (Fig. 2D, 4th panel, compare lane 1 and 2). All tagged GHR fusions proteins have an increased ratio mature:precursor in the case of Jak2 overexpression (Fig. 2D, 4th panel), when compared to the situation where Jak2 was not overexpressed (Fig. 2B). By immunoprecipitating GHR complexes from the cell lysateswe confirmed that all the fusion proteins are able to interact with Jak2 (Fig. 2D, 1st panel).We conclude that the fusion proteins created for the analysis of GHR-JAK2 and GHR-βTrCP interactions by BRET are functional and properly expressed.

Interactions GHR-βTrCP, and GHR-JAK2 can be measured specifically, *in vivo*, using BRET.

GHR, Jak2 and TrCP fusion proteins were tested for their ability to elicit BRET signals. HEK293-TR cells were transiently transfected with GHR fusion constructs together with either βTrCP or Jak2 fusion constructs as indicated in Fig. 3A, 1-8. The expression of the transfected proteins was verified by western blotting (Fig. 3B). A fusion protein containing an RLUC and YFP separated by a sequence

of four amino acid residues (DVED) was used as a positive control (4). The BRET signal of this positive control was corrected by the condition of donor only (condition in which only RLUC tag was expressed), resulting in a BRET ratio of 341 mBU. None of the combinations of our fusion proteins resulted in a BRET ratio of such a magnitude. Presumably, the distance between the donor and the acceptor in the positive control leads to the highest possible resonance. The BRET ratios obtained for all the combinations are shown in Fig. 3A, 1-8.

Expression of GHR WT-RLUC with YFP-βTrCP resulted in a BRET ratio approximately 3 times higher than the one obtained when GHR F327A-RLUC construct was expressed with YFP-βTrCP (Fig. 3A, compare 1 and 2) reflecting a decreased interaction of GHR F327A with βTrCP, as expected. Specific BRET signals were also measured when the same interaction was addressed by co-expressing RLUC-βTrCP in combination with either GHR WT-YFP (5) or GHR F327A-YFP (6). Although the measured BRET ratios were low, the assay is able to differentiate the interaction of βTrCP with GHR WT, with a higher BRET ratio, from that with the GHR F327A, with a lower BRET signal. This confirms the functionality of these fusion proteins and validates the assay to address GHR-βTrCP interaction in real time.

To address the specificity of the BRET measurements for the GHR-JAK2 interaction, Jak2 Y119E was used as a negative control. Phosphorylation of Y119 causes JAK2 dissociation from the GHR (22). Y119E mutation works as a phosphomimetic and therefore prevents JAK2 binding to GHR (22). Expression of GHR-RLUC with YFP-Jak2 WT resulted in a BRET ratio 10 times higher than that with YFP-Jak2 Y119E (Fig. 3A, compare 3 and 4). The same interaction was addressed by expressing GHR-YFP together with RLUC-Jak2 WT or Y119E (Fig. 3A, compare 7 and 8).

The specificity of our measurements was judged by dividing the BRET signal obtained for the WT situations (GHR WT-βTrCP and GHR-Jak2 WT), with that of the respective negative controls (GHR F327A- βTrCP and GHR-Jak2 Y119E) (Fig. 3A). According to this criterion, for both cases, placing the RLUC tag on GHR and the YFP tag on βTrCP or Jak2 resulted in a more specific BRET ratio.

In Fig. 3A we showed that in transient transfections, the combination of GHR-RLUC with either βTrCP-YFP or Jak2-YFP resulted in a specific BRET signal. However, BRET measurements in stable cell lines may be advantageous since all the proteins are expressed homogenously in the cell population. In addition, that will enable high-throughput screening. HEK293-TR cell lines stably expressing GHR WT-RLUC (clone A2) and GHR F327A-RLUC (clone B4) were generated. These cell lines, stably expressing GHR WT-RLUC and GHR F327A-RLUC as donor, were then transiently transfected with YFP-βTrCP as acceptor; the measured BRET ratios were 19 and 10 mBU respectively (Fig. 3C, 1st and 2nd bar). The transient overexpression of YFP-Jak2 WT in GHR WT-RLUC cell line resulted in a BRET ratio of 24 mBU, and if YFP-Jak2 Y119E was overexpressed instead, the measured BRET was 1 mBU (Fig. 3C, 3rd and 4th bar). In Fig. 3D the expression levels of the proteins were analyzed. The BRET ratio from the stable cell lines expressing GHR-RLUC constructs was specific and therefore they were used to create double stable cell lines that simultaneously expressed donor (GHR WT/ F327A –RLUC) and acceptor proteins (βTrCP-YFP, Jak2 WT-YFP, or Jak2 Y119E –YFP). These double stable cell lines were used in the BRET measurements described in the next sections.

A

	Acceptor	Donor	BRET (mBU)
1	YFP-βTrCP2	GHR WT-RLUC	38
2	YFP-βTrCP2	GHR F327A-RLUC	14
3	YFP-Jak2 WT	GHR WT-RLUC	22
4	YFP-Jak2 Y119E	GHR WT-RLUC	2
5	GHR WT-YFP	RLUC WT-βTrCP	57
6	GHR F327A-YFP	RLUC WT-βTrCP	37
7	GHR WT-YFP	RLUC-Jak2 WT	43
8	GHR WT-YFP	RLUC-Jak2 Y119E	13
	RLUC-DVED-YFP	-	341

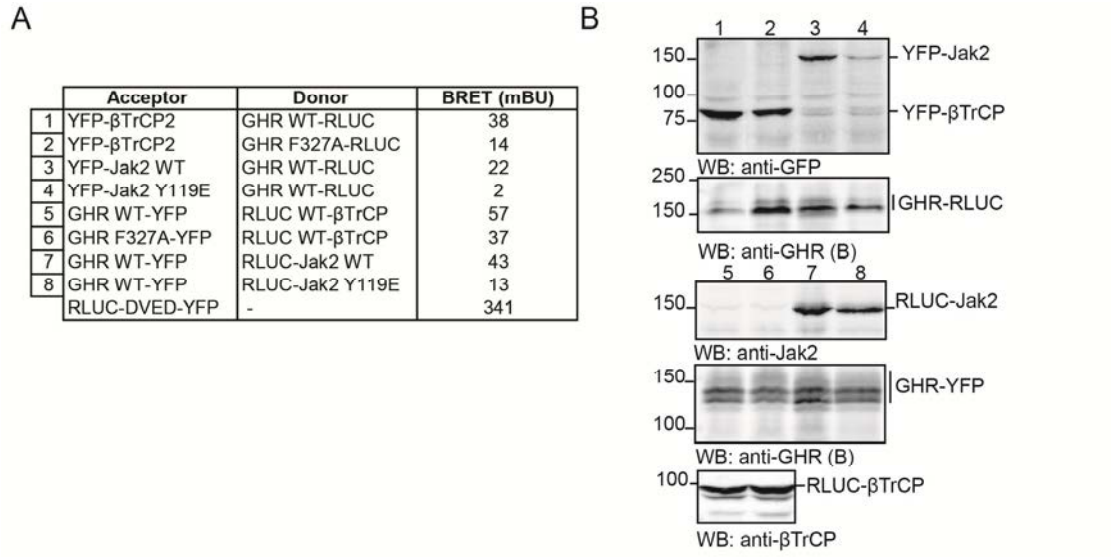

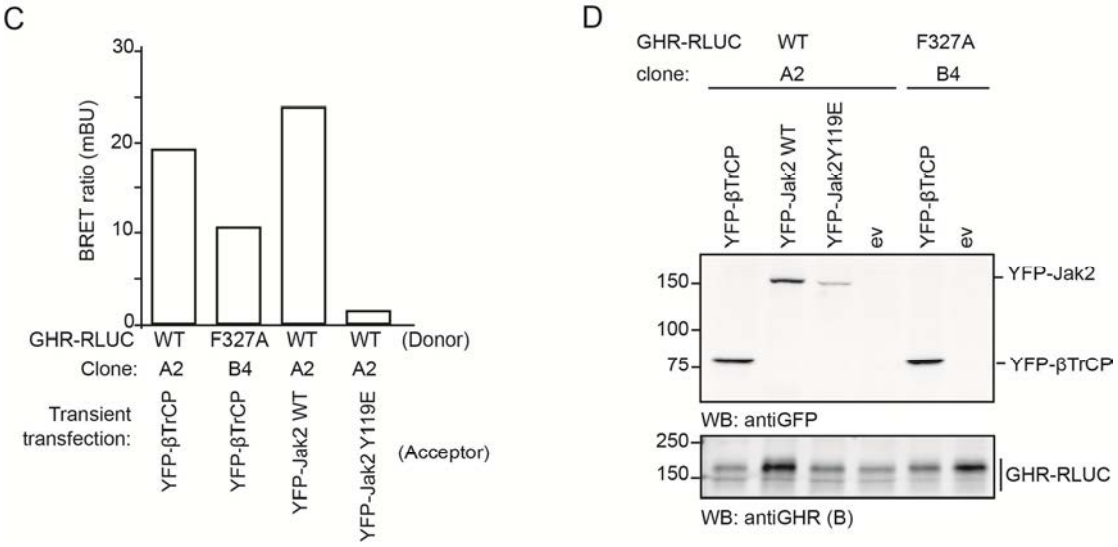

Fig. 3. Interactions GHR-βTrCP, and GHR-JAK2 can be measured specifically, *in vivo*, using BRET. (A) HEK293-TR cells were transiently transfected with all possible combinations of donor and acceptor molecules. RLUC-DVED-YFP was used as positive control. The transfected cells were cultured 24 hours in presence of doxycycline, after which BRET measurements were performed. The table shows the BRET ratios expressed in mBU, obtained for each donor:acceptor combination (1-8). **(B)** Representative cells from the cells subjected to BRET measurements showed in A were lysed. Equal aliquots of the cell lysates (1-8) were analyzed by western blotting (WB), using the indicated antibodies. **(C)** Stable cell lines expressing GHR WT-RLUC (A2) or GHR F327A-RLUC (B4) were transiently transfected with YFP-βTrCP, YFP-JAK2 WT, or YFP-JAK2 Y119E. The transfected cells were cultured 24 hours in presence of doxycycline, after which BRET measurements were performed. The graph shows BRET ratios expressed in mBU. **(D)**. Cell cultures as subjected to BRET measurements shown in C were grown in parallel, then lysed and analyzed by western blotting (WB), using the indicated antibodies.

GH decreases BRET ratio for GHR-JAK2 interaction, by inducing JAK2 release from GHR.

To investigate the dynamics of the GHR-Jak2 interaction with BRET, HEK293-TR cell lines stably expressing GHR-RLUC with Jak2-YFP (WT or Y119E) were used. In the absence of doxycycline, hardly any YFP-Jak2 acceptor protein is expressed (Fig. 4B, lane 1), and, therefore, it is considered a control condition of donor only (GHR-RLUC). Addition of

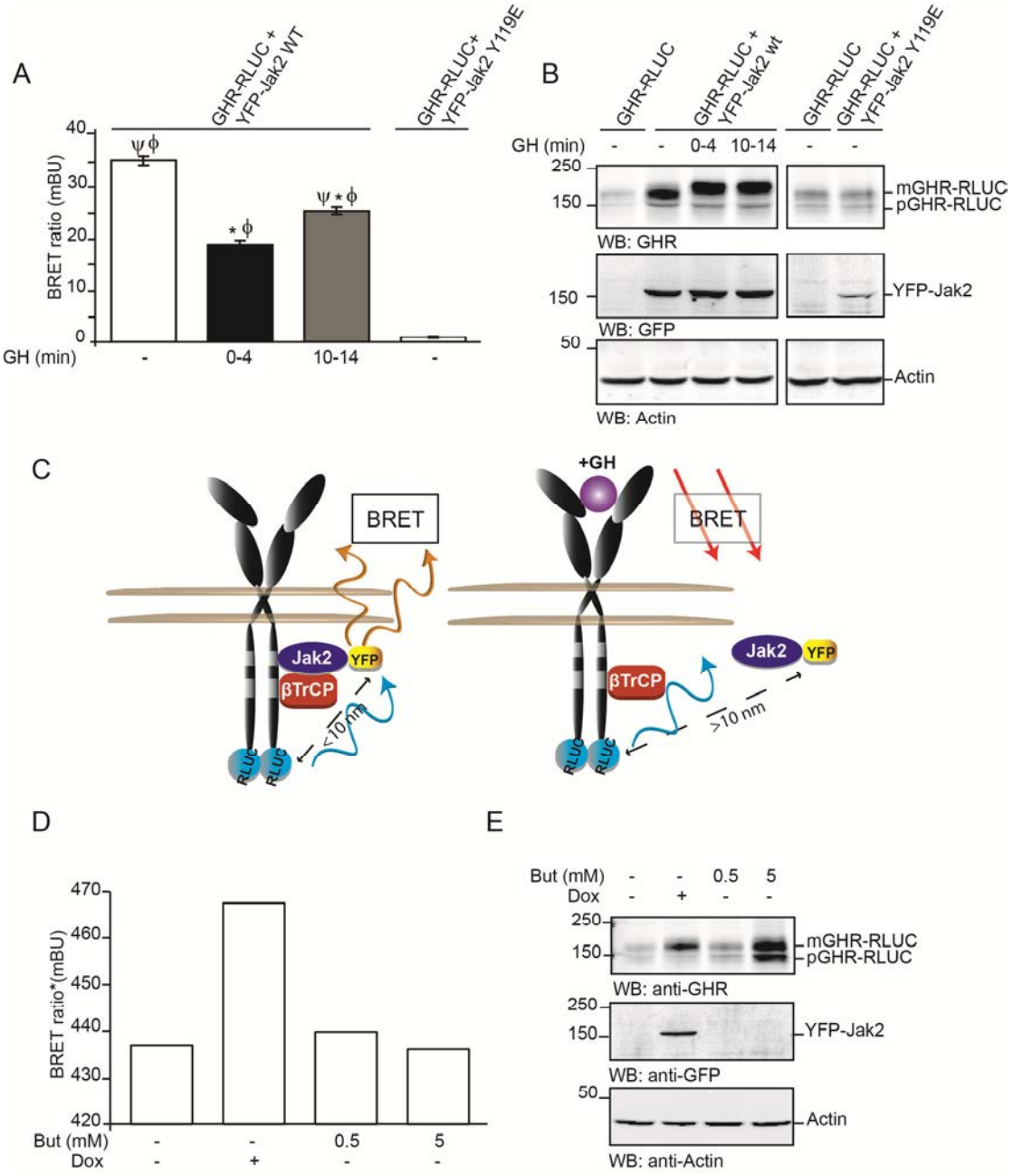

Fig. 4. GH decreases BRET ratio for GHR-JAK2 interaction, by inducing JAK2 release from GHR. **(A)** HEK293-TR stable cell lines expressing GHR-RLUC and YFP-JAK2 (WT or Y119E) were seeded 24 hours before the measurements; doxycycline was added in order to stimulate the expression of YFP-JAK2 constructs. BRET measurements were started immediately after GH addition (interval t = 0-4 min), or 10 min later (interval t = 10-14 min). The graph shows BRET ratios expressed in mBU, representative of eight independent measurements ± S.E.M. (*) significantly different from GHR-RLUC+YFP-JAK2 WT, minus GH condition, $p<0.01$; Φ significantly different from GHR-RLUC+YFP-JAK2 Y119E condition, $p<0.01$; ψ significantly different from GHR-RLUC+YFP-JAK2 WT, plus GH [0-4 min] condition, $p<0.01$). **(B)** Cell cultures as subjected to BRET measurements shown in A were grown in parallel, then lysed and analyzed by western blotting, using the indicated antibodies. Data are representative of three independent experiments. **(C)** Scheme summarizing the effect of GH stimulation on GHR-JAK2 interaction. **(D)** HEK293-TR stable cell lines expressing GHR-RLUC and YFP-JAK2 were seeded 24 hours before the measurements; doxycycline was added when indicated in order to stimulate the expression of YFP-JAK2. When indicated, butyrate (But) was added to the cells overnight, in 0.5 or 5 mM concentration, in order to stimulate the expression of GHR-RLUC. The graph shows BRET ratios expressed in mBU, without subtracting the condition "donor only" (*). **(E)** Parallel cell cultures as shown in D were lysed and analyzed by western blotting, using the indicated antibodies.

doxycycline resulted in YFP-Jak2 expression that induced accumulation of GHR-RLUC (Fig. 4B, compare lanes 2-4 with lane 1). Expression of the binding mutant, YFP-Jak2 Y119E, did not stabilize

GHR-RLUC, consistent with lack of interaction between the two proteins (Fig. 4B, lanes 5 and 6). The obtained BRET ratios for each condition are shown in the Fig. 4A. In the absence of GH, a clear interaction between GHR-RLUC and YFP-Jak2 was detected (Fig 1A, 1st bar), consistent with the constitutive association of JAK2 with the cytoplasmic tails of GHR. Hardly any BRET signal could be detected in the cell line where YFP-Jak2 Y119E was expressed, indicating a lack of interaction with GHR-RLUC. It is important to note that the expression levels of the YFP-Jak2-Y119E are much lower than YFP-Jak2 WT, which can be justified by recent studies in the group, where we verified that Jak2-GHR interaction results in reciprocal stabilization of both proteins (data not shown, Nespital T., manuscript in preparation). Nevertheless, when we calculated the donor:acceptor ratios for both BRET pairs, GHR-RLUC:YFP-Jak2 WT and GHR-RLUC:YFP-Jak2 F327A, similar values were obtained. For this reason, in spite of the different expression levels, the BRET ratios can be compared.

Next, the effect of GH stimulation on GHR-JAK2 interaction was evaluated. Addition of GH to the cell line expressing GHR-RLUC and YFP-Jak2 WT elicited a fast reduction (time interval: 0-4 min) of the BRET signal (of 46 %) when compared to basal state. After 10 min, the BRET ratio recovered to the level of 65 % of the basal signal. The stimulation with GH was sufficient to cause a decreased migration of the mature GHR in the gel probably due to GHR phosphorylation (Fig. 4B, lanes 3 and 4). These results support a scenario where, at early time points after GH stimulation, JAK2 dissociates from the receptor due to its phosphorylation, but soon after it re-associates in a dynamic fashion, probably due to phosphorylation/dephosphorylation cycles. Since the expression of Jak2 affects the levels of GHR, neither saturation nor competition assays could be performed. Therefore, no quantitative data regarding the interaction could be obtained (17). A schematic representation of the contribution of the BRET technology to the model is shown in Fig. 4C.

When calculating the BRET ratio, a correction was made by subtracting the background BRET signal of the "donor only" condition, from the BRET value obtained when both donor and acceptor were expressed. For the analysis of the GHR-RLUC/YFP-Jak2 interaction, in the condition "donor only" the expression levels of GHR-RLUC were much lower than when the expression of YFP-Jak2 was induced by doxycycline. For an appropriate correction, the expression levels of GHR-RLUC should be the same in both conditions. To increase expression levels of GHR-RLUC in the condition "donor only", butyrate was added (19) at two concentrations (0.5 and 5 mM). YFP-Jak2 expression, induced by doxycycline, resulted in intermediate GHR-RLUC levels between the two concentrations (Fig. 4E, compare lane 2 to lanes 3 and 4). Importantly, different expression levels of GHR-RLUC in the three "donor only" conditions resulted in the same BRET signal (Fig. 4D, bar 1, 3 and 4). Thus, the correction of the BRET signal as performed in GHR-RLUC/YFP-Jak2 interaction analysis is reliable. Taken together, we conclude that the dynamics of the interaction between GHR and JAK2 can be measured specifically in the stable cells lines.

GH stimulation did not change BRET ratio for the GHR-βTrCP interaction

The dynamics of the interaction GHR-βTrCP was analyzed by BRET in HEK293-TR stable cell lines expressing YFP-βTrCP with either GHR WT-RLUC (clones A2.1.1 and A2.1.4) or GHR F327A-RLUC (clone B4.1.4). The expression of YFP-βTrCP was induced by addition of doxycycline (Fig. 5B, lanes 2, 4, 6 and 8). Without doxycycline addition, hardly any YFP- βTrCP acceptor protein is expressed (Fig. 5B, lanes 1, 3, 5 and 7), and, therefore, it is considered a control condition of donor only (GHR-RLUC WT or F327A). In the absence of GH, the expression of GHR WT-RLUC together with YFP-βTrCP resulted in low BRET signal (ratio) of ~10 mBU in both clones (Fig. 5A, 1st and 2nd bar), while the BRET signal was approximately 5 times lower when GHR F327A-RLUC was expressed together with YFP-βTrCP (Fig. 5A, compare 1st bar with 3rd bar). Herewith we confirm that GHR-βTrCP interaction is dependent on the UbE domain and occurs constitutively. Unfortunately, as the BRET ratios were very low, the sensitivity of the assay is low, and this may hamper drawing certain conclusions. For instance, the assay is not sensitive enough to detect the significant binding of βTrCP occurring through the DSGxxS motif in basal conditions (*da Silva Almeida AC*, manuscript submitted); this should be detectable in the cell line expressing GHR F327A-RLUC together with YFP-βTrCP.

GH stimulation causes a faster GHR endocytosis (23, 24). Since βTrCP is essential for this process, we hypothesized that GH-induced JAK2 detachment from GHR (Fig. 4) results in increased

GHR-βTrCP interaction (17). In the results reported in Fig. 4, 5 min of GH stimulation resulted in Jak2 detachment, and after 10 min Jak2 interaction with the receptor is partially reestablished. If our hypothesis is correct, we would predict the effects of GH stimulation on GHR-βTrCP interaction to occur in the interval 5-10 minutes. Cells expressing GHR WT-RLUC together with YFP-βTrCP (clone A2.1.1) were stimulated for 5 min with GH, after which BRET measurements were started (5-9 min GH stimulation). GH stimulation did not change the BRET signal for the GHR-βTrCP interaction. Based on this we conclude that GHR-βTrCP interaction is not affected by GH stimulation and JAK2 detachment. This would imply that JAK2 and βTrCP are able to bind GHR dimers simultaneously.

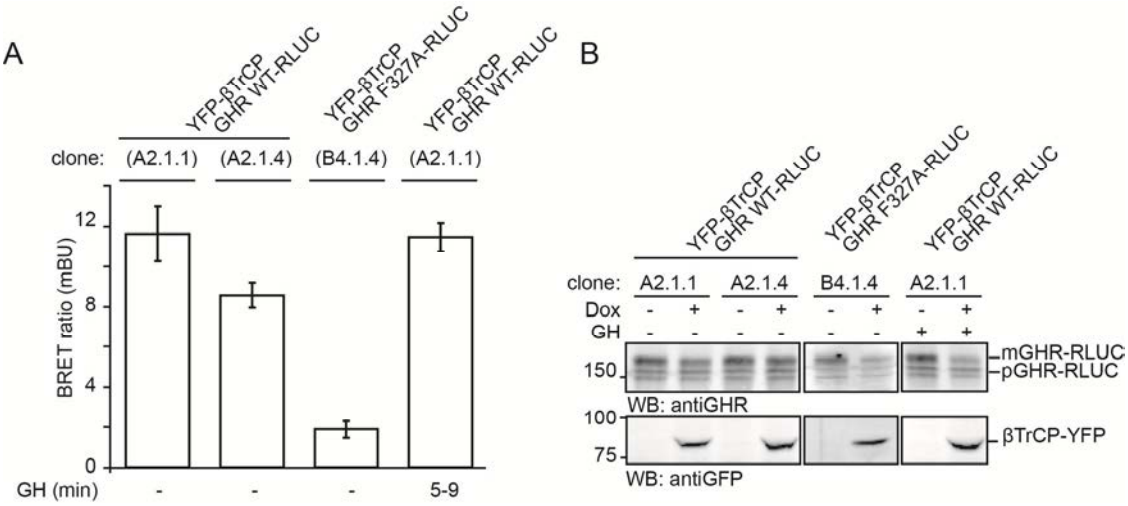

Fig. 5. GH stimulation did not change BRET ratio for the GHR-βTrCP interaction. (A) HEK293-TR stable cell lines expressing GHR-RLUC, WT (clone A2.1.1 or clone A2.1.4) or F327A (clone B4.1.4) together with YFP-βTrCP were seeded 24 hours before the measurements; doxycycline was added in order to stimulate the expression of YFP-βTrCP. When indicated 180 ng/ml GH was added and 5 min after, the BRET measurements were started (5-9 min). The graph shows BRET ratios expressed in mBU, representative of three independent measurements ± S.E.M. **(B)** Cells as subjected to BRET measurements shown in A were grown in parallel, then lysed and equal aliquots of the cell lysates were analyzed by western blotting, using the indicated antibodies. Data are representative of three independent experiments. mGHR, mature GHR; pGHR, precursor GHR in the endoplasmic reticulum; Dox, doxycycline.

Interplay of JAK2 and βTrCP on GHR

JAK2 and βTrCP are key players in the regulation of GHR endocytosis. We recently found that association of JAK2 to the receptor inhibits its endocytosis (17). One explanation could be that the binding of JAK2 to GHR partially shields the UbE motif sequence. Evidence for this comes from a study by Pelletier *et* al. showing that JAK2 binding involves a large area of GHR containing the previously described box-1 as well as the UbE motif (25). This could potentially hinder the binding of βTrCP to the receptor and as such prevent GHR endocytosis. According to our model, GH stimulation results in JAK2 detachment from the receptor allowing efficient binding of SCF (βTrCP) that will mediate GHR endocytosis. If this model is correct, we would expect JAK2 and βTrCP to compete for the binding to GHR. To test whether the relative expression levels of these two proteins determine the regulation of GHR endocytosis, the BRET assay was used. HEK293-TR cells stably expressing GHR-RLUC and doxycycline-inducible YFP-Jak2 were transiently transfected with Flag-βTrCP or empty vector. Doxicyclin induction of YFP-Jak2 expression increased the levels of GHR-RLUC, confirming the stabilizing effect of Jak2 expression on GHR (Fig. 6A, lanes 2 and 4). Flag-βTrCP expression did not have a significant effect on BRET ratio (around 40mBU in both cases), suggesting that βTrCP is not able to compete with Jak2 for GHR binding. However, either the expression levels or the transfection efficiency of βTrCP might have been too low to affect the BRET ratio and measure a competition effect on Jak2-GHR binding. The reverse approach was also performed. HEK293-TR cells stably expressing GHR-RLUC together with YFP-βTrCP (A2.1.1 and A2.1.4 clones) were transiently transfected with Flag-Jak2 or empty vector. Overexpression of Flag-Jak2 did not result in decreased BRET ratio in both clones (Fig. 6B, compare 1st with 3rd bar and 2nd with 4th bar). In

agreement with Fig. 6A, Fig. 6B did not support a scenario where Jak2 and βTrCP are competing for GHR binding. However, the transfection of Flag-Jak2 was probably inefficient since it did not cause accumulation of GHR-RLUC (Fig. 6B, 1st panel, compare the first 4 lanes with the 4 last). Therefore, the lack of competition between Jak2 and βTrCP using both approaches (Fig. 6A and 6B) may have suffered from unfavorable conditions. In summary, the BRET measurements do not support a scenario where the two key players JAK2 and βTrCP compete with each other for binding to GHR cytoplasmic tails.

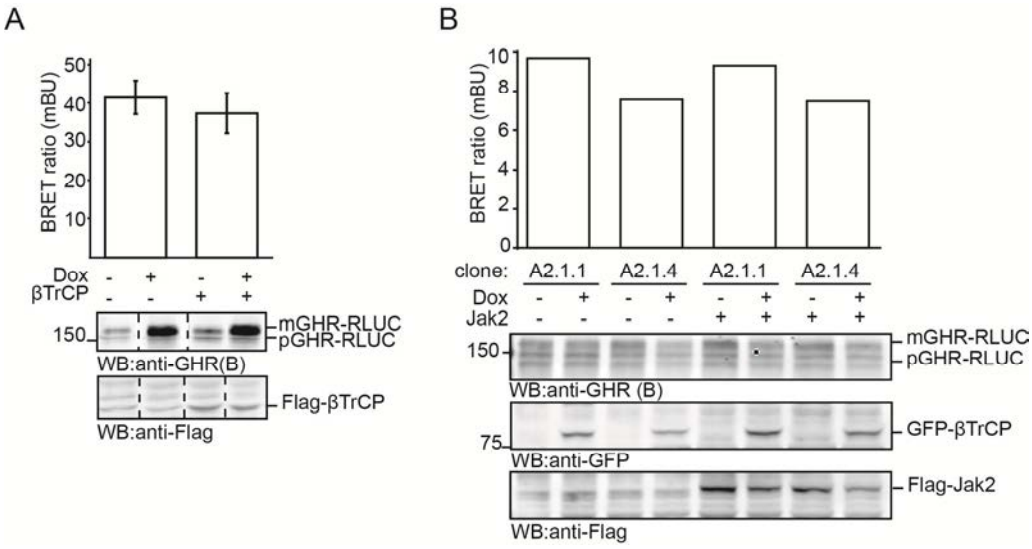

Fig. 6. Interplay of JAK2 and βTrCP on GHR. (A) HEK293-TR stable cell lines expressing GHR-RLUC WT together with YFP-JAK2 were transiently transfected (+ βTrCP) or not (-βTrCP) with Flag-tagged βTrCP; when indicated doxycycline was added in order to stimulate the expression of YFP-JAK2. The graph shows BRET ratios expressed in mBU, representative of two independent measurements ± S.E.M. Cells as subjected to BRET measurements were grown in parallel, then lysed and equal aliquots of the cell lysates were analyzed by western blotting, using the indicated antibodies. Note that in the lanes where doxycycline was added, Flag-JAK2 overexpression resulted in stabilization of GHR. mGHR, mature GHR; pGHR, precursor GHR in the endoplasmic reticulum; Dox, doxycycline. **(B)** HEK293-TR stable cell lines expressing GHR-RLUC WT together with YFP-βTrCP were transiently transfected (+ JAK2) or not (-JAK2) with Flag-tagged JAK2; when indicated doxycycline was added in order to stimulate the expression of YFP-βTrCP. The graph shows BRET ratios expressed in mBU. Cells as subjected to BRET measurements were grown in parallel, then lysed and equal aliquots of the cell lysates were analyzed by western blotting, using the indicated antibodies. mGHR, mature GHR; pGHR, precursor GHR in the endoplasmic reticulum; Dox, doxycycline.

Discussion and applications (perspectives)

In this study we validated the use of our BRET fusion proteins for measuring in real-time and in a dynamic fashion the interactions underlying GHR endocytosis regulation: GHR-JAK2 and GHR-βTrCP. By using appropriate negative controls the specificity of the assay for both protein interactions was confirmed. BRET measurements support the model where GH stimulation induces detachment of JAK2 from the GHR (17). On the other hand, an effect of GH stimulation on GHR-βTrCP interaction was not detected. Possibly, this was due to the low sensitivity of the BRET signal is the cell lines used. Additionally, no evidence was found for a competition between JAK2 and βTrCP for the binding to GHR, as a regulatory mechanism of GHR endocytosis. Perhaps the critical relative levels Jak2: βTrCP were not reached, in part due to low transfection efficiency. Performing similar analysis in cells where GHR, Jak2 and βTrCP are all stably expressed may represent an improvement. Furthermore, other mechanisms may explain the inhibitory effect of JAK2 binding in GHR endocytosis. JAK2 binding to the GHR in the proximity of the UbE motif may cause steric interference with the assembly of the SCF complex instead of directly inhibiting βTrCP binding.

BRET is increasingly used to monitor interactions of receptors and its regulators, and it has contributed immensely for their molecular understanding. The BRET technology has some limitations.

Besides the proximity of the interactors, other factors may influence the efficiency of the resonance energy transfer such as donor lifetime, relative orientation and degree of spectral overlap (3). Additionally, BRET cannot be used to measure interactions between endogenous proteins, requiring at least the donor to be part of a fusion protein. The selection of the tagging methodology of the proteins of interest needs be cautiously planed. If the donor and acceptor tags are placed at opposite ends of the interacting proteins they may not be close enough for efficient resonance transfer to occur. Moreover, the placement of the BRET tags should not interfere with the ability of the proteins to interact. For this reasons, the functional validation of the fusion proteins is very important. The proteins in this study remained functional after being fused to the BRET tags. However, the measured BRET signals, although specific, were quite low. This could be potentially improved by changing the tagging methodology. Inserting linker regions between the BRET tag and the proteins of interest will increase the freedom of movement of the donor and the acceptor and may improve the relative orientation of the BRET tags pair, at least part of the time. Additionally, the incorporation of the linker regions may reduce the steric hindrance of the tags and therefore improve the functionality of the fusion proteins. Another limitation is the fact that BRET signals cannot be localized without cellular fractionation. For this reason we cannot be sure that the BRET signals represent events occurring at the plasma membrane. In fact, it is possible that association of JAK2 and βTrCP with GHR occur already in the ER. Importantly, when the effects of GH addition in the interactions were studied at early time points of stimulation, we were most likely detecting the phenomenon occurring at the plasma membrane.

The results presented in this paper were originated from single point assays at a single protein level ratio donor:acceptor. These data can only be interpreted in a qualitative way. Quantitative data can be obtained by titrating the protein levels, using saturation and competition assays. However, saturation curves for the analysis of GHR-Jak2 or GHR-βTrCP could not be obtained due to the fact that the variation of the acceptor levels (Jak2 and βTrCP) resulted in a change of GHR levels. The effects of ligands or other reagents can be quantitatively analyzed with BRET by performing dose-response or kinetic experiments. Parameters as half-maximal effective concentration, and apparent association/dissociation rate constants can then be determined. The BRET methodology has been used for determining the concentration of insulin required for its half-maximal effect on the association of the protein tyrosine-phosphatase 1B (PTP1B) with the insulin receptor (IR) (8). It would be interesting to use the same approaches for determining the GH concentration required for its half-maximal effect on Jak2 dissociation from GHR. Additionally, GH dose-response curve should be performed for evaluating its potential influence in GHR-βTrCP more precisely.

The BRET measurements in stable cell lines rather than in transient transfection experiments are favorable, as the cell population expresses the proteins homogeneously. Additionally, stable cells lines are easily adaptable to a screening platform. Although transient transfections result in heterogeneous expression of proteins, this does not seem to affect the overall measured BRET signal (5). For the analysis of the interaction GHR-βTrCP, transient transfections resulted in higher BRET signals (Fig. 3A), and consequently more sensitivity than the use of stable cell lines (Fig. 5). The ratios donor:acceptor resulting from the transient co-transfection of the BRET partners probably allowed a better resonance to occur, when compared to the ratio donor:acceptor ratio existing in the tested stable cell lines. Thus, it seems advantageous to use transient transfections for answering scientific questions related to the regulation of GHR-βTrCP interaction. This strategy was successfully adopted for analyzing the interactions of IR with PTP1B (8), Grb14 (9) and FGF receptor with Grb14 and phospholipase C gamma (PLCγ)(10). One aspect to consider is that high expression levels of the interacting proteins increase the chance of measuring BRET resulting from random collisions. Therefore, independently of using transient overexpression or stable cell lines, negative controls should be included. The expression levels should be the nearest to physiological levels while still providing detectable BRET signal. The specificity of our measurements was ensured by measuring specific negative controls for the particular interactions. The BRET signal was always specific in the range of expression levels existing after transient transfections and in the stable cell lines.

Studying simultaneously several interactions, using different acceptors for a common donor, is possible with BRET(26). Different coelenterazines may be used as substrates in different aliquots of the same cell sample, resulting in different wavelengths of luminescence that will stimulate different fluorophores in the acceptor proteins. Oxidation of coelenterazine H (or its protected forms, as ViviRen) excites proteins tagged with YFP ($BRET^1$), while oxidation of coelenterazine-400a excites

proteins tagged with GFP ($BRET^2$). Another BRET combination was developed involving a mutated red fluorescent protein (mOrange) and a mutated Renilla luciferase (RLUC8), which results in the emission of red light, that is less likely quenched by biological tissues, allowing the imaging of protein-protein interactions in living organisms(27). BRET multiplexing would allow the simultaneous monitoring of GHR interaction with JAK2 and βTrCP, for instance after GH stimulation. This would help to understand the interplay between the two interactors in GHR endocytosis regulation. Perroy *et al* used this BRET multiplexing to prove that the ubiquitination of β-arrestin coincides with its recruitment to GPCRs in real time in live cells, by monitoring the attachment of GFP-Ubiquitin to RLUC-β-arrestin, and the interaction of RLUC-β-arrestin with V2-vasopressin receptor-YFP(28). Additionally, this study validated the principle of using BRET for monitoring covalent attachment of proteins, such as ubiquitination. GHR ubiquitination coincides with its recruitment to clathrin coated pits and endocytosis (29), but it does not seem to be necessary for it(18). Therefore, the role of GHR ubiquitination is still not understood. It could be that GHR ubiquitination is a side effect of the necessary ubiquitination event that occurs in the vicinity of GHR. More complexity was added to the system by the introduction of Ubc13/CHIP pair as a new regulator of GHR endocytosis (Slotman et al, in preparation). This finding suggested a role for K63 ubiquitin chains in the process, in addition to the role of K48 chains catalyzed by $SCF^{\beta TrCP}$. It would be interesting to apply BRET technology to follow in real time the order and interplay of K63 and K48 poly-ubiquitination, and to get a better understanding of how ubiquitination regulates GHR endocytosis.

BRET technology is increasingly used in high-throughput screening for drug discovery. In particular, screenings of ligands able to cause the recruitment of β-arrestin to GPCRs are very popular. With this strategy, these ligands are selected as promoting the internalization and desensitization of GPCRs(30). The proof of principle comes from study by Angers *et al.* who verified that β-arrestin is recruited to the β_2-adrenergic receptor by addition of agonist(4). Additionally, BRET methodology has been suggested as a proper tool for looking for molecules able to activate insulin receptor autophoshorylation or inhibit its dephosphorylation. These drugs could be used to treat patients which are insulin resistant or insulin deficient(31).

GHR endocytosis is a very appealing process for drug discovery. On one side, drugs inhibiting GHR endocytosis would result in increased sensitivity of the cells to GH, with application in patients suffering from GH resistance, such as cachexia patients(32, 33). For this purpose live cells may be screened for compounds inhibiting GHR-βTrCP interaction using the BRET technology. On the other side, increasing the rate of GHR endocytosis can be achieved by inhibiting GHR-JAK2 interaction. This would be interesting for cancer treatment, since excessive GH signaling has been connected to certain cancers (34, 35), as well as acromegaly treatment. BRET technology is a good platform to search for compounds in live cells that act on GHR-JAK2 interaction and decrease the sensitivity of cells to GH. The results reported in this paper prove that GHR-JAK2 and GHR-βTrCP interactions can be assessed specifically using the BRET methodology. However, the sensitivity of the assay when using the tagged constructs and cell lines described is quite low, especially in case of GHR- βTrCP; optimization of the tagging of the constructs may be necessary. In the case of the GHR-JAK2 interaction, the sensitivity was high enough to detect GH-induced reduction of the BRET signal. Therefore, compounds that would cause similar effects on GHR-JAK2 interaction as GH stimulation would be selected as hits in an anti-cancer drug screening.

To our knowledge this is the first time that BRET technology has been used for monitoring protein interactions with GHR. The results presented in this study establish the proof of principle of the potentialities of BRET for answering scientific questions related to the regulation of GHR endocytosis, and the possibility of applying the assay as platform for drug discovery for disorders connected to GH signaling.

Acknowledgements

We are grateful to all other members of the GHR. We would like to thank Prof. Tomoki Chiba for supplying us with βTrCP DNA constructs, Prof. Carter-Su for the kind gift of the mouse Jak2 DNA-construct, Prof. Bouvier for the RLUC-DVED-YFP fusion construct, and Madelon Maurice for the HEK-293-TR cells.

This research was supported by the European Network of Excellence, Rubicon "Role of ubiquitin and ubiquitin-like modifiers in cellular regulation" (Grant LSHG-CT-2005-018683), and the Marie Curie network, "UbiRegulators", (Grant MRTN-CT-2006-034555).

References

1. Eidne KA, Kroeger KM, Hanyaloglu AC 2002 Applications of novel resonance energy transfer techniques to study dynamic hormone receptor interactions in living cells. Trends Endocrinol Metab 13:415-421
2. Pfleger KD, Eidne KA 2006 Illuminating insights into protein-protein interactions using bioluminescence resonance energy transfer (BRET). Nat Methods 3:165-174
3. Wu P, Brand L 1994 Resonance energy transfer: methods and applications. Anal Biochem 218:1-13
4. Angers S, Salahpour A, Joly E, Hilairet S, Chelsky D, Dennis M, Bouvier M 2000 Detection of beta 2-adrenergic receptor dimerization in living cells using bioluminescence resonance energy transfer (BRET). Proc Natl Acad Sci U S A 97:3684-3689
5. Terrillon S, Durroux T, Mouillac B, Breit A, Ayoub MA, Taulan M, Jockers R, Barberis C, Bouvier M 2003 Oxytocin and vasopressin V1a and V2 receptors form constitutive homo- and heterodimers during biosynthesis. Molecular endocrinology 17:677-691
6. Gales C, Rebois RV, Hogue M, Trieu P, Breit A, Hebert TE, Bouvier M 2005 Real-time monitoring of receptor and G-protein interactions in living cells. Nat Methods 2:177-184
7. Lan TH, Kuravi S, Lambert NA 2011 Internalization Dissociates beta(2)-Adrenergic Receptors. PLoS One 6:e17361
8. Boute N, Boubekeur S, Lacasa D, Issad T 2003 Dynamics of the interaction between the insulin receptor and protein tyrosine-phosphatase 1B in living cells. EMBO reports 4:313-319
9. Nouaille S, Blanquart C, Zilberfarb V, Boute N, Perdereau D, Burnol AF, Issad T 2006 Interaction between the insulin receptor and Grb14: a dynamic study in living cells using BRET. Biochem Pharmacol 72:1355-1366
10. Browaeys-Poly E, Blanquart C, Perdereau D, Antoine AF, Goenaga D, Luzy JP, Chen H, Garbay C, Issad T, Cailliau K, Burnol AF 2010 Grb14 inhibits FGF receptor signaling through the regulation of PLCgamma recruitment and activation. FEBS Lett 584:4383-4388
11. Xu X, Soutto M, Xie Q, Servick S, Subramanian C, von Arnim AG, Johnson CH 2007 Imaging protein interactions with bioluminescence resonance energy transfer (BRET) in plant and mammalian cells and tissues. Proc Natl Acad Sci U S A 104:10264-10269
12. Xie Q, Soutto M, Xu X, Zhang Y, Johnson CH 2011 Bioluminescence resonance energy transfer (BRET) imaging in plant seedlings and mammalian cells. Methods Mol Biol 680:3-28
13. Brown RJ, Adams JJ, Pelekanos RA, Wan Y, McKinstry WJ, Palethorpe K, Seeber RM, Monks TA, Eidne KA, Parker MW, Waters MJ 2005 Model for growth hormone receptor activation based on subunit rotation within a receptor dimer. Nat Struct Mol Biol 12:814-821
14. Govers R, ten Broeke T, van Kerkhof P, Schwartz AL, Strous GJ 1999 Identification of a novel ubiquitin conjugation motif, required for ligand-induced internalization of the growth hormone receptor. Embo J 18:28-36
15. van Kerkhof P, Putters J, Strous GJ 2007 The ubiquitin ligase SCF(betaTrCP) regulates the degradation of the growth hormone receptor. J Biol Chem 282:20475-20483
16. Deng L, He K, Wang X, Yang N, Thangavel C, Jiang J, Fuchs SY, Frank SJ 2007 Determinants of growth hormone receptor down-regulation. Molecular endocrinology 21:1537-1551
17. Putters J, da Silva Almeida AC, van Kerkhof P, van Rossum AG, Gracanin A, Strous GJ 2011 Jak2 is a negative regulator of ubiquitin-dependent endocytosis of the growth hormone receptor. PLoS One 6:e14676
18. van Kerkhof P, Govers R, Alves dos Santos CM, Strous GJ 2000 Endocytosis and degradation of the growth hormone receptor are proteasome-dependent. J Biol Chem 275:1575-1580
19. Strous GJ, van Kerkhof P, Govers R, Ciechanover A, Schwartz AL 1996 The ubiquitin conjugation system is required for ligand-induced endocytosis and degradation of the growth hormone receptor. Embo J 15:3806-3812

20. Strous GJ, van Kerkhof P, Govers R, Rotwein P, Schwartz AL 1997 Growth hormone-induced signal tranduction depends on an intact ubiquitin system. J Biol Chem 272:40-43
21. Strous GJ, van Kerkhof P, Govers R, Ciechanover A, Schwartz AL 1996 The ubiquitin conjugation system is required for ligand-induced endocytosis and degradation of the growth hormone receptor. EMBO J 15:3806-3812
22. Funakoshi-Tago M, Pelletier S, Matsuda T, Parganas E, Ihle JN 2006 Receptor specific downregulation of cytokine signaling by autophosphorylation in the FERM domain of Jak2. EMBO J 25:4763-4772
23. Murphy LJ, Lazarus L 1984 The mouse fibroblast growth hormone receptor: ligand processing and receptor modulation and turnover. Endocrinology 115:1625-1632
24. Gorin E, Goodman HM 1985 Turnover of growth hormone receptors in rat adipocytes. Endocrinology 116:1796-1805
25. Pelletier S, Gingras S, Funakoshi-Tago M, Howell S, Ihle JN 2006 Two domains of the erythropoietin receptor are sufficient for Jak2 binding/activation and function. Mol Cell Biol 26:8527-8538
26. Breton B, Sauvageau E, Zhou J, Bonin H, Le Gouill C, Bouvier M 2010 Multiplexing of multicolor bioluminescence resonance energy transfer. Biophys J 99:4037-4046
27. De A, Ray P, Loening AM, Gambhir SS 2009 BRET3: a red-shifted bioluminescence resonance energy transfer (BRET)-based integrated platform for imaging protein-protein interactions from single live cells and living animals. FASEB J 23:2702-2709
28. Perroy J, Pontier S, Charest PG, Aubry M, Bouvier M 2004 Real-time monitoring of ubiquitination in living cells by BRET. Nat Methods 1:203-208
29. van Kerkhof P, Sachse M, Klumperman J, Strous GJ 2001 Growth hormone receptor ubiquitination coincides with recruitment to clathrin-coated membrane domains. J Biol Chem 276:3778-3784
30. Alvarez-Curto E, Pediani JD, Milligan G 2010 Applications of fluorescence and bioluminescence resonance energy transfer to drug discovery at G protein coupled receptors. Anal Bioanal Chem 398:167-180
31. Issad T, Boute N, Boubekeur S, Lacasa D, Pernet K 2003 Looking for an insulin pill? Use the BRET methodology! Diabetes Metab 29:111-117
32. von Laue S, Ross RJ 2000 Inflammatory cytokines and acquired growth hormone resistance. Growth Horm IGF Res 10 Suppl B:S9-14
33. Crown AL, Cottle K, Lightman SL, Falk S, Mohamed-Ali V, Armstrong L, Millar AB, Holly JM 2002 What is the role of the insulin-like growth factor system in the pathophysiology of cancer cachexia, and how is it regulated? Clin Endocrinol (Oxf) 56:723-733
34. Waters MJ, Barclay JL 2007 Does growth hormone drive breast and other cancers? Endocrinology 148:4533-4535
35. Kleinberg DL, Wood TL, Furth PA, Lee AV 2009 Growth hormone and insulin-like growth factor-I in the transition from normal mammary development to preneoplastic mammary lesions. Endocr Rev 30:51-74

Summarizing discussion

Ana C. da Silva Almeida

Department of Cell Biology and Institute of Biomembranes,
University Medical Center Utrecht, Heidelberglaan 100, 3584
CX Utrecht, The Netherlands

Drug Discovery Factory BV, Albrechtlaan 14A, 1404 AK
Bussum, The Netherlands

Discussion

Important molecular details involved in the regulation of GHR endocytosis are characterized in this thesis. In chapter 2 we described that βTrCP binds to GHR through two different motifs, UbE and DSGRTS, both important for the constant basal degradation of the receptor. The amino acid residues involved in the unique UbE-βTrCP interaction were described in the chapter 3, where a computational model of the interaction was constructed. The role of a potential phosphorylation of serine 323 in the UbE motif as a regulatory mechanism of GHR endocytosis was analyzed in chapter 4. In chapter 5, we explored the unconventional UbE-βTrCP interaction as a target for drugs that might be used for treatment of cachexia, by alleviating the GH resistance phenotype in these patients. Finally, in chapter 6, BRET technology was used for studying, in real time, interactions of GHR with important regulators of its endocytosis, βTrCP and JAK2. In this section we discuss in detail the molecular mechanisms, some of which uncovered in this thesis, that make GHR endocytosis a flexible process with great physiological and therapeutic relevance for the regulation the sensitivity of cells to GH.

Regulation of GH sensitivity of the cells

GH signaling not only depends on the amounts of GH in circulation, but also on the levels of GHR at the cell surface. The responsiveness of the cells to GH is dynamically regulated, reflecting a balance of receptor endocytosis/degradation, and transport of newly synthesized receptors to the plasma membrane (*1*). Endocytosis and degradation of GHR occur continuously, in the absence of GH, and depend on the action of the $SCF^{\beta TrCP}$ E3 ligase, which mediates ubiquitination event(s) essential for GHR endocytosis (2). βTrCP is recruited to the UbE motif in the cytoplasmic tail of GHR. In addition to this motif, GHR contains a DSGRTS sequence, which corresponds to the classical DSGxxS degron present in other βTrCP substrates. In chapter 2, we found that this conserved DSGRTS sequence, present downstream of the UbE motif, binds βTrCP as well, and thereby contributes to GH-independent GHR degradation. The binding of βTrCP to the DSGxxS motif occurs when both serines are phosphorylated by a specific kinase. In the case of GHR, very likely the serine residues in the DSGRTS sequence are fully phosphorylated under basal conditions, independently of GH stimulation. Future studies need to be performed to find the kinase responsible for the phosphorylation of DSGRTS of GHR. This will give more insight into GH-independent mechanisms of regulation of GHR endocytosis. In the absence of GH stimulation, both UbE and DSGxxS motifs contribute equally to GHR degradation while no role of the DSGRTS sequence was detected upon GH stimulation. Therefore, in addition to the UbE motif, the DSGRTS sequence significantly contributes to the GHR homeostasis of cells; the combined action through both motifs ensures that the levels of GHR are kept at the right level at the cell surface, so that the cells are appropriately sensitive to GH. βTrCP was proposed to bind certain substrates through multiple motifs (3-5). The cooperative binding to multiple motifs, under the regulation of several phosphorylation events, allows a fine-tuned βTrCP action. However, it remains unclear whether both UbE and DSGRTS motifs can be active and occupied by βTrCP at the same time. In fact, since GHR exists as a dimer at the cell surface (6), and the $SCF^{\beta TrCP}$ complex has been reported to dimerize (7, 8), multiple $SCF^{\beta TrCP}$ complexes may be present in each GHR unit.

GH-signaling termination

GH binding to GHR results in the activation of several signaling pathways mainly through JAK2-mediated phosphorylation events. GH signaling plays a major role in body growth and metabolic regulation, as well as in cellular differentiation and proliferation. However, its duration needs to be tightly controlled. Excessive GH signaling has recently been linked with cancer (9, 10). Additionally, cycles of desensitization/ re-sensitization of cells are necessary for achieving maximal activation of GH signaling cascades. In males, the high pulsatile pattern of GH secretion by the pituitary results in the maximal GH signaling activation, while the nearly continuous secretion pattern in females reduces the levels of activated STAT5. Differences in sex-specific gene expression in the liver have been attributed to this dimorphic pattern of GH release (11). During a pulse of GH stimulation, the signaling

is down-regulated, through several mechanisms at several levels, including by GHR endocytosis. The cells are then reset for another round of GH signaling.
GHR endocytosis, although occurring constitutively, is accelerated in presence of GH (12, 13). In this thesis we studied two motifs that bind βTrCP and are both needed for GHR endocytosis: UbE motif and DSGRTS sequence. The function of the DSGRTS sequence is restricted to steady state conditions, without GH stimulation (chapter 2). On the other hand, the UbE motif is active both at steady state and upon GH stimulation. Therefore, the termination of GH-signaling through endocytosis depends on βTrCP action through the UbE motif. In chapter 4, we present evidence that the serine 323 in the UbE motif may be phosphorylated after GH stimulation, which results in increased affinity of βTrCP binding to the UbE motif and, consequently, in a faster endocytosis. This constitutes a very efficient mechanism by which GH signaling can be rapidly terminated. Further investigation is needed to find the kinase responsible for the phosphorylation of serine 323, and the GH-induced signaling pathways involved. Serine 323 is contained in a CK2 consensus site, and, therefore, this is an obvious candidate as the kinase responsible for this phosphorylation. Although JAK2 has been regarded as the major effector of GH signaling, there is growing evidence that Src family kinases are activated by GH, independently of JAK2 (14, 15). Future studies are needed to find which of these GH-induced pathways lead ultimately to S323 phosphorylation. The possibility of quickly increasing the rate of GHR endocytosis via a phosphorylation event, confirms the versatility of the endocytosis process as a regulatable mechanism.

Influence stressors in GHR endocytosis

In this thesis we identified serine phosphorylation events as important regulators of GHR endocytosis. While the phosphorylation of the serines in the DSGRTS sequence seems to occur independently of GH stimulation (chapter 2), the phosphorylation of serine 323 in the UbE is triggered by GH (chapter 4). These serines might work as targets where several pathways converge to modulate the rate of GHR endocytosis and consequently the sensitivity of the cells to GH. Therefore, different stressors besides GH may affect the phosphorylation status at these sites. Insulin has been suggested to reduce GHR levels and GH signaling in PI-3 kinase and MAPK dependent manners (16-18). It is interesting to consider that insulin might accelerate GHR endocytosis by stimulating phosphorylation of serine 323, since insulin treatment was shown to decrease the pool of GHRs at the cell surface (17). Pro-inflammatory cytokines such as TNFα and IL-6 (19) as well as glucocorticoids have been described to induce GH insensitivity (20-22). These studies have suggested that the GH insensitivity phenotype is due to decreased GHR mRNA level. As an additional mechanism, it could be that these stimuli are able to induce faster GHR endocytosis by triggering phosphorylation at Ser323. Further experiments need to be performed to evaluate this possibility. These studies would benefit from an antibody able to detect specifically phosphorylated S323 in GHR.

GH anabolic actions imply a very big demand of energy to the cells. Obviously, under stress the available cellular energy needs to be canalized to processes necessary for coping with the stressful situations. This is in part ensured by fast downregulation of the cellular levels of GHR, and consequent decrease of the sensitivity of the cells to GH.

The DSGRTS sequence in GHR seems to be phosphorylated in basal conditions under the conditions of our experiments, without applying any special treatment or stressor to the cells (chapter 2). However, we cannot exclude that this is an artifact e.g. of GHR overexpression conditions. Under physiological conditions the phosphorylation status of DSGRTS might also be regulatable upon certain stimuli, as the ones described above. Additionally, in some situations that require high levels of GH signaling, the body would benefit from higher sensitivity to GH at steady state, e.g. in the process of chondrogenesis at children's growth plate, or maybe during adolescence to stimulate breast growth (23, 24). A decreased kinase activity towards the DSGRTS serines would result in decreased basal degradation of GHR, increase in cellular levels of GHR, and consequently increase in GH sensitivity.

Regulation of endocytosis of GHR versus other cytokine receptors

$SCF^{\beta TrCP}$ E3 ligase is involved in the endocytosis of several cytokine receptors. Interferon receptor (IFNAR1) was the first cytokine receptor found to depend on $SCF^{\beta TrCP}$ for its degradation (25).

Subsequently, $SCF^{\beta TrCP}$ was reported to be needed for prolactin receptor (PRLR) and erythropoietin receptor (EPOR) endocytosis and degradation (26, 27). Presumably, $SCF^{\beta TrCP}$ binds exclusively to the DSGxxS motif present in these receptors, when both serines are phosphorylated after ligand binding, mediating their ubiquitination and degradation. The phosphorylation of the DSGxxS motif in PRLR is triggered by prolactin (28). In the case of IFNAR, the treatment of cells with IFNα/β induces the phosphorylation of the serine 535 in the DSGxxS motif, in a Tyk2 kinase-dependent manner (29). The DSGxxS motif of the EPOR gets phosphorylated upon stimulation with its ligand, depending on JAK2 activation (27). Therefore, βTrCP acts as a negative regulator of signaling of these receptors. Whether $SCF^{\beta TrCP}$ is general machinery employed by the cells for the degradation of all cytokine receptors remains to be investigated. Although $SCF^{\beta TrCP}$ most likely leaves the receptors after its ubiquitination activity, it is important to note that, in many cases, cells harbor many different cytokine receptors that would all depend on the availability of the complete set of factors needed to build an active SCF complex.

$SCF^{\beta TrCP}$ is also essential for GHR endocytosis, but with a more complex regulatory mechanism. In this case, two motifs are able to bind $SCF^{\beta TrCP}$, in a GH-independent manner, ensuring the continuous endocytosis and degradation of the GHR, thereby setting the GH sensitivity at a low steady state level. The kinase responsible for DSGRTS phosphorylation at steady state is unknown but it seems to be different from the kinases involved in IFNAR and PRLR (CK1 and GSK3β, respectively), as it was concluded by using specific inhibitors. Upon GH stimulation, the DSGRTS sequence is not functional anymore through mechanisms not yet understood, which differs from the situation occurring in the other cytokine receptors. The UbE motif is able to bind βTrCP both in the absence and presence of GH stimulation, although with higher affinity under GH stimulation because S323 phosphorylation is triggered. Another peculiar aspect to consider is the fact that the ubiquitination of GHR itself is not needed for its endocytosis. We prove in chapter 4 that $SCF^{\beta TrCP}$ mediates GHR ubiquitination *in vitro*, and previous results in the group also supported this scenario in cells (30). However, this event does not seem to be crucial for GHR endocytosis, since a lysine-less GHR construct that cannot be ubiquitinated, is endocytosed normally in an ubiquitin system-dependent manner (31). The current model is that another factor in the vicinity of GHR needs to be ubiquitinated by the ubiquitination machinery recruited through GHR before the endocytosis can occur. The ubiquitination of this factor might precede its proteasomal degradation, or it might turn it into an endocytic adaptor which, by binding to the endocytic machinery, facilitates GHR endocytosis. In other cytokine receptors that depend on $SCF^{\beta TrCP}$ for their endocytosis, specific lysines need to be ubiquitinated. GHR endocytosis occurs basally and rapidly, which is responsible for the short half-life of GHR compared to other cytokine receptors. These aspects may justify the fact that, although the endocytosis of GHR needs similar components, the regulation is different.

Model of GHR endocytosis

In this thesis we uncovered novel features of GHR endocytosis regulation. Initially, we proposed that the basal and GH-induced GHR endocytosis use the same mechanisms. In both cases the endocytosis depends on clathrin, ubiquitin system, $SCF^{\beta TrCP}$, and the UbE motif (30). However, my study revealed additional mechanisms. First of all, the DSGRTS sequence was identified as a novel factor to consider in GHR endocytosis regulation. The role of the DSGRTS sequence is restricted to basal conditions, in the absence of GH stimulation, which indicates that the field of action of this motif is the systemic regulation of GHR responsiveness of the cells (eg. age-related physiological changes, disease situations, among others). On the other hand, the UbE motif is required for both basal and GH-induced endocytosis. Upon GH stimulation certain events, centered on the UbE motif, result in faster GHR endocytosis. Therefore, an important aspect of the UbE motif is its ability to quickly regulate GH responsiveness of the cells.

One of the events that is likely responsible for the GH-induced fast GHR endocytosis is S323 phosphorylation, which occurs after GH stimulation and results in increased affinity of GHR- βTrCP interaction (chapter 4). In addition, GH-stimulation induces JAK2 detachment from GHR (reported in chapter 6 and (30)) which may also contribute to faster GHR endocytosis. In fact, JAK2 binding has been proposed to prevent the selection of the GHR for endocytosis by the $SCF^{\beta TrCP}$. We hypothesized that JAK2 release, after GH stimulation, allows βTrCP to bind more effectively to the receptor.

Studies by Pelletier and collaborators showed that the binding of JAK2 involves a large area including box-1, and some residues up to and within the UbE motif, which could potentially affect βTrCP binding (32). Therefore, competition between JAK2 and βTrCP for GHR binding could be an explanation for the negative effects of JAK2 on GHR endocytosis. In this case, the relative expression levels of JAK2 and βTrCP might be important determinants of GHR endocytosis. We did not find evidence for competition using our BRET assay (chapter 6). However, we cannot exclude that the critical relative protein levels JAK2:βTrCP were not reached. On the other hand, other mechanisms may explain the inhibitory effect of JAK2 on GHR endocytosis. JAK2 binding to the GHR in the proximity of the UbE motif may cause steric interference with the assembly of the SCF complex instead of directly inhibiting βTrCP binding. Additionally, it is interesting to consider the possibility that phosphorylation of serine 323 and JAK2 release from GHR are interlinked processes. It could be that the phosphorylation of serine 323 occurs only after JAK2 dissociation, or that serine 323 phosphorylation facilitates JAK2 release. Further studies are needed to evaluate this scenario.

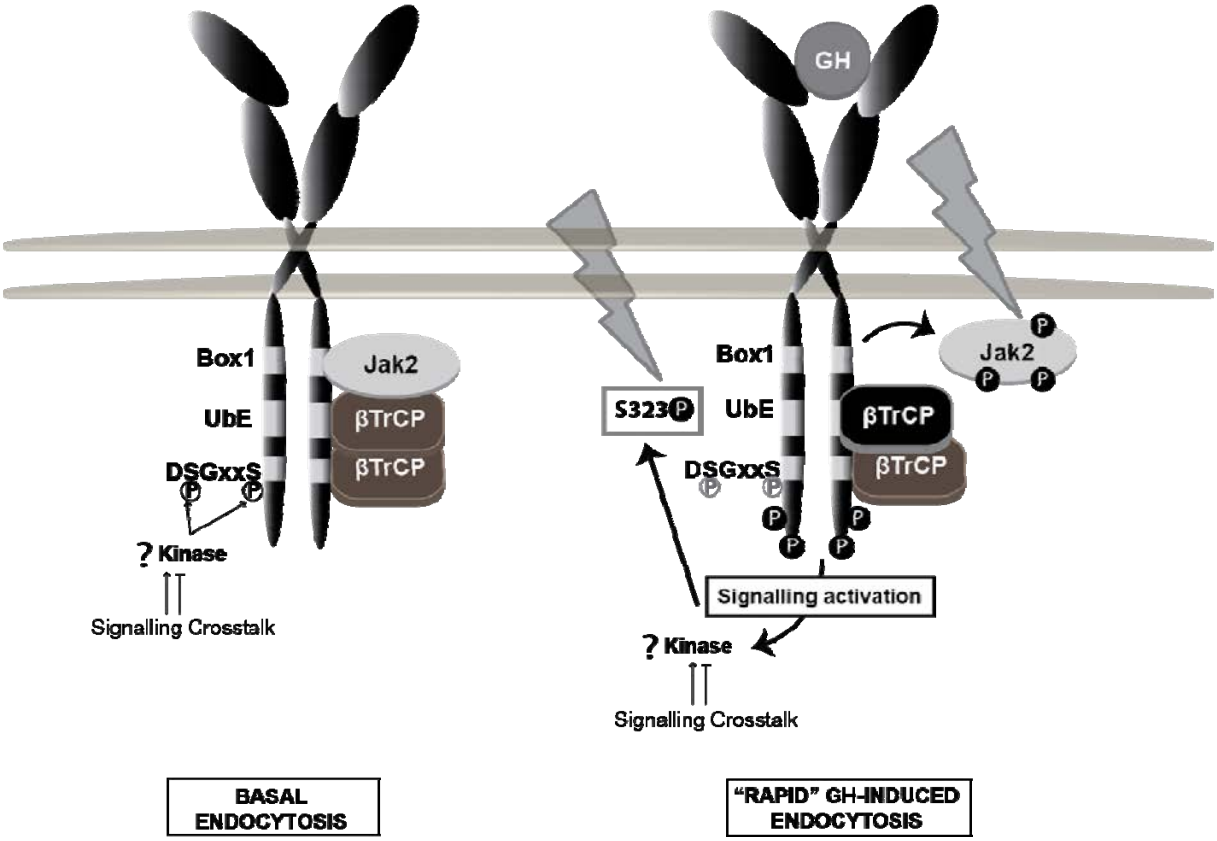

Fig. 1: Model of GHR endocytosis regulation. Under basal conditions βTrCP binds to the UbE motif and to the constitutively phosphorylated DSGRTS sequence. Both motifs contribute equally to the continuous GH-independent turnover of the GHR. This is essential to guarantee a proper regulation of the GH sensitivity of the cells. The kinase responsible for the DSGRTS phosphorylation is unknown. Other pathways may influence GHR cellular levels by modulating DSGRTS phosphorylation status. Under conditions of GH stimulation JAK2 is released from the receptor, and the serine 323 of the UbE motif gets phosphorylated by an unknown kinase. These events l increase the affinity of βTrCP for the UbE motif, and, reduce the role of the DSGRTS sequence. Overall GH stimulation results in faster GHR endocytosis.

The reason why the DSGRTS sequence only acts on GHR endocytosis in basal conditions, and not under GH stimulation remains unclear. The serines of the DSGRTS seem to be basally phosphorylated, allowing βTrCP to bind. One possible scenario is that GH stimulation causes de-phosphorylation of these serines, by inhibiting the kinase responsible, or by activating specific phosphatases. Alternatively, events triggered by GH stimulation may result in a predominant role of the UbE motif in such a way that the DSGRTS sequence, even if kept phosphorylated, becomes redundant. Such events might be the phosphorylation of the serine 323, and the consequent increase of βTrCP affinity to the UbE motif. Additionally, JAK2 detachment from GHR might also result in increased binding of βTrCP to the UbE motif. A combination of both events, which might be

interconnected, is also possible. It is reasonable to conclude that the DSGRTS sequence is only needed if the UbE motif is not at a status of maximal βTrCP binding capacity. Specific antibodies against the phosphorylated serines in the DSGRTS sequence would be very helpful in future experiments, to understand when and through which pathways the DSGRTS function is regulated. It remains unclear whether $SCF^{\beta TrCP}$ can bind to the DSGRTS sequence while Jak2 is bound to GHR. In Jak2 overexpression experiments GHR is stabilized to an extent (T1/2~20 h) that is not reached by shutting off the ubiquitination system (T1/2~9h)(30, 33). Therefore, the inhibitory effect of JAK2 on GHR endocytosis seems to be a dominant factor over $SCF^{\beta TrCP}$ action. For this reason, the most likely scenario is that the binding of JAK2 to GHR inhibits $SCF^{\beta TrCP}$ action through both UbE motif and DSGxxS sequence. The function of the UbE and the DSGRTS motifs in steady state conditions is dependent on the dynamic cycles of JAK2 association/disassociation to the receptor, in a model where the amount of free available JAK2 is the main determinant of GH sensitivity of the cells. In Fig.1 a schematic representation of the current knowledge on GHR endocytosis regulation is shown.

The GHR-βTrCP interaction as a drug target against cachexia

The GH resistance phenotype is characterized by elevated concentrations of GH in circulation, accompanied by decreased concentrations of GHBP and IGF-1 (34). This phenotype occurs in patients with severe illness, in particular cachexia patients (34) (35). In chapter 5, we showed for the first time that in tumor-bearing mice, suffering from cachexia, the GHR levels are indeed substantially down-regulated. Previous studies have shown that patients suffering from GH resistance have reduced GHBP levels in circulation when compared to controls, which was suggested as an indirect indication of reduced GHR cellular levels (36-38). Therefore, the GH resistance phenotype in cachexia patients is probably caused by decreased amount of GHRs in cells. Since pro-inflammatory cytokines have been regarded as the main mediators of cachexia, anti-inflammatory agents have been tried for cachexia treatment. As GH resistance seems to be an important component of the cachexia syndrome, treatments that increase the amount of GHRs in the cells, and as such their GH sensitivity, would be beneficial for these patients as well.

GHR levels in the cells can be modulated by interfering with GHR endocytosis. Inhibition of GHR endocytosis will ultimately result in increased sensitivity of the cells to GH. A specific way of achieving this is by inhibiting the interaction of GHR with βTrCP, which is an essential factor for GHR endocytosis. Since βTrCP is responsible for the ubiquitination and degradation of many substrates, the targeting of GHR- βTrCP interaction needs to be very specific so that other interactions are not affected. In the chapters 2 and 3, we conclude that the binding of βTrCP to the UbE motif has unique characteristics, as expected from the different amino acid sequence (DDSWVEFIELD), when compared to the classical DSGxxS motif present in other βTrCP substrates. Therefore, the interaction GHR UbE- βTrCP represents a promising specific target for drug discovery against cachexia. In chapter 5 the development of a screening platform to find such drugs is described. After an *in vitro*, molecular based high-through-put screening for finding compounds able to inhibit the interaction, the effects of the positive compounds were validated in cell based assays, and ultimately tested in mice. One compound was able to stabilize the mature GHR in mice livers, representing a potential compound for further development as a therapy for cachexia. Additionally, the structural data obtained on the UbE- βTrCP interaction in chapter 3 opens the opportunity of designing drugs that specifically interfere with the interaction. Importantly, in the initial step of the screening the compounds were selected based on their ability to interfere with the βTrCP binding in a non-phosphorylated form of the UbE peptide. The UbE peptide phosphorylated at Ser323 may interact with βTrCP in a different way. Future aspects will address this aspect. Therefore, we need to consider that a compound effective in inhibiting the interaction between βTrCP and the non-phosphorylated UbE motif might not be as effective in interfering with the βTrCP binding to the phosphorylated UbE motif. The therapeutic implications of this scenario would be that the compounds selected on the screen will increase the steady state levels of GHR in cells, making the cells more sensitive to GH, without affecting the GH-induced GHR endocytosis. In this case, the action of the compound would keep the physiological regulation that guarantees that each receptor is able to signal only once. Another important factor to consider is that GHR is expressed in almost all the cells of the body and it is difficult to predict how the different cells will respond to the drug; the accumulation of GHRs might have a different effect on

liver versus muscles or fat cells. One factor determining the effectiveness and specificity of the drug in the different tissues could be the different cellular levels of Jak2. Perhaps in cells with high Jak2 levels, a drug interfering with the UbE- βTrCP interaction is less effective, as Jak2 will be probably the dominant GHR stabilizing factor.

As cachexia is a multifactorial syndrome, a combination of several treatments might be needed to achieve successful therapeutic results. The combination of already developed agents that interfere with cytokine synthesis or activity, with compounds that ameliorate the GHR resistance phenotype directly, potentially the compound found in our screen, may lead to substantial improvement in the effectiveness of cachexia treatment.

The findings reported in this thesis represent important contributions for the understanding of the mechanisms regulating GHR endocytosis, and GH sensitivity, where we explored the acquired knowledge for discovery of drugs able to fight cachexia.

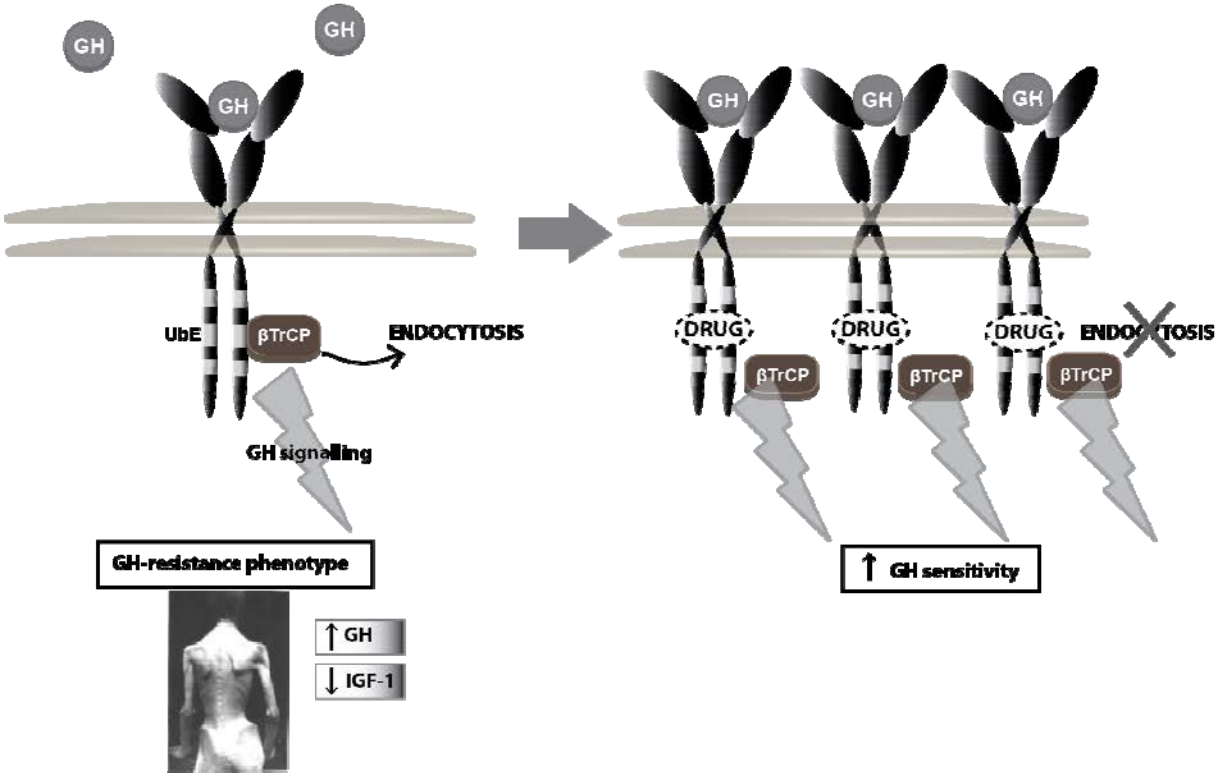

Fig. 2: Strategy for cachexia treatment. Cachexia syndrome is very often marked by a GH-resistance phenotype, characterized by low levels of IGF-1 despite of the high levels of GH in circulation. This phenotype may be caused by decreased amount of GHRs in these patients. We used the interaction GHR UbE – βTrCP as target for specific drugs that will inhibit GHR endocytosis, increase the amount of GHRs at the cell surface, and consequently improve the sensitivity of these patients to GH.

References

1. Strous GJ, van Kerkhof P 2002 The ubiquitin-proteasome pathway and the regulation of growth hormone receptor availability. Mol Cell Endocrinol 197:143-151

2. van Kerkhof P, Putters J, Strous GJ 2007 The ubiquitin ligase SCF(betaTrCP) regulates the degradation of the growth hormone receptor. J Biol Chem 282:20475-20483

3. Jia J, Zhang L, Zhang Q, Tong C, Wang B, Hou F, Amanai K, Jiang J 2005 Phosphorylation by double-time/CKIepsilon and CKIalpha targets cubitus interruptus for Slimb/beta-TRCP-mediated proteolytic processing. Dev Cell 9:819-830

4. Inuzuka H, Tseng A, Gao D, Zhai B, Zhang Q, Shaik S, Wan L, Ang XL, Mock C, Yin H, Stommel JM, Gygi S, Lahav G, Asara J, Xiao ZX, Kaelin WG, Jr., Harper JW, Wei W 2010

Phosphorylation by casein kinase I promotes the turnover of the Mdm2 oncoprotein via the SCF(beta-TRCP) ubiquitin ligase. Cancer Cell 18:147-159
5. Tempe D, Casas M, Karaz S, Blanchet-Tournier MF, Concordet JP 2006 Multisite protein kinase A and glycogen synthase kinase 3beta phosphorylation leads to Gli3 ubiquitination by SCFbetaTrCP. Mol Cell Biol 26:4316-4326
6. Gent J, van Kerkhof P, Roza M, Bu G, Strous GJ 2002 Ligand-independent growth hormone receptor dimerization occurs in the endoplasmic reticulum and is required for ubiquitin system-dependent endocytosis. Proc Natl Acad Sci U S A 99:9858-9863
7. Suzuki H, Chiba T, Suzuki T, Fujita T, Ikenoue T, Omata M, Furuichi K, Shikama H, Tanaka K 2000 Homodimer of two F-box proteins betaTrCP1 or betaTrCP2 binds to IkappaBalpha for signal-dependent ubiquitination. J Biol Chem 275:2877-2884
8. Chew EH, Poobalasingam T, Hawkey CJ, Hagen T 2007 Characterization of cullin-based E3 ubiquitin ligases in intact mammalian cells--evidence for cullin dimerization. Cell Signal 19:1071-1080
9. Waters MJ, Barclay JL 2007 Does growth hormone drive breast and other cancers? Endocrinology 148:4533-4535
10.Kleinberg DL, Wood TL, Furth PA, Lee AV 2009 Growth hormone and insulin-like growth factor-I in the transition from normal mammary development to preneoplastic mammary lesions. Endocr Rev 30:51-74
11.Rinn JL, Snyder M 2005 Sexual dimorphism in mammalian gene expression. Trends Genet 21:298-305
12.Murphy LJ, Lazarus L 1984 The mouse fibroblast growth hormone receptor: ligand processing and receptor modulation and turnover. Endocrinology 115:1625-1632
13.Gorin E, Goodman HM 1985 Turnover of growth hormone receptors in rat adipocytes. Endocrinology 116:1796-1805
14.Rowlinson SW, Yoshizato H, Barclay JL, Brooks AJ, Behncken SN, Kerr LM, Millard K, Palethorpe K, Nielsen K, Clyde-Smith J, Hancock JF, Waters MJ 2008 An agonist-induced conformational change in the growth hormone receptor determines the choice of signalling pathway. Nat Cell Biol 10:740-747
15.Barclay JL, Kerr LM, Arthur L, Rowland JE, Nelson CN, Ishikawa M, d'Aniello EM, White M, Noakes PG, Waters MJ 2010 In vivo targeting of the growth hormone receptor (GHR) Box1 sequence demonstrates that the GHR does not signal exclusively through JAK2. Mol Endocrinol 24:204-217
16.Ji S, Guan R, Frank SJ, Messina JL 1999 Insulin inhibits growth hormone signaling via the growth hormone receptor/JAK2/STAT5B pathway. J Biol Chem 274:13434-13442
17.Leung KC, Doyle N, Ballesteros M, Waters MJ, Ho KK 2000 Insulin regulation of human hepatic growth hormone receptors: divergent effects on biosynthesis and surface translocation. J Clin Endocrinol Metab 85:4712-4720
18.Bennett WL, Keeton AB, Ji S, Xu J, Messina JL 2007 Insulin regulation of growth hormone receptor gene expression: involvement of both the PI-3 kinase and MEK/ERK signaling pathways. Endocrine 32:219-226
19.Wang P, Li N, Li JS, Li WQ 2002 The role of endotoxin, TNF-alpha, and IL-6 in inducing the state of growth hormone insensitivity. World J Gastroenterol 8:531-536
20.Beauloye V, Ketelslegers JM, Moreau B, Thissen JP 1999 Dexamethasone inhibits both growth hormone (GH)-induction of insulin-like growth factor-I (IGF-I) mRNA and GH receptor (GHR) mRNA levels in rat primary cultured hepatocytes. Growth Horm IGF Res 9:205-211
21.King AP, Carter-Su C 1995 Dexamethasone-induced antagonism of growth hormone (GH) action by down-regulation of GH binding in 3T3-F442A fibroblasts. Endocrinology 136:4796-4803
22.Jux C, Leiber K, Hugel U, Blum W, Ohlsson C, Klaus G, Mehls O 1998 Dexamethasone impairs growth hormone (GH)-stimulated growth by suppression of local insulin-like growth factor (IGF)-I production and expression of GH- and IGF-I-receptor in cultured rat chondrocytes. Endocrinology 139:3296-3305
23.De Luca F 2006 Impaired growth plate chondrogenesis in children with chronic illnesses. Pediatr Res 59:625-629

24.Gevers EF, Hannah MJ, Waters MJ, Robinson IC 2009 Regulation of rapid signal transducer and activator of transcription-5 phosphorylation in the resting cells of the growth plate and in the liver by growth hormone and feeding. Endocrinology 150:3627-3636
25.Kumar KG, Tang W, Ravindranath AK, Clark WA, Croze E, Fuchs SY 2003 SCF(HOS) ubiquitin ligase mediates the ligand-induced down-regulation of the interferon-alpha receptor. Embo J 22:5480-5490
26.Li Y, Kumar KG, Tang W, Spiegelman VS, Fuchs SY 2004 Negative regulation of prolactin receptor stability and signaling mediated by SCF(beta-TrCP) E3 ubiquitin ligase. Mol Cell Biol 24:4038-4048
27.Meyer L, Deau B, Forejtnikova H, Dumenil D, Margottin-Goguet F, Lacombe C, Mayeux P, Verdier F 2007 beta-Trcp mediates ubiquitination and degradation of the erythropoietin receptor and controls cell proliferation. Blood 109:5215-5222
28.Plotnikov A, Li Y, Tran TH, Tang W, Palazzo JP, Rui H, Fuchs SY 2008 Oncogene-mediated inhibition of glycogen synthase kinase 3 beta impairs degradation of prolactin receptor. Cancer Res 68:1354-1361
29.Kumar KG, Krolewski JJ, Fuchs SY 2004 Phosphorylation and specific ubiquitin acceptor sites are required for ubiquitination and degradation of the IFNAR1 subunit of type I interferon receptor. J Biol Chem 279:46614-46620
30.Putters J, da Silva Almeida AC, van Kerkhof P, van Rossum AG, Gracanin A, Strous GJ 2011 Jak2 is a negative regulator of ubiquitin-dependent endocytosis of the growth hormone receptor. PLoS One 6:e14676
31.Govers R, ten Broeke T, van Kerkhof P, Schwartz AL, Strous GJ 1999 Identification of a novel ubiquitin conjugation motif, required for ligand-induced internalization of the growth hormone receptor. Embo J 18:28-36
32.Pelletier S, Gingras S, Funakoshi-Tago M, Howell S, Ihle JN 2006 Two domains of the erythropoietin receptor are sufficient for Jak2 binding/activation and function. Mol Cell Biol 26:8527-8538
33.Strous GJ, van Kerkhof P, Govers R, Ciechanover A, Schwartz AL 1996 The ubiquitin conjugation system is required for ligand-induced endocytosis and degradation of the growth hormone receptor. Embo J 15:3806-3812
34.Jenkins RC, Ross RJ 1996 Acquired growth hormone resistance in catabolic states. Baillieres Clin Endocrinol Metab 10:411-419
35.Anker SD, Volterrani M, Pflaum CD, Strasburger CJ, Osterziel KJ, Doehner W, Ranke MB, Poole-Wilson PA, Giustina A, Dietz R, Coats AJ 2001 Acquired growth hormone resistance in patients with chronic heart failure: implications for therapy with growth hormone. J Am Coll Cardiol 38:443-452
36.Ross RJ, Miell JP, Holly JM, Maheshwari H, Norman M, Abdulla AF, Buchanan CR 1991 Levels of GH binding activity, IGFBP-1, insulin, blood glucose and cortisol in intensive care patients. Clin Endocrinol (Oxf) 35:361-367
37.Counts DR, Gwirtsman H, Carlsson LM, Lesem M, Cutler GB, Jr. 1992 The effect of anorexia nervosa and refeeding on growth hormone-binding protein, the insulin-like growth factors (IGFs), and the IGF-binding proteins. J Clin Endocrinol Metab 75:762-767
38.Menon RK, Arslanian S, May B, Cutfield WS, Sperling MA 1992 Diminished growth hormone-binding protein in children with insulin-dependent diabetes mellitus. J Clin Endocrinol Metab 74:934-938

Nederlandse samenvatting

Ana C. da Silva Almeida, Agnes G S H van Rossum

Department of Cell Biology and Institute of Biomembranes,
University Medical Center Utrecht, Heidelberglaan 100, 3584
CX Utrecht, The Netherlands

Drug Discovery Factory BV, Albrechtlaan 14A, 1404 AK
Bussum, The Netherlands

Publications

The interaction of βTrCP with the Ubiquitin- dependent endocytosis motif of GHR is unconventional

Ana C da Silva Almeida[1, 2], Henry G. Hocking[3], Rolf Boelens[3], Ger J Strous[1], Agnes G S H van Rossum[1, 2].

[1]Department of Cell Biology and Institute of Biomembranes, University Medical Center Utrecht, Heidelberglaan 100, 3584 CX Utrecht; [2]Drug Discovery Factory BV, Albrechtlaan 14A, 1404 AK Bussum, The Netherlands; [3] Department of NMR Spectroscopy, Bijvoet Center for Biomolecular Research, Utrecht University, Padualaan 8, 3584 CH Utrecht, The Netherlands

Growth Hormone Receptor endocytosis and degradation are regulated by phosphorylation of serine 323 in the Ubiquitin-dependent Endocytosis motif

Ana C. da Silva Almeida[1,2], Agnes G S H van Rossum[1,2], Ger J Strous[1]

[1]Department of Cell Biology and Institute of Biomembranes, University Medical Centre Utrecht, Heidelberglaan 100, 3584 CX Utrecht; [2]Drug Discovery Factory BV, Albrechtlaan 14A, 1404 AK Bussum, The Netherlands

βTrCP controls growth hormone receptor degradation via two different motifs
Ana C da Silva Almeida[1, 2], Ger J Strous[1], Agnes G S H van Rossum[1, 2].

[1]Department of Cell Biology and Institute of Biomembranes, University Medical Center Utrecht, Heidelberglaan 100, 3584 CX Utrecht; [2]Drug Discovery Factory BV, Albrechtlaan 14A, 1404 AK Bussum, The Netherlands.

Abbreviations: GH, Growth Hormone; GHR, Growth Hormone Receptor; PRLR, prolactin receptor; IFNAR, interferon α receptor; EpoR, erythropoietin receptor; UbE, ubiquitin-dependent endocytosis βTrCP, β-transducing repeat-containing protein; SCF, Skp, Cullin, F-box containing complex; MVBs, Multivesicular bodies; JAK2, Janus kinase 2; STAT5, Signal transducer and activator of transcription 5; WT, wild type.

Study of GHR endocytosis in living cells using bioluminescence resonance energy transfer (BRET).

Ana C da Silva Almeida[1,2], Ger J Strous[1,], Agnes G S H van Rossum[1,2]

[1]Department of Cell Biology and Institute of Biomembranes, University Medical Center Utrecht, Heidelberglaan 100, 3584 CX Utrecht; [2]Drug Discovery Factory BV, Albrechtlaan 14A, 1404 AK Bussum, The Netherlands.

Partially published in:

Putters J, da Silva Almeida AC, van Kerkhof P, van Rossum AG, Gracanin A, Strous GJ. JAK2 is a negative regulator of ubiquitin-dependent endocytosis of the growth hormone receptor. PLoS One 6: e14676, February 2011

A high-throughput small molecule screen targeted to the growth hormone receptor – βTrCP interaction

Ana Almeida[1,2], Daphne Lelieveld[1], Peter van Kerkhof[1], Henk Viëtor[2], Peter Maas[3], Adri Slob[4], Jan A. Mol[4], Ger J. Strous[1], Agnes G.S.H. van Rossum[1,2]

[1]Department of Cell Biology, University Medical Center Utrecht, Heidelberglaan 100, Utrecht, The Netherlands, [2]Drug Discovery Factory (Recharge) B.V., Albrechtlaan 14A, 1404 AK, Bussum, The Netherlands, [3]Compound Handling B.V. (Specs), Kluyverweg 6, 2629 HT, Delft, The Netherlands. [4]Department of Clinical Sciences of Companion Animals, Faculty of Veterinary Medicine, Utrecht University, Yalelaan 198, Utrecht, The Netherlands.

Nederlandse samenvatting

voor de leek

Groeihormoon zorgt ervoor dat het lichaam groeit. Het hormoon wordt geproduceerd door de voorkwab van de hypofyse en uitgescheiden in het bloed. Als de hoeveelheid groeihormoon in de jeugd te laag is ontstaat er dwerggroei, terwijl te veel groeihormoon leidt tot overmatige groei, het zogenaamde gigantisme, ofwel reuzengroei. Behalve bij de groei speelt groeihormoon ook een belangrijk rol bij andere fysiologische processen zoals metabolisme, spiergroei, vruchtbaarheid, afweer, ontwikkeling van het hart, botvorming en algemene veroudering. Bijgevolg heeft ontregeling van de groeihormoonfunctie ernstige gevolgen, ook bij volwassenen. Verminderde groeihormoonactiviteit veroorzaakt vetophoping rond de organen, verminderde spiermassa en -kracht, en verminderde kwaliteit van leven. Te veel groeihormoon ontstaat meestal ten gevolge van tumorgroei van de hypofyse. Dit resulteert in acromegalie, die gekenmerkt wordt door vergrote handen, voeten en vingers. Ten gevolge van het verstoorde metabolisme is er kans op diabetes.

Hoe reageren cellen op groeihormoon, met andere woorden, hoe vertalen cellen de aanwezigheid van het hormoon in de typische acties? Alle cellen van het lichaam bezitten een specifiek bindingseiwit (receptor) voor groeihormoon aan hun oppervlak. Zodra het rondcirculerend groeihormoon aan de receptor bindt, wordt het kinase, JAK2, dat doorgaans al aan de receptor gebonden is, actief, en het fosforyleert (activeert) zichzelf, de receptor en andere signaalmoleculen in de buurt. Dit leidt in de lever tot veranderingen van het metabolisme (bijvoorbeeld in gluconeogenese) en uiteindelijk tot productie van eiwitten die de verschillende activiteiten van groeihormoon moeten uitvoeren. De belangrijkste factor, waarvan de synthese wordt gestimuleerd, is insulin-like growth factor-1 (IGF-1). De signaleringsroutes, die groeihormoon kan activeren in de cellen, zijn STAT5, MAPK en PI3-K. De signaalsterke, die in een cel ontstaat, hangt dus niet alleen af van de groeihormoonconcentratie in het bloed maar evenzeer van de hoeveelheid groeihormoonreceptoren aan het celoppervlak. Hoeveel receptoren er aan het oppervlak zijn wordt bepaald door: (1) de synthesesnelheid en het transport van nieuw-gesynthetiseerde receptoren naar het celoppervlak en (2) de afbraaksnelheid van receptoren aan het celoppervlak. Receptorafbraak start door de receptoren vanaf het celoppervlak te transporteren naar blaasjes (endosomen) binnenin de cel. Dit proces wordt endocytose genoemd. Vanaf endosomen gaan de receptoren naar lysosomen waar ze worden afgebroken. Endocytose van de receptor is heel precies geregeld. Hierdoor kan de gevoeligheid van cellen voor groei¬hormoon op het juiste niveau worden ingesteld (precies goed voor de situatie waarin de cel zich op dat moment bevindt). Om op snelle veranderingen te kunnen reageren vindt aanmaak en afbraak van de receptor voortdurend plaats, onafhankelijk van de aanwezigheid van groeihormoon. Zodra cellen worden gestimuleerd met groeihormoon, gaat de endocytose en afbraak van de receptor sneller. Hierdoor neemt de gevoeligheid van de cellen voor groeihormoon tijdelijk af. Al sinds 1996 weten we dat endocytose van de receptor afhangt van het ubiquitine-proteasoom systeem, dat werkt via het ubiquitine-afhankelijke endocytose motief (UbE motief) wat zich bevindt in het intracellulaire gedeelte van de receptor. Ubiquitinering is het proces waarbij ubiquitine, een klein eiwit (7 kDa), wordt vastgemaakt aan andere eiwitten. Hierdoor worden ze voorbestemd om te worden afgebroken, of krijgen ze een andere functie in de cel.

Het onderzoek in dit proefschrift concentreert zich met name op één factor van de groeihormoonreceptor endocytose machinerie: βTrCP. βTrCP is een onderdeel van een eiwitcomplex (SCFβTrCP) dat een specifieke aminozuurvolgorde herkent in andere eiwitten, het DSGxxS motief, indien beide serines (S) gefosforyleerd zijn. Na de "herkenningsstap" plakt SCFβTrCP ubiquitine-moleculen aan het eiwit (het substraat), waarna het door het proteasoom wordt afgebroken. SCFβTrCP was eerder geïdentificeerd in onze groep als een essentiële factor

voor de endocytose van de groeihormoonreceptor. In hoofdstuk 2 laten we zien dat βTrCP twee motieven herkent in de receptor: het UbE motief (DDSWVEFIELD) en de DSGRTS sequentie. De laatste komt overeen met het klassieke DSGxxS substraatbindende motief van βTrCP. In afwezigheid van groeihormoon zijn beide motieven betrokken bij de endocytose en afbraak van de receptor. Na groeihormoonstimulatie bindt βTrCP niet meer aan de DSGRTS sequentie. Het UbE motif is daarentegen noodzakelijk voor zowel groeihormoon-afhankelijke als –onafhankelijke receptor endocytose. De rol van de DSGRTS sequentie lijkt zich te beperken tot het reguleren van de basale receptor niveaus in cellen en de daarbij behorende groeihormoon gevoeligheid. Het UbE motief heeft een additionele rol, namelijk de snelle beëindiging van groeihormoonsignalering. In hoofdstuk 4 laten we zien dat groeihormoonstimulatie fosforylering van serine 323 in the UbE motief teweeg brengt. Deze modificatie verhoogt de affiniteit van het UbE motief voor βTrCP, hetgeen endocytose en afbraak van de receptor aanzienlijk versnelt. De binding van groeihormoon aan de receptor veroorzaakt ook dat het kinase, JAK2, loslaat van de receptor (hoofdstuk 6). Dit faciliteert de binding van βTrCP aan de groeihormoonreceptor en initiëert endocytose van de receptor. De combinatie van beide, wellicht onafhankelijke, gebeurtenissen (serine 323 fosforylering en JAK2 loskoppeling), zorgt voor snellere endocytose en afbraak van de receptor na groeihormoonbinding.

Andere receptoren, gerelateerd aan de groeihormoonreceptor zoals de prolactine receptor, de interferon receptor en de erythropoietin receptor, maken ook gebruik van βTrCP. Bij deze receptoren bindt βTrCP aan hun DSGxxS motieven, nadat de serines gefosforyleerd zijn na binding van het hormoon aan de receptor¬. De endocytoseregulatie van deze receptoren verschilt dus van die van de groeihormoon¬receptor. Het belangrijkste verschil is het UbE motief zelf, dat in geen enkel ander eiwit voorkomt. De aminozuurvolgorde van het UbE motief veschilt substantieel van het DSGxxS motief in de andere βTrCP substraten. Desondanks bewijzen we in hoofdstuk 2 dat βTrCP direct bindt aan het UbE motief, hetgeen resulteert in de ubiquitinering van de groeihormoonreceptor in vitro. Structuuranalyse met behulp van nucleaire magnetische resonantie (NMR) toonde aan dat de UbE-βTrCP interactie inderdaad niet conventioneel is in vergelijking met de interactie van βTrCP met andere substraten. De UbE-βTrCP interactie is daarom een veelbelovend, specifiek "drug target" voor medicijnontwikkeling: Een stof die de UbE-βTrCP interactie kan verhinderen of onderbreken is in staat de afbraak van de receptor te vertragen en daarmee zowel het aantal receptoren per cel als de gevoeligheid voor groeihormoon te verhogen. Een dergelijke drug zal specifiek werken op de UbE-βTrCP interactie zonder de binding van βTrCP met andere substraten te beïnvloeden. Patiënten die ongevoelig zijn voor groeihormoon zullen hiervan profijt hebben. Groeihormoonresistentie komt vooral voor bij patiënten met cachexia. Cachexia is een catabole situatie die wordt gekarakteriseerd door een enorm verlies van spiermassa ten gevolge van een onderliggende ziekte zoals kanker, AIDS, rheumatoïde arthritis. In hoofdstuk 5 laten we voor het eerst zien dat muizen die lijden aan cachexia ten gevolge van kanker 9 keer lagere groeihormoonreceptor niveau's in de lever hebben. Hieruit kunnen we concluderen dat de groeihormoonreceptoren in patiënten met cachexia versneld worden afgebroken. Uitgaande van deze stelling hebben we een geautomatiseerde drug screening procedure opgezet om stoffen te identificeren die de UbE-βTrCP interactie kunnen verstoren. In een tweede screen konden we stoffen identificeren die inderdaad de endocytose en afbraak van de groeihormoon¬receptor verhinderde. Eén stof was in staat de hoeveelheid groeihormoonreceptoren in muizenlevers, het belangrijkste "target" orgaan, te verhogen en biedt een goede basis voor verdere therapeutische ontwikkeling.

De bevindingen in dit proefschrift dragen in belangrijke mate bij aan inzicht in de mechanismen die de endocytose van de groeihormoonreceptor en de gevoeligheid van cellen voor groeihormoon regelen. De verkregen kennis biedt belangrijke mogelijkheden om nieuwe geneesmiddelen te ontdekken die in staat zijn cachexia te genezen of te remmen.

Sumário em Português

A hormona do crescimento é uma molécula produzida na hipófise responsável pelo crescimento do nosso corpo. Durante a infância, quantidades insuficientes em circulação da hormona resultam em nanismo, enquanto quantidades excessivas resultam em crescimento descontrolado, conduzindo ao desenvolvimento de gigantismo. A hormona do crescimento desempenha outras funções fisiológicas importantes no organismo para além de promover o crescimento, tais como o controlo do metabolismo, crescimento muscular, fertilidade, imunidade, desenvolvimento cardíaco, ossificação, envelhecimento, entre outras. Desta forma, desregulações na função da hormona do crescimento aquando da idade adulta, em que o corpo completou o crescimento, têm consequências prejudiciais. A redução da atividade da hormona do crescimento em adultos causa acumulação de gordura na zona visceral, com uma redução relativa de massa muscular, de energia e de qualidade de vida. Por outro lado, um excesso de atividade da hormona do crescimento, que ocorre frequentemente devido a um tumor na hipófise que secreta esta hormona, causa acromegalia. Esta condição é caracterizada por desfiguração facial, aumento do tamanho dos pés e mãos, bem como desregulação metabólica que origina diabetes.

Mas de que forma detetam as células a hormona do crescimento? A maior parte das células do nosso organismo contêm na sua superfície um recetor específico para a hormona do crescimento. Quando a hormona se liga ao recetor, são ativadas vias de sinalização, desencadeadas inicialmente pela ativação da proteína JAK2, uma quinase associada às caudas citoplasmáticas do recetor. Em consequência, ocorre a ativação da expressão de genes importantes para as ações da hormona do crescimento no organismo. O principal fator cuja expressão resulta da estimulação pela hormona do crescimento é o IGF-1 (Insulin-like growth factor 1). As vias de sinalização ativadas pela hormona do crescimento são a STAT5, MAPK e PI3-K. A sinalização ativada pela hormona do crescimento depende não só da quantidade de hormona em circulação, mas também do número de recetores na superfície das células. Os níveis de recetor representam um balanço dinâmico de dois processos: (1) síntese e transporte dos recetores sintetizados para a superfície das células e (2) degradação dos recetores. A degradação dos recetores é iniciada depois da "entrada" dos recetores da superfície para o interior das células, num processo denominado endocitose. Subsequentemente, os recetores da hormona do crescimento são transportados para os lisossomas, onde são degradados. O processo de endocitose do recetor é estritamente regulado, de forma a que a sensibilidade das células para a hormona do crescimento seja ajustada ao nível adequado. A endocitose e degradação do recetor da hormona do crescimento ocorrem continuamente e independentemente da estimulação com hormona do crescimento. A estimulação das células com a hormona acelera a endocitose do receptor, o que contribui para a terminação da sinalização. A endocitose do recetor implica um sistema de ubiquitinação funcional e depende de uma região na cauda intracelular do recetor denominada UbE (Ubiquitin-dependent Endocytosis motif). A ubiquitinação é o processo através do qual a proteína regulatória ubiquitina é adicionada a outras proteínas, marcando-as para destruição ou direcionando-as para localizações diferentes na célula.

A presente tese foca-se particularmente num componente da maquinaria de endocitose do recetor da hormona do crescimento: βTrCP. βTrCP é parte de um complexo de proteínas (SCFβTrCP) que reconhece sequências específicas de aminoácidos nos seus substratos, classicamente a sequência DSGxxS (aspartato, serina, glicina, x – resíduo hidrofóbico, serina), quando as duas serinas são fosforiladas. Subsequentemente, o complexo SCFβTrCP medeia a ubiquitinação e concomitante degradação dos seus substratos. SCFβTrCP foi identificado como sendo essencial para a endocitose do recetor da hormona do crescimento. No capítulo 2, demonstramos que βTrCP se liga a duas regiões do recetor: ao UbE (sequência: DDSWVEFIELD) e à sequência DSGRTS, que corresponde à sequência que normalmente é reconhecida em outros substratos de βTrCP. Na ausência de estimulação com a hormona do crescimento, as duas regiões são necessárias para a endocitose e degradação do recetor. Quando as células são estimuladas

com a hormona, βTrCP não se liga à sequência DSGRTS, e não é necessária para a endocitose do recetor induzida pela hormona do crescimento. Por outro lado, o motivo UbE é necessário tanto para a endocitose basal como para a endocitose induzida pela hormona do crescimento. Isto deve-se provavelmente ao facto da estimulação pela hormona do crescimento despoletar certos eventos nas células que conferem um papel predominante ao motivo UbE em relação à sequência DSGRTS na endocitose do recetor. Desta forma, o papel da sequência DSGRTS é restrito à regulação dos níveis basais de recetor, contribuindo substancialmente para a regulação da sensibilidade das células à hormona do crescimento. O motivo UbE tem um papel adicional na terminação rápida da sinalização desencadeada pela hormona do crescimento. No capítulo 4, demonstramos que a hormona do crescimento ativa a fosforilação da serina 323 no motivo UbE, resultando numa maior afininidade para βTrCP e, consequentemente, numa endocitose mais rápida do recetor. Um outro evento mediado pela hormona do crescimento é a "libertação" da quinase JAK2 do recetor para o citosol (capítulo 6). Este processo poderá facilitar a ligação de βTrCP ao recetor e, como tal, a sua ação na endocitose do recetor. Os dois eventos poderão ser inter-dependentes, e asseguram a rápida endocitose e degradação do recetor depois da ligação da hormona do crescimento.

Outros recetores homólogos ao recetor da hormona do crescimento – tais como o recetor de prolactina, interferão e eritropoetina - necessitam de βTrCP para serem endocitados. Nestes recetores, βTrCP liga-se a sequências DSGxxS, quando as duas serinas são fosforiladas após estimulação com os respetivos ligandos. Portanto, a regulação da endocitose destes recetores difere da observada no recetor da hormona do crescimento. A principal diferença é o facto do motivo UbE, cuja sequência difere substancialmente de DSGxxS, não existir em nenhum outro substrato. Não obstante, no capítulo 2, provamos que βTrCP se liga diretamente ao motivo UbE, o que resulta na ubiquitinição do recetor, in vitro. Contudo, análise estrutural através de NMR (ressonância magnética nuclear) demonstrou que a interação entre o motivo UbE e βTrCP é única quando comparada com a interação entre βTrCP e outros substratos. Portanto, a interação entre βTrCP e o motivo UbE representa um alvo promissor para descoberta de compostos que, interferindo com a interação, resultam num aumento do número de recetores da hormona do crescimento nas células e, consequentemente, no aumento da sua sensibilidade para a hormona do crescimento. Esta terapêutica actuaria especificamente na interacção UbE- βTrCP sem afetar a interação de βTrCP com os seus outros substratos. Pacientes que sofrem de resistência/ insensibilidade à hormona do crescimento beneficiariam deste composto. A resistência à hormona do crescimento é uma característica frequente em pacientes que sofrem de caquexia. A caquexia é uma condição catabólica caracterizada por uma perda extensa de massa muscular, estando normalmente associada a uma patologia crónica subjacente como o cancro, a SIDA, artrite reumatóide entre outras. No capítulo 5, demonstramos pela primeira vez que ratos com caquexia derivada de um tumor contêm 9 vezes menos recetores da hormona do crescimento nos seus fígados. Por extrapolação destes resultados, pode assumir-se que a degradação dos recetores em pacientes a sofrer de caquexia poderá ocorrer mais rapidamente. Partindo deste princípio, desenvolvemos um sistema de rastreio para identificar compostos capazes de interferir com a interação UbE-βTrCP, inibir a degradação do recetor da hormona do crescimento, aumentar o número de recetores nas células e desta forma melhorar a sensibilidade de pacientes a sofrer de caquexia à hormona do crescimento. Um exemplo de um composto capaz de aumentar os níveis de recetor em fígados de rato é demonstrado.

As descobertas desta tese representam contribuições importantes para a compreensão dos mecanismos que regulam a endocitose do recetor da hormona do crescimento e a sensibilidade celular para a hormona do crescimento, onde nós exploramos o conhecimento adquirido na descoberta de compostos capazes de lutar contra caquexia.

Curriculum Vitae

Ana Almeida was born in Caracas, Venezuela, in 28th September 1984, and soon after moved to Portugal. In June 2002 she completed the High School studies in the public high school in Sever do Vouga, Portugal. In the same year in September, she started her studies in Biochemistry at the Faculty of Sciences in University of Oporto. In 2006, she performed the final research project of her Biochemistry degree in the Department of Biochemistry and Biophysics at Stockholm University, under the European Union Erasmus program. In September 2006, she completed the degree in Biochemistry. From October 2006 to April 2007 she performed a diagnostics and research fellowship in the Department of Genetics of the Faculty of Medicine of Oporto, with a fellowship from the Portuguese Foundation for Science and Technology. In April 2007 Ana moved to The Netherlands to start her PhD studies under the supervision of Prof. Ger Strous, inserted in a Marie Curie Network UbiRegulators. After her PhD promotion, she will become a Post-doctoral in the group of Dr. Adolfo Ferrando, at Columbia Medical Center in New York.